

Phonons 98

Lancaster

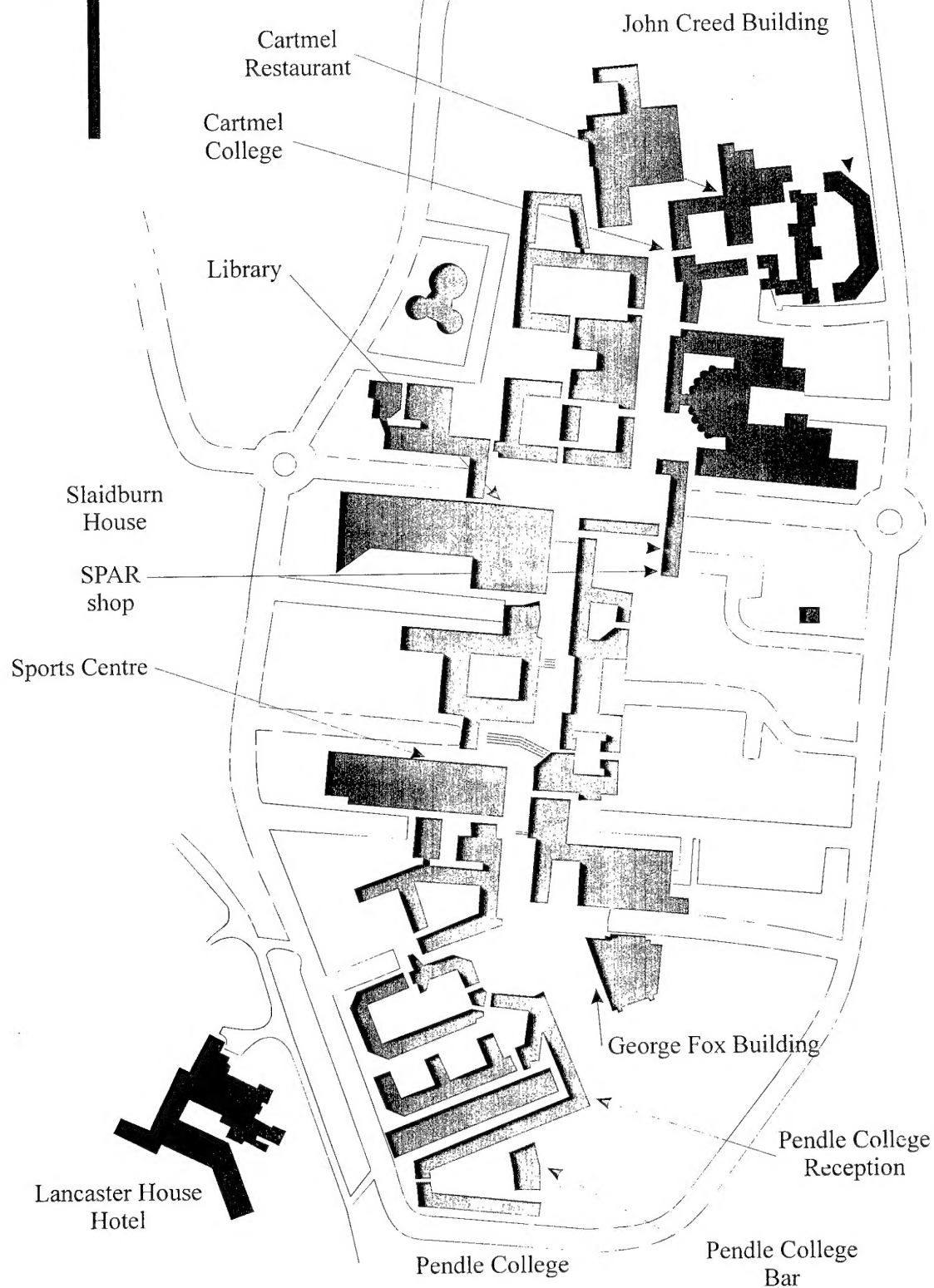


Programme and Abstracts

19981006 039

*Ninth International Conference on Phonon
Scattering in Condensed Matter*

July 26-31, 1998, Lancaster, United Kingdom



Lancaster University Campus Plan

PHONONS 98

**9TH INTERNATIONAL CONFERENCE ON PHONON
SCATTERING IN CONDENSED MATTER**

LANCASTER, ENGLAND

26-31 July 1998

Sponsors

**Engineering and Physical Sciences Research Council (UK)
European Commission
European Physical Society
European Research Office of the U.S. Army
Institute of Physics (UK)
International Union of Pure and Applied Physics
Lancaster University Physics Department**

INTERNATIONAL ADVISORY COMMITTEE

J.L. Beeby (UK)
L.J. Challis (UK)
J.I. Dijkhuis (Netherlands)
A. Every (South Africa)
J. Inkson (UK)
J.C. Lasjaunias (France)
H.J. Maris (USA)
T. Miyasato (Japan)
R.L. Orbach (USA)
R.O. Pohl (USA)
K. Suzuki (Japan)
F. Vallee (France)
M.N. Wybourne (USA)

B. Cabrera (USA)
W. Dietsche (Germany)
W. Eisenmenger (Germany)
S. Hunklinger (Germany)
A.A. Kaplayanskii (Russia)
Y.B. Levinson (Israel)
L.P. Mezhov-Deglin (Russia)
T. Nakayama (Japan)
T. Paskiewicz (Poland)
B. Sadoulet (USA)
S. Tamura (Japan)
J.P. Wolfe (USA)

PROGRAMME COMMITTEE

W. Dietsche (Germany)
H.J. Maris (USA)
A.G. Kozorezov (UK) **(chair)**

A.J. Kent (UK)
C.J. Mellor (UK)

LOCAL ORGANISING COMMITTEE

P. Boyd
A. G. Kozorezov
D.J. Meredith

J. Hesletine
C.J. Lambert
J. Taylor

A. Krier
P.V.E. McClintock
J.K. Wigmore **(chair)**

PRESENTATIONS

All scientific sessions will take place in the George Fox Conference Centre, which is a no-smoking area. A plan of the building is on the inside back cover. Oral presentations will be made in the Auditorium (R1 in the programme) and in Lecture Theatre 5/6 (R2 in the programme). Posters will be displayed in the foyer, where refreshments and lunches will also be served.

Oral presentations

Plenary presentations are scheduled for 40 minutes, invited talks for 30 minutes, and oral presentations for 20 minutes, all times to include 5 minutes for questions or brief discussion. You are requested to keep closely to these times. Before the beginning of a session, speakers should introduce themselves to the chair and make arrangements with the session assistant regarding slides or any other special requirements. Overhead projector, microphone and laser pointer will be provided as standard.

Although the conference language is English, for many participants this is not their first language. Therefore, please speak slowly, clearly and loudly.

In responding to contributions from the audience, first repeat the question or the point raised for discussion.

Discussion sessions

The two largest areas of interest at the conference are **Glasses/Disorder**, and **Nanostructures**. Special discussion sessions on these topics will be held to chart progress and identify important problems. It would help the session chairs (Raymond Orbach and Martin Wybourne) to have advance notice of your intention to speak, but this is not essential.

Highlights

The sessions on **Particle and Photon Detectors** and on **Isotope Effects** will highlight two important areas of physics to which the effects of phonons are becoming increasingly relevant.

Posters

Poster presentations should be prepared to fit into an area of 0.91m (horizontal) \times 1.22m (vertical). Material will be attached to the felt-covered boards with "Velcro" which will be provided.

Please mount your poster on the numbered board some time in the morning of your session before 12.00, and remove it before 09.00 the following morning.

Prizes will be awarded at each poster session for the best posters prepared by students describing work in which they have had a major input. Judging criteria will focus on quality of presentation and clarity of explanation.

PROCEEDINGS

The conference proceedings will appear as a regular issue of Physica B. Please help us to maintain the tight schedule that is necessary.

Authors

If you have not already provided your manuscript and disc, take them to the **conference office** immediately. Watch the PROCEEDINGS NOTICEBOARD regularly. Notification to authors of any manuscripts that require modification will be posted here. If you do not see your name at anytime, you may assume that your manuscript has been accepted without modification. The final deadline for receipt of revised manuscripts by the conference is 30 September.

Referees

Please return all manuscripts, together with reports, to the **conference office** as soon as possible, but not later than 09.00 on Thursday morning. Thank you for carrying out this important task.

ASSISTANCE

If you require assistance on anything at any time please go to the **conference office**, which is up the winding staircase to the left of the entrance, or contact one of the persons wearing a blue sweatshirt or a blue badge.

Monday 27 July

09.00	Opening ceremony [R1]	
09.30	Plenary session [R1]	
10.50	<i>Refreshments</i>	
11.20	Nanostructures 1 [R1]	Lattice dynamics 1 [R2]
13.00	<i>Lunch</i>	
14.00	Nanostructures 2 [R1]	Lattice dynamics 2 [R2]
15.30	Poster Session A (<i>Refreshments</i>)	
17.00	Coherent phonons 1 [R1]	Phase transitions [R2]
19.00	<i>Dinner</i>	
20.30	<i>Conference reception</i>	

Tuesday 28 July

09.00	Glasses 1 [R1]	
10.50	<i>Refreshments</i>	
11.20	Electron-phonon interactions 1 [R1]	Raman scattering [R2]
13.00	<i>Lunch</i>	
14.00	Glasses 2 [R1]	Nanostructures 3 [R2]
15.30	Poster session B (<i>Refreshments</i>)	
17.00	Nanostructures (discussion) [R1]	
19.00	<i>Dinner</i>	

Wednesday 29 July

09.00	Glasses 3 [R1]	New techniques 1 [R2]
10.30	<i>Refreshments</i>	
10.50	Electron-phonon interactions 2 [R1]	Phonon Interactions 1 [R2]
12.30	<i>Lunch</i>	
13.30	<i>Excursion departure</i>	
20.00	<i>Dinner</i>	

Thursday 30 July

09.00	Coherent phonons 2 [R1]	Particle detectors (highlight) [R2]
11.00	<i>Refreshments</i>	
11.30	Disordered systems [R1]	Phonon interactions 2 [R2]
13.00	<i>Lunch</i>	
14.00	New techniques 2 [R1]	Isotope effects (highlight) [R2]
15.30	Poster session C (<i>Refreshments</i>)	
17.00	Glasses and disordered systems (discussion) [R1]	
18.30	<i>Conference banquet departure</i>	
19.00	<i>Dinner</i>	

Friday 31 July

09.00	Interfaces and quantum fluids [R1]	Phonon interactions 3 [R2]
10.30	<i>Refreshments</i>	
10.50	Electron-phonon interactions 3 [R1]	Defects [R2]
12.15	Closing plenary session [R1]	
13.00	Conference close	
13.30	<i>Lunch</i>	

ORAL PRESENTATIONS

PLENARY SESSION (Monday 09.30) Chair: Beeby [R1]

PL1 M. Roukes

Yoctocalorimetry : Quantum Phonon Optics in Nanostructures

PL2 F. Nori

Phonon Squeezed States : Quantum Noise Reduction in Solids

NANOSTRUCTURES 1 (QUANTUM WIRES / WELLS) (Monday 11.20) Chair: Dietsche [R1]

NS1.1 M.P. Blencowe

Quantum Energy Flow in Mesoscopic Dielectric Structures

NS1.2 M.A. Stroscio G. Belenky M. Dutta V.B. Gorfinkel G.I. Haddad G.J. Iafrate K.W. Kim M. Kisin S. Luryi J.P. Sun H.B. Teng S. Yu

Tailoring of Optical Phonon Modes in Nanoscale Semiconductor Structures: Role of Interface-Optical Phonons in Quantum-Well Lasers

NS1.3 N. Nishiguchi M.N. Wybourne

Thermal Relaxation of Coherent Charge Oscillation in Coupled-Quantum Wells

NS1.4 C.R. Bennett B.K. Ridley N.A. Zakhleniuk M. Babiker

The Hybrid Model for Optical Phonon Confinement in AlN/GaN Quantum Wells

LATTICE DYNAMICS 1 (Monday 11.20) Chair: Cardona [R2]

LD1.1 P. Pavone T. Pletl U. Engel D. Strauch

First-Principles Study of Lattice-Dynamical and Elastic Trends in Tetrahedral Semiconductors

LD1.2 G. Srivastava H.M. Tütüncü

Surface Dynamics of AlSb(110) and GaP(110)

LD1.3 J. Li

Interpretation of Inelastic Neutron Scattering Spectra by Lattice and Molecular Dynamic Simulations

LD1.4 A. Bussmann-Holder

Local Structural Anomalies in Perovskite-Type Lattices

NANOSTRUCTURES 2 (NANOCRYSTALS) (Monday 14.00) Chair: Stroscio [R1]

NS2.1 J.I. Dijkhuis M. van der Voort A.V. Akimov G.D.J. Smit N.A. Feoktsitov A.A. Kaplyanskii A.B. Pevtsov

Decay of Nonequilibrium Phonons in Nanocrystalline Silicon

NS2.2 **H. Yang** S.P. Feofilov B.M. Tissue R.S. Meltzer W.M. Dennis
One Phonon Relaxation Processes in $\text{Y}_2\text{O}_3\text{:Eu}^{3+}$ Nanocrystals

NS2.3 **T. Maeda** C. Horie
Phonon Modes in Single-Wall Nanotubes with a Small Diameter

NS2.4 **Y. Kogure**
Simulation of Phonon Propagation in Fine Particles

LATTICE DYNAMICS 2 (Monday 14.00) Chair: Inkson [R2]

LD2.1 **S.M. Bennington** J. Li M. Harris D.K. Ross
Phonon Softening in Ice Ih

LD2.2 **E. Burkel** C. Seyfert C. Halcoussis H. Sinn R.O. Simmons
Phonon Dispersion Curves in HCP 3He and $\alpha\text{-SiO}_2$ Determined by Inelastic X-Ray Scattering

LD2.3 **W. Reichardt** M. Braden
Anomalous Features in the Mn-O Bond-Stretching Vibrations of $\text{La}_{1-x}\text{Sr}_x\text{MnO}_3$

LD2.4 **A. Kolesnikov** V.E. Antonov S.M. Bennington B. Dorner V.K. Fedotov G. Grosse J.C. Li
S.F. Parker F.E. Wagner
The Vibrational Spectrum and Giant Tunnelling Effect of Hydrogen dissolved in $\alpha\text{-Mn}$

COHERENT PHONONS 1 (Monday 17.00) Chair: Wolfe [R1]

CP1.1 **H. de Wijn** P.A. van Walree A.F.M. Arts
Coherent Phonon Avalanches

CP1.2 **S. Baumhoff** J.-Y. Prieur J. Joffrin
Amplification of Sound in the Coherent Regime at Low Temperatures in Glass

CP1.3 **J.H. Page** M.L. Cowan H.P. Schriemer P. Sheng D.A. Weitz
Diffusive Transport of Acoustic Waves in Strongly Scattering Media.

CP1.4 **Y. Abe** **A. Iobe**
Chaotic Behaviour in a Surface Acoustic Wave Resonator

PHASE TRANSITIONS (Monday 17.00) Chair: Maynard [R2]

PT1 **M.J. Harris** D.F. McMorrow
Phonon Softening at a Continuous Melting Transition: Lattice Melting in Ferroelastic Na_2CO_3

PT2 **M. Takesada** M. Kasahara T. Yagi
Premelting Phenomena of $\text{LiH}_3(\text{SeO}_3)_2$ Studied by Brillouin Scattering

PT3 **J.C. Marmeggi** R. Currat G.H. Lander
Phonons softening in Alpha-U Metal at Low Temperature

PT4 **B. Hehlen** L. Arzel A.K. Tagantsev E. Courtens Y. Inaba A. Yamanaka K. Inoue
Observation of the Coupling Between TA and TO Modes in SrTiO₃ in Brillouin Scattering

GLASSES 1 (Tuesday 09.00) Chair: Strehlow [R1]

GL1.1 **T. Nakayama**
The Boson Peak in Network-Forming Glasses

GL1.2 **M. Yamaguchi** T. Nakayama T. Yagi
Effects of High Pressure on the Boson Peak in a-GeS₂ Studied by Light Scattering

GL1.3 **R.L. Orbach** T. Nakayama
Heat Transport Above the Plateau Temperature in Glasses

GL1.4 **M. Foret** B. Hehlen E. Courtens R. Vacher
Is there a Ioffe-Regel Limit for Sound Propagation in Glasses?

GL1.5 **M. Arai** Y. Inamura T. Otomo N. Kitamura S.M. Bennington A.C. Hannon
Novel Coexistence of Propagating Collective Mode and Strongly Localized Mode in Vitreous Silica

ELECTRON-PHONON INTERACTIONS 1 (Tuesday 11.20) Chair: Dutta [R1]

EP1.1 **A.J. Kent** A.J. Naylor I.A. Pentland M. Henini
Electron-Phonon Interaction in Quantum Wires

EP1.2 **M. Rokni** Y. Levinson
The Absorption of Surface Acoustic Waves by an Array of Quantum Wires

EP1.3 **N.Z. Vagidov** V. I. Pipa V.V. Mitin
Relaxation Rates of 2D Electron Gas Due to Near-Surface Acoustic Phonon Scattering

EP1.4 **D. Lehmann** Cz. Jasiukiewicz A.J. Kent A.J. Cross P. Hawker
Angular and Mode Distribution of Acoustic Phonon Emission by Hot 2D Electrons in GaAs: The Effect of Acoustic Anisotropy and Screening.

RAMAN SCATTERING (Tuesday 11.20) Chair: Kaplyanskii [R2]

RS1 **K. Shirai** H. Katayama-Yoshida
Raman Spectrum of α -Rhombohedral Boron and its Anharmonic Effects

RS2 **T. Kume** T. Tsuji S. Sasaki H. Shimizu
Raman Study of Solid HBr Under High Pressure and Low Temperature

RS3 **K. Wakamura** J. Katagi H. Takahashi
Temperature Dependence of Vibrational Spectra in Glass Superionic Conductors(AgI)_x-(AgPO₃)_{1-x}

RS4 **H. Kuroe** H. Seto T. Sekine M. Isobe Y. Ueda
Spin-Peierls Transition in α' - $\text{Na}_{1.8}\text{V}_2\text{O}_5$ observed by Raman Scattering

GLASSES 2 (Tuesday 14.00) Chair: Nakayama [R1]

GL2.1 **S. Hunklinger** P. Strehlow C. Enss
Macroscopic Quantum State of Tunnelling Systems

GL2.2 **P. Strehlow** M. Meissner
Thermodynamically Consistent Determination of the Specific Heat of Vitreous Silica Down to 15 Millikelvin

GL2.3 **R. Geilenkeuser** T. Porschberg M. Jäckel
Influence of High Pressure on Thermal Properties of Amorphous Polystyrene

GL2.4 **C. Laermans** M. Coeck
Low Frequency Raman Scattering in Bulk Neutron Disordered Silicon

NANOSTRUCTURES 3 (SUPERLATTICES) (Tuesday 14.00) Chair: Maris [R2]

NS3.1 **S.I. Tamura**
Dynamic Properties of Phonons in Superlattices

NS3.2 **M. Schmitt** A.P. Mayer D. Strauch
Lifetimes of Acoustic Phonons and Thermal Conductivity in Superlattices

NS3.3 **M. Giehler** T. Ruf M. Cardona K.H. Ploog
Standing Acoustic Waves in GaAs/AlAs Mirror-Plane Superlattices and Cavity Structures Studied by Raman Spectroscopy

NS3.4 **D.N. Talwar** S. Zaraneek
Anion-Related Differences in the Phonons of $(\text{GaY})_m/(\text{Ga}_{1-x}\text{Al}_x\text{Y})$, $\text{Y}=\text{As}, \text{N}$ Superlattices

NANOSTRUCTURES : DISCUSSION (Tuesday 17.00) Chair: Wybourne [R1]

GLASSES 3 (Wednesday 09.00) Chair: Hunklinger [R1]

GL3.1 **A. Wurger**
Dissipative Dynamics of Two-State Defects

GL3.2 **M. van der Voort** G.D.J. Smit A.V. Akimov J.I. Dijkhuis
Phonon Generation by Carrier Recombination in A-Si:H

GL3.3 **S.G. Lushnikov** S.N. Gvasaliya I.G. Siny
Phonons and Fractons in the Vibration Spectrum of the Relaxor Ferroelectric $\text{PbMg}_{1/3}\text{Nb}_{2/3}\text{O}_3$

GL3.4 **R. Kühn** U. Horstmann
Spin-Glass Approach to Low-Temperature Anomalies in Glasses

NEW TECHNIQUES 1 (Wednesday 09.00) Chair: Miyasato [R2]

NT1.1 **W. Grill** K. Hillmann T.J. Kim O. Lenkeit J. Ndop M. Schubert
Scanning Acoustic Microscopy with Vector Contrast

NT1.2 **S. Knauth** K. Hillmann W. Grill
Scanning Second Sound Microscopy with Vector Contrast

NT1.3 **D.J. Dieleman** A.F. Koenderink M.G.A. van Veghel M.A. de Vries A.F.M. Arts H.W. de Wijn
Physical and Geometrical Optics of Phonons

NT1.4 **J.P. Wolfe** R.E. Vines
Scanning Phononic Lattices with Ultrasound

ELECTRON-PHONON INTERACTIONS 2 (Wednesday 10.50) Chair: Levinson [R1]

EP2.1 **A.V. Akimov**
Exciton-Phonon Interaction in Single and Double Quantum Wells.

EP2.2 **W. Dietsche** S. Roshko L.J. Challis
Spectroscopic Evidence for Cyclotron Phonon Emission from Si-MOSFETs in Strong Magnetic Fields

EP2.3 **A. Sergeev** B.S. Karasik N.G. Ptitsina G.M. Chulkova K.S. Il'in E.M. Gershenzon
Electron-Phonon Interaction in Disordered Conductors

EP2.4 **O.B. Wright** P.L.G. Ventzek V.E. Gusev
Electron-Phonon Dynamics in Metals on Ultrashort Timescales

PHONON INTERACTIONS 1 (Wednesday 10.50) Chair: Kozorezov [R2]

PI1.1 **H.J. Maris** H.-Y. Hao
Acoustic Solitons

PI1.2 **V. Hizhnyakov** M. Selg R. Kink J. Maksimov
Step-Wise Multiphonon Anharmonic Decay of Local Modes: Theory and Experiment

PI1.3 **A. Debernardi** M Cardona
First Principle Calculation of the Real Part of Phonon Self Energy in Compound Semiconductors

PI1.4 **M.R. Geller** W.M. Dennis
Phonon-Phonon Interactions in Disordered Systems

COHERENT PHONONS 2 (Thursday 09.00) Chair: Wright [R1]

CP2.1 **A. Bartels** T. Dekorsy H. Kurz K. Köhler
Coherent Acoustic Phonons in GaAs/AlAs Superlattices

CP2.2 **K. Mizoguchi** M. Hase S. Nakashima M. Nakayama
Study of coherent folded acoustic phonons in semiconductor superlattices by pump-probe technique

CP2.3 **K. Kisoda** M. Hase H. Harima S. Nakashima
Pump Power Dependence of Coherent Phonons in η -Mo₄O₁₁

CP2.4 **F. Vallée** N. Del Fatti S. Tzortzakis C. Flytzanis
Coherent Acoustic Mode Oscillation in Silver Nanoparticles

CP2.5 **O.V. Misochko** M. Tani K. Sakai K. Kisoda S. Nakashima V.N. Andreev F.A. Chudnovsky
Phonons in V₂O₃ Above and Below Mott Transition: A Comparison of Time and Frequency Domain Spectroscopy Results

CP2.6 **P. Kocevar** M. Schullatz J. Kuhl
A Monte-Carlo Analysis of the Picosecond Raman Spectroscopy of Germanium

PARTICLE AND PHOTON DETECTION (Thursday 09.00) Chair: Booth [R2]

PP1 **B. Cabrera**
Particle Detectors Using Superconducting Transition Edge Sensors

PP2 **A. Peacock**
X-Ray Detectors and Photon Counters Using Superconducting Tunnel Junctions

PP3 **S.R. Bandler** J.S. Adams C. Enss A. Fleischmann S. Hunklinger Y. Kim J. Schönefeld G.M. Seidel
Particle Detection Using Cryogenic Magnetic Calorimeters

PP4 **A. Poelaert** R. den Hartog A. Peacock A. Kozorezov J.K. Wigmore
The Role of Phonon Processes in the Performance of Superconducting Tunnel Junctions used as Photon Detectors

PP5 **P. Clegg** M. Bravin N.E. Booth M. Bruckmayer K. Djotni E. Esposito E.P. Houwman H. Kraus G.L. Salmon
Determination of Quasidiffusive Phonon Propagation in BaF₂ Using Pulse Shape Analysis and Possible Implications for Particle Detection

DISORDERED SYSTEMS (Thursday 11.30) Chair: Laermans [R1]

DS1 **W. Eisenmenger** R. Eilenberger K. Lassmann
Anharmonic Resonators in Electron-Irradiated α -Quartz

DS2 **C. Enss** M. Kreft S. Ludwig C.P. An F. Luty
Dielectric Relaxation of Interacting Hydroxyl Ions in KCl

DS3 **T. Damker** H. Böttger
Phonon Hopping in Disordered Systems

DS4 **G. Fagas** V.I. Falko C.J. Lambert
Wigner-Dyson Statistics of Phonon Resonances in Chaotic Acoustic Resonators

PHONON INTERACTIONS 2 (Thursday 11.30) Chair: Paskiewicz [R2]

PI2.1 **L.P. Mezhov-Deglin** V.B. Efimov
Phonon Scattering in HTS Cuprate Crystals

PI2.2 **M. Ikebe** H. Fujishiro
Two-Level-Like Phonon Scattering in the Oxide Superconductor, $\text{La}_{2-x}\text{Sr}_x\text{CuO}_4$

PI2.3 **S.P. Feofilov** A.A. Kaplyanskii A.B. Kulinkin R.I. Zakharchenya
Optical Studies of Terahertz Phonons Dynamics in Small-Grain Polycrystalline Corundum

PI2.4 **S. Ivanov** L.M. Zhukova E.N. Khazanov Y.M. Soifer A.V. Taranov
The Scattering of Nonequilibrium Phonons on Grain Boundaries in Single Phase Ceramics

NEW TECHNIQUES 2 (Thursday 14.00) Chair: Mellor [R1]

NT2.1 **R.M. Koehl** C.J. Brennan T.F. Crimmins K.A. Nelson
Spatiotemporal Imaging, Spatiotemporal Pulse Shaping, and Spatiotemporal Coherent Control

NT2.2 **B. Perrin** C. Rossignol B. Bonello J.-C. Jeannet
Interferometric Detection in Picosecond Ultrasonics

NT2.3 **W. Sturhahn** E.E. Alp P. Hession M. Hu T.S. Tollner
Vibrational Density of States obtained from Inelastic Nuclear Resonant Absorption of Synchrotron Radiation

NT2.4 **R. Röhlberger** E.E. Alp A. Bernhard E. Burkel A.I. Chumakov E. Gerdau O. Leupold K.W. Quast R. Rüffer W. Sturhahn T.S. Tollner
Techniques for Inelastic X-ray Scattering with μeV - Resolution

ISOTOPE EFFECTS (Thursday 14.00) Chair: Klemens [R2]

IS1 **M. Cardona**
Optical Studies of Isotopically Pure Semiconductors : Phonons and Electronic Structures

IS2 **F. Widulle** T. Ruf A. Göbel I. Silier E. Schönherr M. Cardona A. Cantarero J. Camacho
Raman Studies of Isotope Effects in Si and GaAs

IS3 **K. Lassmann** N. Aichele C. Linsenmaier F. Maier F. Zeller E.E. Haller K.M. Itoh L.I. Khirunenko B. Pajot H. Müssig
Isotopic Shifts of the Low-Energy Excitations of Interstitial Oxygen in Germanium

IS4 **G. Weiss** M. Hübner C. Enss
Sound Velocity and Internal Friction of Li Doped KCl

GLASSES AND DISORDERED SYSTEMS : DISCUSSION (Thursday 17.00) Chair: Orbach [R1]

INTERFACES AND QUANTUM FLUIDS (Friday 09.00) Chair: Eisenmenger [R1]

IQ1 **A.G. Every** A.A. Maznev G.A.D. Briggs
Acoustic Wave Propagation at a Solid-Liquid Interface

IQ2 **M.E. Msall** A. Klimashov W. Dietsche K. Friedland
Direct Phonon Transmission Across Wafer Bonded Crystals

IQ3 **Y. Okuda** S. Yamazaki T. Yoshida Y. Fujii K. Matsumoto
Observation of Melting of Solid ^4He by Sound Wave

IQ4 **N. Gov** E. Akkermans
Hybridization of Localized and Density modes in Superfluid $\text{He } ^4$

PHONON INTERACTIONS 3 (Friday 09.00) Chair: Dijkhuis [R2]

PI3.1 **R. Maynard** A. Smontara J.-C. Lasjaunias R. Bressoux
Poiseuille Flow of Phonons in a Quasi-One Dimensional Crystal

PI3.2 **A.F.M. Arts** P.J. Rump H.W. de Wijn
Diffusion of Phonons in $\text{Li}_{1-x}\text{Ho}_x\text{F}_4$

PI3.3 **V.B. Efimov** L.P. Mezhov-Deglin
Heat Transport in Fullerite Samples

PI3.4 **S. Voltz** G. Chen
Lattice Dynamic Simulation of Silicon Thermal Conductivity

ELECTRON-PHONON INTERACTIONS 3 (Friday 10.50) Chair: Mitin [R1]

EP3.1 **C.J. Mellor** U. Zeitler A.M. Devitt S.H. Roshko A.J. Kent K.A. Benedict T. Cheng M. Henini
Angle-Resolved Ballistic Phonon Absorption Spectroscopy in the Lowest Landau Level

EP3.2 **J. Riess** D. Bicout T. Duguet P. Magyar
Increase of Quantum Hall Plateau Width by Electron-Phonon Interaction

EP3.3 S. Dickmann

Acoustic Phonon Absorption by a 2D Electron Gas in the Quantised Hall Regime for Odd Filling Factors

EP3.4 V.W. Rampton I. Kennedy C.J. Mellor B. Bracher M. Henini Z.R. Wasilewski P.T. Coleridge
Surface Acoustic Wave Interactions with Composite Fermions and the Acousto-Electric Effect

DEFECTS (Friday 10.50) Chair: Lassmann [R2]

DE1 P. Klemens

Phonon Scattering by Oxygen Vacancies in Ceramics

DE2 A.M. Kosevich A.V. Tutov

Peculiarities of Acoustic Phonon Scattering from a Planar Crystal Defect and Pseudosurface Phonons

DE3 F. Zeller K. Lassmann W. Eisenmenger

Phonon Scattering Related to Oxygen Precipitation in CZ-Silicon

DE4 B. Danilchenko D. Poplavsky S. Roshko

Phonon spectroscopy of D-Band Tails of Shallow Impurities in Ge

CLOSING PLENARY SESSION (Friday 12.15) Chair: Wigmore [R1]

L.J. Challis

Phonons 98 perspective

POSTER PRESENTATIONS

POSTER SESSION A (Monday)

lattice dynamics
phase transitions
phonon interactions
Raman scattering

PosA1 **S.M. Bennington** N. Kitamura M.G. Cain M.H. Lewis M. Arai
The Structure and Dynamics of Hard Carbon Formed From C_{60} Fullerene

PosA2 **A. Bussmann-Holder** K.-H. Michel N. Dalal
Anharmonicity-Induced Cooperative Proton Ordering in H-Bonded Systems

PosA3 **A. Cantarero** A. García-Cristóbal M. Cardona C. Trallero-Giner
Resonant Hyper-Raman Scattering in Semi-Conductors: Excitonic Effects

PosA4 **B. Danilchenko** V. Guzenko T. Paskiewicz M. Bockowski I. Grzegory T. Suski
Propagation of Phonon Pulses in GaN

PosA5 **P. Dashora** J. Dashora G. Gupta
Thermal Conductivity of Semi-Crystalline Isotropic and Oriented Polymers

PosA6 **H.W. de Wijn** E.P.N. Damen A.F.M. Arts
Anharmonic Phonon Decay in TeO_2 : Confirmation of Herring's Theory

PosA7 **S.L. Dong** A.I. Kolesnikov J.C. Li
Neutron Scattering Study and Lattice Dynamical Simulation of H_2O+He Clathrate

PosA8 **V.B. Efimov** L.P. Mezhov-Deglin M.K. Makova
Phonon Scattering in Diamond Films

PosA9 **A. Eifler** J.-D. Hecht G. Lippold V. Riede W. Grill G. Krauß V. Krämer
Combined Infrared and Raman Study of the Optical Phonons of Defect-Chalcopyrite Single Crystals

PosA10 **K. Flachbart** M. Reiffers S. Molokác A. Belling J. Bischof E. Konovalova Y. Paderno
Thermal Conductivity of LaB_6 - The Role of Phonons

PosA11 **H. Fujishiro** M. Ikebe T. Kikuchi T. Fukase
Sound Velocity Anomaly Related to the Charge Ordering in $La_{(1-x)}Sr_xMnO_3$ and $La_{(1-x)}Ca_xMnO_3$

PosA12 **H. Furuta** S. Endo
Raman Scattering Study of $PbZrO_3$ Under High Pressure

PosA13 **T.I. Galkina** A.I. Sharkov A.Yu. Klovov R.A. Khmel'nitskii V.A. Dravin A.A. Gippius
Nonequilibrium Acoustic Phonons in Diamond: Generation, Scattering, Reflection

PosA14 **S.C.A. Gay** H.M. Tütüncü G.P. Srivastava
Surface Phonons on $Si(001)/As(2 \times 1)$

- PosA15 **V.E. Gusakov** A.P. Saiko A. Jezowski
Phonon Scattering in Crystals with Strongly Correlated Bistable Sublattice and Hysteretic Behaviour of Thermal Conductivity in HTSC Compounds
- PosA16 **R. Heid** K.-P. Bohnen
Ab Initio Phonon Spectra from a Supercell Approach
- PosA17 **T. Hirata**
Oxygen Concentration Dependence of Raman Active Phonons with Variable Gruneisen Parameter in $\text{YBa}_2\text{Cu}_3\text{O}_x$
- PosA18 **H. Fujishiro** M. Ikebe
Phonon Scattering Anomaly in the Doped Manganese Oxide, $\text{La}_{(1-x)}\text{Sr}_x\text{MnO}_3$
- PosA19 **V. Keppens** D. Mandrus B.C. Sales B.C. Chakoumakos P. Dai R. Coldea M.B. Maple D.A. Gajewski E.J. Freeman S. Bennington
Local-Mode Thermodynamics of Filled Skutterudite Antimonides
- PosA20 **K. Kirimoto** K. Nobugai T. Miyasato
Ultrasonic Attenuation in Yttria-Stabilized Zirconia
- PosA21 **A.I. Kolesnikov** J.C. Li N.C. Ahmad C.-K. Loong J. Nipko D. Yocum S.F. Parker
Neutron Spectroscopy of High-Density Amorphous Ice
- PosA22 **A.I. Kolesnikov** V.E. Antonov I.O. Bashkin J.C. Li A.P. Moravsky E.G. Ponyatovsky J. Tomkinson
Neutron Spectroscopy of Fullerite Hydrogenated Under High Pressures
- PosA23 **H. Kuroe** H. Seto T. Sekine R. Masuda I. Tsukada K. Uchinokura
Raman Scattering in Mg-doped CuGeO_3
- PosA24 **S. Kramp** N.M. Pyka M. Loewenhaupt M. Braden
Phonons in the Non-Converted State of DyCu_2
- PosA25 **V. López-Richard** G.E. Marques
Polaron Renormalization and Life-Time Broadening Effects on Raman Scattering Under Magnetic Field
- PosA26 **E.V. Manzhelii** E.S. Syркин
Dynamics of the Cubic Lattices with Long-Range Interaction
- PosA27 **I. Morrison** S. Jenkins
Ab-Initio Lattice Dynamics Studies of the Vibrational Spectra of Ice
- PosA28 **K. Motida** K. Suzuki
Evidence of Strong Electron-Phonon Coupling in Double Layered Cuprate Superconductors
- PosA29 **S. Murata** S. Isida M. Suzuki Y. Kobayashi K. Asai K. Kohn
Elastic Anomalies with the Two Spin-State Transitions in LaCoO_3

PosA30 **H. Nakayama** Y. Minagawa S. Yajima K. Ishii
Pseudolattice Vibrations in Smectic Liquid Crystals

PosA31 **D. Nevedrov** V. Hizhnyakov
Nonlinear Quantum Dynamics of Local Modes: Perfect and Disordered Alkali Halide Crystals

PosA32 **N. Noda** K. Shimizu R. Nozaki Y. Shiozaki
Phase Transition and Excess Specific Heat in RS-ARS Mixed Crystals

PosA33 **N. Ogita** Y. Tsunazumi O. Fujita J. Akimitsu M. Udagawa
Raman Scattering Study of $\text{Cu}(\text{Ge}_{1-x}\text{Si}_x)\text{O}_3$

PosA34 **T. Okabe** H. Yamada
Dynamical Properties of One-Dimensional Lennard-Jones Lattice

PosA35 **L.G. Quagliano** D. Orani A. Ricci
Phonon Study of Temperature Evolution of Strain in GaAs/Si(001) and GaAs/Si(111) Heterostructures

PosA36 **I. Saitoh** S. Kojima
Soft Phonon and Bismuth Content in Ferroelectric $\text{SrBi}_2\text{Ta}_2\text{O}_9$

PosA37 **S. Sasaki** K. Kambuchi T. Kume H. Shimizu
High-Pressure Brillouin Study on Hydrogen Chloride up to 8 GPa

PosA38 **I. Savatinova** E. Liarokapis I. Savova
Raman Study of Highly Protonated LiNbO_3 Thin Film Waveguides

PosA39 **A. Sergeev** C. Preis J. Keller
Optical Phonon Attenuation in d-Wave Superconductors

PosA40 **S.A. Smirnov** V.A. Konstantinov V.G. Manzhelii V.P. Revyakin
Phonon Scattering in Orientationally Disordered Phase of Solid Methane

PosA41 **A. Smontara** A. Bilusic E. Tutis H. Berger F. Lévy
Role of the Nb Impurities on the Thermal Conductivity $(\text{Ta}_{1-x}\text{Nb}_x\text{Se}_4)_2\text{I}$ Alloys in the Vicinity of the Peierls Transition

PosA42 **A. Smontara** A. Bilusic H. Berger
Minimum Thermal Conductivity of the $\text{Nb}_4\text{Te}_{17}\text{I}_4$

PosA43 **A.V. Sologubenko** D.F. Brewer G.E. Ekosipididis A.L. Thomson
Influence of Zn Substitution on the Thermal Conductivity of Pr_2CuO_4

PosA44 **A.V. Sologubenko**
Lower Limit of Phonon Mean Free Path in the Debye Model of Thermal Conductivity

PosA45 **S. Takasaka** Y. Tsujimi T. Yagi
Anisotropy of Thermal Relaxation Mode in KHCO_3 Studied by Impulsive Stimulated Thermal Scattering

- PosA46 **T. Takase** Y. Sun T. Miyasato
SAW Attenuation in C_{60} Thin Films at Low Temperatures
- PosA47 **A. Taranov** S.N. Ivanov E.P. Smirnova E.N. Khazanov
Transport of Non-Equilibrium Phonons in Highly Disordered Ferroelectrics Ceramics
- PosA48 **E.V. Tartakovskaya** B.A. Ivanov
Spin-Phonon Interaction in Thin Magnetic Films
- PosA49 **M. Udagawa** S. Nimori H. Hata N. Ogita F. Nakamura S. Sakita N. Kigugawa T. Fujita
Phonon Raman Study in $La_{1.475}Nd_{0.4}Sr_{0.125}CuO_4$
- PosA50 **J. Watanabe** M. Kasahara T. Yagi
Phase Transition of Zero-Dimensional Hydrogen-Bonded Crystals Studied by Raman Scattering
- PosA51 **F. Widulle** A. Göbel T. Ruf A. Debernardi R. Lauck M. Cardona
The Phonon Dispersion of Wurtzite CdSe
- PosA52 **N. Wiele** H. Franz O. Leupold W. Petry
Anharmonicity of $Fe_{72}Pt_{28}$ Measured with Elastic and Inelastic Nuclear Scattering of Synchrotron Radiation
- PosA53 **C.-C. Wu** C.-J. Lin
Effect of Nonparabolicity on Free-Carrier Absorption in n-Type InSb Films for Polar Optical Phonon Scattering
- PosA54 **S. Yoshioka** Y. Tsujimi T. Yagi
High-Frequency Dielectric Constant of KDP Obtained by Polariton Dispersion
- PosA55 **M. Zoli**
Phonon Dispersion Effects on the Motion of Small Polarons in Molecular Solids

POSTER SESSION B (Tuesday)

coherent and acoustic phonons
electron-phonon interaction
nanostructures
new techniques

PosB1 **H. Al Jawhari** A.G. Kozorezov J.K. Wigmore
Observation of Energy Loss by a Hot Two-Dimensional Electron Gas into Coupled Plasmon-Optic Phonon Modes

PosB2 **S.M. Badalyan** M. Aghasyan
Electron-Phonon Relaxation in Quantum Wires in a Quantizing Magnetic Field

PosB3 **R. Bauer** A. Schmid P. Pavone D. Strauch
Ab Initio Lattice Dynamics, Group Velocities and Electron-Phonon Coupling in Metals

PosB4 **C.R. Bennett** K. Güven B. Tanatar
Confined Optical Phonon Effects on the Band Gap Renormalisation in Quantum Wire Structures

PosB5 **M.P. Blencowe** A.Y. Shik
Phonoconductance of Quantum Wires

PosB6 **P. Bury** I. Jamnický V.W. Rampton
Acoustic Spectroscopy of Deep Centres in GaAs/AlGaAs Heterostructures

PosB7 **G. Chen**
Phonon Wave and Particle Heat Conduction in Superlattices

PosB8 **T.F. Crimmins** A.A. Maznev K.A. Nelson
Transient Grating Detection of Picosecond Acoustic Pulses

PosB9 **A.J. Cross** A.J. Kent P. Hawker D. Lehmann Cz. Jasiukiewicz M. Henini
Phonon Emission by Warm Electrons in GaAs Quantum Wells: The Effect of Well Width on the Acoustic-Optic Crossover

PosB10 **M. Dutta** D. Alexson L. Bergman K.W. Kim S. Komirenko R.J. Newanich B.C. Lee M.A. Strosio S. Yu
Confined Phonons and Phonon-Mode Properties of III-V Nitrides with Wurtzite Crystal Structure

PosB11 **N.I. Grigorchuk**
Account for the Optical Phonon Dispersion in Exciton Attenuation

PosB12 **T. Gwizdalla**
Phonons in Self-Consistent Metallic SLAB

PosB13 **P. Hawker** A.J. Kent T.S. Cheng C.T. Foxon
Heat Pulse Studies of the Energy Relaxation Rate of Hot Electrons in N-Type GaN Epilayers

- PosB14 **P. Hawker** A.J. Kent M. Henini
Measuring the Size of Buried Quantum Dots Using Phonons
- PosB15 **P. Kinsler** R.W. Kelsall P. Harrison
Interface and Confined Phonons in Stepped Quantum Wells
- PosB16 **S. Knauth** A. Boehm W. Grill
Observation of Thermally Activated Quasiparticle Interaction by Ballistic Electron Transport and Electron Focusing
- PosB17 **Z. Kojro** W. Grill T. Gudra T.J. Kim M. Schmachtl M. Schubert
Confocal Scanning Acoustic Microscopy in Air at Normal Conditions at MHz-Frequencies Close to the Phonon-Cutoff-Regime
- PosB18 **S.M. Komirenko** K.W. Kim V.A. Kochelap M. Dutta M.A. Strosio
Renormalization of Acoustic Phonon Spectra and Rudiments of Peierls Transition in Free-Standing Quantum Wires
- PosB19 **Y.A. Kosevich**
Generalized Interface Acoustic Waves Piezoelectrically Coupled to Embedded Two-Dimensional Electron System
- PosB20 **A.V. Kulikowski** M. Giltrow A.G. Kozorezov M. Sahraoui-Tahar J.K. Wigmore J.H. Davies C.R. Stanley B. Vogel C.D.W. Wilkinson
Energy Loss of Hot Electrons in Double Barrier Resonant Tunnelling Structures
- PosB21 **S. Lamari**
Electron-Phonon Interaction of the 2DEG in an InSb MOSFET
- PosB22 **K. Lambert G.P. Srivastava**
Confinement of Optical Phonon Modes in Thin $(\text{GaAs})_n(\text{AlAs})_n$
- PosB23 **H.J. Maris** W.S. Capinski T. Ruf M. Cardona K. Ploog D.S. Katzer
Thermal Conductivity of Short Period $(\text{GaAs})_n/(\text{AlAs})_n$ Superlattices
- PosB24 **A. Mascarenhas** H.M. Cheong F. Alsina J.M. Olson
Vibrational Properties of Spontaneously Ordered GaInP_2
- PosB25 **A.A. Maznev** T.F. Crimmins K.A. Nelson
Heterodyne Transient Grating Detection of Acoustic and Optic Phonons
- PosB26 **S. Mizuno S.I. Tamura**
Surface Vibrational Modes and Reflection Times of Phonons in a Finite-Size Superlattice
- PosB27 **S. Nakashima** M. Hase K. Mizoguchi H. Harima K. Sakai S. Cho A. DiVenere J.B. Ketterson
Coherent Phonons in Mixed Semimetals and Semimetal Superlattices
- PosB28 **H. Okabe** K. Kuboyama K. Hara S. Kai
Anomalous Velocity Change of Surface Wave Near the Gelation Point

- PosB29 **Y.M. Olikh** V.F. Machulin R.K. Savkina
Acoustodynamic Methods of Investigation of Semiconductors Defects
- PosB30 **F.F. Ouali** H.R. Francis H.C. Rhodes
Acoustic Phonon Scattering in Two Dimensional Carriers in GaAs
- PosB31 **F.F. Ouali** S.A. Cavill A.V. Akimov L.J. Challis A.J. Kent M. Henini
Stimulated Phonon Emission in Superlattices
- PosB32 **S. Ozawa** R. Komuro Y. Hiki
Computer Experiment on Surface Waves in Non-Linear Crystal
- PosB33 **T. Paszkiewicz** A. Duda
Second and Third-Order Elastic Constants for Effective Isotropic Media for all Laue Groups
- PosB34 **N. Perrin**
Confined Acoustic Phonons and Electron Transport in Quantum Wires: A Numerical Analysis of the Characteristic Parameters
- PosB35 **D. Poplavsky** B. Danilchenko H. Kostial
Destruction of Weak Localization by Phonon Flux in δ -doped GaAs
- PosB36 **N.M. Pyka** M. Loewenhaupt S. Kramp
Panda: A Novel Triple-Axis Spectrometer Under Construction at the High Flux Reactor FRM-II of Munich
- PosB37 **V.W. Rampton** I. Kennedy C.J. Mellor B. Bracher M. Henini Z.R. Wasilewski P.T. Coleridge
SAW Attenuation by the Localized States of a 2D Carrier System in a Magnetic Field
- PosB38 **M. Reiffers** E. Kacmarčíková T. Salonoová
Point-Contact Spectroscopy of the Electron-Phonon Interaction in $RENi_5$ (RE -Rare Earths)
- PosB39 **R. Röhlberger** A. Bernhard E.E. Alp E. Burkel A.I. Chumakov J. Metge R. Rüffer W. Sturhahn T.S. Toellner
Vibrational Density of States of Thin Films Measured by Inelastic Scattering of Synchrotron Radiation
- PosB40 **E. Rokuta** A. Itoh T. Tanaka K. Yamashita S. Otani C. Oshima
Phonon Measurement on Graphite and Hexagonal Boron Nitride Films on Ni(755)
- PosB41 **E. Rokuta** C. Oshima
Phonons in Hexagonal Boron Nitride Films on Transition Metal Surfaces and Analysis of Dispersion Curves Based on Lattice Dynamics
- PosB42 **S.M. Sadeghi** J. Meyer
Exciton-Phonon Scattering Effects on the Coherent Control of Exciton Decay
- PosB43 **M. Sanada** T. Yagi
High-Resolution Brillouin Scattering Observation of Ferroelastic Soft Phonon, Using Spherical Fabry-Perot Interferometer and Computer Controlled Spectra Accumulation

PosB44 **A.V. Scherbakov** A.V. Akimov V.P. Kochereshko

Detection of Nonequilibrium Phonons by the Exciton Luminescence in CdTe/CdMnTe Quantum Wells

PosB45 **P.C. Sharma**

Proposed Model of Mixed Electron (Hole)-Phonon Scattering in the Intermediate Concentration Region

PosB46 **U. Straube** J. Beige

Measuring System for the Determination of Nonlinear Elastic and Electromechanical Properties in Solids

PosB47 **D.N. Talwar**

Localized Excitations in Diluted Magnetic $\text{Cd}_{1-x}\text{Mn}_x\text{Te}/\text{Cd}_{1-y}\text{Mn}_y\text{Te}$, $\text{ZnSe}/\text{Zn}_{1-y}\text{Mn}_y\text{Se}$ Semiconductor Superlattices

PosB48 **S.I. Tamura** T. Aono Y. Tanaka

Surface Phonons in One-Dimensional Periodic Superlattices

PosB49 **Y. Tanaka** S.I. Tamura

Two-Dimensional Phononic Crystals: Surface Acoustic Waves

PosB50 **A.V. Tkach**

Magnetoacoustic Determination of Deformation Potential

PosB51 **F. Tsuruoka**

Phonon Hole Burning at Low Temperature

PosB52 **L. Valente**

Non-Linear Excitations in One-Dimensional Electron-Phonon Systems

PosB53 **M. Wagner** A. Sauerzapf

Quantum Decay of Self-Localized Modes in Anharmonic Systems

PosB54 **A. Yoshihara**

Elastic Properties of TiN/ZrN Superlattices: A Brillouin Scattering Study

PosB55 **N.A. Zakhleniuk** C.R. Bennett B.K. Ridley M. Babiker

Interaction of Non-Equilibrium Electrons with Phonons in Bulk GaN and GaN/AlGaN Quantum Wells

POSTER SESSION C (Thursday)

disordered systems

glasses

defects

interface and quantum fluids

particle and photon detectors

PosC1 **S. Abens** A. Gladun M. Jäckel D. Lipp S. Sahling

The Influence of Hydrogen Charging on the Glassy Low Temperature Properties of a Polycrystalline NbTi-Alloy

PosC2 **V.A. Andrianov** P.N. Dmitriev V.P. Koshelets M.G. Kozin I.L. Romashkina S.A. Sergeev V.S. Shpinel

Back Tunneling and Phonon Exchange Effects in Superconducting Tunnel Junction X-Ray Detectors

PosC3 **M.M. Shukla** J.R. Campanha

An Ad Hoc Dynamical Model Study of Lattice Dynamics of Metallic Glass $\text{Mg}_{70}\text{Zn}_{30}$

PosC4 **J. Classen** I. Rohr C. Enss S. Hunklinger C. Laermans

Low Frequency Acoustic Properties of Neutron-Irradiated Quartz

PosC5 **J. Classen** M. Heitz J. Meier S. Hunklinger

Elastic Properties of Neon and Argon Films

PosC6 **M. Coeck** C. Laermans E. Peeters

Ultrasonic Velocity Changes in Bulk Neutron-Disordered Silicon

PosC7 **Th. Eggert** G. Köbernig M. Jäckel A. Gladun

Frequency Dependent Dielectric Investigations of Polycarbonate from 100mK to 300K at Hydrostatic Pressures

PosC8 **G. Fagas** A.G. Kozorezov C.J. Lambert J.K. Wigmore

Lattice Dynamical Calculation of Phonon Scattering at a Disordered Interface

PosC9 **V. Fleurov** Y. Ben-Ezra

Hierarchical Structure of the Potential Landscape in Glass

PosC10 **A.M. Gulian**

Microrefrigeration and the Phonon Deficit Effect

PosC11 **K. Hara** A. Nakamura N. Hiramatsu A. Matsumoto

Evolution of Low-Frequency Raman Scattering Spectrum, Thermal and Elastic Properties of Dehydrated Polyacrylamide Gel with Increasing Temperature

PosC12 **M.J. Harris** M.T. Dove J.M. Parker

On the Wavevector Dependence of the Boson Peak in Silicate Glasses and Crystals

PosC13 **M.R. Hauser** R. Gaitskell J. Short J.P. Wolfe

Imaging Phonons in Superconductors

PosC14 **Y. Hiki** H. Takahashi Y. Kogure
Relaxation of Thermal Properties Observed in Glasses

PosC15 **H. Ikari**
Nonequilibrium Phonon Propagation in Vitreous Silica

PosC16 **Y. Inamura** M. Arai O. Yamamuro T. Matsuo N. Kitamura T. Otomo S.M. Bennington
Peculiar Suppression of the Specific Heat and Boson Peak Intensity of Densified SiO₂ Glass

PosC17 **H. Kawashima** K. Shirahama K. Kono
Fluctuation Properties of Third Sound Transmission in Random Media

PosC18 **V.P. Kisel**
Micromechanisms of Dislocation-Phonon Interaction in Solids at Low and High Temperatures

PosC19 **N. Kitamura** I. Matsubara R. Funahashi H. Ohta H. Nojiri S. Mitsudo T. Sakon M. Motokawa
Spin-Lattice Relaxation of Paramagnetic Spin in Phosphate Glass Under High Magnetic Field

PosC20 **S. Kojima** M. Kodama
Boson Peak in Alkali Borate Glass

PosC21 **H. Kobayashi** T. Kosugi Y. Kogure
Internal Friction and Relaxation Mechanisms of Ge- and F-Doped SiO₂ Glasses

PosC22 **A.M. Kosevich** E.S. Syrkin A.V. Tutov
Acoustic Waves Localized at a Planar Defect in Crystal

PosC23 **T. Kosugi** H. Kobayashi Y. Kogure
Internal Friction of TiO₂-SiO₂ Glass

PosC24 **C. Laermans** D.A. Parshin
Tunneling - Thermal Activation Crossover in Neutron Irradiated Quartz

PosC25 **C. Laermans** V. Keppens
Unexpected Behaviour of the Tunneling States-Phonon Coupling in Neutron-Irradiated Quartz as a Function of Dose.

PosC26 **D.V. Lioubtchenko** T.A. Briantseva T.J. Bullough
SAW Diagnostics of GaAs Surface Structure

PosC27 **V.N. Lisin** A.M. Shegeda B.M. Khabibullin V.A. Zuikov V.V. Samartsev
Heat Pulse Ballistic Phonons Interaction with Optical Coherent Excited Impurity System

PosC28 **F. Maier** K. Lassmann
Phonon Scattering and IR-Spectra of Oxygen-Related Defects in Gallium Arsenide - Aspects of Quantative Phonon Spectroscopy

PosC29 **G. Matsui** S. Kojima
Brillouin Scattering Study of Acoustic Phonons in Supercooled Liquid of Lower Alcohols

- PosC30 **M. Matsukawa** M. Yoshizawa K. Noto Y. Yokoyama A. Inoue
Anisotropic thermal transport of 2D quasicrystals of decagonal Al-Ni-Co systems
- PosC31 **V.G. Mazurenko** V.I. Sokolov A.N. Kislov
Localised Vibrations Induced by 3d Charged Impurities in II-VI Semiconductors - A Novel Approach
- PosC32 **A. Nakamura** K. Hara N. Hiramatsu A. Matsumoto
Low Frequency Raman Peak and Elastic Anomaly of Dehydrated Heat-Treated Egg-White Gel
- PosC33 **M. Nakamura** O. Matsuda Y. Wang K. Murase
A Study of Network Dimensionality in Chalcogenide Glass by Low Frequency Raman Scattering
- PosC34 **V.N. Novikov**
Anharmonicity of Vibrations and Quasielastic Scattering in Glasses
- PosC35 **T. Ozaki** T. Ogasawara T. Kosugi T. Kamada
Dielectric Dispersion of SiO₂ Glass at Low Temperatures
- PosC36 **T. Paszkiewicz** M. Pruchnik
Comparison of Ballistic Propagation of Molecular and Phonon Beams
- PosC37 **M. Pruchnik** M.P. Blencowe T. Paszkiewicz
Computer Experiments on Anomalous Diffusive Propagation of Phonon Beams in Cubic Elastic Media Containing Point Mass Defects
- PosC38 **R. Saburova** G. Busiello
Tunneling Electric Dipole Defects in Insulating Glass: Soft Mode and Spin-Glass Like Transition
- PosC39 **W. Schirmacher** G. Diezemann C. Ganter
Harmonic Vibrational Excitations in Disordered Solids and The "Boson Peak"
- PosC40 **R. Schmidt** Th. Franke P. Häussler
Thermal Conductivity of Cu_xSn_{100-x} Films at Low Temperatures
- PosC41 **A. Sergeev**
Inelastic Electron-Boundary Scattering in Thin Films
- PosC42 **K. Shibata** Y. Yamazaki K. Matsuzaki H. Takakura K. Suzuki
Low Energy Vibrational Excitations in Metallic Glass (Mo_{0.6}Ru_{0.4})₈₀B₂₀ and its Anomalies Induced by Superconductivity
- PosC43 **W. Sturhahn** R. Röhlberger T.S. Toellner E.E. Alp
Localized Vibrational States in Amorphous Tb_{1-x}Fe_x Films and Phonon - Fracton Crossover in Amorphous Fe₉-Zr
- PosC44 **M. Suzuki** M. Hieda H. Yano N. Wada K. Torii
Mechanical Responses of Helium Film Adsorbed on Two-Dimensional Mesoporous Hectorite
- PosC45 **Y. Takagi** T. Yano M. Mikami S. Kojima
Temperature Dependence of Depolarized Spectra in n-Propanol

PosC46 **T. Terao** T. Nakayama
Vibrational Characteristics of Cluster-Cluster Aggregations

PosC47 **Y. Tsujimi** M. Kobayashi T. Yagi
Frequency and Time-Resolved Spectroscopic Study of Liquid-Glass Transition in D-Sorbitol

PosC48 **D. Van Vechten** K.S. Wood G.G. Fritz J.S. Horwitz R.H. Stroud R.C.Y. Auyeung J. Kim
S.B. Qadri A.L. Gyulamiryan V.R. Nikogosyan A.M. Gulian
Studies of Anisotropic Thermoelectricity in Layered Oxide Materials and Time Resolved Phonon Kinetics

PosC49 **Y. Wang** M. Nakamura O. Matsuda K. Murase
Rigidity Percolation and Structure of Ge-Se System

PosC50 **I.A. Weinstein** A.F. Zatsepin Yu.V. Shchapova
The Phonon Assisted Shift of the Energy Levels of Localized Electron States in Statically Disordered Solids

PosC51 **O.B. Wright**
Thermodynamics of Irreversible Heat Generation in Glasses at Low Temperatures

PosC52 **T.-M. Wu** W.-J. Ma
Voronoi Analysis on Microstructures of Localized Instantaneous Normal Modes in Liquid Na

PosC53 **H. Yamada**
Dynamical Delocalization of One-Dimensional Disordered System with Lattice Vibration

PosC54 **P. Zielinski** Z. Lodziana
Anharmonic Effects of Phonon Scattering from Crystal Surfaces

PosC55 **N.V. Zuev** V.V. Bolko N.E. Dyumin V.N. Grigor'ev
Phonon-Assisted Diffusion of Vacancies in Solid Helium

ABSTRACTS

PL1 (09.30)

Towards Yoccalorimetry, Phonon Counting,
and Quantum Phonon Optics in Nanostructures.

Michael L. Roukes*
Condensed Matter Physics
Caltech 114-36
Pasadena, CA 91125 USA

Thermal transport and energy equilibration in nanostructures are intriguing, but still largely unexplored, areas of mesoscopic physics. In part, this stems from the fact that the nanofabrication methods and measurement techniques that might permit such investigations have not been available. We have recently developed surface nanomachining techniques enabling the definition of miniature, freely-suspended, monocrystalline semiconductor devices with separately-patterned thermal transducers and (insulating) thermal conductors.¹ I will describe our experiments with these devices, which now permit us to carry out direct thermal conductance measurements on nanostructures. Additional recent motivation for these efforts comes from theoretical work carried out in our group² and elsewhere,³ which establishes analogies between electrical and thermal conductance quantization in nanostructures at low temperatures.

Among our current experimental efforts, we are now attempting to employ suspended nanodevices for calorimetry at millikelvin temperatures. I will describe our novel dc SQUID-based measurement approach, designed to provide minimal back action on these ultralow heat capacity structures. It appears that this route should offer—ultimately—energy resolution at the level of *individual* phonons. This sensitivity will allow access to an exotic regime where single-phonon phenomena, with analogs in classical and quantum optics, should become manifested. I will describe intriguing possibilities such as observing phonon shot noise, phonon bunching, anticorrelated electron-phonon relaxation, and the phonon-by-phonon energy decay of a quasi-isolated, *nm*-scale thermal reservoir.

*In collaboration with Dan E. Angelescu, Michael C. Cross, Warren C.-W. Fon, Erik A. Henriksen, Keith C. Schwab, Thomas S. Tighe, and John M. Worlock.

¹ T. S. Tighe, J. M. Worlock, and M. L. Roukes, *Appl. Phys. Lett.* **70**, 2687 (1997).

² D. E. Angelescu, M. C. Cross and M. L. Roukes, *Superlattices and Microstructures*, (Special Issue in Honor of Rolf Landauer on the Occasion of his 70th Birthday) **23**, 673-689 (1998).

³ Luis G. C. Rego and George Kirczenow, *to be published*.

PL2 (10.10)

PHONON SQUEEZED STATES:
QUANTUM NOISE REDUCTION IN SOLIDS

Franco Nori

Physics Department, University of Michigan, Ann Arbor, MI 48109-1120

This talk presents an introduction and an overview of the new subject of squeezed phonons—which allow the reduction of quantum noise in solids. We will discuss quantum fluctuation properties of a crystal lattice and, in particular, phonon squeezed states [1-3]. Specifically, we will review several different proposals to generate phonon quadrature squeezed states, including second-order Raman scattering [1,2], a phonon parametric down-conversion process [1], and a polariton mechanism [1,3]. The first two can generate two-mode squeezed states in the relevant acoustic phonon modes of opposite wavevectors, while the last one can generate squeezing in the optical phonon modes involved. Here we focus on both continuous-wave and impulsive second-order Raman scattering mechanisms. The later approach was used to experimentally suppress (by one part in a million) noise in the atomic displacements. Moreover, we have calculated changes in macroscopic properties, such as the dielectric constant, due to two-mode phonon squeezed states, and also pointed out possible approaches for detection of phonon squeezing. Additional information, including preprints and further references, is available in [4].

- [1] X. Hu and F. Nori, *Phys. Rev. Lett.* **76**, 2294 (1996); *Bull. Am. Phys. Soc.* **39**, 466 (1994); **41**, 657 (1996); X. Hu, Ph.D. Thesis, Univ. of Michigan (1996).
- [2] X. Hu and F. Nori, *Phys. Rev. Lett.* **79**, 4605 (1997).
- [3] X. Hu and F. Nori, *Phys. Rev. B* **53**, 2419 (1996).
- [4] <http://www-personal.engin.umich.edu/~nori/squeezed.html>

NS1.1 (11.20)

QUANTUM ENERGY FLOW IN MESOSCOPIC DIELECTRIC STRUCTURES

M. P. Blencowe

The Blackett Laboratory, Imperial College, London SW7 2BZ, UK.

We investigate the phononic energy transport properties of mesoscopic, suspended dielectric wires. The mean of the energy current is determined and the Landauer formula for the thermal conductance extracted. It is found that each phonon subband contributes to the reduced conductance κ/T the *universal* quantum $\pi k_B^2/6\hbar \approx 9.465 \times 10^{-13} \text{ WK}^{-2}$. Conductance steps cannot be resolved, however, because of the broadness of the Bose-Einstein distribution as compared with the subband edge separation. We then determine the variance of the energy current in the presence of a steady state current flow. A Johnson-Nyquist equilibrium noise formula is recovered in the special case where the mean current flow is zero. In the final part, some initial results are presented concerning the nature of the temperature fluctuations of a mesoscopic electron gas thermometer due to the absorption and emission of wire phonons. The remarkable possibility to detect *single* phonons through the temperature fluctuations is a consequence of the very small volume and hence heat capacity of the electron gas. From the magnitude of a given temperature fluctuation the energy of the absorbed or emitted phonon is known and, thus, there is the possibility for high resolution phonon spectroscopy. We find that the fluctuations give direct information concerning the energy dependence of the phonon scattering matrix for the wire.

NS1.2 (11.40)

TAILORING OF OPTICAL PHONON MODES IN NANOSCALE SEMICONDUCTOR STRUCTURES: ROLE OF INTERFACE-OPTICAL- PHONONS IN QUANTUM-WELL LASERS

Gregory Belenky (a), Mitra Dutta (b), Vera B. Gorfinkel (a), George I. Haddad (c), G. J. Iafrate (d), K. W. Kim (e), Mikhail Kisin (a), Serge Luryi (a), Michael A. Strosio (b), J. P. Sun (c), H. B. Teng (c), SeGi Yu (c)

(b) U.S. Army Research Office, PO Box 12211, RTP, NC 27709 USA

(c) ECE Dept., North Carolina State U., Raleigh, NC 27695 USA

(e) EECS Dept., U. of Michigan, Ann Arbor, MI 48109 USA

(a) EE Dept., SUNY Stony Brook, Stony Brook, NY 11794 USA

(d) EE Dept., University of Notre Dame, Notre Dame, IN 46556 USA

This paper discusses the concept of enhancing semiconductor laser performance through tailoring of scattering rates of confined polar-optical phonons. Studies of optically pumped intersubband scattering in coupled quantum-well lasers [1] have demonstrated that interface-phonon-assisted transitions are important in such structures; furthermore, Strosio [2] has derived simple analytical expressions that indicate the importance of interface-phonon scattering in quantum-well lasers. These calculations reveal that the interface-phonon-assisted transitions are dominant for small quantum well dimensions of approximately 40 Angstroms; such dimensions are typical of novel lasers including both the unipolar quantum cascade laser and the tunneling injection laser. In recent numerical calculations, of Kisin et al. and Teng et al. [3] have confirmed these effects and have extended them to indicate how confined and interface phonons also affect critical laser properties such as optical gain. The application of confined phonon effects to intersubband lasers is perhaps the most important application of confined-phonon physics to the present time.

1. Jin Wang, J.-P. Leburton, F. H. Julien, and A. Sa'ar, "Design and Performance Optimization of Optically-pumped Mid-Infrared Intersubband Semiconductor Lasers," *IEEE Photonics Technology Letters*, Vol 8, 1001-1003 (1996).
2. Michael A. Strosio, "Interface-phonon-assisted Transitions in Quantum Well Lasers," *Journal of Applied Physics*, Vol 80, 6864-6867 (1996).
3. Mikhail V. Kisin, Vera B. Gorfinkel, Michael A. Strosio, Gregory Belenky, and Serge Luryi, "Influence of Complex Phonon Spectra on Intersubband Optical Gain," *J. Appl. Phys.*, 82 2031-2038 (1997); Mikhail V. Kisin, Michael A. Strosio, Gregory Belenky, Vera B. Gorfinkel, and Serge Luryi, "Effects of Interface Phonon Scattering in Three-Interface Heterostructures," to be published (1998); H. B. Teng, J. P. Sun, G. I. Haddad, Michael A. Strosio, SeGi Yu, and K. W. Kim, "Phonon Assisted Intersubband Transitions in Step Quantum Well Structures," to be published (1998).

THERMAL RELAXATION OF COHERENT CHARGE OSCILLATION IN COUPLED-QUANTUM WELLS

Norihiko Nishiguchi^{*} and Martin N. Wybourne

Department of Physics and Astronomy, 6127 Wilder Laboratory, Dartmouth College, Hanover, NH 03755-3528, U.S.A.

Coherent oscillation of photoexcited electron wave packet in coupled-quantum-well structures has been observed in recent experiments of GaAs/AlGaAs double quantum wells.^[1,2] The wave packet is a superpositional state of two or more lowest conduction subband states, tunnelling through the potential barrier and oscillating between the potential wells. A frequency of the oscillation, corresponding to the energy difference between the conduction subbands, is in terahertz region which overlaps phonon frequency region. Hence the coherent charge oscillation is expected to resonantly interact with phonons with the same frequency. If this is the case, the coherent charge oscillation may decay by emitting coherent phonons with the same frequency as the coherent charge oscillation or will be amplified by absorbing phonons.

In this work, we consider the attenuation of the coherent charge oscillation in coupled-quantum wells of GaAs/AlGaAs by acoustic phonon emission as well as by absorption via both the deformation and piezoelectric potentials, using the time-dependent perturbation theory.

Quantum mechanically, the coherent charge oscillation decays accordingly to the de-
 vation of the wave packet from the initial state with time, which is due to both inter-
 and intrasubband transitions between the constituent electron states. We examine the
 transition probabilities by means of Fermi's golden rule, and find that the intrasubband
 piezoelectric scattering plays a dominant role in the relaxation of the wave packet. The
 reason is twofold: first, due to the double quantum well structures, the matrix elements of
 intersubband transitions for both the deformation potential and piezoelectric coupling are
 of much smaller magnitude than those for intrasubband transitions at small wavenumber.
 Second, the piezoelectric coupling is stronger than the deformation potential coupling for
 low frequency phonons. The resonant interaction between the coherent charge oscillation
 and phonons of intersubband energy is shown not to be important in phase relaxation of
 coherent charge oscillations in coupled-quantum wells. Rather, intrasubband transitions
 are shown to dominate dephasing of the wave packet. The predicted wave packet relaxation
 time will be compared with that measured.^[1,2]

References

- [1] H.G.Roskos, M.C.Nuss, J.Shah, K. Leo, D.A.B. Miller, A.M. Fox, S. Schmitt-Rink,
 and K. Köhler, Phys. Rev. Letters **68**, 2216 (1992).
- [2] P.C.M. Planken, I. Bremner, M.C.Nuss, M.S.C. Luo, and S.L.Chuang, Phys. Rev. B **48**,
 4903 (1993).

^{*}Permanent address: Department of Applied Physics, Hokkaido University, Sapporo 060-
 8628, Japan

THE HYBRID MODEL FOR OPTICAL PHONON CONFINEMENT IN AlN/GaN QUANTUM WELLS

C.R. Bennett, B. K. Ridley, N. A. Zakhleniuk, and M.Babiker

Department of Physics, University of Essex, Colchester, CO4 3SQ, England

Since the experimental confirmation of optical phonon confinement in AlAs/GaAs quantum wells by Raman scattering about a decade ago, many theoretical continuum models have been suggested. Previously, the dielectric continuum (DC) model, which is distinguished by the use of only electrostatic boundary conditions and which predicts two separate type of polar optical modes, namely confined and interface modes, was the main model employed. This model, however, fails to explain the symmetries of the various optical modes obtained by Raman scattering. Nevertheless, the DC model provides a shortcut for calculation of confinement effects in electron-phonon scattering in quantum-well structures.

More recently, it has been realised that in order to account for the Raman symmetries some mechanical boundary conditions involving lattice displacement must be included. This has led to the hybridisation of the confined and interface phonons in the system and to the prediction of the correct symmetries at small wavevectors. The hybrid model has also given rise to results similar to those due to the DC model for electron-phonon scattering. The primary feature of the hybrid model is that it incorporates spatial dispersion of the optical vibrations and in the limit of no dispersion the DC model is retrieved at the range of wavevectors appropriate for electron scattering in quantum wells.

The hybrid theory has only been applied to the AlAs/GaAs system where the spectra of the optical modes are very different for the two materials and they do not overlap. This is not the case in the AlN/GaN system where the *resistral* bands overlap and it is possible for one mode to travel across the whole structure, albeit with a change in wavevector across the interfaces. Here we present an extended version of the hybrid model for this system, which requires the use of an additional set of mechanical boundary conditions: the continuity of stress associated with optical vibrations. The optical modes satisfying these continuity conditions are obtained and used in the evaluation of the electron-phonon scattering in GaN-based quantum wells. A comparison with the results emerging from the DC model is made. Finally, a sum-rule is put forward which confirms the expectation that the DC model will always provide a good approximation of the total electron-phonon scattering rate which would otherwise emerge from more comprehensive models, such as the hybrid model.

LD1.1 (11.20)

FIRST-PRINCIPLES STUDY OF
LATTICE-DYNAMICAL AND ELASTIC TRENDS IN
TETRAHEDRAL SEMICONDUCTORS

Thomas Piel, Pasquale Pavone, Ulrike Engel, and Dieter Strauch

*Institut für Theoretische Physik, Universität Regensburg, D-93040 Regensburg,
Germany*

Although the structural, elastic, and lattice-dynamical properties of prototype group-IV and III-V semiconductors such as Si or GaAs have been extensively studied both from the theoretical and the experimental point of view, a comprehensive theoretical analysis of the general trends in the vibrational and elastic properties for this class of materials is still missing. In particular, the comparison of the properties of different tetrahedral semiconductors becomes fundamental when dealing with the study and characterization of complex semiconductor systems with mixed composition (e.g., superlattices, semiconductor alloys) where, from the experimental side, tools such as Raman spectroscopy have been shown to be very efficient. Within this context, the investigation of the growth properties of new materials cannot leave apart the analysis of the elastic behavior of the constituents, in connection with the response to hydrostatic or uniaxial stresses. From the theoretical point of view, moreover, first-principles methods based on density-functional (DFT) and density-functional perturbation (DFPT) theory are now allowing the determination of the elastic and vibrational properties of solids with an unprecedented degree of accuracy.

In this work, we present a complete first-principles study of trends in the lattice dynamics of tetrahedral semiconductors in the zincblende or diamond structure, using the plane-wave pseudopotential method within DFPT. The interatomic force constants of the different materials have been obtained and analyzed, especially concerning the scaling properties with the volume. As a result, we find that the short-range parts of the force constants have a well defined quadratic dependence on the lattice parameter for the considered compounds. Furthermore, the effect of long-range forces on the lattice dynamics of these materials is discussed in terms of the Born effective charges. As a general trend, we find that the value of the effective charge of a given group-III atom decreases with the mass of the considered group-V atom. This trend has an extreme case for the heaviest Boron compounds where the signs of the effective charge of the two constituents are exchanged.

For all the considered materials, we present vibrational properties such as phonon dispersion curves, eigenvector phases, and internal strain parameters. Concerning the phonon dispersion curves, we analyze in particular the ratio between the longitudinal and transversal optical frequencies at the X point and find a dependence on the ratio of the atomic masses which is discussed in the framework of a linear-chain model. Moreover, we discuss the flatness at the border of the Brillouin zone of the transverse acoustic branches which is typical for tetrahedral semiconductors except for those containing first-row elements.

Finally, we present results of the calculation of the linear and nonlinear elastic constants for the studied class of materials, extracting trends in dependence of the reduced mass and the density of the various semiconductors.

LD1.2 (11.50)

SURFACE DYNAMICS OF AISb(110) AND GaP(110)

H. M. Tütüncü^{1,2} and G.P. Srivastava¹

¹ *Department of Physics, University of Exeter, Stocker Road, Exeter EX4 4QL, UK*

² *Sakarya Üniversitesi, Fen-Edebiyat Fakültesi, Fizik Bölümü, Adapazarı, Turkey.*

(March 10, 1998)

Abstract

We have investigated the surface dynamics of the (110) surface of AISb and GaP by employing the adiabatic bond-charge model based on the surface atomic geometry obtained from *ab initio* pseudopotential calculations [1]. The results for both surfaces are in very good overall agreement with a recent high-resolution electron-energy-loss spectroscopy (HREELS) experiment [2] and an *ab initio* calculation [3]. We present a detailed analysis of polarization characteristics of important surface phonon modes of both surfaces. From a comparison of the phonon spectra of these surfaces we find that the AISb(110) surface does not show any gap phonon states in the middle of acoustic-optical gap region unlike the GaP(110) surface. The gap phonon modes for the AISb(110) surface are found to lie very close to the optic bulk edge in good agreement with the recent HREELS experiment [2]. Moreover we have observed that the highest surface optical phonon modes are localized on the cation atoms for AISb(110) but the reverse is true for GaP(110) due to smaller anion mass.

[1] H. M. Tütüncü, Ph D Thesis (University of Exeter, U.K.) 1998.

[2] H. Nienhaus, Phys. Rev. B **56**, 13194 (1997).

[3] C. Eckl, (private communication) (1996).

LD1.3 (12.10)

Interpretation of Inelastic Neutron Scattering Spectra by Lattice and Molecular Dynamic Simulations

Jichen Li

Department of Physics, UMIST, PO Box 88, Manchester, M60 1QD, UK

The vibrational spectrum measured by inelastic neutron scattering (INS) techniques can be simulated by either lattice dynamic (LD) or molecular dynamic (MD) methods. In the LD approach, the calculation begins with the adiabatic approximation which enables us to treat the solutions in the electronic problem as interaction potentials in the nuclear problem. By assuming harmonic forces and periodic boundary conditions, we can obtain a normal mode distribution function of the nuclear displacements. The problem is then reduced to a classic system of coupled oscillators. Under these conditions the one-phonon dispersion relation can be evaluated and hence the one-phonon density of states can be calculated. On the other hand, the MD calculations are based on numerically integrating Newton's equations for a multi-body system. Then the Fourier transformation of velocity auto-correlation function will yield the phonon density of states. Because of the self-convolution of the velocity involved in the MD calculations, it is essentially the same as incoherent INS measurements - intensity is proportional to the displacement of each individual atoms (or molecules), it is therefore most suitable for interpreting the data obtained from INS [1]. In this paper, we demonstrate that the advantages and the disadvantages of each of simulation techniques in the case of calculations of vibrational dynamics for the exotic phases of ice [2,3]. Combining their advantages, we were able to simulate a range of effects, such as size effect, proton disordering effect and long range interaction effect which are essential in order to reproduce the measured phonon density of states.

1. J.C. Li and D.K. Ross, *Nature* 365, 327 (1993) and J.C. Li, *J. Chem. Phys.* 105, 6733 (1996).
2. C.J. Bunham, J.C. Li and M. Leslie, *J. Phys. Chem.* 101, 6192 (1997).
3. J.C. Li, *J. Phys. Chem.* 101, 6237 (1997).

LD1.4 (12.30)

LOCAL STRUCTURAL ANOMALIES IN PEROVSKITE-TYPE LATTICES

A. Bussmann-Holder

Max-Planck-Institut für Festkörperforschung
Heisenbergstr. 1, 70569 Stuttgart, Germany
fax: +49-711-689-1091, email: annet@vaxf2.mpi-stuttgart.mpg.de

Abstract

All perovskite oxides show unusual local displacement patterns which are not compatible with their average crystallographic structure. The ultrafast dynamics induce stripe- and tweed-type patterns on a much faster time scale than phonon dynamics. The experimental data are reproduced by an anharmonic electron-lattice interaction model with higher-order density-density multiphonon processes. The model is solved exactly for arbitrary q and leads, depending upon the degree of anharmonicity, to stripe and tweed formation in the oxygen ion dynamics. It is found that, in general, only the oxygen ions exhibit these unusual ultrafast dynamics, whereas the transition metal ions show mostly harmonic motion.

NS2.1 (14.00)

DECAY OF NONEQUILIBRIUM PHONONS IN NANOCRYSTALLINE SILICON

M. van der Voort¹, A.V. Akimov^{1,2}, G.D.J. Smit¹, J.L. Dijkhuis¹, N.A. Feoktistov²,
A.A. Kaplyanskiy², and A.B. Pevitsov²

¹ Department of Condensed Matter, Debye Institute, Utrecht University, P.O. Box 80.000, 3508 TA Utrecht, The Netherlands

² A.F.Ioffe Physical-Technical Institute, 194021 St. Petersburg, Russia

Numerous studies of low-dimensional semiconductor nanostructures have been carried out to elucidate and control the static confinement effects on charge carriers and phonons. However, the effects of confinement on the dynamical properties have received much less attention. In this contribution we present novel experimental results on lifetimes of nonequilibrium THz-phonons in thin (0.5 μm) amorphous a-Si:H PECVD-grown films containing crystalline (nc-Si) nanoparticles. The Stokes Raman spectrum shows the familiar broad lines centred at 120 cm^{-1} , 300 cm^{-1} , and 480 cm^{-1} typical for the TA, LA and TO vibrations in a-Si, respectively, and a 15 cm^{-1} wide line at 515 cm^{-1} that corresponds to TO vibrations in nc-Si. From a detailed analysis of the Raman spectrum, an average nanocrystallite size of 4 nm and a 20% volume fraction of nc-Si were estimated [1].

In order to study the dynamics of phonons in a-nc-Si:H, we use the well-known fact that the anti-Stokes (I_{AS}) and the Stokes (I_{S}) Raman intensities directly relate to the average phonon occupation number, N_{ω} . Nonequilibrium phonons are generated in our experiments at 2 K as a result of fast (<1 ps) relaxation of hot carriers. These are created by absorption of intense 10-ns frequency doubled Nd:YAG laser pulses with a repetition rate of 30 Hz and an average intensity up to 0.3 Wcm^{-2} at the sample. Other Nd:YAG laser pulses synchronously or at a controlled time delay excite the Raman spectra. It is revealed in synchronous experiments that the TO nonequilibrium phonon contribution to $I_{\text{AS}}(\omega)$ from the nanoparticles peaks at a 10- cm^{-1} lower energy than the nc-Si Raman contribution in the Stokes spectrum I_{S} . This points to an increase of the TO phonon lifetime for nanoparticles that have their Raman shift at lower ω . This is also supported by experiments with a controlled delay. In agreement with data obtained on a-Si:H samples without nc-Si [2], a decay time of 50 ns was measured at the amorphous TO peak. For higher $\hbar\omega$, however, where the predominant part of the Raman intensity corresponds to the vibrations of the nanocrystallites, the phonon decay appears to become gradually faster until it becomes too fast (<10 ns) to measure in our setup for $\hbar\omega = 515 \text{ cm}^{-1}$. It is well known that the Raman peak position of nanoparticles shifts to higher energies for increasing size until it reaches the bulk value in c-Si. Therefore, the experimental results lead to the important conclusion that the smaller nanoparticles have slower anharmonic decay. It is quite natural to relate the slowing down of the anharmonic decay for smaller particles to phonon confinement effects that become important as soon as the wavelength of THz phonons approaches the size ($\sim 1 \text{ nm}$) of the nanocrystallites. Then the phonon spectrum exhibit gaps large enough to lead to suppression of decay by anharmonic break up [2,3].

We finally note that we observe a big difference in the phonon decay in a-nc-Si:H and a-Si:H in the TA ($\hbar\omega = 150 \text{ cm}^{-1}$) spectral region. In a-nc-Si:H we measure a 50-ns decay time which is much longer than in a-Si:H without nc-Si [2]. This may be explained by the contribution of long-living Lamb modes [4] from the smallest nanocrystallites to the Raman spectrum in the TA region.

1. V.G.Golubev et al, Phys.Solid State 39, 1197 (1997)

2. A.J.Scholten et al, Phys.Rev.B 47, 13910 (1993); Phys.Rev.B 53, 3837 (1996)

3. R.Orbach and A.Jagannathan, J.Phys.Chem. 98, 7411 (1994)

4. S.P.Feofilov et al. Journal of Luminescence 66/67, 349(1996).

NS2.2 (14.20)

One phonon relaxation processes in $\text{Y}_2\text{O}_3:\text{Eu}^{3+}$ nanocrystals

Ho-Soon Yang^a, S. P. Feoflov^b, Brian M. Tissue^c, R. S. Meltzer^a,
and W. M. Dennis^a

^aDepartment of Physics and Astronomy, University of Georgia,
Athens, GA 30602-2451, USA

^bA. F. Ioffe Physical-Technical Institute, St. Petersburg,
Russia 194021

^cDepartment of Chemistry, Virginia Polytechnic Institute and
State University, Blacksburg, VA 24061-0212, USA

In bulk systems, the phonon density of states (DOS) is known to be a continuous function which at low frequencies is well described by the Debye model. However, in nanocrystalline materials, the DOS is modified due to the finite particle size and for isolated nanoparticles the phonon spectrum is expected to become discrete with a gap opening up at very low frequencies.

In this paper, we investigate the effect of the nanoparticle phonon spectrum on the one phonon relaxation rate. The $\text{Y}_2\text{O}_3:\text{Eu}^{3+}$ nanocrystals used in this study are prepared by gas phase condensation using CO_2 laser heating of ceramic pellets. Nanocrystals prepared in this way crystallize in a monoclinic phase which possesses three crystallographically distinct cation sites (labeled A, B, and C). Particles were prepared with a nominal diameter of 23 nm.

The lowest energy splittings of the $^5\text{D}_1$ manifold of Eu^{3+} are 25 cm^{-1} and 39 cm^{-1} for the B sites and 4 cm^{-1} and 7 cm^{-1} for the C sites. We measure the one phonon relaxation of these excited components of $^5\text{D}_1$ by monitoring their time-resolved emission to $^7\text{F}_3$ for both the B and C sites. We compare results for the 23 nm particles with these for larger ($\sim \mu\text{m}$) monoclinic particles.

PHONON MODES IN SINGLE-WALL NANOTUBES WITH A SMALL DIAMETER

Toshiteru Maeda and Chuji Horie

Department of Basic Science, Ishinomaki Senshu University
Minamisakai, Ishinomaki, Miyagi 986-8580, Japan

With the recent development in method for synthesizing samples containing high concentrations of single-wall nanotubes (SWNTs) of carbon, it has been possible to prove the properties of these quasi one-dimensional crystals in some detail[1]. In particular, studies of the Raman scattering from the SWNT have revealed that the size-dependent properties of SWNT manifest themselves in the phonon structure observed in the Raman spectra. Theoretical studies of phonon structure, so far, have been based on zone-folding of the phonon dispersion relations for a two-dimensional graphene sheet[2]. Thus, this approach evidently neglects the effects of tubule curvature on the phonon dispersion relations.

It is the objective of the present paper to calculate the phonon structure by taking proper account of the effects of tubule curvature. Our calculations based on the assumption that the equilibrium distance between the nearest neighbor carbons (bond length) is same as that for a graphite and the three bond angles are equal against each other on tubule surface. This basic assumption comes from the strong bonding nature of carbons, even though the sp^2 -character of graphene sheet is thought to be slightly deformed by adding sp^3 -character of tetrahedral bondings. Thus, we can treat the curvature effects beyond the zone-folding model. It is convenient to introduce cylindrical coordinates to describe the positions of carbon atoms. We employ the Born-von Kármán model containing interactions up to the fourth nearest neighbors. The force constants first employed by Jishi et al.[2] to fit the phonon dispersion relations obtained by electron energy loss experiment on 2D graphene sheet are slightly revised to yield a better agreement with the experimental results. Eliminating degrees of freedom of atomic motions other than vibrations around the lattice sites we can derive important constraints for the force-constants to satisfy. The effects of tubule curvature are elucidated in the comparison with the results based on zone-folding method.

Obviously, the effects of tubule curvature are emphasized for SWNT with a small diameter. The polarization of phonon modes which have been decoupled in 2D graphene sheet is generally altered from the original one on account of the tubule curvature, so that the symmetry arguments developed in the zone-folding model are not exactly correct. It is remarkable that frequencies of so-called "breathing mode" are most sensitive for a small diameter independently of chiralities of tube. The frequency of "breathing mode" is inversely proportional to the tubule diameter. It is shown that the present results are useful for analyzing the size distribution of SWNT in the synthesized samples. We will present the comparison of calculated results and Raman spectra measured for the samples of mono-size SWNTs.

[1] M. S. Dresselhaus et al., *Science of Fullerenes and Carbon Nanotubes* (Academic Press, New York, 1996).

[2] R. A. Jishi et al., *Chem. Phys. Lett.*, **209**, 77 (1993).

SIMULATION OF PHONON PROPAGATION IN FINE PARTICLES

Yoshiaki Kogure

Teikyo University of Science & Technology
Uenohara, Yamanashi 409-0193, Japan

Molecular dynamics simulation of atomic vibration in fine particles of copper has been done. The model particles are consisted of $10^3 - 10^4$ atoms. EAM potential was adopted for the interaction of atoms. The potential is smoothly truncated at $1.9r_0$, where r_0 is the nearest neighbor distance in the crystal. The time interval Δt of the molecular dynamics was chosen to be $2 - 5 \times 10^{-15}$ s, which is less than $1/10$ of the period of zone boundary phonons in the crystal. As an initial configuration atoms are arranged in fcc structures. Then a particle velocity corresponded to the temperature higher than 2000 K is given to each atoms and the crystal is melt. The molten particle was quenched and annealed. The fine particles of crystalline or amorphous state are produced by changing the annealing process.

The surface morphology of the particles is visualized by selecting the surface atoms through the coordination number or the potential energy of each atom and connecting nearest neighbor atoms by lines. The atomic structure inside of the particles is examined through the radial distribution function or the potential energy. Well annealed specimens are polycrystals and rapidly quenched specimens are amorphous.

When the particle attains a quasi-stable state, an atom near the center of the particle is displaced and released, and the motions of atoms in the particle are monitored. It is noted that the total mechanical energy is conserved through the molecular dynamics simulations without quenching, then the phonon propagation can be simulated. Emitted waves or phonons are reflected at the surface and go back to the center. A nearly periodic and coherent vibration of the atoms are observed in the crystalline particle, whereas sinusoidal vibration is quickly thermalized due to the disordered structure in the amorphous particles. Point defects, such as the vacancies and the interstitials, are introduced into the crystalline particles and the decay of the waves due to the defect scattering is compared with the decay in amorphous.

One of the purposes of the present study is to realize the wave propagation in a computer made disordered structure, in which the atomic coordinate is completely known. The results may help to understand the mechanism of the phonon scattering and the heat conduction in amorphous materials and nanostructures.

LATTICE DYNAMICS 2 (Monday 14.00) Chair: Inkson [R2]

LD2.1 (14.00)

Phonon Softening in Ice Ih

Stephen M Bennington[†], Jichen Li[‡], Mark J Harris^{*}, & D Keith Ross[‡]

^{*}ISIS Facility, Rutherford Appleton Laboratory, Chilton, Didcot, Oxon. OX11 0QX UK.

[†]Department of Physics, UMIST, Manchester, M1 7HS, UK.

[‡]Department of Physics, University of Salford, Salford, Manchester M5 4WT, UK

With the recent reports of 'fast sound' in ice and the fierce debate that followed, plus the equally contentious debate over the two force constant model used by Jichen Li to model hydrogen bonding in ice there has been a huge interest in the dynamics of ice in recent months. A large amount of effort has been put into molecular dynamics, lattice dynamics and ab-initio calculations. Although there are now several measurements of polycrystalline ice and liquid water there is a serious lack of good quality single crystal data. Apart from a measurement by Renker in 1969, there are no complete measurements of dispersion curves in ice.

We present Phonon dispersion measurements made with inelastic neutron scattering on crystals of ice Ih. These show a discontinuity in the phonon energy as a function of temperature at about 140K. We believe this to be due to a glass type transition where the hydrogen motion freezes and the ordering stops.

LD2.2 (14.30)

PHONON DISPERSION CURVES IN HCP ³He AND α -SiO₂ DETERMINED BY INELASTIC X-RAY SCATTERING

E. Burkel¹, C. Seyfert¹, C. Halcoussis¹, H. Sinn¹ and R. O. Simmons²

¹LS Physik Neuer Materialien, FB Physik Universität Rostock, 18051 Rostock, FRG

² Department of Physics, University of Illinois, Urbana-Champaign, Illinois, USA

The new technique of inelastic X-ray spectroscopy with energy resolution in the meV regime matured with the high photon flux of the third generation synchrotrons of these days.

We demonstrate that the phonon dispersion curves of a complex crystal, like a single crystal of SiO₂, can be resolved appropriately. The dispersion scheme obtained with inelastic X-ray scattering along the $[\bar{c}, 0, 0]$ direction of SiO₂ will be presented. In addition, not only the phonon energy values, but also the phonon intensities, will be used in the comparison of the experimental results with theoretical lattice models.

The inelastic spectroscopy with meV resolution opened new possibilities for the study of the dynamics in condensed matter under high pressures. A special beryllium pressure cell was used in our investigations of solidified single crystalline ³He and ⁴He up to pressures of 90 MPa.

For the first time, the phonon dispersion relation in single crystals of hcp ³He could be observed. The common method to study the dynamics in solids, inelastic neutron scattering has never been applied to this case because of the very high absorption cross section of ³He for thermal neutrons. The measurements were performed at low momentum transfers to emphasize single phonon aspects. The determined phonon dispersion relations and the observed phonon line width will be shown. Comparison of hcp ³He and ⁴He dispersion relations will be accomplished.

ANOMALOUS FEATURES IN THE Mn-O BOND-STRETCHING VIBRATIONS OF $\text{La}_{1-x}\text{Sr}_x\text{MnO}_3$

W. Reichardt and M. Braden
Forschungszentrum Karlsruhe, INFP, POB 3640, D-76021 Karlsruhe, FRG
Laboratoire Leon Brillouin, C.E. Saclay, F-99191 Gif sur Yvette, France

ABSTRACT:

The present interest in ferromagnetic perovskites of type $\text{La}_{1-x}\text{Sr}_x\text{MnO}_3$ ($\text{Me}=\text{Ca}, \text{Sr}$) arises from the discovery of anomalous effects in the magnetoresistance. The tendency towards charge ordering of Mn^{3+} and Mn^{4+} and the Jahn Teller splitting of Mn^{3+} may be reflected in the high frequency Mn-O bond-stretching vibrations.

We present detailed studies on the phonon branches in $\text{La}_{0.5}\text{Sr}_{0.5}\text{MnO}_3$ and $\text{La}_{0.7}\text{Sr}_{0.3}\text{MnO}_3$ by means of inelastic neutron scattering and model calculations. Both single crystal samples used in the experiment had the R3c structure (10 atoms per unit cell) and were twinned. The scattering patterns were found to be very different from those of a cubic perovskite which necessitated to plan the phonon scans and to analyse the data using lattice dynamical models for the rhombohedral structure and accounting for the twinning.

Most of the data are well reproduced by a shell model including screening by nearly free carriers to account for the metallic character of the compounds. The screening manifests itself most pronouncedly in LO branches which start at Γ near 10 THz and shoot up beyond 14 THz near the zone boundary.

Anomalous features were observed in the high frequency branches with breathing (linear, planar and volume) and quadrupolar (planar and volume) character. They start in the zone center at 17.5 THz and rapidly drop below this value already at small wave-vectors. About halfway to the zone boundary they dive into the lower lying phonon bands of bond-bending character and a strong mixing with other branches prevents an unequivocal identification at larger wave-vectors. Compared to predictions by structure factor calculations we observed near the zone boundary enhanced intensities in the range from 9 to 11 THz which we attribute to the strongly renormalized breathing and quadrupolar frequencies. The drop at small wave-vectors is more pronounced in $\text{La}_{0.5}\text{Sr}_{0.5}\text{MnO}_3$ than in $\text{La}_{0.7}\text{Sr}_{0.3}\text{MnO}_3$ suggesting that the anomalies increase with increasing x. The anomalies in the breathing type vibrations resemble those observed in several high T_c superconductors: $\text{Ba}_2\text{K}_2\text{BiO}_3$, $(\text{La}, \text{Sr})_2\text{CuO}_4$, $\text{YBa}_2\text{Cu}_3\text{O}_7$. In $\text{La}_{0.7}\text{Sr}_{0.3}\text{MnO}_3$ the temperature dependence of several phonon frequencies at Γ and at the zone boundary was studied between 12 K and 400 K. Most of the frequencies at Γ exhibit a slight normal softening of the order 1 % with no abrupt changes at the metal-insulator transition ($T_c=358$ K). In contrast the rotational frequency stiffens by 7 %, but again without discontinuity at T_c .

Preliminary studies on a single crystal of $\text{La}_{0.5}\text{Ca}_{0.5}\text{MnO}_3$ with the orthorhombic Pbnm structure showed that the phonon spectra are quite different from those of the rhombohedral compounds and are much more complex. Most of the differences can be explained by the different crystal structure which, in particular, leads to a stiffening of frequencies with rotational character.

THE VIBRATIONAL SPECTRUM AND GIANT TUNNELING EFFECT OF HYDROGEN DISSOLVED IN α -Mn

A.I. Kolesnikov^{1,2}, V.E. Antonov¹, S.M. Bennington³, B. Domet⁴, V.K. Fedotov¹, G. Grosse⁵, J.C. Li², S.F. Parker³ and F.E. Wagner²

¹Institute of Solid State Physics RAS, 142432 Chernogolovka, Moscow District, Russia

²Department of Physics, UMIST, PO Box 88, Manchester, M60 1QD, UK

³ISIS Facility, Rutherford Appleton Laboratory, Chilton, Didcot, Oxon, OX11 0QX, UK

⁴Institute Laue-Langevin, BP 156, 38042 Grenoble Cedex 9, France

⁵Physik-Department E 15, Technische Universität München, D-85747 Garching, Germany

A recent high pressure study showed that the solubility of hydrogen in α -Mn can be increased up to a few atomic percent [1]. A neutron diffraction investigation of α -MnH_{0.07} showed [2] that hydrogen randomly occupies interstitial sites of the 12e type (space group $I\bar{4}3m$) which form dumb-bells positioned rather far apart, at the centres of the edges and faces of the cubic unit cell of α -Mn. Because of the small distance of only 0.68 Å between the 12e sites in a dumb-bell, each dumb-bell can accommodate only one hydrogen atom.

An inelastic neutron scattering (INS) study [2] of α -MnH_{0.07} at 90 K with the KDSOG-M spectrometer at JINR (Dubna, Russia) revealed a band of optic hydrogen vibrations split into three peaks at 73, 105 and 123 meV in accordance with the low site symmetry of the hydrogen positions and also a strong peak at 6.4 meV which was tentatively attributed to the splitting of the vibrational ground state of hydrogen due to tunnelling between the adjacent 12e sites forming a dumb-bell.

This paper reports on the results of further INS studies which strongly corroborated the assignment [2] of the tunnelling origin of the 6.4 meV peak. These include the INS spectra (i) of α -MnH_{0.07} at 5–200 K and (ii) of α -MnD_{0.05} at 5 K measured with the TFXA spectrometer at ISIS, RAL (UK); (iii) the INS spectra of α -MnD_{0.05} at 1.7–180 K measured with the IN6 spectrometer at ILL (Grenoble, France) and (iv) the neutron momentum transfer dependence of the INS spectra of α -MnH_{0.07} at 5–200 K measured with the MARI spectrometer at ISIS.

The most remarkable features of the hydrogen tunnelling peak in the INS spectrum of α -MnH_{0.07} are its anomalously large intensity compared to that of the hydrogen optic band and its anomalously high energy of 6.4 meV which is about 1.5 times larger than the energy of tunnelling splitting observed earlier for hydrogen in other metals. Deuterium tunnelling in metals has not been detected previously by neutron spectroscopy.

[1] V.E. Antonov et al., *Scripta Mater.* **34** (1996) 1331.

[2] V.K. Fedotov et al., *J. Phys.: Condens. Matter*, in press.

COHERENT PHONONS 1 (Monday 17.00) Chair: Wolfe [R1]

CP1.1 (17.00)

COHERENT PHONON AVALANCHES

H. W. de Wijn, P. A. van Walree, and A. F. M. Arts

*Faculty of Physics and Astronomy, and Debye Research Institute,
Utrecht University, P.O. Box 80000, 3508 TA Utrecht, The Netherlands*

Avalanches of acoustic phonons arising from stimulated emission by an inverted one-phonon transition are observed in a single crystal of dilute ruby ($\text{Al}_2\text{O}_3:\text{Cr}^{3+}$). The phonons are resonant with the Zeeman-split $E(2E)$ Kramers doublet, complete initial inversion of which is achieved in a limited volume of the crystal by selective pulsed optical pumping into its upper Zeeman component. The detection is accomplished via the luminescence emanating from the lower $\bar{E}(2E)$ Zeeman component.

The phonon avalanche appears to develop in a way analogous to optical laser action. Following a delay, the avalanche grows rapidly, until it comes to a halt because the phonons leave the active zone. Amplification resumes when the phonons return to the active zone after covering a full round trip through the acoustical cavity formed by the reflecting end faces of the crystal. For frequencies up to 100 GHz, as many as six round trips have been observed before the inversion no longer overcomes the losses. Avalanches of T_1 or T_2 acoustic phonons can be selected by proper orientation of the crystal faces with respect to the crystalline axes.

To describe the phenomena, we developed a theoretical treatment, based on earlier work by Jacobsen and Stevens, and Leonardi et al., which allows for coherence of the phonon-associated spin polarization in the active zone. As it turns out, appreciable coherence is conserved between successive passages of the acoustic wave.

In summary, our experiments to date have established the basic ingredients for an acoustical laser, viz., amplified stimulated emission of a traveling phonon pulse, the presence of an acoustical cavity, and the preservation of coherence.

CP1.2 (17.30)

Amplification of sound in the coherent regime at low temperatures in glass

S. Baumhöff, J.-Y. Prieur^{1,2} J. Joffrin¹

¹Laboratoire de Physique des Solides, Université Paris-Sud, Bât. 510, Centre Scientifique d'Orsay, F-91405 Orsay, France

²Laboratoire d'Acoustique et Optique de la Matière Condensée², Université Pierre et Marie Curie, Tour 13, Case 78, 4 place Jussieu, F-75252 Paris Cedex 05, France

New results on the Amplification of ultrasound by Two-Level Systems (TLS) in BK7 glass samples are reported at low temperatures $T < 50\text{mK}$. Long relaxation times T_1 , T_2 require the consideration of coherency effects for the description of propagating acoustic pulses interacting with resonant TLS. We have adapted a formalism developed in optics for light pulses travelling through resonant atomic levels with inverted population. We obtain four coupled equations, three Bloch equations describing the state of the TLS as a pseudo magnetisation and one wave equation, linking the deformation pulse shape in time and position with the TLS magnetisation vector during its passage through the sample.

Experimentally we reverse the TLS population with an acoustic rapid adiabatic passage technique. Due to this technique we are able to observe acoustic pulse shapes after a passage through amplifying, saturated or attenuating TLS.

We'll show the temperature dependence of the amplification gain between 50 and 30 mK and acoustic pulse shapes found to be characteristic of amplification. A maximum local power gain as strong as 15dB has been observed. The presented measurements were carried out, varying the incident acoustic power over a range of 50dB. They cover the regime of high intensities where nearly all accessible TLS contribute to the amplification as well as the regime of low intensities where all the energy detected after the passage through the sample is due to the amplification effect.

For a good correspondence between computer simulations and experimental pulse shapes, we need to introduce a modified relaxation time T_2' which is about one order of magnitude shorter than the T_2 determined by an acoustic echo technique.

DIFFUSIVE TRANSPORT OF ACOUSTIC WAVES IN STRONGLY SCATTERING MEDIA.*

J.H. Page¹, M.L. Cowan¹, H.P. Schriemer², Ping Sheng³, and D.A. Weitz⁴

¹ Department of Physics, University of Manitoba, Winnipeg, Manitoba, Canada, R3T 2N2

² Department of Physics, Queen's University, Kingston, Ontario, Canada K3L 2N6

³ Dept. of Physics, Hong Kong University of Science & Technology, Clear Water Bay, Kowloon, Hong Kong

⁴ Dept. of Physics and Astronomy, Univ. of Pennsylvania, Philadelphia, PA 19104-6396 U.S.A

The propagation of classical waves through strongly scattering media is a problem of considerable current interest in many areas of physics, where important questions remain to be answered on topics as diverse as the investigation of classical wave localization and the development of novel non-destructive probes of disordered materials. In this presentation, we will discuss recent progress in understanding the diffusive propagation of ultrasonic waves through a simple strongly scattering medium consisting of glass beads immersed in a fluid. In the intermediate frequency regime, where the ultrasonic wavelength is comparable with the size of the scatterers, the propagation is dominated by very strong multiple scattering due to scattering resonances. In this regime, the transport of energy by the scattered waves is shown to be well described using the diffusion approximation. We critically test the validity of diffusion approximation for multiply scattered ultrasound by using a combination of pulsed and quasi-continuous-wave techniques to measure the wave diffusion coefficient D , the transport mean free path l^* and the energy velocity $v_e = 3D/l^*$ over an extended range of frequencies and sample thicknesses. Both D and v_e exhibit a strong frequency dependence, reflecting a substantial slowing down of wave propagation in the medium due to resonant scattering. Insight into this behavior is obtained by comparing the energy¹ and group² velocities that describe the transport of energy by the diffusive and ballistic waves respectively, and by interpreting our results using a simple theoretical model that quantitatively accounts for the scattering delay experienced by a wave pulse. This gives a microscopic physical picture of energy transport by diffusive acoustic waves in strongly scattering media - an important step in facilitating both the search for acoustic wave localization in more strongly scattering samples and the development of a new dynamic phonon scattering technique called Diffusing Acoustic Wave Spectroscopy.

1 H.P. Schriemer, M.L. Cowan, J.H. Page, P. Sheng, Z. Liu and D.A. Weitz, *Phys. Rev. Lett.* 79, 3166 (1997).

2 J.H. Page, P. Sheng, H.P. Schriemer, I. Jones, X. Jing and D.A. Weitz, *Science* 271, 614, (1996).

* Research supported by NSERC of Canada, DAG of HKUST & NSF.

CHAOTIC BEHAVIORS IN A SURFACE ACOUSTIC WAVE RESONATOR

Yutaka ABE and Atsushi IOBE

Department of Applied physics, Hokkaido University, Sapporo, 060, JAPAN

ABSTRACT

According to the fact that the acoustic energy of surface acoustic wave(SAW) is concentrated in a thin layer, it is plausible that it is rather easy to observe nonlinear bifurcation and chaotic behaviors in simple SAW devices. However, in spite of this conjecture, this problem still remains to be explored.

In this report, we investigate both experimentally and theoretically on the detailed behaviors of the bifurcation, indeterminate transition phenomena, and chaotic behaviors observed in a simple SAW resonator on LiNbO₃ substrate. The quality factor Q of the resonator is limited to be relatively low in order to realize the interaction of the driving frequency with higher-harmonics and sub-harmonics, which is essential requirement to observe nonlinear chaotic behaviors in general nonlinear driven oscillators.

It is shown theoretically that the present resonator system can be expressed by Duffing's type nonlinear oscillator, which can only be analyzed by numerical method.

All the sequence of the periodic doubling, quasiperiodicity, and intermittency are observed experimentally, which is very consistent with theoretical investigation. Recently, we have reported new type of phenomena which reveals a characteristic feature of nonlinear driven oscillator [1]. We have observe this indeterminate transition in the present experiment, and we

conjecture that this is one of the universal property in a driven nonlinear oscillator.

The example of control the SAW chaos is also presented.

[1] A. Iobe and Y. Abe, Fractal-like basin-boundaries and indeterminate transition in nonlinear resonance of a Toda oscillator, *Int. J. Bifurcation and Chaos*, 7, 1673-1678 (1997), A. Iobe and Y. Abe, Experimental observation of indeterminate transition in a driven R-L-Diode resonator, *Physica D*, to be published.

PT1 (17.00)

PHONON SOFTENING AT A CONTINUOUS MELTING TRANSITION:
LATTICE MELTING IN FERROELASTIC Na_2CO_3

M. J. Harris, ISIS Facility, Rutherford Appleton Laboratory, Chilton, Didcot,
Oxon, OX11 0QX, United Kingdom
D. F. McMorrow, Department of Solid State Physics, Risø National Laboratory,
DK-4000, Roskilde, Denmark

A crystal melts at the point where the atomic displacements diverge, leading to a complete breakdown of the crystalline order. Theoretical work in the 1970's suggested that a similar divergence of the atomic displacements should also occur at a phase transition that is driven by a two-dimensional softening of the phonons in the crystal. However, in contrast with conventional melting, crystalline order is expected to return continuously on heating above the transition, so that it is fully reversible and continuous. This process is known as lattice melting, and was first observed experimentally in 1993 [1]. Experimental work to investigate this remarkable effect will be described, with particular reference to the compound Na_2CO_3 , which is the only material currently known to undergo full lattice melting.

We will present the results of an inelastic neutron scattering study of the dynamics of lattice melting in Na_2CO_3 [2]. The driving instability is a transverse acoustic mode that softens over a plane of wavevectors. The phonon softening is shown to be in accord with the renormalisation-group predictions from the 1970's. At T_c a wide distribution of excitations is observed in the plane of critical wavevectors, similar to the dynamics of a liquid. Perpendicular to this plane, the system possesses one-dimensional order. Implications for the mechanism behind conventional melting will be discussed.

[1] M. J. Harris, R. A. Cowley, I. P. Swainson and M. T. Dove. *Phys. Rev. Lett.* **71**, 2939 (1993).

[2] M. J. Harris, D. F. McMorrow and K. W. Godfrey. *Phys. Rev. Lett.* **79**, 4846 (1997).

PT2 (17.30)

PREMELTING PHENOMENA OF $\text{LiH}_3(\text{SeO}_3)_2$ STUDIED BY BRILLOUIN
SCATTERING

Masaki TAKESADA, Masaru KASAHARA and Toshiro YAGI
Research Institute for Electronic Science, Hokkaido University, Sapporo 060-0812, JAPAN

Low-frequency acoustic phonon modes of ferroelectric $\text{LiH}_3(\text{SeO}_3)_2$ have been observed by Brillouin scattering around the melting point T_m (383K) as a function of temperature to elucidate a mechanism of the melting process. A longitudinal acoustic phonon mode (LA mode) appears in each scattering wave vectors q parallel to the a , b and c^* axes at approximately 25K below T_m . They show softening dramatically as the temperature approaches T_m accompanied with anomalous broadening and increasing scattering intensity. The temperature dependence for the frequency shift of the LA mode are shown in Fig. 1. In the liquid phase with increasing temperature the LA mode shows hardening slightly just above T_m and decreasing gradually. In contrast to these anomaly, the other acoustic phonon modes do not show any anomalous behavior up to T_m . It is concluded that the anomaly of the LA mode is caused by premelting phenomena. An existence of viscous-fluid layer is suggested on the surface of the crystal below T_m . The result is discussed as precursor phenomena of the solid-liquid transition.

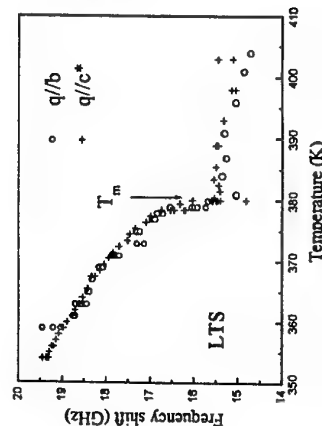


Fig.1 Temperature dependence of the frequency shift for the LA modes of $\text{LiH}_3(\text{SeO}_3)_2$ along the b and c^* axes.

PT3 (17.50)

PHONONS SOFTENING IN ALPHA-U METAL AT LOW TEMPERATURE

J.-C. Marmeggi^{1,2}, R. Currat², G.H. Lander³

¹ Laboratoire de Cristallographie, CNRS-Université J. Fourier, BP 166, 38042 Grenoble Cédex 9, France; ² Institut Laue Langevin, BP 156, 38042 Grenoble Cédex 9, France; ³ European Commission, JRC, EITU, Postfach 2340, 76125 Karlsruhe, Ger.
e-mail: MARMEGGI@polycnrs-gre.fr

Alpha-U has been observed to undergo the following sequence of transformations; ortho.: Cnrm $T_0 = 43\text{K}$, $\text{mono.: C2/m11 (qx, qy, qz) } T_1 = 37\text{K}$, $\text{mono.: P211 (1/2, qy, qz)}$. The phonon dispersion was measured by neutron inelastic scattering in the range (200, 43K) of existence of the high-temperature orthorhombic phase [1] and in the range of the phase transformations at 43, 37 and 22K. Soft branches were associated with the normal-to-incommensurate transitions in Brillouin zone: (201). The main component of the displacement pattern is consistent with the symmetry for a $\Sigma 4$ phonon mode. The static displacements associated with the displacive transition are produced by low-frequency and damped phonons at positions \mathbf{qs} (qx, qy, qz) which on approaching the second-order phase transition (T_0) soften more than those with $\mathbf{qc} = \{1/2, 0, 0\}$, but not totally. Increasing the energy resolution by using cold neutrons on the three axis spectrometer IN14 near (101), we have seen in the range $T-T_0 = 7\text{K}$ a small deviation from the linear law of Curie. The experimental phonon softening which is accompanied by large changes in cell parameters at T_0 is dependent on $\text{qy}(T)$, $\text{qz}(T)$ contrary to predictions of the Yamada theory. Incomplete softening is observed: squared soft mode frequency remains finite at 43K.

[1] J.C. Marmeggi, G.H. Lander, R. Currat, C.M.E. Zeyen, *Physica B*, **234-236**, 129-130 (1997)

PT4 (18.10)

OBSERVATION OF THE COUPLING BETWEEN TA AND TO MODES IN SrTiO_3 IN BRILLOUIN SCATTERING

B. Hehlen,¹ L. Arzel,^{1,2} A.K. Tagantsev,³ E. Courtens,¹ Y. Inaba,⁴ A. Yamanaka,⁴ and K. Inoue⁴

¹ Laboratoire des Verres, UMR 5587 CNRS, Université de Montpellier II, F-34095 Montpellier Cedex 5, France

² Institut Laue-Langevin, BP 156, F-38042 Grenoble Cedex 9, France

³ Laboratoire de Céramique, EPFL, CH-1015 Lausanne, Switzerland

⁴ Research Institute for Electronic Science, Hokkaido University, Sapporo 060, Japan

Some of us had reported previously the Brillouin scattering observation of an unusual low temperature softening of some transverse modes in SrTiO_3 . The early data, complemented by newer Brillouin results, and supplemented by high quality hyper-Raman data on the soft mode, now demonstrate that this anomalous softening is caused by a bilinear coupling of the strain with the gradient of the electrical polarisation fluctuations. This coupling had been identified long ago, in particular in another perovskite KTaO_3 , but this at the large momentum exchanges that are achieved in neutron spectroscopy. To our knowledge, it is the first time that the signature of this coupling is observed in any material at the small wave vectors of optical Brillouin scattering.

GL1.1 (09.00)

The boson peak in network-forming glasses

Tsuneyoshi NAKAYAMA, Department of Applied Physics, Hokkaido University,
Sapporo 060-8628, Japan

Glasses are extremely interesting objects in the physics of condensed matter, with universal properties such as the T -linear specific heat below a few K, the thermal conductivity plateau around 10K, and the low-energy broad-peak observed in Raman spectra, the so-called boson peak. The origins for the latter two, however, remain a question of considerable current interest, for which I discuss from a simple-model for glasses with directional bonds. The model predicts the appearance of three types of excitations in the acoustic band: weakly, strongly, and mesoscopically localized modes, and, in addition, recovers the excess density of states at low energies observed by inelastic neutron scattering experiments and derived from specific heat data of glasses. The latter two excitations constitute two broad-bands at low energies. Namely, the lower band consists of strongly-localized nondispersive-modes and constitute the so-called boson peak. Mesoscopically localized-modes are dispersive and contribute to the second higher-band. Quite recently, the above predictions concluded from the model analysis have been confirmed by high-flux and high-resolution inelastic neutron scattering experiments. I also discuss the origin of the frequency dependence of the Raman coupling coefficient for the boson peak in addition to the pressure dependence of the boson peak spectrum with its significant physical implication.

GL1.2 (09.30)

EFFECTS OF HIGH PRESSURE ON THE BOSON PEAK IN a-GeS₂ STUDIED BY LIGHT SCATTERING

M.Yamaguchi^a, T.Nakayama^a and T.Yagi^b

^a Department of Applied Physics, Faculty of Engineering, Hokkaido University,
Sapporo 060-8628, Japan

^b Research Institute of Electronic Science, Hokkaido University, Sapporo 060-0812,
Japan

We present the results of light scattering study for amorphous germanium disulfide (a-GeS₂) performed under high pressure (up to 2.5 GPa) using the Diamond Anvil Cell (DAC). This study combines Raman scattering and Brillouin scattering experiments to elucidate the effects of high pressure on vibrational properties of glasses.

Raman scattering measurements were performed to investigate the pressure dependence of the boson peak. Brillouin scattering measurements were employed to obtain the pressure dependence of the frequency shift of the longitudinal acoustic (LA) mode in a-GeS₂. The comparison of Raman scattering and Brillouin scattering data allows us to describe the boson peak in relation to low-temperature properties of glasses.

Raman scattering results show a decrease in the boson peak intensity with increasing pressure from the ambient pressure to 2.5 GPa. The frequency shift of the boson peak increases with pressure (Fig. 1). From comparison with the pressure dependence of the longitudinal acoustic mode frequency, the ratio of the third order elastic stiffnesses for these modes is estimated. The results of this analysis show larger anharmonicity for the boson peak reflecting much stronger pressure effect on the boson peak shift compared to the LA mode. These results will be discussed in connection with the thermal conductivity of amorphous materials above the plateau region at low temperatures.

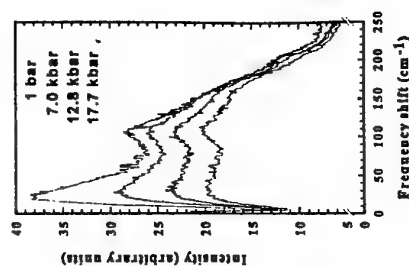


Figure 1.

Heat transport above the plateau temperature in glasses

Tsuneyoshi Nakayama and Raymond L. Orbach*,

Department of Applied Physics, Hokkaido University, Sapporo 060-8628,

*Department of Physics, University of California, Riverside, CA92521.

The plateau in the thermal conductivity κ around 10K for glasses can be explained by the existence of a mobility edge for phonons in the medium. Evidence for localization has been obtained from the extraction of the phonon mean free path as a function of frequency from observed κ . For temperatures above $\hbar\omega_c/3.83k_B$ with an assigned phonon localization frequency ω_c , conventional heat transport can only occur via already excited phonons. Such behavior leads to a saturation in κ , referred to as the plateau, namely, κ from phonon sources will saturate in the Dulong-Petit regime with regard to the extended phonon states. At the high temperature end of the plateau, κ rises with increasing temperature. The rise of κ is certainly at least initially linear with increasing temperature. The increase in κ should be caused by an additional heat conduction channel.

In ordered structures, anharmonicity reduces thermal transport through the Umklapp process, while in disordered structure the anharmonicity is the cause of heat flow. Here we discuss the mechanism of heat transport above the plateau temperature. We demonstrate that the introduction of large anharmonicity for strongly localized modes, contributing to the boson peak spectrum, allows to transport heat by hopping mechanism.

IS THERE A IOFFE-REGEL LIMIT FOR SOUND PROPAGATION IN GLASSES ?

Marie Foret, Bernard Hehlen, Eric Courtens, and René Vacher

Laboratoire des Verres, UMR 5587 CNRS, Université de Montpellier II

F-34095 Montpellier Cedex 5, France

There is considerable current activity and debate on the inelastic scattering from glasses at frequencies and momentum exchanges that correspond to vibrations at the scale of a few structural elements. This end region of acoustic branches is expected to correspond to the onset of strong phonon scattering by structural inhomogeneities, which leads to corresponding low temperature thermal anomalies. Moreover one observes in glasses at these low frequencies an excess in the vibrational density of states over the Debye value (the so-called boson peak) whose origin is still a matter of discussion.

New spectroscopic results obtained on glassy selenium using coherent inelastic neutron scattering are presented. For the first time with neutrons both Brillouin scattering under kinematic conditions and the boson peak have been observed. Two neutron spectrometers were necessary, thermal neutron three-axes and cold neutron time-of-flight spectroscopies. The absolute calibration of both spectroscopies allows to unravel the quantitative strength of the various spectral contributions in this frequency range. One finds that the most plausible interpretation of the overall data is that a Ioffe-Regel transition occurs for longitudinal acoustic waves around 1 THz. Umklapp scattering via the static structure factor is also seen. It provides unique information on transverse acoustic modes. Its fast disappearance for frequencies beyond 1 THz is once again a strong indication that acoustic excitations cease to propagate.

NOVEL COEXISTENCE OF PROPAGATING COLLECTIVE MODE
AND STRONGLY LOCALIZED MODE IN VITREOUS SILICAM.Araji¹, Y.Inamura¹, T.Otomo¹, N.Kitamura², S.M.Bennington³ and A.C.Hannon³¹High Energy Accelerator Research Organization, 1-1 Oho, Tsukuba 305, Japan²Government Industrial Research Institute of Osaka, 1-8-31 Midorigaoka, Ikeda, Japan³Rutherford Appleton Laboratory, Chilton, Didcot, Oxon OX11 0QX, UK

Abstract

One of the most important definition of non-crystalline system is that there is no Bragg-Peaks in diffraction pattern because of lack of periodic long range order and well defined Brillouin zones. The non-periodic atomic structure could give peculiar thermo-dynamic behaviours, discovered by Pohl and Zeller in 1971 [1], unexplainable by the well established theory of solid state physics on crystalline material.

A two level model [2] and a soft-potential model as a extension of the former were introduced to explain the low temperature thermo-dynamics and low energy dynamics, i.e. the Boson peak, as a localized elgen mode of a certain intermediate range structure [3]. A lot of works were done to identify the peculiar dynamics by means of various experimental approaches [4], however, it is still controversial problem even after the recent great progress of the experimental techniques in synchrotron x-ray inelastic scattering [5].

In the present neutron inelastic scattering in a wide range of energy-momentum space, we have discovered for the first time that there is a acoustic phonon dispersion with quasi periodic Brillouin zones and, in addition, coexistence with a localized mode of the Boson peak, penetrating through the low energy region of the dispersion. The novel coexistence of coherent phonon and localized states, can be the intrinsic origin of the unexplainable thermo-dynamics of non-crystalline system as was expected by a recent theoretical work by Nakayama [6].

[1] Pohl and Zeller, Phys. Rev. B5 (1971) 2029

[2] P.W.Anderson et al., Phil. Mag. 25 (1972) 1, W.A.Philips, J.Low Temp. Phys. 7 (1972) 351

[3] Buchenau, Phys. Rev. Lett. 53 (1984) 2316

[4] M.T.Dove et al., Phys. Rev. Lett. 78 (1997) 1070, A.P.Sokolov et al., Phys. Rev. Lett. 69 (1992) 1540

[5] M.Foret et al., Phys. Rev. Lett., 77 (1996) 3831, P.Bennasi, et al., Phys. Rev. Lett. 77 (1996) 3835

[6] T.Nakayama, Phys. Rev. Lett. 80 (1998) 1244, J. Phys.: Condens. Matter 10 (1998) L41-L47

EP1.1 (11.20)

Direct Measurements of the Electron-Acoustic Phonon Interaction
In GaAs Quantum Wire Structures

A J Kent, A J Naylor, I A Pentland and M Henini

Department of Physics, University of Nottingham, University Park,
Nottingham NG7 2RD UK*Abstract*

In this paper we describe new direct measurements of the emission and absorption of acoustic phonons by quasi-one-dimensional (1D) electrons in GaAs quantum wire (QWR) structures. The measurements were made using heat-pulse techniques: for the absorption experiments, nonequilibrium phonons were generated using a metal-film resistive heater and the absorption detected via the change in conductivity induced in the QWR itself (phonoconductivity); in the emission experiments, the electrons in a QWR array were heated electrically and the emitted phonons detected by superconducting bolometers.

Heat pulse phonon techniques have hitherto proved very useful in the study of the interaction of acoustic phonons with two-dimensional electron systems (2DES). Phonon experiments are able to give direct information concerning the electron phonon interaction that cannot be obtained by other means, e.g. by analysing electronic transport measurements. For example, in the case of emission of phonons by a warm 2DES in GaAs, the anomalous weakness of the deformation potential coupled longitudinal-acoustic (LA) phonon mode was observed in phonon emission experiments. Nonequilibrium phonons have also proved to be a powerful spectroscopic probe of 2D electronic states in zero and high (quantizing) magnetic fields. Significant advances in instrumentation and experimental technique made over the last decade of studying 2D electron systems have resulted in sufficient sensitivity for studying devices containing only a very small number of electrons. It is therefore expected that phonon measurements will prove as effective in the study of QWR devices as they have been in studies of the 2DES.

In phonoconductivity measurements on split-gate QWR devices, we observed giant oscillations of the phonon-induced conductivity changes as the QWR was narrowed by increasing the (negative) gate bias. The amplitude of the response reached a maximum when the Fermi energy was close to the bottom of any 1D subband, where the 1D density of states is a maximum. In short wires (ballistic point contacts) the phonoconductivity is negative, i.e. phonons caused a decrease in the conductance, due to phonon backscattering of electrons. However, at large negative gate bias, close to "pinch-off" of the channel, the phonoconductivity became strongly positive. In long wires, $L > l_{\text{ph}}$ where l_{ph} is the localization length of electrons in the structure, the phonoconductivity is always positive due to phonon-induced delocalization of weakly localized electron states in the QWR.

Preliminary phonon emission experiments made using an array of etched QWRs are compared with the results of numerical calculations corresponding to the realistic experimental conditions of electron temperature and subband occupancy. We see evidence that, owing to phase-space restrictions for phonon emission in QWRs, the emitted phonons are mostly low-frequency and piezoelectrically coupled.

EP1.2 (11.50)

THE ABSORPTION OF SURFACE ACOUSTIC WAVES BY AN
ARRAY OF QUANTUM WIRES

Michal Rokni and Y. Levinson

The Weizmann Institute of Science, Rehovot, 76100, Israel Fax: 08-9465110,
Email: cmrokni@wicc.weizmann.ac.il

In this work we describe the absorption of surface acoustic waves (SAW) by an array of quantum wires (QWR's). The work was stimulated by an experiment performed by Nash *et al.* [1] in which the transmission of an SAW through a QWR array, in the presence of a strong perpendicular magnetic field, was measured in two cases. In the first case the SAW propagated parallel to the wires, and in the second case it traveled perpendicular to the wires. The results of the experiment contradicted what is expected from simple energy and momentum conservation considerations. Therefore more sophisticated theoretical methods, that take into account effects of level broadening, should be used.

A SAW interacts with a two dimensional electron gas (2DEG), due to the electric field created by the SAW. This field is screened by the electrons within the 2DEG, bringing about a modification of the absorption of the SAW. In the spatially homogeneous case the screened field will have one Fourier component - that of the SAW field. When the 2DEG is patterned into a periodic array of wires the screened field will have additional Fourier components, so that the dielectric function, that depends on the SAW frequency and wave vector, is in fact a matrix in Fourier space. One has to invert this dielectric matrix in order to describe the SAW absorption, that is directly related to one of the elements of the inverted matrix [2].

We have obtained an integral equation (in space) for the dielectric function in a periodic system of QWR's, in a strong perpendicular magnetic field. We inverted this equation so as to obtain an equation for the inverse dielectric function. This equation was solved for the Fourier components of the inverse dielectric matrix under the condition that the wire width is much smaller than the period of the array. Using the elements of the inverse dielectric matrix we then describe the SAW absorption as a function of the magnetic field applied.

[1] G. R. Nash *et al.*, Phys. Rev. B 54, R8337 (1996).[2] Y. Levinson *et al.*, preprint cond-mat/9712276.

RELAXATION RATES OF 2D ELECTRON GAS DUE
TO NEAR-SURFACE ACOUSTIC PHONON SCATTERINGN. Z. Vagidov¹, V. I. Pipa^{1,2}, V. V. Mitin¹¹ Department of ECE, Wayne State University, Detroit, MI 48202, USA

phone: (313) 577-5507, e-mail: nizami@besm6.eng.wayne.edu, fax: (313) 577-1101

² Institute of Semiconductor Physics, Pr. Nauki 45, Kiev 252028, Ukraine,

e-mail: zinovi@lab2.kiev.ua, fax: 38-044-265-8842

We study the effect of proximity of a quantum well (QW) to the surface of the heterostructure on the energy and momentum relaxation rates of 2D electrons localized in the lowest subband of the QW. The interactions with acoustic phonons via piezoelectric and deformation potentials were taken into account. The surface effect on scattering arises due to the modification of the acoustic field which is caused by: a) the interference between the incident and reflected acoustic waves; b) the mutual conversion of longitudinal and transverse acoustic waves induced by reflection; c) the existence of a Rayleigh wave. Piezoelectric interaction depends also on the boundary conditions of an electric potential. We have considered semiconductor surfaces of two types: 1) which are electrically free to vacuum, and 2) which are covered with a thin metallic film.

Using the elastic-continuum approximation, we have derived the Hamiltonian which describes both the piezoelectric and deformation potential interactions of electrons with all acoustic modes of the semi-infinite homogeneous medium. The interaction via deformation potential has been derived in [1], and via both, piezoelectric and deformation potentials, with a Rayleigh wave in [2], [3].

The relaxation rates of momentum and energy were found from the corresponding balance equations for small deviations from thermodynamic equilibrium. (The surface effect on the energy losses of electrons interacting via the deformation potential has been calculated in [4]). The results obtained show that the influence of the surface on the relaxation rates is substantial at low temperatures (Bloch-Grüneisen regime): $T < 2\pi\hbar^2/k_B$, where s is the longitudinal sound velocity, $\hbar v_F$ is the Fermi momentum, and k_B is Boltzmann's constant. In this temperature range, the contributions of the above-mentioned mechanisms a) and b) to the near-surface scattering are comparable with that of the Rayleigh wave considered in [2]. To stress the surface effects we calculated the ratios of relaxation rates to their bulk values (corresponding to the QW situated infinitely far from the surface). The piezoelectric interaction was assumed to be isotropic in the plane of the QW. These ratios depend nonmonotonically on the distance from the QW to the surface, on the temperature, and on the electron concentration. Our results show that for narrow QWs placed close to the surface the relaxation rates are changed considerably (up to several times for GaAs or InAs-based QWs).

1. S.V. Badalyan and Y.B. Levinson, Soviet Phys. - Solid State, 30, 1592 (1988).

2. A. Knäbchen, Phys.Rev.B, 55, 6701 (1997).

3. A. Knäbchen, Y.B. Levinson, and O. Entin-Wohlman, Phys.Rev.B, 54, 10696 (1997).

4. V.I. Pipa, F.T. Vasko, and V.V. Mitin, Phys.Stat.Sol.(b), 204, 234 (1997).

ANGULAR AND MODE DISTRIBUTION OF ACOUSTIC PHONON
EMISSION BY HOT 2D ELECTRONS IN GaAs

THE EFFECT OF ACOUSTIC ANISOTROPY AND SCREENING

Cz. Jasiukiewicz¹, D. Lehmann², A.J. Kent³, A.J. Cross³ and P. Hawker³¹ Institute of Theoretical Physics, University of Wrocław, PL-50-204 Wrocław, Poland² Institut für Theoret. Physik, Technische Universität Dresden, D-01062 Dresden, Germany³ Department of Physics, University of Nottingham, Nottingham NG7 2RD UK

We report a detailed theoretical study of the angular and polarization dependence of the acoustic phonon emission by a hot two-dimensional electron gas (2DEG) in GaAs/AlGaAs heterojunctions and quantum wells and compare the results with some recent experimental measurements.

The phonon emission by hot 2D electrons has been observed in a number of heat pulse experiments (for a review see [1]). Using this technique angular and temporal resolution of the emitted phonons is possible. Such studies give, in contrast to other methods (eg. transport measurements), direct information concerning the phonon wavevector and mode dependence of the emission process. Common to all the heat pulse experiments was that for 2D electrons in the (001) plane of GaAs heterostructures no signal due to longitudinal acoustic (LA) phonons propagating in a direction close to the 2DEG normal could be detected. Only transverse acoustic (TA) phonons were picked up on a bolometer directly opposite the 2DEG. This result was in strong contradiction to earlier theoretical studies which suggested that the emission of deformation potential coupled LA modes should be dominant at angles close to the [100] direction in the electron temperature range $10K < T_e < 40K$. The inclusion of phonon focussing effects alone does not explain this discrepancy. Strong focussing of TA modes propagating close to [100] will enhance the TA signal. However, the net effect of this would only be to give detected LA and TA signals of about the same strength.

To explain this discrepancy and to understand fully the process of electron-phonon coupling a detailed theoretical analysis of the angular, mode and temperature dependence of the emitted acoustic phonons has been made. We used a model which not only includes the dynamical screening of electron-phonon interaction in the 2D electron gas but also takes proper account of the finite "thickness" of the 2D gas and above all, considers the strong acoustic anisotropy of the phonon emission and propagation processes. Our numerical results for the angular dependence of the emitted phonon modes for quasi-2D electrons in (001) heterostructures and quantum wells show clearly the importance of including all of these four factors.

For quantum wells with different thickness we demonstrate the strong dependence of the angular distribution and TA to LA ratio on the quantum well width. A good qualitative agreement with measurements for different detector positions is found.

[1] A.J. Kent, in: Hot electrons in semiconductors: Physics and Devices, ed. N. Balkan (Oxford University Press, 1998), p. 81

RS1 (11.20)

ANHARMONICITIES IN OPTICAL SPECTRA OF α -RHOMBOHEDRAL BORON

Koun Shirai and Hiroshi Katayama-Yoshida

ISIR, Osaka University
8-1, Mihogaoka, Ibaraki, Osaka, 567 Japan

Since a Raman spectrum was at the first measured for α -rhombohedral boron [1], it has been known that this crystal has a very narrow Raman band at 527 cm^{-1} . A recent study shows that the linewidth $\Delta\omega$ is 0.8 cm^{-1} in FWHM at room temperature [2]; the ratio $\Delta\omega/\omega$ is less than 0.2 %. Several attempts were made for elucidating this band theoretically and experimentally on the basis of phonon scattering, but all such efforts were failed until recently. Accordingly, it is a surprising matter to see a recent study by Vast *et al.*, which demonstrated that this band was due to a usual phonon scattering, and that the relevant phonon was a librational mode [3]. The frequency ω_l of this librational mode is presumably the highest amongst librational modes of bulk crystals.

The frequency ω_l is governed by the intericosahedral angle forces f_a . The value of ω_l which Vast *et al.* found is about five times as high as the previously reported value, from which it was suspected that the angle forces would be unusually large (as large as the stretching forces). Analyzing the result by a force constant model, we found that the angle forces are not at all large. The reason why such a high frequency is obtained in spite of weak angle forces is that the number of angles which participate the librational mode is indeed large [4].

In this way, the question why the ω_l is high has been solved. However, there lefts as yet an answered question why this mode has such a narrow linewidth. We have attempted to solve this problem from the viewpoint of anharmonic effects of phonons.

In terms of phonon decay processes, the phonon lifetime is governed by two factors, beside the thermal factor. The one is the density of states (DOS) for phonon decay processes to occur. It is found that the two-phonon DOS's which are available for all the zone-center mode of boron is rather large. Compared with the optical mode T_{33} of silicon, the two-phonon DOS's of boron are order of magnitude large.

The other is the coupling strength between different phonons involved in decay processes. By observing that the pressure dependence of ω_l is very weak, it is suggested that the anharmonic forces associated with the librational mode must be very small. However, the weakness of pressure dependence of the frequency indicates, in this case, merely that the intericosahedral angles and thereby f_a remain almost unchanged as the pressure is varied. Analyzing the pressure dependence on the phonon frequencies, we found that anharmonic force constants of individual bonds and angles are quite normal, i.e., not so small even for f_a . Even though the anharmonic coupling parameters become very small in a form expressed by normal modes, this reduction is almost compensated with large DOS's.

It is finally found that the essential cause of the narrow linewidth is its exceptionally high frequency. This makes the thermal factor for the up-conversion processes, which govern the decay process of the librational mode, small even at room temperature.

Our study on the anharmonicity of boron provides useful information concerning further features of the Raman spectrum, especially the higher-frequency portion of the spectrum, the thermal expansion and many others.

- [1] W. Richter and K. Ploog, *Phys. Status Solidi B* **68**, 201 (1975).
- [2] D. R. Tallant, T. L. Avelage, A. N. Campbell, and D. Emin, *Phys. Rev. B* **40**, 5649 (1989).
- [3] V. Vast, S. Baroni, G. Zerah, J. M. Besson, A. Pollan, M. Grimsditch, and J. C. Chevin, *Phys. Rev. Lett.* **78**, 693 (1997).
- [4] K. Shirai, *J. Solid State Chem.*, **133**, 215 (1997).

RS2 (11.40)

RAMAN STUDY ON SOLID HBr UNDER HIGH PRESSURE AND LOW TEMPERATURE

T. Kume, T. Tsuji, S. Sasaki, and H. Shimizu

Dept. of Electronics, Gifu University, 1-1 Yanagido, Gifu, 501-1193, Japan
CREST, Japan Science and Technology Corp., Kawaguchi, Saitama, 332-0012, Japan

Solid hydrogen bromide (HBr) is the simplest hydrogen-bonded solid. At ambient pressure, HBr freezes from the liquid into phase I at 186.3 K , and undergoes transitions successively to phase I' (at 116.9 K), II (at 113.7 K) and III (at 89.7 K) [1]. For many years, a great deal of attention have been paid on the interesting structure characterized by hydrogen bonding, the ferroelectricity in phase III, and so on. Although many kinds of experiments have been made for solid HBr, the pressure-temperature (P - T) phase diagram is still little known. In particular, the regions of the phase II and I' were not clear. The purpose of the present work is to determine the P - T phase diagram of solid HBr and to investigate the pressure effect on vibrational modes using Raman spectroscopy.

A HBr specimen was loaded into a diamond-anvil cell (DAC) by splaying its vapor into a hole of the gasket of DAC which was cooled by liquid N_2 . The HBr solidified on the gasket was sealed by translating the lower diamond. The pressure was measured with the ruby-scale method. Raman spectra for the specimen were measured in back scattering geometry over a wide region up to 15 GPa in pressure and down to 20 K in temperature.

Figure 1 shows Raman spectra obtained for various pressures at 200 K . As seen in this figure, the Raman spectrum drastically changes depending on the pressure, which demonstrates the successive transitions from phase I to I', II and III. For higher pressures ($P > 4.5\text{ GPa}$), the pressure regions of phase III and II were identified by the spectral feature, i.e., several intermolecular (lattice) modes and two intramolecular stretching modes in phase III, and no lattice and two stretching modes in phase II. On the other hand, the Raman spectra in lower pressures ($P < 4.5\text{ GPa}$) exhibited only one stretching mode and were similar to each other. However, the spectral feature was found to slightly change depending on pressure. Namely, the peak which was symmetric initially, became asymmetric above 2.3 GPa , as seen in Fig. 1. We consider that the spectral change arises from the transition from phase I to I'.

From the characteristics of the Raman spectra measured over a wide P - T region, we could obtain the P - T phase diagram of HBr. The obtained phase diagram demonstrated that (1) phase III is stable in a wide P - T range, (2) phase II does not exit at room temperature, and (3) there is the triple point of phases I', II and III at $T \sim 230\text{ K}$ and $P \sim 7.5\text{ GPa}$.

References

- [1] J.E. Vesel and B. H. Torrie, *Can. J. Phys.* **55**, 592 (1977).

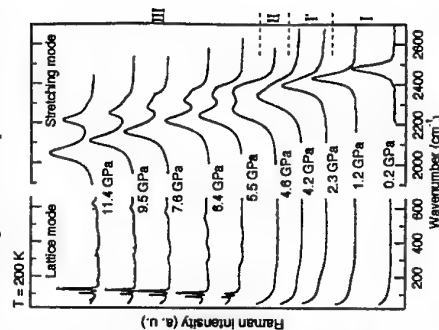


Fig. 1 Raman spectra obtained at 200 K for various pressures.

TEMPERATURE DEPENDENCE OF VIBRATIONAL SPECTRA IN GLASS
SUPERIONIC CONDUCTORS $(\text{AgI})_x-(\text{AgPO}_3)_{1-x}$

K. Wakamura, J. Katagi, and H. Takahashi*

Department of Applied Science, Okayama Science University
1-1 Ridai-cho, Okayama 700, Japan*Applied Physics Group, Faculty of Engineering, Ibaraki University,
4-12-1 Nakanarusawa, Hitachi 316, Ibaraki, Japan

Vibrational modes in superionic conductor (SIC) are noticed from the strong contribution of low energy optical (LEO) phonon to the high ionic conduction through the phonon-mobile ion coupling (1,2). The origin of such a LEO-phonon is attributed to the specific crystal structure of SIC(3). Associated with these results, we are interested in the vibrational modes in glass SIC because an intimate relation of the mode to the characteristics of glass SIC, that is high ionic conductivity at low temperature, is anticipated. However, the work of this field has not been studied enough.

In this report, we investigate the vibrational bands in glass SIC $(\text{AgI})_{0.5}-(\text{AgPO}_3)_{0.5}$ and AgPO_3 by measuring the temperature dependence of infrared reflectivity spectra from 20 to 4000 cm^{-1} under the temperature range from 20K to 400K. Specimen prepared were examined by the X-ray diffraction and thermal analyses. Observed Raman and infrared spectra are shown in Figs.1 and 2, respectively. We find a few bands in the infrared spectra near 1100 cm^{-1} which are not observed in the Raman spectra (4). For this different feature, we can consider the cluster about AgPO_3 phase having the vibrational dipole moments with the infrared and Raman active symmetry.

The frequency shift and damping constant of the bands are evaluated as function of temperature by the classical dispersion relation containing mobile ion term. Determined values show extremely small temperature dependency. These values are discussed in comparison with those of crystal SIC and discussed with respect to the characteristics of glass SIC.

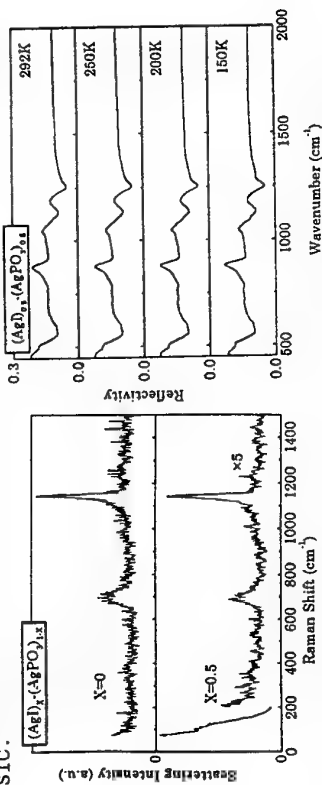


Fig.1 Raman spectra at room temperature

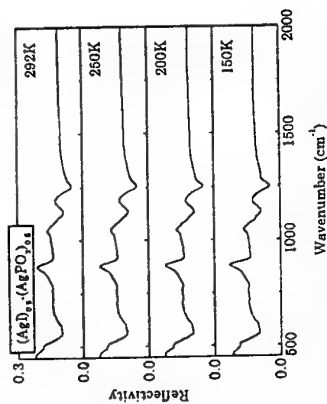


Fig.2 Temperature dependence of infrared spectra.

Refs.

1. K. Wakamura et al., J. Phys. Chem. Solids. 57(1996)75.
2. K. Wakamura, Phys. Rev. B56(1997)11593.
3. K. Wakamura, unpublished.
4. P. Benassi et al., Phys. Rev. B43(1991)1756

SPIN-PEIERLS TRANSITION IN α' - $\text{Na}_{1-x}\text{V}_2\text{O}_5$ OBSERVED BY RAMAN SCATTERING

H. Kurose, H. Sato, T. Sekine, M. Isobe*, and Y. Ueda*

Department of Physics, Sophia University, 7-1 Kioi-cho, Chiyoda-ku, Tokyo
102-8554, Japan*ISSP, The University of Tokyo, 7-22-1 Roppongi, Minato-ku, Tokyo 106-
8666, Japan

We have studied the spin-Peierls (SP) transition in α' - $\text{Na}_{1-x}\text{V}_2\text{O}_5$ ($\delta = 0, 0.01$ and 0.1) by means of Raman scattering. In the SP phase, several new peaks and a new broad band appear. The new peak at 62 cm^{-1} originates from the SP-gap excitation. The new peak at 128 cm^{-1} and the new broad band between 130 and 400 cm^{-1} probably come from the second-order magnetic Raman scattering. The new peaks at $102, 646$ and 944 cm^{-1} are assigned to the folded phonon modes. The Raman spectrum of the folded phonon mode at 944 cm^{-1} is observed both in the (a, a) and the (a, b) polarization configurations, indicating that the possible symmetry of the lattice below T_{SP} is monoclinic $C_2^2(Pn)$ or triclinic $C_1^1(P1)$. In α' - $\text{Na}_{0.99}\text{V}_2\text{O}_5$, the folded phonon modes broaden and weaken, and these are not observed in α' - $\text{Na}_{0.9}\text{V}_2\text{O}_5$. The Na^+ -ion deficiency works as a non-magnetic impurity doping and suppresses the SP transition.

GL2.1 (14.00)

MACROSCOPIC QUANTUM STATE OF TUNNELLING SYSTEMS

S. Hunklinger*, P. Strehlow**, C. Enss*

*Institut für Angewandte Physik, Albert-Ueberle-Straße 3-5

D-69120 Heidelberg, Germany

**Physikalisch-Technische Bundesanstalt, Abbestraße 2-12

D-10587 Berlin, Germany

In contrast to ideal dielectric crystals, which are well understood, glasses exhibit a large variety of interesting and surprising low temperature properties. Irregularities in their structure enable local structural rearrangements even at low temperatures, e.g. via the tunneling motion of small atomic clusters. This is the origin of low energy excitations which determine the thermal, elastic and dielectric properties of glasses at low temperatures.

With decreasing temperature the interaction between the tunneling systems becomes increasingly important. It leads to a transition from coherent to incoherent tunnelling motion resulting in a modification of the dynamic properties of glasses. At very low temperatures a new and totally unexpected phenomenon was found very recently. Below a critical temperature T_c of about 6 mK the dielectric constant of multicomponent glasses becomes highly sensitive to weak magnetic fields although slightly above that temperature the dielectric properties of these glasses are hardly influenced by strong magnetic fields even up to 20 T. In addition, the temperature dependence of the dielectric constants shows a kink at T_c . Both observations indicate the occurrence of a phase transition from a state of uncorrelated and incoherent tunneling to a highly correlated motion of a macroscopic number of tunneling systems. In addition, we have evidence that the low temperature dielectric properties of glasses in magnetic fields are also influenced by the interaction of the tunnelling systems with nuclear spins resulting in relaxation processes. The surprising new phenomena require an extension of the commonly used one-dimensional description of tunnel systems in glasses towards a three-dimensional tunnelling motion of charged particles in electromagnetic fields.

GL2.2 (14.30)

THERMODYNAMICALLY CONSISTENT DETERMINATION OF THE SPECIFIC HEAT OF VITREOUS SILICA DOWN TO 15 MILLIKELVIN

Peter Strehlow and Michael Meißner*

Physikalisch-Technische Bundesanstalt, Abbestraße 2-12, 10587 Berlin, Germany

*) Hahn-Meitner-Institut Berlin, Glienicke Straße 100, 14109 Berlin, Germany

Different theoretical models based on tunneling states have been proposed to explain the specific heat anomaly in glasses at temperatures below 1 K. The most controversially discussed problems concern the introduction of a time-dependent specific heat and the comparison of tunneling state parameters obtained in various heat-pulse and thermal relaxation experiments. The interpretation of all these dynamic measurements requires the solution of proper field equations for boundary and initial values which can be controlled by the experiment.

Based on the coupled Boltzmann equations for phonons and localized tunneling systems nonlinear field equations for phonon energy, tunneling system energy and phonon momentum have been derived. It is shown that the solution of these hyperbolic field equations for given boundary and initial values of heat-pulse experiments are in excellent agreement with new experimental data obtained in vitreous silica at temperatures down to 15 mK.

The experimental setup consists of a framed glass disk (Suprasil I), a point heater at the centre and two sputtered ringlike gold electrodes. The heat flux generated by the heater is assumed to be radially symmetric. Thus, the temperature profiles of heat-pulse experiments were recorded by in situ capacitance thermometry. This represents a direct method in order to determine the temperature of the tunneling states in glasses.

The fits of the heat-pulse profiles are sensitive to both the tunneling density of state \bar{P} and the minimal energy splitting $\Delta_{0,min}$. All heat-pulse profiles measured in Suprasil I at temperatures from 15 mK to 500 mK can be described by the parameter set $\bar{P} = 9 \times 10^{44} \text{ J}^{-1} \text{ m}^{-3}$ and $\Delta_{0,min}/k_B = 18 \text{ mK}$. The relative high value of the minimal energy splitting seems to correspond with a phase transition of tunneling states recently observed in multicomponent glasses.

In the thermodynamic field theory the specific heat of glasses is not explicitly time-dependent, but only depends on time via temperature. Its tunneling states part is given by

$$c_{v,ts}(T) = \frac{\bar{P} k_B^2 T}{\rho} \int_{\Delta_{0,min}/k_B}^{\infty} \left[2 \operatorname{Arctanh} \left(1 - \left(\frac{\Delta_{0,min}}{x k_B T} \right)^2 \right)^{1/2} + \left(1 - \left(\frac{\Delta_{0,min}}{x k_B T} \right)^2 \right)^{-1/2} \right] \frac{x dx}{\exp(x) + 1},$$

where ρ is the mass density. For temperatures $T \gg \Delta_{0,min}/k_B$ it holds

$$c_{v,ts}(T) = \frac{\pi^2}{6\rho} \bar{P} k_B^2 T \left[1.046 + \ln \left(\frac{2 k_B T}{\Delta_{0,min}} \right) \right].$$

INFLUENCE OF HIGH PRESSURE ON THERMAL PROPERTIES OF AMORPHOUS POLYSTYRENE

R. Geilenkeuser*, Th. Porschberg and M. Jäkel

Institut für Tieftemperaturphysik, TU Dresden, D-01062 Dresden, Germany

We investigated both the thermal conductivity λ and the specific heat c_p of amorphous polystyrene in the temperature range 1.7 K < T < 300 K at three different pressure values up to $p=0.4$ GPa. The measurements were performed in a self-clamping pressure cell, using cylindrical samples of $d = 8$ mm diameter and $l = 18$ mm length, embedded in a special oil as pressure transmitting medium. The thermal conductivity data show a visible influence of pressure over the entire temperature range. As the density of the sample increased under pressure, we corrected the data with a method described elsewhere [1] to separate only the pressure effect. After this correction an influence of pressure is still present at the typical plateau of λ at 2 K < T < 10 K. This means, pressure influences the scattering properties in this temperature range. According to the AHPV- and Soft-Potential-Model [2,3] [4] in amorphous solids phonons are scattered by localized Two-Level-Systems (TLS) and Soft-Modes (SM). We therefore fitted the thermal conductivity data, using the corresponding scattering mechanisms to obtain values for the model-parameters $\bar{P}\gamma^2$, γ and W , where \bar{P} is the mean density of TLS or SM, γ describes the coupling between phonons and TLS or SM and W is the crossover-energy between TLS and SM. The product $\bar{P}\gamma^2$ rises from 2.5×10^6 J/m³ at zero-pressure to 3.7×10^6 J/m³ at $p=0.4$ GPa. Fit results for γ reveal an increase by a factor of 5 with the pressure applied in our experiments, the coupling between phonons and TLS or SM becomes stronger. A similar behaviour of λ under pressure was found for two further polymers, Polycarbonate [1] and the epoxy-resin SC-8 [5]. In contradiction, vitreous silica shows the opposite behaviour: with increasing pressure λ is lowered in the plateau region [6]. This can be explained with the different sign of the Grüneisenparameter of vitreous silica and polymers which is supported by measurements of the velocity of sound v_s under pressure. For polymers, v_s increases with pressure whereas the contrary behaviour was found for vitreous silica.

Measurements of the specific heat c_p of amorphous solids show a typical bump, if c_p/T^3 is plotted versus temperature. This bump clearly decreases under pressure for polystyrene and the temperature of the maximum is slightly shifted to higher temperatures. Interestingly, a more detailed analysis of the data shows that the decrease of the bump is due to the lowered Debye contribution and pressure hardly influences the contribution of the TLS and SM.

- [1] R. Geilenkeuser, F. Weise, M. Jäkel Proceedings of the LT21, Czech. J. of Phys., 46, 2251 (1996)
- [2] P.W. Anderson, B.I. Halperin, C.M. Varma, Philos.Mag. 25, 1 (1972)
- [3] W.A. Phillips, J.Low Temp.Phys. 7, 351 (1972)
- [4] D.A. Parshin, Phys.Rev. B 49, 9400 (1994)
- [5] J.M. Grace, A.C. Anderson, Phys.Rev. B 40, 1901 (1989)
- [6] M. Jäkel, K. Wagner, E. Hegenbarth, Physica B 219 & 220, 308 (1996)

* supported by Deutsche Forschungsgemeinschaft through Ja 677/3-2

LOW FREQUENCY RAMAN SCATTERING IN BULK NEUTRON DISORDERED SILICON

C. Laermans¹ and M. Coeck^{1,2}

¹ : Katholieke Universiteit Leuven, Dept. of Physics, Celestijnenlaan 200 D, B-3001 Heverlee, Belgium
² : SCK-CEN, Dept. BR2, Boeretang 200, B-2400 Mol, Belgium

It is well established by several experiments that the universal properties of glasses differ from those in their crystalline counterparts. The low-temperature anomalies, can be described by the tunneling model [1], putting forward the presence of tunneling states with a wide distribution of energy and relaxation times and an almost constant density of states in glasses. Above a few Kelvin the universal properties of glasses deviate from the predictions of the tunneling model. One of the features that can not be explained by this model is the low-frequency Raman scattering. A successful description of this so-called boson peak is given by the soft potential model [2] which is based on the idea that besides two level systems there also exist soft harmonic oscillators.

We have performed Raman scattering experiments on neutron-irradiated bulk silicon in a frequency range from 50 till 600 cm⁻¹, both at room temperature and liquid nitrogen temperature. From the rise of an amorphous band at 490 cm⁻¹ in the irradiated samples together with a decrease of the crystalline peak at 520 cm⁻¹ it is clear that due to fast neutron irradiation the silicon samples become partially amorphous. From the ratio of the integrated intensities of the amorphous and crystalline band an amorphous volume fraction of 4.1 % was calculated for an irradiation dose of 3.2×10^{21} n/cm² [3].

At lower Raman frequencies, around 114 cm⁻¹, a broad band was observed which we interpret as the boson peak. Several arguments can be invoked to support this idea. First of all we know that the investigated material is partly amorphous. The intensity I of the band scales with the Bose factor $n(\omega, T)+1$ and a plot of $I/n(\omega, T)+1$ as a function of ω is constant above 114 cm⁻¹, indicating that the product $C(\omega) \times g(\omega)$ is linear in ω above 114 cm⁻¹. This is a property which is seen in several glasses for frequencies above the boson peak. The position of the maximum at 114 cm⁻¹ is in contradiction to the value of 245 cm⁻¹ proposed by Ivanda et al. [4]. However, a comparison, made in the framework of the soft potential model, with a-SiO₂ where the boson peak is observed at 52 cm⁻¹ supports a maximum for silicon around 114 cm⁻¹.

- [1] P. W. Anderson, B. I. Halperin and C. M. Varma, Phil. Mag. 25 (1972) 1; W. A. Phillips, J. Low Temp. Physics 7 (1972) 351.
- [2] V. L. Gurevich, D. A. Parshin, J. Pelous and H. R. Schober, Phys. Rev. B 48 (1993) 16381; D. A. Parshin, Phys. Solid State 36 (1994) 991.
- [3] M. Coeck, C. Laermans, R. Provoost and R. E. Silverans, Mat. Sc. Forum, 258-263 (1997) 623-628.
- [4] M. Ivanda, I. Hartmann and W. Kiefer, Phys. Rev. B 51 (1995) 1567.

NS3.1 (14.00)

Dynamic Properties of Phonons in Superlattices

Shin-ichiro Tamura

Department of Applied Physics, Hokkaido University, Sapporo 060, Japan

This paper presents an overview of the temporal behavior of phonons propagating through superlattices. A periodic superlattice acts as an opaque barrier for phonons inside frequency gaps analogous to a potential barrier for electrons. We will discuss the time evolution of phonon packets incident normally on the superlattice. The packet assumed is sufficiently narrow in the frequency domain so that it may be effectively confined inside a frequency gap. Numerical simulations reveal a time advance for the phonon packet transmitted through a single-superlattice, while a large time delay is predicted for the phonon packet transmitted through a double-superlattice structure. For the systems consisting of semiconductor superlattices of the size of 1000 Å the time advance or delay of the transmitted and reflected packets range from 10 ps for a single-superlattice structure to 1 ns at resonances for a double-superlattice structure. These results are well described in terms of asymptotic phase times of phonons calculated analytically.

The interaction of phonons with surface vibrational modes in a periodic superlattice with a free surface is another topic discussed in this paper. A phonon incident on the superlattice from a substrate is perfectly reflected, i.e., the reflection rate is unity irrespective of frequency. However, it comes back to the substrate with a large time delay when the frequency coincides with an eigenfrequency of the surface mode. This result is attributable to the resonant interaction of incident phonons with a vibrational mode localized near the surface.

The case for phonon packets incident obliquely to the layer interfaces is also considered.

NS3.2 (14.30)

LIFETIMES OF ACOUSTIC PHONONS AND THERMAL CONDUCTIVITY IN SUPERLATTICES

M. Schmitt, A.P. Mayer, and D. Strauch

Institut für Theoretische Physik, Universität Regensburg,
D-93040 Regensburg, Germany

Motivated by recent experiments on coherent acoustic phonons in semiconductor superlattices [1], the intrinsic lifetime of acoustic phonons in two-component superlattices due to the anharmonicity of the interatomic interactions is calculated for different temperature/frequency regimes. In the hydrodynamic regime, the lifetimes are related to the thermal conductivities and phonon viscosities of the two materials forming the superlattice. In the Landau-Rumer regime, where collisions are negligible, and at zero temperature, quantitative calculations are carried out on the basis of nonlinear elasticity theory. Here, the layers constituting the superlattice have been chosen to be isotropic with respect to their linear elastic properties. The frequencies and the associated displacements of the acoustic phonons are calculated with the help of transfer matrices, and the cubic anharmonic coupling constants have been determined by using the second-order and third-order elastic moduli of the two constituents.

The long-scale periodicity in the direction normal to the plane of stratification in a superlattice gives rise to a special type of Umklapp processes [2] which involves low-frequency acoustic phonons. It can become relevant at low temperatures where ordinary Umklapp processes have become unimportant because of the smallness of thermal occupation numbers of the phonon modes involved. Results of a quantitative calculation of the thermal conductivity of a perfect two-component superlattice at low temperatures are presented, which are based on a Chapman-Enskog expansion of the phonon Boltzmann equation [3] involving the part of the Peierls collision operator that corresponds to these mini-Umklapp processes. The anharmonic coupling coefficients are again evaluated within nonlinear elasticity theory.

[1] A. Bartels, T. Dekorsky, H. Kurz, and K. Köhler, *Verhandl. DPG* (VI) **33**, 766 (1998).

[2] S.Y. Ren and J.D. Dow, *Phys. Rev. B* **25**, 3750 (1982).

[3] V.L. Gurevich, "Transport in Phonon Systems", (North-Holland, Amsterdam 1986).

STANDING ACOUSTIC WAVES IN GaAs/AlAs MIRROR-PLANE SUPERLATTICES AND CAVITY STRUCTURES STUDIED BY RAMAN SPECTROSCOPY

M. Giehler¹, T. Ruf², M. Cardona², and K. H. Ploog¹

¹ Paul-Drude-Institut für Festkörperelektronik, Hausvogteiplatz 5-7, D-10117 Berlin, Germany,

² Max-Planck-Institut für Festkörperforschung, Heisenbergstrasse 1, D-70569 Stuttgart, Germany

Longitudinal acoustic (LA) phonons in mirror-plane superlattices (MPSL's) and cavity structures have recently been studied by Raman spectroscopy [1]. In order to study interference and disorder effects in more detail we investigate MPSL's consisting of SL = (GaAs)₁₅/(AlAs)₁₀ and LS = (AlAs)₁₀/(GaAs)₁₅ units, arranged in (SL)_m/2/(LS)_m sequences ($m/2 = 5, 10, \text{ and } 20$) and cavity structures of the form (SL)₁₀/(GaAs)₁₀/(LS)₁₀ ($9 \leq n < 600$).

The main feature in the spectra of MPSL's is a splitting of each component of the folded LA-phonon doublets into two lines. In the spectra of short-cavity structures (thickness (GaAs)_n = D_{cav} ≈ thickness SL unit) the character of the doublet components changes from unsplit to split depending on D_{cav} . Structures with long cavities (D_{cav} ≈ length (LS)_m block) always exhibit a splitting, where the number of split lines increases with increasing cavity length. Furthermore, all spectra display equidistant satellites, and the Brillouin line is always unsplit. These features can be explained by standing LA-vibrational excitations and the phase shift as well as interference between the fields scattered from the (SL)_m/2 and (LS)_m blocks. For destructive interference (mirror-symmetric structures), a split into an even number of lines occurs, whereas for constructive interference (periodic structures), a split into an odd number of lines is observable. The number of satellites is mainly determined by $m/2$. The measured spectra can be described by the transfer-matrix formalism assuming photoelastic scattering from standing LA-vibrations. This approach also shows that the influence of LA-phonon transmission resonances (gap modes) on Raman spectra is very small.

Fluctuating layer thicknesses cause a stronger broadening of the doublets of periodic superlattices than of the split lines of MPSL's, whereas the Brillouin linewidth does not depend on such type of disorder. In contrast, the attenuation of the exciting and scattered laser light in MPSL's due to absorption smoothes the interference-split lines much more than the pure folded-phonon doublets of superlattices.

[1] M. Giehler, T. Ruf, M. Cardona, and K.H. Ploog, Phys. Rev. B **55**, 7124 (1997).

ANION-RELATED DIFFERENCES IN THE PHONONS OF (GaY)_m/(Ga_{1-x}Al_xY, Y=As, N) SUPERLATTICES

Devki N. Talwar and S. Zaraneek

Department of Physics, Indiana University of Pennsylvania
Indiana, PA 15705 -1087, USA

The cubic phase of group III-nitride semiconductors (GaN, AlN and InN) represents an unexplored material system whose properties can be quite different from those of its wurtzite counterpart. For instance, it has been suggested that the zinc-blende AlN exhibits an indirect band gap ($\Gamma \rightarrow X$) which is approximately ~ 1 eV lower than the wurtzite polytype. The electronic and thermal properties of cubic GaN are expected to be superior than those of the wurtzite material resulting from the reduced phonon scattering in the higher symmetry crystal. These features may allow higher levels of p -doping in cubic crystals, essential in current injection-based optoelectronic devices which has to date proved difficult in the wurtzite materials. As the capabilities of growing cubic group III-nitrides have been demonstrated in recent years [1], it is timely to investigate the electronic and vibrational properties of their quantum well and superlattice structures. Quite recently, Grille and Bechstedt [2] studied the phonon properties of cubic GaY/Al_xGa_{1-x}Y superlattices (SLs) by using a 3-parameter Keating model. In this simplified scheme, aside from the long wavelength optical phonons the values of acoustical and optical modes at the edge of the Brillouin zone are generally over estimated. As the optical and acoustical modes overlap in GaN and AlN, the description of phonon folding and interface characteristics in the GaN/AlN SLs requires a lattice dynamical scheme capable of describing accurately the critical-point phonon frequencies for the bulk materials. The purpose of the present work is to report the results of a microscopic lattice dynamical study of phonons in cubic GaY, AlY, Ga_{1-x}Al_xY alloys and (GaY)_m/(Ga_{1-x}Al_xY)_n SLs based on a second-neighbor rigid-ion model (RIM). This study permits the construction of a dynamical matrix entering into the secular equation for the SL vibrations of a given wavevector, directly from the dynamical matrices of the bulk materials. The optimization of short-range forces in the RIM has become possible due to the availability of infrared and first- and second-order Raman data of phonons at critical-points and the elastic constant values for GaY, AlY and Ga_{1-x}Al_xY [3]. The influence of composition and disorder in Ga_{1-x}Al_xY is described within a random-element isodisplacement model generalized to layered structures with arbitrary wavevectors and composition profiles. The long-range electrostatic (Coulomb) forces are obtained exactly by using the Ewalds transformation method. For ultra thin superlattices, the dependence of phonons on wavevectors both parallel and perpendicular to the growth direction [001] are investigated. Remarkable differences between the lattice dynamical properties of As- and N-based SLs are observed. Theoretical results for the GaN/AlN superlattices are compared and discussed with the GaAs/AlAs system as well as with the existing model calculations [2]. Unlike GaAs/AlAs, the larger optical phonon values and partially changed confinement characteristics in GaN/AlN superlattices are believed to have significant effects on the relaxation properties of electrons in group III-nitride material systems. Impurity vibrational modes in GaY and AlY due to Si-donor and Mg-acceptor impurities are also examined in the Green's function framework and the results are compared and discussed with the existing infrared and Raman data.

[1] For recent reviews see for example, S. Strite, M. E. Lin, and H. Morkoc, *Thin Solid Films* **231**, 197 (1993); R. F. Davis, *Physica B* **185**, 1 (1993).

[2] H. Grille and F. Bechstedt, *Journal of Raman Spectroscopy* **27**, 201 (1996).

[3] A. Cros et al. *Solid State Commun.* **104**, 35 (1997); A. F. Wright, *J. Appl. Phys.* **82**, 2833 (1997).

GL3.1 (09.00)

DYNAMICS OF INTERACTING TUNNELING DEFECTS

Alois Wuerger

Institut Laue-Langevin, Avenue des Martyrs B.P. 156
F - 38042 Grenoble Cedex 09

Tunnel systems in crystalline and amorphous solids show a variety of surprising low-temperature properties. The dynamical behaviour is influenced by coupling to lattice vibrations and the dipolar interaction of nearby defects, resulting in energy dissipation and loss of phase coherence. We discuss the role that dipolar interactions play for the dynamics of substitutional defects in alkali halides (KCl:Li, NaCl:OH₂, ...). At low concentration, the impurities perform coherent oscillations between well-defined tunneling states. With increasing impurity density, the dipolar interaction perturbs this coherent motion and drives a cross-over to collective relaxation. A similar effect occurs in oxide glasses, where the elastic interaction of the two-level systems strongly influences the tunneling dynamics at temperatures below 100 mK.

GL3.2 (09.30)

PHONON GENERATION BY CARRIER RECOMBINATION IN A-Si:H

M. van der Voort, G.D.J. Smit, A.V. Akimov*, J.I. Dijkhuis

Department of Condensed Matter, Debye Institute, Utrecht University, P.O. Box 80.000,
3508 TA Utrecht, The Netherlands

Intense optical interband excitation of amorphous semiconductors is followed by fast carrier cooling and nonradiative recombination, giving rise to the creation of nonequilibrium optical and acoustic phonons. The study of the spectral, spatial and temporal evolution of these nonequilibrium phonons provides important information on the dynamics of both phonons (transport, elastic and inelastic scattering) and electrons (kinetics of carrier relaxation and nonradiative recombination). In this work we concentrate on the phonon generation produced by carrier recombination, a process not yet understood in a-Si:H.

For samples we used 1.0- μm thick a-Si:H films, grown by plasma enhanced chemical vapor deposition (PECVD) and hot-wire assisted chemical vapor deposition (HW), both on crystalline silicon substrates. The samples were immersed in superfluid Helium (1.8 K). Interband excitation was produced by the 10-ns pulses of two frequency doubled Nd:YAG lasers with a repetition rate of 30 Hz and average intensity in the focus of 30 mWcm^{-2} . Pulses of one 'probe' laser had been electronically delayed to those of the other 'pump' laser. The integrated spectral intensity of nonequilibrium phonons was measured by means of an anti-Stokes Raman scattering scheme. By changing the delay between pump and probe pulses, dynamics of nonequilibrium phonons could be investigated in the wide range of 10 ns up to 15 ms.

We obtained a fast ($\ll 10$ ns) decay time of the TA-phonon population and a relatively long (70 ns) decay time for the optical phonons in all the samples studied. Such behavior was observed earlier and explained in terms of phonon localization effects¹. In the PECVD samples, we observed for the first time an additional contribution to the Raman signal of both optical and acoustic phonons, which extends to the millisecond regime. This additional signal was not observed in the HW samples, and is demonstrated to be of electronic origin.

In order to explain the additional contribution to the phonon signal, we analyse the nonradiative recombination process. We propose a model that successfully describes our results, in which the phonons are emitted as a result of nonradiative recombination of free carriers and carriers localized in the tail states. In absence of optical pumping, the lifetime of carriers in the tail states is known to be ~ 1 ms. Therefore, the population of tail states reached during the pump pulse, will be stored until the probe pulse arrives. In this way, tail states filled by the pump pulse give rise to the additional phonon generation by nonradiative recombination of carriers generated by the probe pulse. We believe that the absence of the additional signal in HW samples is due to slower carrier relaxation from free to localized states in these materials.

*Permanent address: A.F. Ioffe Physical-Technical Institute, 194021 St. Petersburg, Russia

¹A.J. Scholten, A.V. Akimov, and J.I. Dijkhuis, Phys. Rev. B **47**, 13 910 (1993);
A.J. Scholten and J.I. Dijkhuis, Phys. Rev. B **53**, 3837 (1996).

PHONONS AND FRACTONS IN THE VIBRATION SPECTRUM OF THE RELAXOR FERROELECTRIC $\text{PbMg}_{1/3}\text{Nb}_{2/3}\text{O}_3$

S.G. Lushnikov, S.N. Gvasaliya and I.G. Siny

A.F. Ioffe Physical Technical Institute, Russian Academy of Sciences,
194021, St. Petersburg, Russia

In our report we present the results of investigation of the vibration spectrum of the model relaxor ferroelectric $\text{PbMg}_{1/3}\text{Nb}_{2/3}\text{O}_3$ (PMN) by Raman and neutron scattering.

The generalized density of states (DOS) has been measured in the powdered PMN compound by inelastic neutron scattering (INS) in the temperature range from 300 K down to 50 K. The INS experiments were performed on a time-of-flight inverse geometry spectrometer KDSOG - M at the fast pulsed reactor IBR-2 (Dubna, Russia). One-phonon approximation was used to calculate the generalized DOS from the measured INS spectra. The temperature degeneracy factor was excluded from generalized DOS to clarify an expected critical contribution to the temperature evolution of DOS.

Analysis of the low-energy part of DOS allowed us to obtain the character of the power law (spectral dimensions) of DOS in the energy range up to 10 meV. We obtained changes in the spectral dimension from $d = 2.9$ to $d = 1.7$ at $T = 50$ K and from $d = 2.8$ to $d = 1.9$ at 77 K. In present report we would like to discuss: 1) the possibility of fractal structures participating in the unique evolution of such relaxors like PMN to a ferroelectric state; 2) a complicated structure of the low-frequency part of Raman spectra of the PMN crystal appearing as a result of contribution of the fractons to the vibrational spectrum of considered compound.

This work was supported by RFBR No. 96-02-17859.

SPIN-GLASS APPROACH TO LOW-TEMPERATURE ANOMALIES IN GLASSES

Uta Horstmann and Reimer Kühn

Institut für Theoretische Physik, Universität Heidelberg
Philosophenweg 19, 69120 Heidelberg, Germany

A spin-glass type approach to the physics of structural glasses¹ is discussed. Its key idea is based on a Born von Karman type expansion of the interaction potential about a set of reference positions, in which we model the glassy aspects by taking the harmonic contribution within this expansion to be random. We derive the justification for such a procedure from the observation of universality: since the low-temperature anomalies observed in amorphous systems are apparently to a large extent insensitive to the detailed form of the interaction, any interaction might be taken as a starting point, as long as it does give rise to a glassy low-temperature phase. Moreover, several groups have recently stressed the fundamental similarity between self-induced disorder, as it occurs in glasses proper, and the truly quenched disorder on which our analysis is based².

Our approach leads to a class of models of spin-glass type³ which exhibit both, glassy low-temperature phases, and double- and single-well configurations in their potential energy. The distribution of parameters characterizing the local potential energy configurations can be computed, and differ from those assumed in the standard tunneling model and its variants. Still, the low-temperature anomalies characteristic of amorphous systems are reproduced, and we are able to distinguish properties which can be expected to be universal from those which cannot. Our theory also predicts the existence, under suitable circumstances, of amorphous phases without low energy tunneling excitations. Recent experiments of Liu et al.⁴ are discussed in this context.

Specifically, we compute phase diagrams, the glass transition temperature, excitation spectra in local potential energy configurations, densities of state, the low-temperature specific heat, which comes out linear at low T and which exhibits the typical bump in $C(T)/T^3$, and we consider the interaction between localized excitations and a heat bath provided by Debye phonons.

1. R. Kühn, in: *Complex Behaviour of Glassy Systems*, Proceedings of the XIVth Sitges Conference, edited by M. Rubi, Springer Lecture Notes in Physics (Springer, Berlin, Heidelberg, 1996); R. Kühn and U. Horstmann, Phys. Rev. Lett. **78**, 4067 (1997); R. Kühn and U. Horstmann, *A New Look at Low-Temperature Anomalies in Glasses*, preprint Heidelberg, to appear in Festkörperprobleme/Advances in Solid State Physics (1998)
2. T. Kirkpatrick and D. Thirumalai, J. Phys. A **22**, L149 (1989); J.P. Bouchaud and M. Mézard, J. Phys. I (France) **4**, 1109 (1994); E. Marinari, G. Parisi, and F. Ritort, J. Phys. A **27**, 7615 (1994); — ibid. 7647 (1994)
3. D. Sherrington and S. Kirkpatrick, Phys. Rev. Lett. **35**, 1792 (1975)
4. X. Liu, B.E. White Jr., R.O. Pohl, E. Iwanizko, K.M. Jones, A.H. Mahan, B.N. Nelson, R.S. Crandal, and S. Veprek, Phys. Rev. Lett. **78**, 4418 (1997)

NT1.1 (09.00)

SCANNING ACOUSTIC MICROSCOPY WITH VECTOR CONTRAST

W. Grill, K. Hillmann*, T. J. Kim, O. Lenkeit, J. Ndop, M. Schubert

Institut für Experimentelle Physik II der Universität Leipzig

Linnéstr. 5, D-04103 Leipzig, Germany

* Forschungszentrum für Medizintechnik und Biotechnologie e.V., Geranienvweg 7

D-99947 Bad Langensalza, Germany

Based on the developed high resolution phase and amplitude contrast (vector contrast) for scanning acoustic microscopy [1] in the frequency regime up to 2 GHz, a variety of novel schemes, capable to collect spatially resolved information on the mechanical properties of the observed objects has been developed. This includes high resolution acoustic topography in the reflection mode, imaging of the absorption and velocity of ultrasonic waves by surface focused transmission microscopy and the observation of dynamic processes and heat transport by differential phase contrast with single or multiple imaging.

Applications concerning the characterisation of various materials including biological or medical samples are presented. Limiting effects, new schemes of vector-image processing and results of combinatory microscopy including force and near field acoustic microscopy are demonstrated.

[1] W. Grill, K. Hillmann, K. U. Würz, J. Wesner.

Scanning Ultrasonic Microscopy with Phase Contrast.

In: Advances in Acoustic Microscopy, Volume 2, edited by A. Briggs and W. Arnold
Plenum Press, New York 1996, pages 167-218

NT1.2 (09.30)

SCANNING SECOND SOUND MICROSCOPY WITH VECTOR CONTRAST

S. Knauth, K. Hillmann, and W. Grill

Institut für Experimentelle Physik II der Universität Leipzig,

Linnéstr. 5, D-04103 Leipzig, Germany

A scanning confocal second sound microscope operating in liquid helium has been developed. The principal of operation is similar to scanning confocal laser microscopy or scanning acoustic microscopy with amplitude and phase contrast but second sound waves are employed for imaging. The contrast does therefore depend on the heat transport characteristics of the observed samples including the helium-sample interface.

The developed microscope is based on focusing spherical transducers. Meandrically structured evaporated granular aluminium film deposited in a spherical cap of an acrylic glass substrate have been employed as transducers. For generation the film is electrically heated by a pulsed oscillatory electrical current. The film is subsequently operated as a superconducting bolometer for detection. The aperture angle of the focusing transducer device is about 55°. The working distance is in the range of 1.5 mm. The microscope is operated in a liquid-⁴He immersion cryostat in the temperature range of 1.3 K to 2 K. Second sound with a frequency of 125 kHz correlating to a wavelength of about 160 µm has been employed.

Images in phase and amplitude contrast are obtained by scanning the focusing transducer in two dimensions. Based on this data three dimensional representations of reflecting surfaces are constructed. For structured samples observed in the reflection mode a lateral resolution of 170 µm and a height resolution of 5 µm is demonstrated. For electrically heated emitting samples, a lateral resolution of 210 µm was observed. The basic detection schemes are presented and examples for applications are demonstrated.

PHYSICAL AND GEOMETRICAL OPTICS OF PHONONS

D. J. Dieleman, A. F. Koenderink, M. G. A. van Veghel, M. A. de Vries,
A. F. M. Arts, and H. W. de Wijn

*Faculty of Physics and Astronomy, and Debye Research Institute,
Utrecht University, P.O. Box 80000, 3508 TA Utrecht, The Netherlands*

We have performed experiments on the physical and geometrical "optics" of phonons in the frequency range 1–5 GHz by the use of a recently developed technique generating narrow Fresnel-diffracted monochromatic phonon beams [1]. The specimen is a single crystal of lead molybdate (PbMoO_4). The phonons, of longitudinal polarization and propagating along the c axis, are generated by periodic heating of a thin (400–900 nm) Au transducer deposited onto a (001) surface. This heating is in turn achieved by interference of two cw single-frequency dye lasers, whose beams are focused on the Au film to a spot 40- μm in diameter. The generated acoustic beam, having a frequency equal to the difference frequency of the lasers, is detected via Brillouin scattering, which is selective for the direction of propagation, and enables in-situ measurement of the acoustic power as a function of the distance from the transducer. This permits to extract both the phase and group velocities.

Sweeping the phonon beam. Introducing an angle between the interfering laser beams results in a sideways traveling spatial modulation of the heating, and thus a lateral component of the phonon wavevector. The direction of the phonon beam, i.e., the acoustic group velocity, may be swept over as many as $\pm 15^\circ$. The group and phase velocities are found to be in conformity with the slowness surfaces calculated from the elastic anisotropy of the crystal.

Multiple slits. A transducer in the form of a microscopic Au grating rather than a uniform film leads to the phonon equivalent of optical Fraunhofer diffraction by multiple slits. The angles at which the spectral orders arise as well as their intensities appear to agree with ordinary diffraction theory, provided due account is taken of phonon focusing. The wavevector selectivity of Brillouin spectroscopy furthermore permits to measure the phonon-focusing parameter.

Phonon lens. We further considered the situation in which the foci of the interfering laser beams do not coincide, but are mutually shifted along the beam axis. The resulting curvature of the wave fronts at the transducer induces radially symmetric phase shifts in the periodic heating, which are passed on to the phonon beam. The effects are analogous to a positive phonon lens positioned at the transducer, i.e., the phonon beam first narrows to a waist and subsequently diverges by Fresnel diffraction.

Transmission by a superlattice. Finally, we measured the frequency dependence of the transmission of the phonon beam through a superlattice of alternating Au and Ag layers. Good agreement was obtained between the measured spectra and the calculated transmission with inclusion of phonon damping. Several stop bands were discerned.

[1] E. P. N. Damen, A. F. M. Arts, and H. W. de Wijn, Phys. Rev. Lett. 74, 4249 (1995).

SCANNING PHONONIC LATTICES WITH ULTRASOUND*

R.E. Vines and J.P. Wolfe

Physics Department and Materials Research Laboratory
University of Illinois at Urbana-Champaign, Urbana, IL 61801

Abstract

Photonic lattices have received wide attention in the last few years. The existence of frequency gaps for electromagnetic waves in these periodic structures has potential for modifying the radiative strength of optical transitions and for manipulating microwaves and light beams. Analogous to photonic structures are phononic lattices, which support vibrational waves in elastic media.

We introduce a method for probing the elastic properties of periodic structures with acoustic waves. Highly anisotropic ultrasonic transmission of surface acoustic waves is observed by continuously scanning the wavevector angle. We examine the properties of two basic phononic structures – a multilayer and a 2D hexagonal lattice. Preliminary models of wave propagation through these structures explain general features of the experimental results, such as the existence of frequency gaps and wave channeling along certain directions, but the details require more realistic modeling of surface acoustic waves in elastically modulated media.

*Research supported by Department of Energy grant DOE 45439.

EP2.1 (10.50)

EXCITON-PHONON INTERACTION IN QUANTUM WELLS

A.F.Ioffe *Physical-Technical Institute, 194021 St.Petersburg, Russia*
A.V.Akimov

At low temperatures photo-excited electrons and holes can be bound to free quasiparticles, the so-called excitons. In two-dimensional (2D) semiconductor structures the interaction of such excitons with acoustic phonons is strongly modified in comparison to bulk material due to the lateral confinement of carriers. Phonons remain 3D and the electron confinement breaks down the momentum conservation for exciton-phonon transitions in the direction perpendicular to the plane of 2D layer.

In this talk we present the results of nonequilibrium phonon experiments where the exciton-phonon interaction in GaAs/AlGaAs quantum wells (QWs) was studied by phonon-induced changes in the luminescence [1]. Nonequilibrium phonons are generated in the constant heater, pass through the GaAs substrate, reach 2D excitons in the QW created by cw Ar-ion laser excitation, and produce phonon-induced changes in the exciton luminescence spectrum. So it was revealed that the effective temperature of the 2D excitons in the presence of nonequilibrium phonons depends on the QW width, d , and exciton density, n_x . For low $n_x < 10^9 \text{ cm}^{-2}$ the 2D excitons appeared to be heated more effectively in wide ($d > 10 \text{ nm}$) QWs. In contrast, for high $n_x > 10^{10} \text{ cm}^{-2}$, the temperature of the 2D exciton in the presence of nonequilibrium phonons increases with the decreasing d . The experimental results were analysed by solving the kinetic equation for the exciton energy distribution function in the presence of nonequilibrium phonons [2]. The phonon distribution was taken anisotropic in q -space prescribed by the geometry of the experiment. Further the high-energy cutoff due to scattering of phonons in GaAs substrate was taken into account. A good agreement with experiment is obtained. The analysis leads to the conclusion that the dependence on the QW width of the effective temperature reached by the 2D excitons can be traced back to the angular and energy dependence of the matrix elements for the exciton-phonon interaction. We find in wide QWs that the range of phonon energies active in the exciton-phonon interaction is smaller and the angular momentum distribution of active phonons is wider in comparison with narrow QWs.

We also studied asymmetric double QWs. The acoustic phonon-assisted tunneling transitions between four (two direct, DX, and two indirect, IX) exciton states were examined by the luminescence for wide range of temperature (5 - 40 K) and applied electric fields [3]. We show that for the case of a hole in the same QW the pairs of DX and IX are in thermal equilibrium while for excitons with a hole in a different QWs, thermal equilibrium is not reached during the exciton lifetime ($\sim 10^{-9} \text{ s}$). We conclude that phonon-assisted tunneling transition is fast ($< 10^{-9} \text{ s}$) for "excitonic" electrons and slow for "excitonic" holes.

Finally, the exciton luminescence was used to detect nonequilibrium phonons in CdTe QWs with semimagnetic CdMnTe barriers in an external magnetic field [4]. In these experiments the interaction of phonons with Mn ions turns out to reduce the giant Zeeman splitting of the exciton states in QW and to change the exciton luminescence spectrum. The results show that our method has a potential to perform sensitive high resolution phonon spectroscopy.

References:

- [1] E.S.Moskalenko et al. *Ann Physik* **4**, 127 (1995)
- [2] L.E.Golub et al. *J.Phys.:Condens. Matter* **8**, 2163 (1996)
- [3] A.V.Akimov et al. *Phys.Stat.Solids b* **204**, 400 (1997)
- [4] A.V.Akimov et al. *Phys.Rev.B* **56**, 12100 (1997)

EP2.2 (11.20)

Spectroscopic evidence for cyclotron phonon emission from Si-MOSFETs in strong magnetic field

S. Roshko^(a,e), W. Dietsche^(a) and L.J.Challis^(b)
(a) Max-Planck-Institut für Festkörperforschung, Stuttgart, Germany
(b) Physics Department, University of Nottingham, U.K.

Spectroscopic investigations of the phonon emission from two-dimensional electron gases (2DEG) in high magnetic fields were more or less impossible in the past because of the lack of suitable phonon spectrometers. Therefore, for example, it was not possible to establish if the phonons emitted in the quantum-Hall-effect (QHE) regime had energies corresponding to the cyclotron-resonance energy or not. Here, we present new experiments on 2DEGs in Si-MOSFET structures in which we use the intrinsic doping of the substrate as a threshold detector with which we establish that phonons emitted in the QHE state fulfill indeed the cyclotron resonance-condition.

Our substrates contain 10^{13} cm^{-3} Boron acceptors which were partially converted into B^+ centers (boron atoms with an additional hole) by illumination with visible light. Acoustic phonons with energies exceeding a threshold of about 2 meV neutralise these centers and lead to a conductivity increase [1]. The threshold energy increases weakly with magnetic field as was established independently [2]. In the experiment, current is passed through the 2DEG leading to phonon emission and its effect on the photo-conductivity of the substrate is monitored simultaneously. With increasing magnetic field we observe a clear signal onset when the cyclotron energy of the 2d electrons crosses the detection threshold of the B^+ centers of the substrate. This can only be explained by the presence of cyclotron-resonance phonons. Tilting the sample decreases the cyclotron energy and leads to a shift of the onset magnetic field as expected. However, the cyclotron phonon emission is particularly large only if the 2DEG is in the QHE state. This is surprising at first since the electron transport is nearly dissipationless in the bulk of the 2DEG. Therefore the cyclotron phonons are emitted by the two "hot spots" which are located in two opposite corners of the current contacts. These hot spots must be heated to temperatures of the order of the cyclotron energy ($\approx 2 \text{ meV}$) for the cyclotron emission to occur because otherwise no transitions between the Landau levels are possible. From the known relation between electron temperature and dissipated power density we can estimate the size of the hot spots and arrive at reasonable values of 10 to 50 μm depending on current. Outside the QHE state, the balance between phonon emission and power dissipation is achieved at lower electron temperatures, therefore the cyclotron phonon emission is much less likely.

The cyclotron emission in the QHE state increases roughly linearly with current for small currents but shows a distinct kink towards less emission at a current which is still much less than the breakdown current for the QHE. This indicates that the emission processes of the hot spots change with current in a regime where there are no measurable effects in the electric transport measurements. We suspect that a part of the dissipation does now take place in the contacts themselves instead of the 2DEG.

(c) permanent address: Ukrainian Academy of Science, Kiev, Ukraine
[1] W. Burger and K. Lassmann, *Phys. Rev. Lett.* **53**, 2035 (1984)
[2] S. Roshko and W. Dietsche, *Sol. State Comm.* **98**, 453 (1996)

ELECTRON-PHONON INTERACTION IN DISORDERED CONDUCTORS

A. Sergeev^{1,3}, B.S. Karasik^{2,3}, N.G. Pitsina³, G.M. Chulkova³,
K.S. Il'in³, and E.M. Gershenzon³

¹ Dep. of Physics, University of Regensburg, D-93040 Regensburg, Germany

² Jet Propulsion Laboratory, Pasadena, CA 91109, USA

³ Moscow Pedagogical University, Moscow 119482, Russia

Interrelation between the elastic electron scattering from impurities, defects, bound-aries ($1/\tau$) and the inelastic electron-phonon scattering ($1/\tau_{e-ph}$) has been puzzled people working in this area for years. We discuss the current status of the problem and suggest an explanation of experimental data obtained at helium temperatures.

Recently there has been significant progress in understanding of the electron-phonon interaction in metallic films with a small value of the electron mean free path. It was found that the resistance of Au, Al, Nb, Be and NbC films contains a significant T^2 -contribution that is proportional to the residual resistance [1]. This contribution is attributed to the interference between electron-phonon and elastic electron scattering. Fitting the data to the theory, we obtained the constants of effective electron coupling with longitudinal and transverse phonons (effect of transverse phonons dominates in impure conductors). These constants allow us to evaluate the inelastic electron-phonon scattering rate, which is found to be in excellent agreement with the electron dephasing rate measured at $T \geq 10K$.

At lower temperatures the inelastic scattering rate is determined from experiments with hot electrons, where thin films should be used. At helium temperatures different dependencies of $1/\tau_{e-ph}$ on temperature and $1/\tau$ have been measured.

Theoretical description of the interaction in disordered systems is complicated. Besides 'pure' electron-phonon scattering, there is an additional basic process: inelastic electron scattering from vibrating impurities or boundaries. This mechanism generates a wide variety of the interference processes, however, in an impure bulk metal leading scattering processes neglect each other at low temperatures [2]. Cancellation of leading processes may be incomplete in strong nonhomogeneous systems such as thin films. For example, if impurities or defects in the thin film are acoustically connected with a substrate stronger than with film phonons, and the sound velocity in the substrate is significantly larger than in the film, impurities and defects may be considered as quasistatic. According to Ref. 3, in this case $1/\tau_{e-ph} \propto 1/\tau$, while for an impure bulk metal it is expected that $1/\tau_{e-ph} \propto \tau$ [2,4].

The research of A.S. is supported by the Alexander von Humboldt Stiftung.

[1] N.G. Pitsina, G.M. Chulkova, K.S. Il'in, A.V. Sergeev, F.S. Pochinkov, E.M. Gershenzon and M.E. Gershenzon, Phys. Rev. B 56 10089 (1997).

[2] M.Yu. Reizer and A.V. Sergeev, JETP, 63, 616 (1986).

[4] B.L. Altshuler, JETP 75, 1328 (1978).

[3] A. Schmid, Z. Phys. 259, 421 (1973).

ELECTRON-PHONON DYNAMICS IN METALS ON ULTRASHORT TIMESCALES

Oliver B. Wright¹, Peter L. G. Ventzek² and Vitaliy E. Gusev³

¹ Faculty of Engineering, Hokkaido University, Sapporo, Japan (and PRESTO, Japan Science and Technology Corporation (JST), Kawaguchi 332, Japan)

² Motorola, Predictive Engineering Laboratory, MD-K10, 3501 Ed Bluestein Blvd, Austin TX 78721, USA

³ Laboratoire d'Acoustique de l'Université du Maine, CNRS, Le Mans, France (and International Laser Center, Moscow State University, Russian Federation)

Analytic and numerical solutions for the ultrafast athermal relaxation of hot electrons in free electron metals after excitation with an ultrashort optical pulse have been obtained using the linearised Boltzmann equation including the effect of electron-electron (e-e) and electron-phonon (e-p) scattering terms. The analytical model gives predictions for the variation of the total nonequilibrium energy density (E) and electron number density (N) [1,2]. The evolution in space and time of the perturbed electron distribution depends on the ratio of the sample thickness d to the optical absorption depth ζ ; for $d/\zeta \ll 1$, as in a very thin film, conditions are approximately spatially homogeneous provided that no electrons diffuse out the sample; for $d/\zeta \gg 1$ the electrons can diffuse into the bulk. We have solved for both cases with a one-dimensional treatment. Here, we compare the analytical predictions to a numerical solution to the same problem under spatially homogeneous conditions, making use of a Monte Carlo technique.

The relaxation of the electrons is governed by the characteristic times for nonequilibrium electron energy loss (τ_E) and for thermalisation to a Fermi-Dirac distribution (τ_T). The analytical model predicts that the total excess energy, for times $t \lesssim \tau_E$ and temperatures above the Debye temperature, is given by

$$\frac{E}{E_V} = 1 - \left(\frac{t}{\tau_E} \right)^{3/2} + \beta \left(\frac{t}{\tau_E} \right)^3, \quad (1)$$

where $\tau_E = \tau_0^{1/3} \tau_3^{2/3} / \pi^{1/3}$, $\beta = (1 + 3\pi^2/16)/2\pi \approx 0.45$, and E_V is the initial excess energy. Here, τ_0 and τ_3 are the characteristic e-e and e-p scattering times. The electron number N is related to E through $\partial E / \partial t = -N e F / \tau_5$, where $e F$ is the Fermi energy. We find Eq. (1) to be in excellent agreement with the numerical calculations for $t \lesssim \tau_E$ (~ 0.75 ps for gold). In the analytical model the thermalisation time τ_T can also be derived for metals in which $\tau_T \ll \tau_E$ ($\tau_T \sim 0.5$ ps for gold at 300 K); we couple the athermal stage of the relaxation ($t < \tau_T$) with the thermalised stage ($t > \tau_T$) that makes use of the two-temperature model, a model in which the phonon and electron distributions are assumed to be separately thermalised. In contrast, the numerical model is based on the linearised Boltzmann equation that becomes less and less accurate as time progresses, eventually breaking down when the average energy per nonequilibrium electron becomes of the order of kT . Ways of improving the modelling are discussed.

[1] V. E. Gusev and O. B. Wright, Phys. Rev. B 57, 2878 (1998)

[2] O. B. Wright and V. E. Gusev, Physica B 219&220, 770 (1996)

PI1.1 10.50)

Direct Observations of Phonon Dispersion and Solitons in Crystal Lattices

Hsin-Yi Hao and Humphrey Maris

Department of Physics, Brown University, Providence, Rhode Island 02912

Although the dispersion relation of phonons in crystal lattices has been studied theoretically and experimentally for many years, direct observation of the effects of dispersion on phonon propagation has been difficult to achieve. We will describe recent experiments in which we have been able to observe the effects of dispersion on the propagation of longitudinal acoustic phonons. In these experiments we are also able to study the formation and propagation of solitons.

PI1.2 (11.20)

Step-Wise Multiphonon Anharmonic Decay of Local Modes:
Theory and Experiment

V. Hizhnyakov¹, M. Selg², R. Kink², M. Kink², J. Maksimov²

¹Institute of Theoretical Physics of Tartu University, Tähel 4, Tartu EE2400, Estonia

²Institute of Physics of Tartu University, Riia 142, Tartu EE2400, Estonia

Recently a nonperturbative theory of anharmonic relaxation of strongly excited local mode has been worked out [1, 2], which predicts explosion-like decay of the mode energy. The speed of two-phonon processes abruptly increases in the immediate vicinity of a critical amplitude and slowly diminishes towards larger amplitudes. Three and more phonon processes switch on jump-like at corresponding critical amplitudes and slow down monotonously with decreasing amplitude. The theory has been verified computationally and experimentally by studying the hot luminescence (HL) of self-trapped excitons in Xe crystal. The experiment was based on a novel method in spectroscopy of rare gas crystals - two-photon laser excitation (using an excimer laser emitting at 193 and 248 nm). In addition, HL spectra of solid Xe under X-ray excitation were recorded.

Quantum-mechanical calculation of Franck-Condon factors for the quasi-molecule Xe_2^+ has been carried out. HL starts on the level $n = 44$ and is situated between 6 and 8.3 eV (Fig. 1). The new relaxation theory was applied to the two-phonon decay allowed for the levels $n \geq 20$ only, while the three-phonon decay of the lower levels has been described within the frames of the standard perturbation theory. Good accordance between the experimental and calculated spectra proved that the vibrational relaxation rate of the quasi-molecule Xe_2^+ has a sharp maximum at an amplitude near 0.3 Å, which fully confirms the predictions of the new nonperturbative theory.

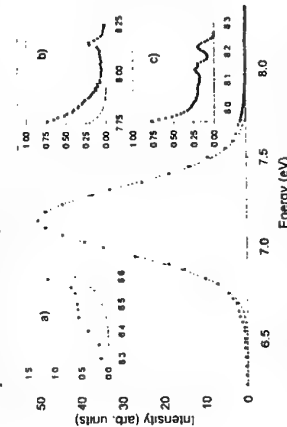


Figure 1. Experimental (dots) luminescence spectrum of a Xe crystal at $T = 10$ K: a and b - X-ray excitation, c - two-photon excitation with ArF excimer laser (193 nm). Dashed line corresponds to a Gaussian fit of the band.

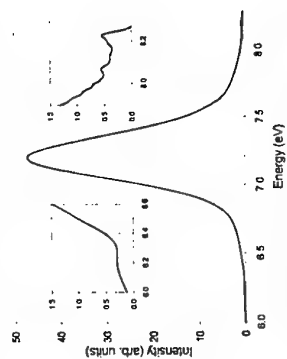


Figure 2. Calculated hot luminescence spectrum of the quasi-molecule Xe_2^+ in solid Xe.

1. V. Hizhnyakov, Phys. Rev. B 53, 13981 (1996).
2. V. Hizhnyakov, Z. Phys. B 104, 675 (1997).

FIRST PRINCIPLE CALCULATION OF THE REAL PART OF PHONON SELF ENERGY IN COMPOUND SEMICONDUCTORS

Alberto Debernardi and Manuel Cardona

Max-Planck-Institut für Festkörperforschung, Heisenbergstr. 1, 70569 Stuttgart,
Germany

In the last years an increasing amount of experimental data were collected concerning the Raman lineshape of phonon peaks in semiconductors. The main ingredients to determine the lineshape are: the harmonic frequency of the phonon mode *i.e.* the quadratic term in a Taylor expansion of the total energy with respect the phonon displacements of the atom from the equilibrium position, and the complex self energy which takes into account the higher order, anharmonic corrections. A theoretical computation of the phonon self energy can be of considerable help for interpreting the mechanisms which determine the asymmetry and linewidth of Raman peaks and their dependence on temperature and pressure. Twice the imaginary part of the phonon self energy is essentially the inverse of the phonon lifetime and is responsible for the linewidth of the Raman peak. An *ab initio* calculation of the imaginary part of the self energy was become available only recently.^[1]

In this work we present first principles calculations of the real part of the self energy for some compound semiconductors. Up to the leading order in the perturbative diagrammatic expansion the real part of the self energy at zero temperature consists of two contributions: one arising from the square modulus of the third order term in the energy expansion with respect to the phonon displacements, and a second one that is proportional to a forth order term. While it was generally believed that both terms can have the same order of magnitude we found that at zero temperature in the materials we have studied the former is the dominant contribution whereas the latter is considerably smaller. The effects due to anharmonicity will be thoroughly analysed and discussed together with the implicit term induced by the thermal expansion.

[1] A. Debernardi, S. Baroni and E. Molinari, Phys. Rev. Lett. 75, 1819 (1995).

PHONON-PHONON INTERACTIONS IN DISORDERED SYSTEMS

Michael R. Geller and W. M. Dennis

Department of Physics and Astronomy, University of Georgia, Athens, Georgia 30602-2451 USA

We study the effects of disorder and anharmonicity on acoustic phonons in the long wavelength limit. In the absence of disorder, the three-phonon anharmonic decay rate is found to vary with phonon energy according to the well-known ω^5 scaling. The presence of disorder, treated here in the second-order Born approximation, leads to an elastic (Rayleigh) scattering rate equal to $\tau_{el}^{-1} = \Delta(\omega/\Delta)^4$, where Δ is an energy scale that depends on the strength and nature of the disorder. The elastic scattering also leads to an enhancement of the anharmonic phonon decay rate, and, in addition, to a crossover—at energies less than Δ —from the ω^5 law to an ω^8 dependence, in agreement with the recent theoretical result of Bose *et al*.¹ The form of the crossover is found to be universal, independent of the strength of the disorder. Experimental implications will be discussed.

¹S. K. Bose, S. M. Kirkpatrick, and W. M. Dennis (preprint).

CP2.1 (09.00)

COHERENT ACOUSTIC PHONONS IN GaAs/AlAs SUPERLATTICESA. Bartels¹, T. Dekorsy¹, H. Kurz¹, K. Köhler²¹Institut für Halbleitertechnik II, RWTH Aachen, Sommerfeldstr. 24, D-52056 Aachen, Germany, E-Mail: bartels2@ih2-ii.rwth-aachen.de²Fraunhofer-Institut für Angewandte Festkörperphysik, D-79108 Freiburg, Germany

Acoustic phonons comprise a broad spectrum of low energy lattice excitations in a solid. In the semiconductor GaAs they cover the range from 0 to 30 meV. However, their investigation by light scattering experiments is limited to the μeV range because for momentum conservation reasons photons only couple to phonons, which are very close to the Brillouinzone-centre (BZ) centre. Semiconductor superlattices exhibit zone-folding of the bulk acoustic dispersion into the mini-BZ because of the artificial periodicity along the growth direction. In contrast to a bulk crystal, now acoustic modes with energies in the meV range appear at the BZ-centre and thus become accessible by light scattering experiments in principle. We impulsively generate a burst of those backfolded modes by a laser pulse of 50 fs duration, derived from a mode-locked Ti:sapphire laser and observe the lattice motion in amplitude and phase by means of time resolved pump-probe spectroscopy, detecting reflectivity and transmission changes.

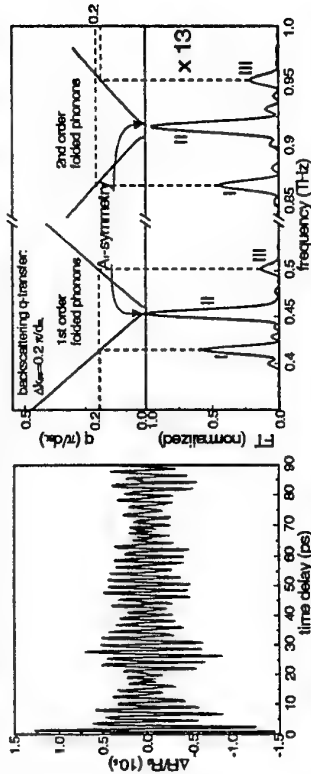


figure 1: Oscillatory component of the transient reflectivity changes in a $(\text{GaAs})_{19}(\text{AlAs})_{19}$ superlattice after excitation with a fs-laserpulse and the spectrum of the time resolved data. Three modes of each backfolded order are observed. We compare the spectrum to the calculated dispersion on top in order to identify the modes.

The vibrational contribution to the signal of a $(\text{GaAs})_{19}(\text{AlAs})_{19}$ superlattice is shown in fig. 1. A numerically obtained Fourier transform reveals three modes of first and second backfolded order around 0.45 THz and 0.9 THz. We identify the peaks comparing the spectrum to a dispersion, calculated with a model, treating the superlattice as layered elastic continuum [1]. The modes labelled I and III can be assigned to a backscattering excitation with twice the light k -vector. The central peaks of each order labelled II are A_1 modes at the BZ-centre. A second BZ-centre mode is not observed in agreement with selection rules discussed in ref. [2]. We calculate scattering intensities assuming a Raman interaction via the photoelastic effect and find good agreement with the experiment. This points towards impulsive stimulated Raman scattering as the driving process of coherent zone-folded acoustic phonons in semiconductor superlattices. A resolution of 1 GHz is yet achieved in the experiments, which is about an order of magnitude less than in high resolution Raman spectroscopy. The linewidths are in the range of 3 GHz, corresponding to dephasing times of approx. 110 ps.

[1] S.M. Rytov, Akust. Zh. 2 71 (1956)

[2] B. Jusserand, D. Paquet, F. Molloy, F. Alexandre and G. Le Roux, PRB 35 2808 (1987)

CP2.2 (09.20)

Study of coherent folded acoustic phonons in semiconductor superlattices by pump-probe technique

K. MIZOGUCHI¹, M. HASE¹, S. NAKASHIMA¹, and M. NAKAYAMA²¹Department of Applied Physics, Osaka University, Yamadaoka 2-1, Suita 565, Japan.²Department of Applied Physics, Osaka City University, Sugimoto, Sumiyoshi-ku, Osaka 558, Japan.

The study of coherent oscillations by using ultrashort laser pulses is an interesting subject since the time evolution of carriers and phonons is directly observed in time-domain [1,2]. While various coherent phonons are observed by a reflection-type pump-probe method [1,2], little is known about the nature and generation mechanism of the coherent phonons. The two-color pump-probe measurements are expected to obtain the information on the wavevector of the coherent folded acoustic phonons. In the present study, we report the results of the measurement on the coherent folded acoustic phonons in $(\text{GaAs})_n(\text{AlAs})_n$ superlattices (SLs) by using a two-color pump-probe technique, where the subscript m and n denotes the monolayer numbers of the GaAs and AlAs, respectively.

The time derivative traces of reflectivity changes for $(\text{GaAs})_{24}(\text{AlAs})_{24}$ SL observed by using one-color (1C) and two-color (2C) pump-probe techniques showed oscillatory structures with beats. The observed oscillations arise from the folded longitudinal acoustic (LA) phonons. While the coherent oscillations obtained by the 1C pump-probe method were observed in a time range of more than 200 ps, the oscillations observed by the 2C pump-probe technique almost disappeared after 150 ps.

In order to study the coherent phonons observed in $(\text{GaAs})_{24}(\text{AlAs})_{24}$ SL in more detail we performed Fourier-transform of the time-domain data as depicted in Fig. 1. The 1C pump-probe spectrum shows that a strong first-order peak (0.39 THz) accompanies weak peaks at the lower- and higher-frequency sides (0.35 and 0.43 THz). The 2C pump-probe spectrum shows that the strong peak at 0.39 THz is hardly observed and only two peaks appeared at 0.35 and 0.43 THz. From group theory analysis and a comparison between the peak frequencies and the calculation of the dispersion curves of the zone-folded LA modes, these peaks obtained by the 1C pump-probe method are attributed to the folded LA modes with A_1 symmetry at and near the zone center, while two peaks obtained by the 2C pump-probe method arise from dominantly the folded

LA modes near the zone center.

If the coherent phonons are generated via impulsive stimulated Raman scattering with both forward and backward scattering transfers by pump pulses [2], the frequencies of the coherent oscillations near the zone center should change with the wavelength of the pump laser. Our results that the frequencies of the phonons near the zone center are independent of the wavelength of pump laser are not affirmative to the coherent phonon generation by stimulated Raman process. A plausible explanation is that the coherent oscillations with various wavevectors are generated by pump pulses and that the coherent phonons with a certain wavevector which are phase-matched with probe pulses are detected. This two-color pump-probe technique will give light on the generation mechanism of the coherent phonon in superlattices.

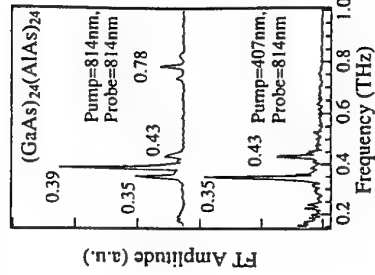


FIG. 1 The Fourier transform spectra of the folded acoustic phonons obtained by one-color and two-color pump-probe techniques.

References

- [1] W. A. Kütt, et al, IEEE, J. Quantum Electron., 28, (1992) 2434, H. J. Zeiger, et al, Phys. Rev. B45, (1992) 768.
- [2] R. Merlin, Solid State Commun., 102, (1997) 207.

PUMP POWER DEPENDENCE OF COHERENT PHONONS IN η - Mo_4O_{11}

Kisoda Kenji, Muneaki Hase, Hiroshi Harima, and Shin-ichi Nakashima

Department of Applied Physics, Osaka University

2-1 Yamadaoka, Suita, Osaka 565-0871, Japan

Kiyomi Sakai and Masahiko Tani

Kansai Advanced Research Center, Ministry of Posts and Telecommunications

Kobe 651-2401, Japan

Hiroshi Negishi and Masasi Inoue

Department of Materials Science, Hiroshima University

Kagamiyama 1-3-1, Higashi Hiroshima 739-0046, Japan

We will report on the pump power dependence of coherent phonons in η - Mo_4O_{11} . Quasi-two-dimensional conductor η - Mo_4O_{11} undergoes two charge density wave (CDW) phase transitions at $T_{c1}=105$ K and $T_{c2}=35$ K as confirmed by electrical resistivity and electron diffraction measurements, etc. The purpose of this report is to elucidate the relation between the generation of the coherent phonons and the CDW state.

In our previous pump-probe study on η - Mo_4O_{11} using fs-laser excitation, several coherent phonons with frequency below 100 cm^{-1} were strongly observed at temperatures $T < T_{c1}$. This result suggests that the coherent phonon generation is closely correlated with the lattice distortion due to the CDW phase transition. Since two CDW phase transitions occur in η - Mo_4O_{11} , it is expected that coherent phonons behave differently in the two CDW states. To confirm this idea, pump-probe measurement at various excitation power levels was examined at 300 K (above T_{c1}), 80 K (between T_{c1} and T_{c2}), and 20 K (below T_{c2}). At 80 K , the amplitudes of the coherent phonons with frequency below 100 cm^{-1} decrease with increasing the power and eventually disappear, while that of the 120 cm^{-1} mode grows. The decrease in the amplitude of coherent phonons with frequency below 100 cm^{-1} at higher pump powers can be ascribed to the heating effect by the pump laser. The heating leads to the destruction of the CDW state. Therefore we can conclude that these modes are excited by a mechanism related to the lattice distortion due to the CDW transition. On the other hand, increase in the amplitude of the 120 cm^{-1} mode suggests that this mode is unrelated to the CDW.

At 20 K , the modes below 100 cm^{-1} show the strong pump power dependence, although these modes are always observable in the used pump power range and the peak frequencies are unchanged. As the pump laser power increases, the mode at 98 cm^{-1} decreases while the mode at 85 cm^{-1} increases. On the other hand, the amplitude of the 120 cm^{-1} mode is negligibly small. This observation supports that the modes below 100 cm^{-1} is intimately related to the CDW and that the 120 cm^{-1} mode is not.

The Hall measurement showed that the carrier density in the CDW state decreases by about one (at 80 K) and three orders (at 20 K) compared to that in the normal state. It is recognized that the coherent phonon signal is enhanced with increasing the ratio of photogenerated carriers to the background carriers. In the normal state, the photogenerated carrier density is much smaller than the background carrier density, and hence the amplitude of coherent phonon showed no remarkable pump power dependence. In the CDW state, however, the coherent phonons are strongly dependent on the pump power because the photogenerated carrier ratio to the background carrier goes up.

Our results show that the generation mechanism of the coherent phonons in η - Mo_4O_{11} are closely related to the CDW transitions.

COHERENT ACOUSTIC MODE OSCILLATIONS

IN SILVER NANOPARTICLES

N. Del Fatti, S. Tzortzakis, F. Vallée, and C. Flytzanis

Laboratoire d'Optique Quantique du CNRS

Ecole Polytechnique, 91128 Palaiseau cedex, France

Tel: 33-1-69 33 41 26/27 - email: vallee@leonardo.polytechnique.fr

The reduction of the size of a material to nanometric scales leads to drastic modification of its electronic and phonon properties. In particular, in small nanoparticle systems, fundamental properties determined in the bulk material by the bulk acoustic phonons, such as the heat capacity and electron-lattice interactions, are expected to be strongly influenced by the low frequency mechanical oscillations of the nanoparticles. We show here that the spheroidal (breathing) mode of metal nanoparticles can be coherently excited and probed in the time domain via its coupling with the electrons, permitting a precise determination of its frequency and damping.

Experiments were performed using a femtosecond pump-probe technique in silver nanoparticles embedded in a glass matrix. A nonequilibrium electron distribution is created by intraband absorption of a femtosecond infrared pulse (30fs) delivered by a frequency tunable Ti:sapphire oscillator. The electron gas excess energy is quickly damped to the lattice on a time scale (~ 1 ps) faster than the oscillation period, T_{sp} , of the lowest energy spheroidal nanoparticle mode ($T_{sp} \propto R$ ranges from 2 to 10ps for nanoparticle radius R ranging from 3 to 15nm). Our results demonstrate that an impulsive excitation of the spheroidal mode is thus realized leading to coherent mechanical oscillations of the nanoparticles.

These are detected in real time by measuring the induced transmission change $\Delta T/T$ of a time delayed femtosecond probe pulse in the vicinity of the collective electron motion in a nanoparticle (i.e., the surface plasmon resonance around 420nm). The frequency of this morphological resonance, consequence of the confinement, is directly related to the real part of the interband dielectric function making it very sensitive to its modification. After a fast transient that reflects energy injection in the electron gas and its transfer to the lattice with a $\sim 800\text{fs}$ time constant, the measured transmission change exhibits oscillations with a time period proportional to the nanoparticle radius (for the investigated sample with $R = 3, 4.9, 6.4, 12, 15\text{nm}$, respectively) and in good quantitative agreement with the theoretical estimates. Measurements performed as a function of the probe wavelength demonstrate that the $\Delta T/T$ oscillations result from modulation of the surface plasmon resonance frequency Ω_{sp} due to modulation of the interband part of the optical dielectric constant of the metal nanoparticles by the spheroidal mode (through deformation potential coupling).

The oscillation decay time can also be determined and is found to be faster than that due to the particle size distribution (i.e. due to inhomogeneous broadening) permitting the determination of the intrinsic damping time of the spheroidal mode. Because of their low frequency ($3 - 15\text{ cm}^{-1}$ range) and large damping ($\sim 10\text{ ps}$), these parameters are very difficult to measure in the frequency domain and are determined here for the first time in metal nanoparticles.

PHONONS IN V₂O₅ ABOVE AND BELOW MOTT TRANSITION: A COMPARISON OF TIME AND FREQUENCY DOMAIN SPECTROSCOPY RESULTS

O.V. Misochko,¹ M. Tani,¹ K. Sakai,¹ K. Kisoda,² S. Nakashima,² V.N. Andreev,³ and F.A. Chudnovsky²

¹Kansai Advanced Research Center, CRL, Iwaoka, Kobe, Hyogo 651-24, Japan

²Department of Applied Physics, Osaka University, Osaka 565, Japan

³Ioffe Physical-Technical Institute, 194021 St. Petersburg, Russia

We report the results of an optical study of the Mott transition in V₂O₅ carried out by time and frequency domain spectroscopies. We observe that although the spectra obtained by the two techniques are essentially similar, there are distinct differences in phonon lineshape. This is tentatively ascribed to the fact that along with first-order coherence, responsible for temporal interference pattern, the phonon field generated in the pump-probe experiment exhibits higher-order coherences.

Vanadium sesquioxide, V₂O₅, undergoes a metal-insulator phase transition at T_M=150 K. The crystal is considered as a prototype for the physics of Mott transition and its properties may be related to ground state properties of high-T_c superconductors. Although the phase transition in V₂O₅ has been intensively studied, information on lattice dynamics is scarce.

Using a time domain spectroscopy one observes phonons that are excited coherently rather than thermally. Instead of analyzing energies and lineshapes of frequency-domain spectra, one deals with time dependent oscillations and their decay profile. Most solids are equally easily studied in either time or frequency domain, but sometimes one domain is more convenient than the other. To make such a comparison for V₂O₅ was the goal of the study.

The V₂O₅ crystals were polished and mounted on a temperature-controlled stage of an optical cryostat. Excitation and detection of coherent phonons were carried out with a conventional pump-probe setup using mode locked Ti:sapphire laser pulses of 50 fs duration centered at 800 nm. Raman spectra were recorded using a cw Ti:sapphire laser tuned to the same wavelength as in the pump-probe experiments.

The pump induced reflectivity changes at positive time contain an oscillating signal due to phonon modes. The oscillatory part depends linearly on pump intensity. At T > T_M, there is a single oscillatory feature, which can be assigned to one of the two A_{1g} phonons in triclinic V₂O₅. The oscillation decay and frequency in the metallic state do not appreciably depend on either temperature or pump power. Below the transition, the oscillation pattern becomes quite complicated, signaling the larger number of phonon modes accessible for excitation. These oscillations decay more slowly than in the metallic phase and are still observable at time delays up to 10 ps.

At the Mott transition, a change in the spectrum is also observed in the Raman scattering. In the metallic state, the phonon lineshape is strongly asymmetric being steeper at high frequency shifts. In striking contrast to the pump-probe data, the Raman linewidth and frequency of the A_{1g} phonon in the metallic phase are strongly temperature dependent. Additional information about lattice dynamics can be obtained by analyzing lineshape of the Raman phonon and that of the Fourier transformed intensity of the reflected light. Unlike the spectrum, which is formed by density fluctuation, lineshape is determined by higher order correlation functions. By making such a comparison we discovered that lineshape of the phonons observed in the time and frequency domain spectroscopies is distinctly different. Since in this work the same crystals were used for both experiments, the difference cannot be intrinsic to the samples but must be due to the different experimental techniques.

A MONTE-CARLO ANALYSIS OF THE PICOSECOND RAMAN SPECTROSCOPY OF GERMANIUM

P. Kocevski^a, M. Schullatz^a, and J. Kuhl^b

^a Inst. f. Theor. Physik, Karl-Franzens-Universität, A-8010 Graz, Austria

^b Max-Planck-Inst. f. Festkörperforschung, D-70506 Stuttgart, Germany

A former investigation of one of the present authors (JK) and coworkers (H.D. Fuchs et al., Phys. Rev. B 44, 8633 (1991)), concerning the role of isotopic scattering of optical zone-center phonons in natural and isotopically enriched Ge crystals, had revealed that the phonon-population decay times, as obtained from pump-probe picosecond anti-Stokes Raman spectroscopy, are systematically longer than the phonon lifetimes derived from linewidth studies of 1st-order Raman spectra. The authors explained this discrepancy as arising from the interference of the phonon-decay dynamics with the phonon-generation dynamics during the laser pulses, obtaining quantitative agreement with the experimental data by modeling the time evolution of the phonon population by appropriate foldings of phenomenological generation and relaxation rates.

The purpose of the present work is to critically re-examine this original interpretation through a detailed k-space Ensemble-Monte-Carlo simulation of the two-pulse Raman experiment. This technique is best suited to monitor the nonelectronic phonon decays and the phonon generation and reabsorption by the photo-excited electrons and holes within the full time interval during and between the first and the second laser pulse. By use of well-established three-band photoexcitation models, of standard carrier-phonon couplings, and of experimentally determined nonelectronic phonon decay rates, we find very good agreement between the simulated time evolution of the Raman sensitive optic-phonon populations and the experimental data of Fuchs et al., substantiating the original explanation of the discrepancy between population- and phonon-lifetimes as due to the interplay of the carrier-induced generation dynamics (with negligible contributions of the reabsorptions) and the non-electronic phonon decays in the time-resolved Raman measurements.

PP1 (09.00)

Particle Detectors using Superconducting Transition Edge Sensors
Blas Cabrera, Stanford University

Superconducting transition edge sensors (TES) have been used for many years in phonon physics experiments. The recent advance of negative electrothermal feedback (ETF) for the biasing and readout of W and Al-normal metal bilayer TES devices has lead to substantial improvements in the sensitivity of TESs and in the resolution of cryogenic particle detectors. These TES detectors have sharp resistive transitions at a temperature below 100 mK and have demonstrated the best energy resolution of any energy dispersive spectrometer for single photon counting over a wide range from the near infrared (0.1 eV FWHM at 1 eV) through x-ray (3 eV FWHM at 1.5 keV). An understanding of the phonon physics plays an important role in the design and optimization of these devices. In addition, large mass phonon-mediated detectors also use W ETF-TES devices together with quasiparticle trapping from Al films to W and are now operating in the CDMS (Cryogenic Dark Matter Search) experiment. We will summarize these advances, and report on recent advances.

PP2 (09.30)

Superconducting Tunnel Junction Detectors For use in Astrophysics

T Peacock : Astrophysics Division, European Space Agency -
ESTEC, Noodwijk, Netherlands
apeacock@estec.esa.nl

Superconducting Tunnel Junctions (STJ's) have now reached a stage in development where they can be considered as practical detectors for use in astrophysics over the wavelength regime from the near infrared (5 microns) to soft X-rays (1 nm). The ability to efficiently photon count at these wavelengths coupled to a high time resolution and an inherent energy resolution ensure that these detectors will become an important additional tool for astrophysicists in the next century.

The physical principles governing the operation and performance of this new generation of detectors are presented. The principal performance characteristics are reviewed for each key wavelength region and those areas requiring further development highlighted. The use of alternative superconductor materials such as hafnium will allow the current performance of devices, which are based on niobium and tantalum, to be significantly improved. Early results on the physical and electrical properties of thin films of such materials will be described.

For any practical applications arrays of STJ's are required to provide an overall imaging capability to complement the obvious inherent characteristics of the device. Recent results on the development of arrays will be discussed and the longer term activity relating to the fabrication of very large format arrays identified.

PARTICLE DETECTION USING CRYOGENIC MAGNETIC CALORIMETERS

J.S. Adams,¹ S.R. Bandler,¹ C. Ens,² A. Fleischmann,² S. Hunklinger,² Y. Kim,¹
J. Schönefeld,² and G.M. Seidel,¹

¹ Department of Physics, Brown University
Providence, RI 02912, USA

² Institut für Angewandte Physik, Universität Heidelberg
Albert Ueberle-Str. 3-5, 69120 Heidelberg, Germany

We are developing magnetic microcalorimeters suitable for the high resolution detection of X-rays in a broad energy band up to about 10 keV. In these devices a measurement of the magnetization of paramagnetic ions is used to determine very small temperature changes resulting from the absorption of energy. The ions are embedded in metals, the intrinsically fast thermalization time ($\approx 1 \mu\text{sec.}$) allowing fast detector count rates. They have a predicted resolution for 6 keV X-rays of under 2 eV at 50 mK, and even less than 1 eV at lower temperatures. Unlike other technologies we can have some measure of confidence in these predictions since they are based purely upon equilibrium statistical thermodynamics. The parameters relevant for this calculation are magnetization and heat capacity, which we know from theory and experiment, and which have also been recently verified by our group for samples which are directly suitable for the calorimetric measurements. These results (between 200 μK and 100 mK) demonstrated the expected low exchange coupling between localized $4f$ electrons in rare earth ions and conduction electrons in metals, which makes these paramagnetic systems ideal for using in microcalorimeters and also for use as fast very low temperature thermometers. We will present the first results of a microcalorimeter developed using a commercially available miniature susceptometer in which the sample is located inside of a 50 micron diameter evaporated coil, and report on the progress towards the development of an optimally designed device.

THE ROLE OF PHONON PROCESSES IN THE PERFORMANCE OF SUPERCONDUCTING TUNNEL JUNCTIONS USED AS PHOTON DETECTORS

Authors: A. Poelaert,¹ R. den Hartog,¹ A. Peacock,¹ A. Kozorezov,²
and J.K. Wigmore²

Affiliations: ¹ Astrophysics Division of the European Space Agency, ESTEC,
Noordwijk, The Netherlands.

² School of Physics and Chemistry, University of Lancaster,
Lancaster, England.

Abstract:

Phonons play an important role in the photon detection process in a superconducting tunnel junction (STJ). The absorption of a photon in a STJ produces a cloud of charge carriers (quasiparticles). Phonons can thereafter be generated by relaxation of quasiparticles down to lower energy states, or by recombination of two quasiparticles into a Cooper pair. These phonons can be re-used to produce new quasiparticles or excite existing quasiparticles, or can be lost from the system. The balance between the re-use and the loss of phonons can affect the performance of the STJ, in terms of charge output, count rate, energy linearity and resolution. This paper summarises the influence of the phonons on the various parameters involved in photon detection. The attention is particularly focused on three topics: (i) quasiparticle de-trapping via recombination and its effect on the energy linearity; (ii) influence of the recombination on the energy resolution (edge effect); (iii) role of phonons with energy less than the Cooper pair binding energy. A model using adequate balanced equations is used to account for experiments performed on Nb-Al-AlO_x-Al-Nb STJs.

DETERMINATION OF QUASIDIFFUSIVE PHONON PROPAGATION IN BaF_2 USING PULSE SHAPE ANALYSIS AND POSSIBLE IMPLICATIONS FOR PARTICLE DETECTION

P. Clegg, M. Bravin, N.E. Booth, M. Bruckmayer, K. Djotni, E. Esposito¹, E. P. Houwman², H. Kraus, G.L. Salmon.

Department of Physics, Oxford University, Keble Road, Oxford OX1 3RH, UK.

¹ Present address Istituto di Cibernetica del CNR, Via Tolano 6, 80072 Napoli, Italy.

² Present address Drukker International, Beversestraat 20, Cuyk, The Netherlands.

When a particle interacts in a solid a fraction of its energy is usually converted into phonons. This is used in particle detectors to make sensitive measurements of weakly interacting particles. In order to achieve good energy resolution and detection efficiency a small sensor is often mounted on a large absorber. Dielectrics can be used as absorbers to minimize the heat capacity and to reduce the likelihood of long lived excitations. It is essential to understand the phonon transport mechanisms in the absorber in order to establish what information about the particle interaction can be determined from the phonon flux reaching the sensor. If the phonon propagation in a specific crystal was primarily ballistic then it would facilitate the detection of phonon flux anisotropy. This in turn may make it possible to discriminate between nuclear recoil events and interactions with electrons. Such information is critical to dark matter detection experiments. Alternatively the number of background events in a rare event search can be reduced by identifying and discounting signals which originate close to the surface of the crystal.

We have characterised the phonon propagation in a BaF_2 single crystal at low temperature. Our crystal was bombarded with α -particles and the phonon flux originating from two sites was measured using a Series Array of Superconducting Tunnel Junctions. Our data exhibit a diffusive pulse shape with displacement-dependent diffusion coefficient, a behaviour characteristic of so-called quasidiffusive propagation, whose theory is well established. Based on this theory, we derived a simplified model for the expected pulse shape. Our measurements were found to be in strong agreement with this model, in contrast to a ballistic model. This demonstrates that phonon propagation in BaF_2 is quasidiffusive in character.

An advantage with using BaF_2 as an absorber material is that it has almost perfect elastic isotropy, hence it does not exhibit phonon focusing which would mask phonon flux anisotropy. Quasidiffusive propagation implies however, that large angle elastic scattering will occur between the interaction site and the sensor. As a result it will probably not be possible to detect phonon flux anisotropy in BaF_2 . Despite this, the fact that the diffusion coefficient depends on distance travelled means it may be possible to determine the position of interaction from pulse shape analysis. For quasidiffusive propagation the diffusion coefficient $D = K L^{2/3}$ which is consistent with our results for BaF_2 . In order to find the position of an unknown interaction the pulse shape would have to be evaluated at a number of sensors on the absorber. Further experiments will be required to validate this concept. We intend to extend this work to lower energy scales using Transition Edge Sensors.

DS1 (11.30)

ANHARMONIC RESONATORS IN
ELECTRON-IRRADIATED α -QUARTZ

R. Eilenberger, K. Laßmann and W. Eisenmenger

Universität Stuttgart, 1. Physikalisches Institut, Pfaffenwaldring 57, D-70550 Stuttgart

In search of possible building-blocks of the anharmonic systems in amorphous SiO_2 we investigated α -quartz before and after electron-irradiation with doses of $0.8 - 3.0 \cdot 10^{19} \text{ e}^-/\text{cm}^2$ with phonon spectroscopy using superconducting tunnelling junctions. We find in all irradiated samples two anharmonic series of sharp acoustic scattering resonances with energies in the meV region. Good fits to the two series are possible by assuming transitions within anharmonic or soft potential type deep double well potentials. Rather large masses and/or soft compliances are associated with these fits. We find the characteristic soft-potential energy W to be only one third of its value in glassy SiO_2 . Furthermore we did not observe a broadening of the resonances with increasing electron dose as one might expect as a result of increasing amorphization. This raises the question, whether the anharmonic systems underlying the observed phonon resonances are related to the glassy state.

DS2 (11.50)

DIELECTRIC RELAXATION OF INTERACTING HYDROXYL IONS IN KCl

C. Enss,¹ M. Krefl,¹ S. Ludwig,¹ C.P. An,² and F. Luty²

¹ Institut für Angewandte Physik, Universität Heidelberg
Albert Ueberle-Str. 3-5, 69120 Heidelberg, Germany

² Department of Physics, University of Utah
201 James Fletcher Building, Salt Lake City, Utah 84112, USA

Impurity ions like Li^+ , OH^- , and CN^- in potassium chloride crystals are known to give rise to orientational tunneling states. At very low concentrations such tunneling systems in KCl can be considered as isolated and their properties can be described from a microscopic point of view. With rising concentration mutual interaction between the defects leads to a cross-over from coherent to incoherent tunneling, which in turn changes the energy spectrum and the dynamics of the defects. Hydroxyl ions in KCl are a special case because the electric and elastic coupling between the defects is of similar magnitude for this system. We have investigated the dielectric properties of OH^- and OD^- ions in KCl at frequencies between 30 Hz and 2 GHz, concentrations between 2 and 6000 ppm and the temperature range from 6 mK to 120 K. We find that with rising concentration the dielectric response is increasingly dominated by relaxational processes. Surprisingly, even at lowest temperatures a large relaxational absorption is observed at low frequencies and high defect concentrations. In addition, the results of detailed measurements of the thermal activated relaxation of closeby pairs of hydroxyl ions at temperatures above 3 K are presented.

PHONON HOPPING IN DISORDERED SYSTEMS

T. Damker, H. Böttger

Institute of Theoretical Physics, Otto-von-Guericke-University Magdeburg, Germany
and

V. V. Bryksin

A. F. Ioffe Physico-Technical Institute, St. Petersburg, Russia

Anharmonic interactions between localized vibrational states and extended low-energy phonons can lead to thermally activated hopping of the localized states. Such a mechanism has been proposed to explain the thermal conductivity behaviour of dielectric glasses and amorphous films above the so called "plateau temperature", i.e. in the high temperature regime. This hopping mechanism explains the increase in thermal conductivity with temperature, which is opposite to the behaviour of crystals.

To investigate this transport scenario we derive rate equations for the occupation numbers of the localized states. We have shown, that by taking the anharmonic effects in higher order perturbation theory into account, the tendency to saturation at higher temperatures can be explained as well [1], without having to invoke the anharmonic life time broadening proposed by Orbach *et al.* in the fracton hopping model [2]. Furthermore, we find a diffusive contribution to the (heat-)current, which decreases the thermal conductivity in sufficiently disordered systems, compared to a simple approach based on Fermi's golden rule.

Extending our model, we calculate the localized state life times and find an increase with the energy of the state, in accordance with recent experiments (Scholten *et al.*, e.g. [3]) as well as with the fracton hopping model (the functional form differs though). This is in contrast to another model to explain the high temperature behaviour of glasses, namely the model of diffusive transport by non-propagating modes [4]. Furthermore, the latter model predicts a decrease of the conductivity with increasing frequency of an ac temperature gradient. In our hopping model, on the other hand, the conductivity is frequency independent or even increases. This could provide an additional approach to experimentally distinguish between these two models.

To assess the practical relevance of our model we calculated the extension of the localized states required to explain the measured thermal conductivity and life times of the high-energy states. We find the localization length to be of the order of 10 to 40 Å for amorphous silicon, which seems to be a reasonable value (several atomic distances).

[1] H. Böttger and T. Damker, Phys. Rev. B **50**, 12509 (1994)[2] A. Jagannathan, R. Orbach and O. Entin-Wohlman, Phys. Rev. B **39**, 13465 (1989)[3] A. J. Scholten and J. I. Dijkhuis, Phys. Rev. B **53**, 3837 (1996)[4] P. B. Allen and J. L. Feldman, Phys. Rev. B **48**, 12581 (1993)WIGNER-DYSON STATISTICS OF PHONON RESONANCES
IN CHAOTIC ACOUSTIC RESONATORS

G. Fagas, Vladimir I. Falko, C.J. Lambert

School of Physics and Chemistry, Lancaster University LA1 4YB, Lancaster UK

Statistics of phonon eigenmodes in acoustic resonators, such as aluminum and quartz blocks, has been studied experimentally [1] in order to find indication of universal level statistics specific to the wave mechanics in classically chaotic systems. The experimentally investigated samples were manufactured in such a way that the classical counterpart of the Fresnel wave-packet propagation is chaotic, i.e. the trajectory of an elastic wave fills densely the whole kinematically-allowed phase space. Statistical analysis of the resonant frequencies of such blocks revealed a strong level repulsion. The closest neighbour distribution of the spectra resembles that of the eigenvalues of a Gaussian orthogonal matrix in the random matrix theory [2].

The aim of this study was to model numerically a solid-state acoustic resonator with chaotic properties. As a frame, we chose a fcc cubic crystal with central nearest neighbour interactions. The chaotic scattering of phonons is introduced by a compositional disorder, i.e. random variation of the mass at each lattice site throughout the sample. Such a system can be regarded as some kind of a solid mixture of isotopes.

In the numerical procedure, we construct the exact dynamical matrix and calculate its eigenvalues (ω_n^2). Then, we obtain the density of states of phonon modes and use it to normalize the eigenvalues. The nearest-level-spacing distribution function $P(s)$ was found to be of the universal form obeying the Wigner-Dyson law. As long as the time-reversal symmetry is preserved, and both transverse and longitudinal phonon modes are strongly mixed, our results coincide with what is expected for the Gaussian orthogonal ensemble and are in agreement with the experimental observations. All the simulations were performed in the intermediate disorder limit, so that no localization of lattice vibrations was found within the body of the acoustic phonon band. The presence of localized modes can be indicated by an admixture of Poissonian statistics of eigenmode frequencies, which slightly modifies the law of the distribution function $P(s)$. We observe this only in a narrow spectral interval close to the acoustic band edge.

[1] C. Ellegaard, T. Guhr, K. Lindemann, H.Q. Lorensen, J. Nygård, and M. Oxenford, Phys. Rev. Lett., **75**, 1546 (1995); C. Ellegaard, T. Guhr, K. Lindemann, J. Nygård, and M. Oxenford, Phys. Rev. Lett., **77**, 4918 (1996)

[2] 'Quantum Chaos', K. Nakamura, Cambridge University Press (1994); 'Supersymmetry in Disorder and Chaos', K. Efetov, Cambridge University Press (1997)

PI2.1 (11.30)

PHONON SCATTERING IN HTSC CUPRATE CRYSTALS.

V.B.Efimov, L.P.Mezhov-Deglin

Institute of Solid State Physics RAS, Chernogolovka, Moscow distr., 142432, Russia

From results of measurements of transport coefficients: thermal conductivity (κ_{ab} and κ_c) and electric resistivity (ρ_{ab} and ρ_c) in-plane and out-of-plane made on a series of HTSC $\text{YBa}_2\text{Cu}_3\text{O}_{7-x}$ and $\text{Bi}_2\text{Sr}_2\text{CaCu}_2\text{O}_{8-y}$ specimens with the transition temperatures T_c close to 90K one can obtain an information on the mechanisms of the heat transport in normal and superconducting states, hence the main processes of scattering of phonons and carriers in HTSC cuprate crystals.

Our general finding is that above T_c YBCO and BSCCO specimens behave like conventional phonon-dominated layered heat conductors. No correlation has been observed in behavior of the in-plane resistivity ρ_{ab} and thermal conductivity κ_{ab} above and below T_c . More over the relative height of the maximum on $\kappa_{ab}(T)/\kappa_{ab}(T_c)$ curves in superconducting state can reach 2 and its position is shifted toward lower temperatures $T_m < 0.4T_c$ with increasing this ratio both in less anisotropic Y-crystals and highly anisotropic Bi-specimens in contrast to predictions of the theory of electron heat transport in layered HTSC crystals. From this we can conclude that:

- 1). In studied sufficiently perfect crystals the lattice (phonon) contribution to heat conduction is dominating not only above but below T_c , too.
- 2). Near T_c the mean free path of phonons is restricted by the phonon-carrier scattering in bulk, and below T_c its value increases quickly due to near exponential decrease of the density of normal carries like in conventional superconducting metal alloys with a strong electron-phonon coupling.

PI2.2 (12.00)

TWO-LEVEL-LIKE PHONON SCATTERING IN THE OXIDE SUPERCONDUCTOR, $\text{La}_{2-x}\text{Sr}_x\text{CuO}_4$

M. Ikebe and H. Fujishiro

Faculty of Engineering, Iwate University, 4-3-5 Ueda, Morioka 020-8551, Japan.

The phonon thermal conductivity κ_{ph} of $\text{La}_{2-x}\text{Sr}_x\text{CuO}_4$ ($0 < x \leq 0.3$) polycrystals has been measured between 10K and 150K and phonon scattering mechanisms operating in this system have been analyzed as a function of temperature T and the Sr concentration X . Assuming the additive scattering rate approximation, various scattering mechanisms, i.e., dislocations, charge carriers, sheet-like faults, point defects and phonon-phonon interaction are taken into account. In order to enhance the reliability of the analyses, the thermal diffusivity α_{ph} has also been measured and the specific heat C_{ph} of each sample is monitored by use of the relation $C_{ph} = \kappa_{ph}/\alpha_{ph}$. The κ_{ph} and α_{ph} have been measured under an identical experimental setup by the use of a continuous heat flow method for κ_{ph} and by the use of an arbitrary heating method for α_{ph} measurement.¹⁾ The phonon thermal conductivity κ_{ph} is remarkably reduced by the substitution of La by Sr ions. The reduction of κ_{ph} is more conspicuous in the low temperature region ($T < 40\text{K}$) and the scattering strength increases roughly in proportional to the Sr concentration up to $X=0.2$. However, κ_{ph} recovers by further increase of Sr substitution beyond $X=0.2$. In our analyses, the anomalous enhancement in the phonon scattering in the low temperature region results in an increase of the phonon scattering term linear to phonon frequency ω . The $\text{La}_{2-x}\text{Sr}_x\text{CuO}_4$ system is known to take a structural transformation at around $X=0.21$ from orthorhombic ($X < 0.21$) to tetragonal ($X > 0.21$) phase. The structural change mainly results from a slight shift of the apical oxygen sites of the CuO_4 octahedron. We explain the anomalous phonon enhancement as originating from tunneling motion of apical oxygen. The Sr substitution for La makes the orthorhombic phase locally unstable and makes the tunneling motion of apical oxygen possible. Recently we have observed similar enhanced phonon scattering also in $\text{La}_{1-x}\text{Sr}_x\text{MnO}_3$ near structural transitions.^{2,3)} For $\text{La}_{1.85}\text{Sr}_{0.15}\text{CuO}_4$ which has the highest T_c ($=38\text{K}$) in this system, we have observed a small but clear anomaly in κ_{ph} at T_c . From the anomaly, the electron-phonon coupling constant λ is determined to be $\lambda=0.06$. The analyses of the data of $\text{La}_{1.85}\text{Sr}_{0.15}\text{CuO}_4$ indicate that electron-phonon interaction is weak in comparison to $\text{YBa}_2\text{Cu}_3\text{O}_7$, but can never be neglected also in this oxide superconductor.

¹⁾ M. Ikebe, H. Fujishiro, T. Naito and K. Noto: J. Phys. Soc. Jpn. 63 (1994) 3107.

²⁾ M. Ikebe, H. Fujishiro and Y. Konno: to be published in J. Phys. Soc. Jpn. 67 (1998).

³⁾ H. Fujishiro and M. Ikebe: submitted to this conference.

OPTICAL STUDIES OF TERAHERTZ PHONONS DYNAMICS IN SMALL-GRAIN POLYCRYSTALLINE CORUNDUM

S.P.Feofilov, A.A.Kaplyanskii, A.B.Kulinkin and R.I.Zakharchenya
A.F.Ioffe Physical-Technical Institute, 194021, St.Petersburg, Russia

The ceramics-like small grain corundum is a structured material consisting of densely packed 100 nm crystallites. The samples were prepared by annealing of sol-gel prepared highly porous $\gamma\text{-Al}_2\text{O}_3$ [1] at 1250°C. In order to enable fluorescent detection of terahertz acoustic phonons the samples were doped with Cr^{3+} and Mn^{4+} ions. The nonequilibrium phonon distributions were generated in the material at T=5K with chopped Ar-laser light absorbed by the impurities in the material. The technique [2] of optical detection of resonant phonons by observation of phonon-induced fluorescence from the upper ^2E excited state sublevels of the Cr^{3+} and Mn^{4+} ions was used. The phonons of two frequencies: 29 and 80 cm^{-1} (0.87 and 2.4THz) were detected by observation of Cr^{3+} and Mn^{4+} fluorescence respectively. The slow relaxation of generated phonon distribution was observed, similar to that observed by the similar optical technique in oxide glasses [3]. This phonon relaxation regime drastically differs from that in regular corundum ceramics with micron grain size [4]. The results for sol-gel produced small-grain corundum ceramics are discussed in comparison with that for regular corundum ceramics [4] and for nanocrystalline porous $\gamma\text{-Al}_2\text{O}_3$ [1] taking into account the ratios between the crystallites size and phonon wavelength.

- [1] S.P.Feofilov, A.A.Kaplyanskii, R.I.Zakharchenya, J.Lumin. 66&67 (1996), 349;
- Optics and Spectroscopy 79 (1995), 653.
- [2] K.F.Renk and J.Deisenhofer, Phys.Rev.Lett. 26 (1971), 764
- [3] A.A.Kaplyanskii, A.V.Akimov, S.A.Basun S.P.Feofilov, E.S.Moskalenko, J.Kocka, J.Stuchlik, J.Lumin. 53 (1992), 7.
- [4] S.P.Feofilov, A.A.Kaplyanskii, M.B.Melnikov. Physica B 219&220 (1996), 773.

THE SCATTERING OF NONEQUILIBRIUM PHONONS ON GRAIN BOUNDARIES IN SINGLE PHASE CERAMICS

S.N.Ivanov¹, L.M.Zhukova², E.N.Khazanov¹, Ya.M.Soifer³, A.V.Taranov¹

¹ Institute of Radioengineering and Electronics RAS, Moscow

² AO "Mashinostroitelny Zavod" "Electrostal", Moscow Region

³ Institute of Solid State Physics RAS, Chernogolovka, Moscow Region

The boundary scattering of slightly nonequilibrium phonons transporting through AlN and SiC ceramics has been analyzed on the basis of [1,2]. The phonon propagation inside the ceramic grain supposed to be ballistic. The dependence of time of maximum of phonon pulse signal t_m on temperature has been measured.

The weight density of AlN ceramic is about 97-98% of the density of original material. The polycrystalline structure of such ceramic consists of 10µm hexahedron crystals with junction angle between them about 120 degrees. There is also the second phase consists of $\text{Y}_3\text{Al}_5\text{O}_{12}$. The dependence $\partial t_m / \partial T < 0$ and phonon transition coefficient through the grain boundaries $f_a \approx 0.3$ (T=3.8K) has been observed in ceramic samples made by standard technology (cold forming with subsequent annealing). The samples was annealed during 20 hours to eliminate the influence of phonon scattering on grain boundaries. After annealing the temperature dependence becomes positive ($\partial t_m / \partial T > 0$) and f_a becomes two times higher. At room temperature the thermoconductivity increase from 160 to 200 W/mK and the value of $\lg(\delta)$ decrease at 10%.

The SiC ceramic was made by cold isostatic pressure technology. For α -modification (SiC- α) density $\approx 92\%$, grain size $\approx 10\mu\text{m}$, $\partial t_m / \partial T < 0$, $t_m \sim T^{-2}$, and $f_a \approx 5 \cdot 10^{-2}$ indicate strong boundary scattering. The β -modification (SiC- β) has density $\approx 78\%$, crystallites have the filament structure with diameter $R_0 \approx 1-5\mu\text{m}$ and length $2-3R_0$. The bolometer signal have diffusive shape with $t_m \sim T^{-1.5}$. The main difference between these two groups of samples is the dependence of t_m on the length of sample, i.e. diffusion length. For SiC- α we have $t_m \sim L^2$, i.e. "classic" diffusion and for SiC- β we have $t_m \sim L^{0.6}$. The possible reasons of such an unusual dependence have been discussed.

- [1] S.N.Ivanov, A.G.Kozorezov, A.V.Taranov, E.N.Khazanov. Solid St. Commun., 83, 365 (1992)
- [2] A.G.Kozorezov, J.K.Wignmore, C.Erd, A.Peacock, A.Poelaert. Phys.Rev.B 1997 (to be published)

NT2.1 (14.00)

SPATIOTEMPORAL IMAGING, SPATIOTEMPORAL PULSE SHAPING, AND SPATIOTEMPORAL COHERENT CONTROL

Richard M. Koshi, Claran J. Brennan, Timothy F. Crimmins, Keith A. Nelson

Abstract:

Three new advances have been combined to extend significantly the degree of optical control that can be exercised over coherent excitations in condensed matter. First, it is now possible to drive lattice vibrations in some materials well beyond the harmonic limit through impulsive stimulated Raman scattering (ISRS). Anharmonic vibrational responses have been observed in several materials, providing insight into the corresponding anharmonic crystal potential energy surfaces whose characterization is generally elusive.

The second advance is the real-space imaging of propagating phonon-polariton excitations in crystals. In contrast to earlier observations of phonon-polariton propagation through coherent scattering with probe pulses that were delayed temporally and separated spatially from the excitation pulse by specified amounts (the spatial separation increasing linearly with temporal delay), in the present case a large probe spot which includes the excitation region and the entire surrounding region into which the excitation may propagate is used. The probe pulse is not incident at the phase-matching angle for coherent scattering, but simply passes through the coherent phonon-polaritons which act as a moving phase pattern. The transmitted probe light is imaged directly onto a CCD to reveal the phonon-polariton propagation pattern for the case of crossed-pulse excitation.

The third advance is the extension of femtosecond pulse shaping to the spatial as well as temporal domain, in a manner compatible with automated control through a computer-interfaced 2-dimensional liquid crystal display (LCD). Through automated spatiotemporal pulse shaping, it is now possible to transform a single incident beam consisting of a single pulse into many spatially separated output beams, each one consisting of an independently specified waveform whose time-dependent amplitude and phase profiles are controlled. The output is spatially as well as temporally phase-coherent, so options such as time-varying interference patterns and wavevector shaping are possible. The automated process is still rather crude due to limitations in the LCD hardware used, but already it is possible to specify spatially and temporally shaped waveforms to a computer and obtain them through its interface with the 2-D LCD.

The three advances discussed above can be combined to achieve coherent control over time and position-dependent sample responses, through specification of the time and position-dependent driving field and with feedback from real-space imaging of the responses. Preliminary experiments are under way with phonon-polaritons, and other propagating excitations including exciton-polaritons may also be manipulated by spatially and temporally shaped waveforms. The propagating excitation itself can thereby be "shaped" arbitrarily in a manner which has no analog in molecular or atomic spectroscopy, since direct optical access to different spatial locations into which the excitation moves can be achieved. Optical amplification, directional control, and frequency or wavevector filtering are among the objectives in the linear-response regime. Characterization of nonlinear lattice dynamics, soliton formation, and nonlinear polariton-polariton interactions are current goals of coherent control in the anharmonic regime.

NT2.2 (14.20)

INTERFEROMETRIC DETECTION IN PICOSECOND ULTRASONICS

B. Perrin, C. Rossignol, B. Bonello, J. -C. Jeannet

Laboratoire des Milieux Désordonnés et Hétérogènes, UMR 7603 Université Pierre & Marie Curie -CNRS 75252-Ed, casier 86, 4, Place Jussieu 75252 Paris cedex 05, France.

Picosecond ultrasonics relies on a pump-probe optical technique where the photoacoustic absorption of a femto-second (pico-) laser pulse (the pump) excites either short acoustic pulses in thin films or high frequency acoustic resonances of ultrathin layers. The probe pulse, which is time-delayed, is affected by the acoustic field in various respects. Thus, any of the four quantities which characterize the probe electromagnetic field, namely the amplitude, the propagation direction, the phase or the polarization, can be used to detect the acoustic field. At first, amplitude has been considered in transient reflectance or absorbance measurements. Later, laser beam deflection² was used to detect the slight changes of the propagation direction induced by the bump due to the acoustic pulse on the film surface. In this work, we describe how phase detection of the probe beam can also be used and the type of information which can be obtained from such a measurement.

Expression of the change of the complex optical reflectivity coefficient of a sample induced both by the photoelastic effect and the surface and interfaces motions related to an acoustic wave will be given for any multilayered structure. The discussion about the respective information which can be drawn from amplitude and phase measurements will be emphasized. Different interferometric schemes suitable for pump-probe picosecond optical technique will be described. Then, experimental results, obtained in various systems including metallic single monolayers, multilayered structures and semi-transparent materials, will be given to demonstrate the advantages brought by the combined measurement of the amplitude and phase changes in the study of acoustic pulse shapes, thin layer vibrations or « Brillouin » oscillations (in semi-transparent media).

¹C. Thomsen, J. Strait, Z. Vardeny, H. J. Maris, and J. Tauc, Phys. Rev. Lett. 53, 989 (1984)

²O. B. Wright and K. Kawashima, Phys. Rev. Lett. 69, 1668 (1992)

J. E. Rothenberg, Opt. Lett. 13, 713 (1988)

VIBRATIONAL DENSITY OF STATES FROM INELASTIC NUCLEAR RESONANT ABSORPTION OF SYNCHROTRON RADIATION

W. Sturhahn, E. E. Alp, P. Hession, M. Hu, and T. S. Toellner
Argonne National Laboratory, Advanced Photon Source,
9700 South Cass Ave., Argonne, IL 60439, USA

Inelastic nuclear resonant absorption of synchrotron radiation provides a novel approach to measurements of the vibrational density of states (VDOS.) We explain the basic features of the PHOENIX (PHOnon EXcitation by Nuclear Inelastic absorption of X-rays) technique which permits direct determination of partial VDOS with excellent signal-to-noise ratio even for small amounts of material ($<5 \mu\text{g}$). The energy resolution is variable and can be reduced to sub-meV level by using crystal optics. This method features several remarkable properties. The measurement is selective to the resonant isotope only, the partial VDOS is obtained with a minimum of modelling, and the resonant nuclei probe the lattice vibrations locally. Data obtained at sector 3-ID of the Advanced Photon Source will be presented to exemplify the usefulness of the technique.

This work is supported by US-DOE, BES Materials Science, under contract No: W-31-109-ENG-38.

Techniques for Inelastic X-ray Scattering with μeV - Resolution

R. Röhlsberger¹, E. E. Alp², A. Bernhard¹, E. Burkel¹, A. I. Chumakov⁴, E. Gerdau³,
O. Leupold³, K. W. Quast², R. Rüffer⁴, W. Sturhahn², and T. S. Toellner²

¹ *Universität Rostock, Fachbereich Physik, August-Bebel-Str. 55, 18055 Rostock, Germany*

² *Advanced Photon Source, Argonne National Laboratory, Argonne, Illinois 60439, USA*

³ *III. Institut für Experimentalphysik, Universität Hamburg, Germany*

⁴ *European Synchrotron Radiation Facility, BP 220, 38043 Grenoble Cedex, France*

Inelastic x-ray scattering studies with high energy resolution have gained momentum in recent years, particularly due to third-generation, undulator-based synchrotron radiation sources. Vibrational excitations are studied with meV-resolution by using backscattering monochromators and analyzers [1,2]. A different approach has been introduced to measure the phonon density of states via inelastic nuclear resonant scattering [3]. In that case, Mössbauer nuclei in the sample are used as energetic analyzers, and meV-resolution is achieved by monochromators with subsequent high-order reflections in dispersive geometry. Energy resolutions that go significantly below 1 meV require a qualitatively different approach, because of the limited perfection of crystal monochromators and analyzers. There is currently no x-ray spectroscopic technique available that covers the range from a few μeV to a few meV with μeV resolution. However, vibrational excitations in this energy range are of considerable interest. Examples are the boson - peak in disordered materials, magnons, two-level systems, rotational excitations, etc.

In this contribution, we introduce a novel type of spectrometer that provides a μeV bandpass together with a tunability over a few meV around the 14.4-keV resonance of ^{57}Fe [4]. The narrow energy bandpass is reached by polarization - mixing nuclear resonant scattering. A crystal polarizer/analyzer pair in crossed setting provides a rejection of the nonresonant radiation by a ratio of 10^{-8} . Finally, tunability over a few meV is introduced by high speed Doppler motion. Another approach to ultra-high resolution monochromatization is introduced by nuclear resonant scattering from samples rotating with frequencies of several kHz. Resonantly scattered radiation is deflected from the primary beam by an angle that is proportional to the decay time of the excited nuclear state. This 'nuclear lighthouse effect' allows to extract a μeV wide band out of synchrotron radiation that can be tuned over several meV. First experimental results are presented and perspectives for inelastic scattering experiments are discussed.

- [1] E. Burkel, *Inelastic Scattering of X-Rays with Very High Energy Resolution* (Springer-Verlag, New York, 1991)
- [2] see e.g. F. Sette, G. Ruocco, M. Krisch, C. Masciovecchio, R. Verbeni, and U. Bergmann, *Phys. Rev. Lett.* 77, 83 (1996)
- [3] W. Sturhahn, T. S. Toellner, E. E. Alp, X. Zhang, M. Ando, Y. Yoda, S. Kikuta, M. Seto, C. W. Kimball, and B. Dabrowski, *Phys. Rev. Lett.* 74, 3832 (1995)
- [4] R. Röhlsberger, E. Gerdau, R. Rüffer, W. Sturhahn, T. S. Toellner, A. I. Chumakov, and E. E. Alp, *Nucl. Instrum. Meth. A* 394, 251 (1997)

IS1 (14.00)

Optical Studies of Isotopically Modified Semiconductors: Phonons and Electronic Structure

Manuel Cardona

Max-Planck-Institut für Festkörperforschung

Heisenbergstr. 1, D-70569 Stuttgart, Germany, European Union

During the past ten years a number of crystals, mostly semiconductors, have been grown with tailor made concentrations of stable isotopes. They involve highly isotopically pure and highly isotopically disordered systems. Beside the trivial dependence of phonon frequencies on isotopic mass, often used for characterization purposes, a number of rather basic effects have been observed and theoretically interpreted. Among them the following will be discussed.

1. Dependence of the lattice parameters on isotopic masses.
2. Dependence of anharmonic self-energies (real and imaginary parts) on isotopic masses.
3. Dependence of self-energies on isotopic disorder.
4. Mass-disorder-induced first order Raman spectra.
5. Renormalization of electronic states through electron-phonon interaction and its dependence on isotopic mass.

These effects have been observed in elemental and compound crystals; for the latter the mass dependence of a given physical property is different for the various constituent elements.

Isotope substitution has also been used to determine phonon eigenvectors and, in the cases where one of the constituent atoms is a strong neutron absorber, to grow crystals in which this atom is absent. Using these crystals the phonon dispersion relations can be determined by inelastic neutron scattering (e.g. CdS and CdSe).

IS2 (14.30)

RAMAN STUDIES OF ISOTOPE EFFECTS IN Si AND GaAs

F. Widulle, T. Ruf, A. Göbel, I. Silier, E. Schönherr, and M. Cardona

Max-Planck-Institut für Festkörperforschung, D-70569 Stuttgart, Germany

A. Cantarero and J. Camacho

Universitat de València, Dpt. Física Aplicada, 46100 Burjassot (Valencia), Spain

Using highly enriched stable isotopes it is possible to grow bulk and low-dimensional semiconductors with controlled isotopic composition. This opens new possibilities for studies of their lattice-dynamical and electronic properties. Elemental semiconductors have been made from almost pure single isotopes, e.g., to investigate the dependence of phonon frequencies or linewidths on the atomic mass, as well as from isotope mixtures, which allows one to determine mass-disorder-induced effects. Further possibilities exist in compound semiconductors, where different sublattices can be tuned with respect to each other by varying the anion or cation isotope mass.

We have measured the dependence of the zone-center transverse-optic-phonon (TO) frequency and linewidth in Si and GaAs on the isotopic composition using Raman spectroscopy at low temperatures ($T = 10$ K). The samples were isotopically pure ^{28}Si and ^{30}Si , natural Si ($M = 28.11$ u, slightly disordered), and a highly disordered specimen consisting of ^{28}Si and ^{30}Si in a 50 : 50 ratio. Small single crystals as well as layers made by liquid-phase epitaxy were investigated. As GaAs samples we used the natural compound ($M_{\text{Ga}} = 69.72$ u), which is highly disordered, and the isotopically pure samples $^{69}\text{GaAs}$ and $^{71}\text{GaAs}$. Note that natural arsenic consists of only one isotope namely ^{75}As . Small single crystals were grown by a slow reaction of Ga with As_2 vapour at 820 °C.

The energy of the zone-center TO phonon is expected to vary like the inverse square root of the atomic mass in Si and the reduced mass in GaAs, respectively. This behavior has been observed in the isotopically pure samples. In addition to that, isotope mass fluctuations also affect phonon frequencies and linewidths. We have measured these effects in the isotopically disordered samples and find additional frequency hardenings of $(1.9 \pm 0.8) \text{ cm}^{-1}$ in Si and $(0.31 \pm 0.25) \text{ cm}^{-1}$ for the TO phonon of GaAs as compared to the scaled energies of the isotopically pure samples. A minor part of these additional frequency shifts can be attributed to the mass-dependence of the phonon renormalization due to anharmonicity. An estimate of this effect has been derived for Si by extrapolating the temperature dependence of the phonon energy [1] to $T = 0$ K. Anharmonicity also causes the phonon linewidth to vary with the inverse mass (Si) and the inverse reduced mass (GaAs), respectively. This effect has been qualitatively observed in the isotopically pure samples. In the disordered samples we observe additional broadenings of $(0.09 \pm 0.03) \text{ cm}^{-1}$ in Si and $(0.12 \pm 0.09) \text{ cm}^{-1}$ in GaAs. This reflects a reduced phonon lifetime due to elastic scattering of the TO mode at isotope mass fluctuations.

[1] J. Menéndez and M. Cardona, Phys. Rev. B 29, 2051 (1984)

ISOTOPIC SHIFTS OF THE LOW-ENERGY EXCITATIONS OF
INTERSTITIAL OXYGEN IN GERMANIUM

N Aichele¹, K Laßmann¹, C Linsenmaier¹, F Mäter¹, F Zeller¹,
E E Haller², K M Itoh³, L I Khirunenko⁴,
B Pajot⁵, and H Müssig⁶

March 20, 1998

¹Universität Stuttgart, 1. Physikalisches Institut, Pfaffenwaldring 57,
D-70550 Stuttgart, GERMANY

²Lawrence Berkeley National Laboratory and University of California, Berkeley,

CA 94720 USA

³Department of Applied Physics and Physico-Informatics,

Keio University, 3-14-1, Hiyoshi, Kohoku-ku, Yokohama 223, JAPAN

⁴Institute of Physics of Ukrainian National Academy of Sciences, Prospect Nauki 46,
252650 Kiev-22, UKRAINE

⁵Groupe de Physique des Solides, Tour 23, Université Denis Diderot, 2 place Jussieu,
F-75251 Paris Cedex 05, FRANCE

⁶United Monolithic Semiconductors GmbH, Wilhelm-Runge-Str. 11,
D-89081 Ulm, GERMANY

Key Words: Ge:O, isotope shift, phonon spectroscopy

A series of phonon scattering resonances between .18 meV and 4.08 meV in germanium can be associated with rotational states up to $l = \pm 5$ of interstitial oxygen[1]. For rigid rotation of a free Ge-O-Ge quasi-molecule around its inertial axis parallel to $\langle 111 \rangle$ the momentum of inertia would be given by the reduced mass and by the distance r_0 of the oxygen from the Ge-Ge axis. From the fit to the resonance energies this would lead to $r_0 = 93$ pm and to small Ge-isotope shifts lying within the observed linewidth. To separate the contributions of the oxygen, its immediate germanium neighbours, and the lattice to these states it is necessary to determine the level positions in several isotopically enriched germanium crystals as well as for the oxygen isotopes. We report on such measurements which show that the Ge-associated shifts are distinctly larger and the ^{18}O -associated shift is smaller than calculated with the above assumption. The Ge-associated shifts are even larger than compatible with an isotope-induced inhomogeneous linewidth of the resonances in natural germanium. This would mean that not only the immediate Ge-neighbours contribute to the low-energy motion of the interstitial oxygen but there is some average coupling to a larger Ge surrounding or the lattice in general.

Through the reduction of the strong isotope scattering at high phonon energies the use of isotopically enriched Ge has facilitated the observation of a higher level around 5.8 meV (position depending on Ge-isotope) which probably belongs to the rotational state $l = \pm 6$. Weak further resonances observed near 4.75 meV and 5.3 meV are possibly associated with transitions to the first and second excited radial states. If so, this could mean a relatively low central barrier of about 12 meV.

[1] M Gienger, M Glaser, and K Laßmann 1993 *Sol. St. Comm.* **86**, 285

SOUND VELOCITY AND INTERNAL FRICTION OF LI DOPED KCl

G.Weiss,¹ M. Hübner² and C. Enss,²

¹ Universität Karlsruhe, Physikalisches Institut
76128 Karlsruhe, Germany

² Institut für Angewandte Physik, Universität Heidelberg
Albert Ueberle-Str. 3-5, 69120 Heidelberg, Germany

It is well known that Li^+ impurities in KCl crystals substitute K^+ ions and form tunneling systems. Tunneling occurs between eight equivalent off-center positions. In first approximation the ground state splits into four levels with a 1-3-3-1 degeneracy. The energy difference between the levels is 1.1 and 1.6 K for ^7Li and ^6Li ions, respectively. At low temperatures the sound propagation is strongly influenced by the presence of such tunneling systems. Using a torsional oscillator operating at kHz-frequencies we have investigated the elastic properties of KCl crystals doped with different Li isotopes at different concentrations in the temperature range between 0.05 and 30 K. In contrast to analog dielectric measurements the sound propagation is strongly influenced by relaxational processes even at very low defect concentrations. This is a special property of such eight-level-systems and can be understood by considering the coupling of the sound wave to the different eigenstates. We discuss the isotope dependence of both the resonant and relaxational contribution and we compare the temperature dependence of the elastic properties of doped samples to that of a nominally pure KCl crystal.

IQ1 (09.00)

ACOUSTIC WAVE PROPAGATION AT A SOLID-LIQUID INTERFACE

A.G. Every¹, A.A. Maznev² and G.A.D. Briggs³

¹Department of Physics, University of the Witwatersrand, PO WITS 2050, South Africa

²Department of Chemistry, MIT, Cambridge, MA 02139, USA

³Department of Materials, Oxford University, Oxford OX1 3PH, UK

Abstract

The wave modes that exist at the interface between a solid and a liquid have long been a central concern of cw acoustic microscopy, accounting as they do for the oscillations in the acoustic material signature, $V(z)$. Recent time resolved acoustic microscopy (TRAM) experiments on anisotropic solids using point and line focus acoustic lenses^[1,2] have cast new light on these interfacial modes. Unlike cw measurements in which the surface modes are folded by interference into the $V(z)$ oscillations, TRAM measurements yield the velocity, amplitude and other characteristics of the surface modes directly, and in extraordinarily fine detail. This paper will show how the TRAM technique in effect measures the dynamic displacement response of a fluid-loaded solid surface to an impulsive force, concentrated at a point or along a line, depending on the type of lens used.^[3] Good agreement is obtained between calculated and measured response or Green's functions for anisotropic solids, and to illustrate this, results will be presented for a number of crystals and fibre composites. The responses are represented as 2D images spanned by time and direction in the interface. The images contain a wealth of structures associated with leaky Rayleigh and pseudo-surface waves and with lateral waves, i.e. surface skimming bulk waves of the solid. The Stoneley-Scholte interfacial wave is not observed in TRAM because of phase matching constraints and the finite aperture of the lenses used, but it can be coupled into with laser excitation, Brillouin scattering and other techniques.

[1] R.E. Vines, S. Tamura and J.P. Wolfe, *Phys. Rev. Lett.* **74**, 2729 (1995); R.E. Vines, M.R. Hauser and J.P. Wolfe, *Z. Phys.* **B98**, 255 (1995).

[2] N.N. Hsu, D. Xiang, S.E. Fick and G.V. Blessing, *Proc. IEEE Ultrasonics Symposium* **95**, 867 (1995).

[3] A.G. Every, A.A. Maznev and G.A.D. Briggs, *Phys. Rev. Lett.* **79**, 2478 (1997).

IQ2 (09.30)

DIRECT PHONON TRANSMISSION ACROSS WAFER BONDED CRYSTALS,

M.E. Msa¹, I.² A. Klimashov,² W. Dietsche,¹ and K. Friedland.²

¹Max Planck Institut für Festkörperforschung, Postfach 800665, D-70506 Stuttgart

²Paul Drude Institut für Festkörperelektronik, Hausvogteiplatz 5-7, D-10117 Berlin

³Department of Physics, Bowdoin College, Brunswick, ME 04011

Several factors play an important role in reducing the transport of phonons across a solid-solid interface: the largest factors are the presence of subsurface disorder and imperfect physical contact between the solids. When bonding crystals, micrometer size contaminants of the surface can easily cause voids at the interface which strongly scatter phonons. Typical ultrasonic wavelengths on the order of a micrometer can detect micrometer scale defects at solid-solid interfaces but are easily transmitted through many types of bonded interface. In contrast, the phonons used for most phonon imaging applications have wavelengths of tens of nanometers and do not pass bonded interfaces without extreme attenuation. Recent developments of bonding techniques for hetero- and homo-interfaces, however, have the potential to produce bonded samples with suitable phonon transmission for higher frequency applications. We have studied such a GaAs-GaAs interface using the techniques of phonon imaging. We observe unprecedented phonon transmission through these bonded samples.

Our interfaces were produced by bringing optically flat, atomically clean GaAs surfaces into direct contact (called direct bonding, or wafer bonding) followed by moderate temperature annealing. Our phonon images show that the fraction of phonons in the intermediate frequency range (between 75 and 285 GHz) which travel ballistically through the bonded region is correlated with the quality of the bonded interface. The best bonded sample available to us showed very little diffusive scattering at the bond, demonstrating that wafer bonding is an excellent technique with many possible phonon applications.

We have modelled phonon transmission in the limit of purely diffuse scattering and purely elastic scattering at the bond. The experimental images are consistent with computer simulations of ballistic phonon propagation with some diffuse scattering at the bond. However, the presence of distinctive phonon focusing features in the experimental images makes it clear that a significant fraction of the detected phonons are not diffusively scattered. The relative fractions of focused phonons and diffuse background in the phonon images can provide a sensitive, non-destructive test of both the bond quality and of general models of the interface properties. For our best sample, the frequency dependence of the attenuation of the ballistic phonon transmission was consistent with residual disorder with a length scale less than 100 nm. This is comparable to the 30 nanometer sizes associated with regions of crystalline disorder measured in similar samples using Transmission Electron Microscopy. Unlike the TEM measurements, however, the phonon measurement does not require the sample to be cleaved.

Direct bonding of samples is not constrained by the same limitations of lattice matching necessary for other growth methods. In particular, it is possible to "twist-bond" materials so that the crystallographic orientation of the two pieces are at arbitrary angles. Our computer simulations of twist-bonded GaAs show interesting features in the phonon focusing pattern. Such samples provide interesting opportunities to test acoustic models of the interface.

OBSERVATION OF MELTING OF SOLID ^4He BY SOUND WAVE

Y.Okuda, S.Yamazaki, T.Yoshida, Y.Fujii and K.Matsumoto
Department of Applied Physics, Tokyo Institute of Technology,
Oh-okayama, Meguro-ku, Tokyo 152-8551, Japan

Physics on the crystal shape and the interface of solid ^4He below 1K is a very interesting field and many new exciting phenomena are revealed. As the solid ^4He below 1K is grown from the superfluid phase and the latent heat associated with the transition from the superfluid to the solid phase is very small, the growth rate can be incredibly high below 1K. So crystal growth character is completely different from those of the classical solids.

During the course of the sound transmission experiment through the solid/liquid interface monitoring the shape of the crystal by a video camera, we happened to observe crystal melting, or the depletion of the solid/liquid interface where the strong sound beam was passing.

The crystal was produced around 0.8K with the atomically rough horizontal surface sitting in the middle of the monitor window. The interface was very mobile which was confirmed by a easy excitation of the crystallization/melting wave.

When the received signal through the interface was monitored as a function of the input power, there observed a sudden saturation of the received signal at some power. For well above that power, the melting of the interface was visible both cases of the sound emission from fluid-side and solid-side.

With further stronger pulses emitted from the solid-side transducer, the solid was melted inside the crystal near the transducer, not at the interface. That means the negative crystal, or superfluid droplet inside the crystal was produced. The growth behavior of the droplet is very interesting.

Hybridization of localized and density modes in superfluid Helium 4

Nir Gov and Eric Akkermans

Physics Department, Technion, Haifa

We present a new approach for studying the energy spectrum of superfluid Helium 4. It is based on the assumption that there exist localized modes in addition to the usual Feynman density fluctuations (phonons). They correspond to the short range behaviour in the liquid where effects of quantum statistics are important. We describe in a phenomenological way the hybridization of those two kinds of excitations and we compare the resulting energy spectrum with experimental results, e.g. the structure factor and the single excitation scattering intensity. We also predict the existence of another type of excitation interpreted as a vortex loop. The energy of this mode agrees both with the Raman scattering data and critical velocity experiments of Varoquaux et al..

PI3.1 (09.00)

On the Poiseuille flow in quasi-one dimensional crystal

R. Maynard^a, A. Smontara^{b,c}, J.-C. Lasjaunias^c, R. Bressoux^a

^aPhysique et Modélisation des milieux Condensés, CNRS, Université Joseph Fourier, BP 166, 38042 Grenoble-Cedex 9, France

^bInstitute of Physics, Bijenicka 46, POB 304, HR - 10001 Zagreb, Croatia

^cCentre de Recherches sur les Très Basses Températures, Laboratoire associé à l'Université Joseph Fourier, CNRS, BP 166, 38042 Grenoble Cedex 9, France

Abstract

Thermal conduction measurements of quasi-one dimensional single crystals $[Ta_{1-x}Nb_xSe_4]$ shows exceptionally sharp peaks in the vicinity of 1K. The occurrence of these peaks is analysed in term of phonon Poiseuille flow originating from the strong anharmonicity amplified by lattice anisotropy. Boundary conditions for the flow, anisotropy of the phonon dispersion relations and the nature of the defects are discussed.

PI3.2 (09.30)

DIFFUSION OF PHONONS IN $Li_{1-x}Ho_xF_4$

P. J. Rump, A. F. M. Arts, and H. W. de Wijn

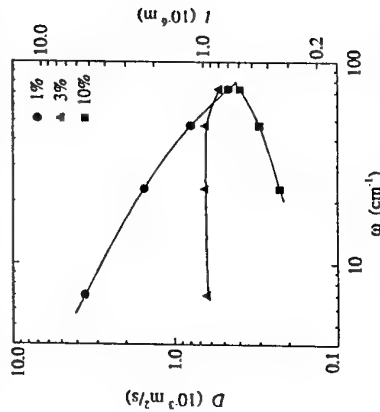
Faculty of Physics and Astronomy, and Debye Research Institute, Utrecht University, P.O. Box 80000, 3508 TA Utrecht, The Netherlands

The evolution in time and space of a nonequilibrium phonon distribution has been studied in single crystals of $Li_{1-x}Ho_xF_4$, with Ho^{3+} concentrations $x = 0.01, 0.03, 0.10$, and 1. The system is unique in that it features a series of closely lying one-phonon transitions in the ground and excited multiplets of the Ho^{3+} ion. Time of flight experiments were performed transverse to the c axis up to distances of several millimeters with a time resolution of order 10 ns. An electrical heater injected a broad initial spectrum of phonons into the crystal, and luminescent detection following pulsed optical excitation probed the occupation numbers of phonons resonant with the various Ho^{3+} electronic transitions. From the spatial distribution of these occupations as a function of time, diffusion constants were obtained for the resonant phonon modes. Quite remarkably, the diffusivity was found to decrease with increasing frequency for $x \approx 0.01$, whereas for $x = 0.10$ the opposite behavior was observed (cf. the figure, which shows the diffusion constant D and the mean free path l versus the phonon frequency).

A detailed analysis shows that the present experiment not only probes the propagation of phonons resonant with the electronic transitions, but that efficient parallel transport channels with a much longer free path are operative. The major part of the acoustic energy is transported away from the heater by the nonresonant part of the phonon spectrum, while resonant phonons remain trapped close to the heater by strong scattering. At larger distances from the heater, anharmonic phonon-phonon interactions equilibrate the local phonon distribution, thus feeding the poorly occupied resonant phonon modes. This mechanism also explains the relatively weak frequency dependence of the observed diffusion constants.

Numerical simulations of the spectral and spatial evolution of the propagating phonon distribution with inclusion of collinear three phonon interactions as well as elastic scattering by localized centers is found to reproduce the frequency dependence of the experimental results.

Finally, in pure $LiHoF_4$, in which the phonons couple strongly to the electronic system, evidence is found for quasi-ballistic propagation of coupled electron-phonon modes.



HEAT TRANSPORT IN FULLERITE SAMPLES.

V.B.Efimov, L.P.Mezhov-Deglin

Institute of Solid State Physics RAS, Chernogolovka, Moscow distr., 142432, Russia

As was shown by our experimental investigations the absolute value of the coefficient of thermal conductivity $k(T)$ of fullerite samples and its temperature dependence strongly depend from conditions on the sample preparation. In our experiments we have studied the transport properties of perfect single crystals and samples compacted at different conditions from a pure C_{60} powder. The compacted samples were two types: pressurized at low temperature (only compacted samples) and polymerized at high pressure and high temperatures.

At room temperature the thermal conductivity of the crystals and of compacted samples was near the same. The thermal conductivity of crystals slightly depended on temperature at range 300-260 K. At SC phase thermal conductivity of single crystals was increasing with cooling and below 80 K the $k(T)$ could be can be described in frames of Debye-Pierls model of phonon-phonon scattering for dielectric crystals: $k(T)=A^*\exp(\theta/T)$, where θ is a Debye temperature and a parameter is close to $\gamma \approx 2$.

Below room temperatures thermal conductivity of compacted samples was decreasing with lowering T . In temperature range 90-250 K $k(T)$ dependence can be described by the Einstein model: heat transfer in an array of buckyballs, vibrating with random phases.

At temperatures near 90 K one can say about some kind of transition in bulk of C_{60} samples - transition into "orientation glassy state". It can be proposed that the phonon scattering on these "frozen" defects can limit the maximal value of phonon mean free path in the crystal at low temperatures: below 15 K $\lambda_{ph} \approx 10^{-3}$ that is much shorter the crystal sizes and slightly depends on temperature. In compacted samples this transition was displayed as a drop of $k(T)$ near two times. But we never observed any demonstration of "glassy-like transition" in polymerized samples in temperature range 20-250 K. It confirms the suggestion that at low temperature the thermal conductivity for both single crystals and compacted samples is determined by interaction with orientation defects. In polymerized fullerite samples with bands between buckyballs the transition into "orientational glassy" state is absent or its temperature is higher then 90 K.

LATTICE DYNAMIC SIMULATION OF SILICON THERMAL CONDUCTIVITY

Sebastian Volz and Gang Chen

Mechanical and Aerospace Engineering Department
University of California, Los Angeles, CA 90095-1597

ABSTRACT

Direct lattice dynamics simulation of the thermal conductivity of single crystal is difficult because of the long time and space characteristic lengths involved by the phonon scattering compared to the size of the computable simulation boxes. For example, the phonon mean free path in single crystalline silicon is about 100 nm and the relaxation time is in the range of 100 ps. A typical molecular dynamic (MD) simulation of a cubic of the order of the mean free path in the suitable duration, should handle with 10^8 atomic trajectories over 10^5 time step, which is a difficult task even for supercomputers. Besides, the finite size of the simulated region implies a wavelength cut-off that excludes a complete range of phonons from contributing to the heat transport. In this work, we perform MD simulations in silicon single crystals where interatomic forces are derived from the Stillinger-Weber potential. To yield the bulk thermal conductivity from a system with dimensions smaller than mean free path; we impose cyclic boundary conditions in all directions and assume that the phonon scattering is not affected since phonon energy and momentum are conserved through the boundaries. The wavelength cut-off issue is corrected via a spectral analysis of the heat flux so that the thermal conductivity values become size independent. The consistency of our assumptions is supported by a set of runs probing the sensitivity temperature and system size. We finally compare the results to recent measurements in isotopically enriched silicon and comment the obtained deviations from the natural Si data.

EP3.1 (10.50)

ANGLE-RESOLVED BALLISTIC PHONON ABSORPTION SPECTROSCOPY
IN THE LOWEST LANDAU LEVELC.J. Mellor, U. Zeiler*, A.M. Devitt, S.H. Roshko, A.J. Kent, K.A. Benedict,
T. Cheng and M. Henini.*Department of Physics, University of Nottingham, Nottingham, NG7 2RD, UK.***Present Address: Institut für Festkörperphysik, Abteilung Nanostrukturen, Universität
Hannover, Appellstraße 2, D-30167, Germany.*

We have performed the first angle-resolved phonon absorption experiments in the fractional quantum Hall and composite fermion regime. These are the first experiments, in this regime, in which a probe with a well-defined, finite, wavevector has been observed to couple to these strongly correlated electron liquids. Thus the technique provides an important new spectroscopic tool for the investigation of these novel states of matter.

Phonons with an approximately Planckian spectral density are created by a thin film constant heater on the rear of a 2mm semi-insulating GaAs substrate. After traversing the GaAs ballistically they transfer a small proportion of their energy to a 2DEG grown on top of the substrate. The absorption of ballistic phonons heats the 2DEG and this is measured by the change in its resistance. In order to generate a detectable signal, the response of a long 2DEG in the form of a meandering line was investigated. We have found similar results for both of wafers ($n=1.14-1.4 \times 10^{15} \text{ m}^{-2}$, $\mu \sim 150 \text{ m}^2 \text{ V}^{-1} \text{ s}^{-1}$) studied.

At odd denominator fractional filling factors with clear resistance minima, the results are consistent with excitation across an energy gap, Δ . Phonon absorption is strongly dependent on the heater spectrum and only takes place as long as phonons of energy Δ are present. The energy absorbed by the 2DEG is therefore proportional to the number of phonons at energy, Δ , emitted by the heater. Using a heater with geometrical acceptance angles between 0° and 27° , only TA phonons are detected; at angles between 27° and 57° , both LA and TA phonons are observed. Different energy gaps are found at the different incident angles. The energies are similar to the predicted magneto-roton energy and considerably higher than those found from activation plots of the magnetoresistance.

Away from the fractional quantum Hall effect, we observe a much weaker dependence of the energy absorbed on the phonon spectrum. In particular, at a filling factor of $1/2$, we find that only low energy phonons interact with the 2DEG, completely consistent with the existence of a $1/\omega$ cut-off, where $1/\omega_0$ is the Fang-Howard parameter. Comparing the two heater angles, a value close to 5nm is obtained for ω_0 . In contrast to fractional filling factors, the 2DEG is found to reach an equilibrium temperature, when the energy loss due to phonon emission balances the gain due to absorption, on a timescale that is short compared to the heater pulse and time resolution of the experiment (50ns). Some previous experiments at $\nu=1/2$ have found effective carrier masses of around $3m_e$; our results are inconsistent with such a high value. From a preliminary analysis of our results we can set an upper limit of $1.5m_e$ for the composite fermion mass at $\nu=1/2$.

EP3.2 (11.10)

INCREASE OF QUANTUM HALL PLATEAU WIDTH
BY ELECTRON-PHONON INTERACTIONJ. Riess^a, D. Bicut^b, T. Duguet^a and P. Magyar^a*a*Centre de Recherches sur les Très Basses Températures, Centre National
de la Recherche Scientifique, B.P. 166, 38042 Grenoble Cedex 9, France
*b*Laboratory of Chemical Physics, NIDDK, NIH, Bethesda, MD 20892

We consider non-interacting electrons in a quasi two-dimensional strip (extended in x-direction) in the presence of a strong perpendicular magnetic field and a constant electric field $E = (0, E_y, 0)$, and subject to simple model disorder potential ("toy model") which allows to obtain the solutions of the time-dependent Schrödinger equation in very good approximation. Further, the electrons are coupled to a heat bath (acoustic phonons), which modifies the coherent Schrödinger time evolution induced by the electric field E_y . After elimination of macroscopically unobservable fluctuations, the time evolution which is relevant for the macroscopic current density can be described by a Boltzmann type equation, which is solved numerically. The steady state solution allows to calculate σ_{yy} and σ_{xy} as a function of any physical parameter of the system. We give results of σ_{yy} and of σ_{xy} for all filling factors and as a function of temperature. Quantized Hall plateaux are obtained with high precision. Between two plateaux, the Shubnikov-de Haas peak spreads out and its maximum decreases with increasing temperature in qualitative accordance with typical quantum Hall samples.

Our model calculations illustrate the interplay between the full Schrödinger time evolution induced by the electric field E_y , which here is known in detail, and the interaction with the phonons. In particular, we show that the Hall current is composed of Schrödinger type velocities and of velocities generated by electron-phonon interaction¹, while the dissipative current is only composed of Schrödinger type velocities. The phonon induced velocities contribute to the so-called compensating current, i.e., to that part of the Hall current which is responsible for the σ_{xy} plateaux. The proportion between the two velocity contributions depends on the parameters of the system. In typical quantum Hall samples (which contain insulating states) the compensating current is mainly composed of Schrödinger type velocities and only to a small extent of velocities originating from electron-phonon interaction. At low temperatures, the latter lead to slightly larger plateaux of σ_{xy} compared to those of σ_{yy} ¹. Such a difference in the plateau widths has actually been known from experiments for a long time, but it seemed unexplained so far.

Further, we investigate the extreme case where all states in the broadened Landau bands are conducting (this occurs when the substrate potential has no spatial fluctuations in the direction of the electric field E_y). Here the dissipative conductivity vanishes only for filling factors close to a band edge. Nevertheless, the calculated Hall conductivity shows broad quantized plateaux, due to a compensating current which in this case is entirely composed of velocities generated by electron phonon interaction. This shows that insulating states are in principle not indispensable for the integer quantum Hall effect, contrary to a widespread belief.

1. D. Bicut, P. Magyar, and J. Riess, Phys. Rev. B, scheduled 15 March, 1998-II.

ACOUSTIC PHONON ABSORPTION BY A 2D ELECTRON GAS AT THE QUANTISED HALL REGIME FOR ODD FILLING FACTORS

S. Dickmann
Institute for Solid State Physics of Russian Academy of Sciences
142423 Chernogolovka, Moscow District, Russia

The absorption of bulk acoustic phonons in GaAs/AlGaAs heterostructures is studied in the clean limit under typical integer quantum Hall conditions and in the case of an odd Landau levels (LL) filling factor ν . As two-dimensional (2D) interacting electrons are the strongly correlated system, the LL width is determined by the character Coulomb interaction energy $E_C = e^2/\kappa l_B$ [κ is the dielectric constant, $l_B = \sqrt{\hbar c/eB}$ is the magnetic length], which is essentially larger than the amplitude of a smooth random potential determining the LL width in the case of one-electron approach [2]. For the odd ν the calculation of the nonequilibrium phonon life time τ may be treated in the most complete form, since the lower part of the 2D electrons spectrum has been exactly calculated for the filled LL and to the first order in $E_C/\hbar\Omega$ [Ω is the cyclotron frequency). In this case the low energy excitations are the chargeless spin excitons having the Zeeman gap $\delta = |g\mu_B B|$ of the same order as e.g. the energy of phonons generated by heating metal films [3]. Correspondingly the electron-phonon interaction may be represented as spin-exciton-phonon interaction, which in addition to spin-independent terms includes small terms arising from the electron spin-orbit coupling.

Exactly these last determine the phonon absorption at $T = 0$. So, the absorption of one phonon generates the spin exciton and diminishes by the unit the both: the spin component S_z and the total electron spin number S . Therefore the phonon absorption rate is proportional to the rate of the spin momentum decreasing. This process is possible only for a small selected group of phonons with wave vectors $\mathbf{k} = (q, k_z)$ satisfying to $\hbar k = \delta + (q l_B)^2/2M$ (s is the sound velocity, $M \sim E_C^{-1}$ is the excitonic mass [1]) and is determined for longitudinal phonons by the deformation electron-lattice interaction. The inverse life time $\tau^{-1}(\mathbf{k})$ for these phonons is of the order of $L_z^{-1}(10^2 \cdot q^2/B)^{1/2} + 10^6 \cdot q^4/B^2 s^{-1}$ (here L_z is the sample length in $z \parallel B$ direction measured in cm, B is in Tesla, q is in cm^{-1}). It turns out even at temperatures $T \sim 1$ K this value of τ^{-1} reaches really the corresponding values, which are determined by spin-independent terms in the spin-exciton-phonon interaction Hamiltonian.

By ignoring the spin-orbit coupling the electron spin state does not change and the rate of phonon absorption is proportional to the conserved number of equilibrium excitons. As a result the electron temperature increases at the corresponding decreasing of the exciton gas chemical potential μ . The value of τ^{-1} at temperatures $T < 1$ K and for $k \gtrsim L_z^{-1}$ is of the order of $(10^{-7} \text{ cm}^3/\text{s}) \cdot \hbar k q s M^{3/2} T^{3/2} \exp[(\mu - \delta)/T - (\hbar s M k/q l_B - q l_B/2)/2MT]/L_z l_B$. Although the both presented formulae for τ^{-1} give the zeroth result for $q = 0$, one can see that actually only phonons having \mathbf{k} with a slight slope to z direction ($q \lesssim 0.1 k_z$) interact effectively with 2D electrons in the both cases.

After the averaging over a certain phonons distribution we find the effective inverse life time and therefore find the rate of the 2D electron gas heating as well as the corresponding contribution to the inverse thermal conductivity. The transition to the limit $k l_B \ll 1$ enables to find the sound wave attenuation. In this case the piezoelectric interaction plays the main role and the transverse wave polarization is considered too.

[1] C. Kallin, B. I. Halperin. Phys. Rev. B 30, 5655 (1984).

[2] S. Iordanskii, Y. Levinson. Phys. Rev. B 53, 7308 (1996).

[3] A. J. Kent et al. Phys. Rev. Lett. 69, 1684 (1992).

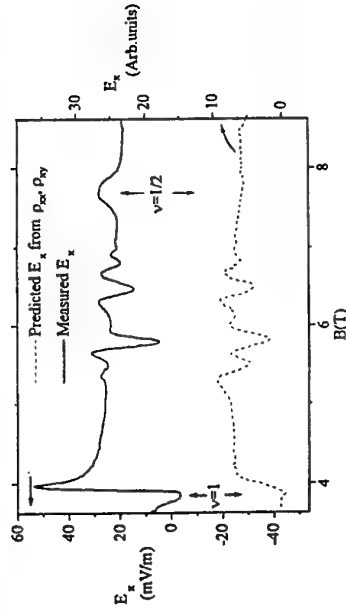
SURFACE ACOUSTIC WAVE INTERACTIONS WITH COMPOSITE FERMIONS AND THE ACOUSTO-ELECTRIC EFFECT

V W Rampton, I Kennedy, C J Mellor, B Bracher*, M Henini, Z R Wasilewski† and P T Coleridge†

Department of Physics, University of Nottingham, University Park, Nottingham NG7 2RD UK
*CMF, Rutherford Appleton Laboratory, Chilton Didcot, OX11 0QX, UK
†Microelectronics Division, NRC, Ottawa, Canada.

The use of surface acoustic waves (SAW) has proved valuable in the study of the fractional quantum Hall effect (FQHE) and gave strong evidence for the existence of a Fermi surface at a filling factor, ν , of one half for a 2 dimensional electron system (2DES). [Willet et al. 1993] These experiments firmly established the composite fermion hypothesis to account for the FQHE.

We have made experiments in the FQHE regime to study the attenuation and dispersion of surface acoustic waves (SAW) by a 2D carrier system at a GaAs/AlGaAs heterojunction. The experiments were made using SAW at frequencies up to 2GHz, magnetic fields to 14T and temperatures down to 340mK. Both 2D electron and 2D hole systems have been used. We have confirmed that features at $\nu=1/2$ can be found in the attenuation and dispersion of SAW by a 2DES. We have also found similar features in the case of the 2 dimensional hole system (2DHS). Measurements have also been made of both the longitudinal and the transverse acousto-electric (AE) voltages. At magnetic fields close to a filling factor of one half, there are features that cannot be explained on the basis of quasi DC measurements of the electrical properties. The figure below shows a typical graph of longitudinal AE voltage versus magnetic field.



Finally we find that a tensor relationship exists in the AE effect similar to that previously reported in the thermoelectric effect.

Reference

Willet R L, Ruel R R, Paalonen M A, West K W and Pfeiffer L N *Phys. Rev. B* 47 7344 (1993)

PHONON SCATTERING BY OXYGEN VACANCIES IN CERAMICS

Paul G. Klemens

Dept. of Physics, University of Connecticut, Storrs CT 06269-3046, U.S.A.

It has long been recognized that vacancies are strong scatterers of phonons and reduce the lattice thermal conductivity. Ratsifantana (1987) showed that their resonance frequency is high, so that perturbation theory can be used over the significant frequency range. Also, distortion scattering is absent, since the nearest linkages, which would make the major contribution, are absent. The perturbation consists of the missing mass, and of the missing linkages of atom pairs. The effective value of $\Delta M/M$ is thus $-2M_v/M$, where M_A is the mass of the missing atom, M the average atomic mass. Oxygen vacancies in ceramics can be produced by radiation damage, by removing oxygen in a reducing atmosphere, or by the addition of solute cations of different valance. Oxygen vacancies cause substantial reductions in thermal conductivity. In stabilized zirconia their concentration is known, and the resulting phonon scattering has been calculated. Unfortunately, the intrinsic lattice thermal conductivity of cubic zirconia cannot be measured but must be estimated from theory, in order to calculate the thermal conductivity of zirconia stabilized by solutes. This causes uncertainty in the theory. However, one can test the theory of phonon scattering by oxygen vacancies in the case of reduced TiO_2 , where the intrinsic conductivity is known, and reductions in thermal diffusivity had been measured in 1978 by Siebenack et al. over a wide temperature range and several vacancy concentrations. It is shown that theory agrees with the data, particularly at low concentrations and at high temperatures, where single vacancies are most likely to occur. This lends confidence to the scattering calculations for vacancies in zirconia. In the important case of yttria-stabilized zirconia, currently used for thermal barrier coatings, the solute atom scatters very weakly, so that vacancy scattering is not affected by any association between the oxygen vacancy and the solute. For other solutes which scatter by mass differences, association would affect phonon scattering, at least at low temperatures.

PECULIARITIES OF ACOUSTIC PHONON SCATTERING FROM A PLANAR CRYSTAL DEFECT AND PSEUDOSURFACE PHONONS

A.M.Kosevich and A.V.Tutov,

B.I.Verkin Institute for Low Temperature Physics and Engineering of the Ukrainian National Academy of Sciences, 310164 Kharkov, Ukraine

A scattering of long wavelength acoustical phonons from a planar crystal defect is studied. A resonance reflection of the transverse phonons from the planar defect is discovered and conditions of such a reflection are investigated. It is shown that the resonance conditions are connected with existence of longitudinal phonons localized at the planar defect and travelling along it with a phase velocity c_{ph} where $c_t < c_{ph} < c_l$ (c_t and c_l are the transverse and longitudinal sound velocities respectively). A set of stationary eigen solutions pseudolocalized at the defect interface (similar to so called resonance vibrational states) is constructed, and a density of states of the pseudosurface phonons is calculated. It is shown that the density of pseudosurface states has the features at the edge of the frequency band of the longitudinal phonons in the case of the weak defect. A non-symmetrical stationary solution which consists of (1) a homogeneous transverse wave propagating only in one elastic semispace and (2) longitudinal localized waves in the both elastic semispaces is found. The condition of the resonance reflection of the transverse phonons from the defect layer coincides with a condition under which the non-symmetrical stationary vibration exists.

PHONON SCATTERING RELATED TO OXYGEN PRECIPITATION IN CZ-SILICON

F. Zeller, K. Laßmann, W. Eisenmenger

1. Physikalisches Institut, Universität Stuttgart, D-70550 Stuttgart, Germany

Since Czochralski-silicon contains a supersaturated solution of interstitial oxygen in its as-grown state heat treatment causes the formation of various types of oxygen precipitates, whose morphology, size and composition depends on crystal growth conditions, doping and thermal history. Much attention has been focused on this field during the past decades due to its influence on device yield and performance. Using time- and energy-resolved phonon spectroscopy with superconducting tunneling junctions we have demonstrated in a recent study [1] the effect of heat treatments on the scattering of acoustic phonons in Cz-silicon. Measurements in transmission as well as backscattering showed increased scattering over the whole energy range as well as rather narrow-band phonon scattering, possibly due to geometrical phonon resonances. Here we report on new results based on multistep annealing cycles of a wider range of samples with different oxygen and carbon concentrations. The most striking result of these experiments is the appearance of a series of at least three phonon resonances with minima at 2.9 meV, 3.9 meV and 5.7 meV (line width approximately 0.6 meV), which evolve after annealing around 1050°C for at least ten minutes in samples with measurable carbon concentration. Increased annealing time results in a slight shift of the resonance positions. IR spectra of these samples show a change of the precipitate-related absorption bands around 1100 cm⁻¹. We therefore assume that the observed phonon scattering is caused by the resonant excitation of geometric eigenvibrations of oxygen agglomerates, whose size would then be expected to be around $\lambda/2_{\text{trans}}$, which is 3.6 nm in the case of the lowest-lying absorption. Since the phonon absorption at 5.7 meV appears at twice the energy of the 2.9 meV resonance within experimental accuracy, it is ascribed to the respective λ -resonance. The observed shifts of resonance positions may be indicative of agglomerate growth or shrinkage.

Phonon spectroscopy appears to be an interesting tool to investigate oxygen precipitation in silicon, it may as well offer new insight into the scattering of phonons at extended crystal defects.

[1] G. Schrag, M. Rebmann, C. Wurster, F. Zeller, K. Laßmann, W. Eisenmenger, submitted to phys. stat. sol. (a)

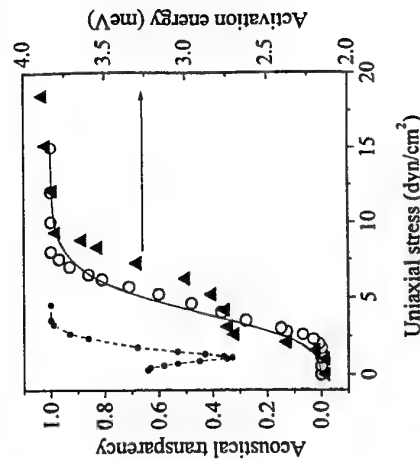
Phonon spectroscopy of D' band tails of shallow impurity in Ge

B. Danilchenko, D. Poplavsky, and S. Roshko

Institute of Physics of NASU, Prosp. Nauki 46, 252650 Kiev, Ukraine

The broadening of impurity electron states driven by both electron correlations and disorder in impurity atoms distribution is one of the factors leading to the metal-insulator transition in doped semiconductors. In many-valley semiconductors the value of broadening can be governed by uniaxial stress applied along one of the valleys. We report on the study of D' band formed from the D' state that represents the second electron attached to impurity atom.

Phonon absorption in intermediately doped bulk Ge:Sb with donor concentration $5 \cdot 10^{16}$ cm⁻² was studied by means of time-of-flight phonon spectroscopy. Phonons were generated by metal film and detected by superconducting bolometer deposited on the opposite side of the crystal. Three phonon modes - LA, FTA and STA - were resolved. Uniaxial stress along $\langle 111 \rangle$ direction was applied in order to reduce the contribution of different valleys to the overlapping integral between neighboring impurities thus decreasing the band width. Also transport measurements in order to determine the energy activation dependence on uniaxial stress were carried out. Acoustical transparency with respect to FTA phonon mode and activation energy dependence on uniaxial stress is represented on Figure (open circles). Its behavior is essentially different from that for weakly doped Ge:Sb (dashed line). The same behavior of acoustical transparency was observed for LA mode while STA mode signal was independent on uniaxial stress. The observed acoustical transparency behavior is attributed to phonon assisted electron transitions from impurity ground state to D' band tails caused by disorder in impurity distribution. Uniaxial stress reduces the D' band width thus increasing the energy gap between ground state and D' band. This leads to increase of acoustical transparency and activation energy of conductivity as seen from Figure. Also numerical calculations of acoustical transparency based on the phenomenological model were performed and are in a good agreement with experimental results.



PosA1

The structure and dynamics of hard carbon formed from C₆₀ fullerene

Stephen M Bennington¹, Naoyuki Kitamura¹, Markys G Cain², Mike H Lewis³ & Masa

Arai⁴

¹ISIS Facility, Rutherford Appleton Laboratory, Chilton Didcot, Oxon. OX11 0QX, UK.

²Osaka National Research Institute 1-8-31 Midorigaoka, Ikeda-shi, Osaka. 563 Japan.

³Physics Department, University of Warwick, Coventry CV4 8PP, UK.

⁴National Laboratory for High Energy Physics (KEK) 1-1, Tsukuba, Ibaraki, 305, Japan.

Subjecting C₆₀ to high pressures and temperatures reveals a wide range of new carbon structures ranging from polymeric through to amorphous diamond like phases. When C₆₀ is compressed at 3GPa and heated to 700°C it produces a form of carbon that is semimetallic and has a hardness that is approximately two thirds that of diamond.

Since C₆₀ became available in large quantities there have been many studies of the phases produced by subjecting it to high pressure and temperature. Most of these phases occur because of the molecules abilities to polymerise through a [2+2] cycloaddition process, where the double bonds on two molecule break and reform into an sp³ bonded dimer C₆₀ molecule. Under hydrostatic pressures the molecules remain intact at pressures up to 20 GPa, but the application of a shear or uniaxial component to the pressure may initiate polymerisation at pressures as low as 3.3 GPa.

We present elastic and inelastic neutron scattering measurements that show that the material is graphitic and, using this data coupled with electron microscopy, we show that the graphitic planes are regularly warped much like corrugated cardboard or iron. This gives the material its stiffness and resistance to shear and accounts for its remarkable hardness.

PosA2

ANHARMONICITY-INDUCED COOPERATIVE PROTON ORDERING IN H-BONDED SYSTEMS

A. Bussmann-Holder

Max-Planck-Institut für Festkörperforschung
Heisenbergstr. 1, 70569 Stuttgart, Germany
fax: +49-711-689-1091, email: annet@vaxf2.mpi-stuttgart.mpg.de

K.-H. Michel and N. Dalal
Florida State University, Tallahassee, FL 32306, USA

Abstract

In many organic and anorganic hydrogen-bonded systems cooperative proton ordering is observed at a certain critical temperature, which in anorganic systems mostly coincides with the onset of ferro- or antiferroelectricity. Upon deuteration the ordering temperature is, in general, dramatically enhanced, and the conventional interpretation of this phenomenon is based on the pseudospin tunneling model. Yet, from recent X-ray diffraction data, severe doubts of the applicability of this model arose. A new model, which combines the pseudospin tunneling model with the anharmonic polarizability model, is introduced here which convincingly accounts for experimental data, correctly reproduces the isotope effect, combines order/disorder-displacive phenomena, and most importantly, includes the O - H ... O bond geometry. The temperature-dependent tunnel and lattice mode frequencies are discussed which exhibit important peculiarities due to their coupling as compared to the uncoupled systems.

RESONANT HYPER-RAMAN SCATTERING IN SEMICONDUCTORS: EXCITONIC EFFECTS

A. García-Cristóbal*, A. Cantarero*, M. Cardona*, and C. Trallero-Giner†

*Departamento de Física Aplicada, Universidad de Valencia, E-46100
Burjassot, Spain

*Max Planck Institut für Festkörperforschung, Heisenbergstrasse 1, 70569
Stuttgart, Germany

†Departamento de Física Teórica, Universidad de La Habana, 10400 La
Habana, Cuba

A theoretical model of resonant hyper-Raman scattering in semiconductors involving two incident photons of frequency ω_L is developed. The model is valid for energies $2\hbar\omega_L$ around the absorption edge (either dipole-allowed or forbidden) of the solid, and takes into account Wannier excitons as intermediate states in the scattering process. The relevant matrix elements of the exciton-photon and exciton-phonon interaction are obtained and used to evaluate the hyper-Raman cross-section. Both deformation potential and Fröhlich interaction are included in the model. It is found that in the case of resonances around allowed optical transitions, Fröhlich-mediated scattering becomes dipole-allowed whereas it is forbidden when induced by the deformation potential, and the opposite situation holds for scattering around a forbidden absorption edge. We have performed numerical calculations of the resonance profile (hyper-Raman cross-section vs $2\hbar\omega_L$) and used them to interpret the existing experiments on ZnSe (allowed edge) and rutile TiO_2 (forbidden edge). In the case of ZnSe the resonant enhancement occurs when $2\hbar\omega_L$ matches the energy of the $2p$ exciton state, while in the case of TiO_2 the resonant state is the s exciton. Finally, we discuss the feasibility of hyper-Raman scattering to study electronic states not accessible to one-photon spectroscopy, both for symmetry reasons or for energy reasons as is the case in large band-gap semiconductors, like GaN.

Propagation of phonon pulses in GaN

B. Danilchenko†, V. Guzenko†, T. Paszkiewicz‡, M. Boćkowski§, I. Grzegory§, and T. Suski§

† Institute of Physics of NASU, Prosp. Nauki 46, 252650 Kiev, Ukraine

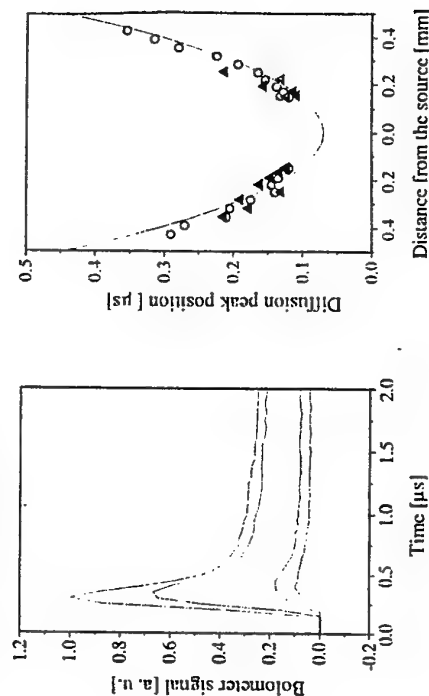
‡ Institute of Theoretical Physics, University of Wrocław, PL 50-204 Wrocław, Poland
§ UNIPRESS, Polish Academy of Sciences, Sokolowska 29, 01-142 Warsaw, Poland

We studied propagation of beams of acoustic phonons in crystalline n -type specimens of gallium nitride grown in the Center of High Pressure Studies of Polish Academy of Sciences in Warsaw. These undoped specimens have the form of platelets of linear dimensions $0.15 \text{ mm} \times 60 \div 100 \text{ mm}^2$. The crystalline symmetry axis is perpendicular to the surface of platelets.

Various measurements indicate that such GaN crystals contain nitride vacancies of density 10^{19} cm^{-3} , gallium vacancies of density $10^{17} \div 10^{18} \text{ cm}^{-3}$ as well as some amount of oxygen impurities. Additionally, the nitride vacancies behave like a shallow donor. Therefore, the diffusive propagation of phonon beams is expected.

Phonon pulses were generated by photoexcitation of the clean crystal surface. Phonons were detected using an indium superconducting film. The measured quantity is the flux of phonons J . Phonon pulses are characterized by broad diffusive maximum followed by the long-time tail (Fig. 1). We studied the dependence of arrival time of flux maxima t_{max} on the distance r between the source of phonons and the detector and obtained that the t_{max} is proportional to r^2 (Fig. 2). We also studied the dependence of flux peaks height J_{max} on the distance r . We obtained that the J_{max} goes as r^{-1} .

Using our data we found the group velocity of phonons traveling along c -direction to be $6 \times 10^3 \text{ cm/s}$. The values of the diffusion coefficient D and mean free path l were estimated to be $0.085 \text{ m}^2/\text{s}$ and $35 \text{ }\mu\text{m}$ respectively.



THERMAL CONDUCTIVITY OF SEMI-CRYSTALLINE ISOTROPIC AND ORIENTED POLYMERS

P. Dashora, J. Dashora and G. Gupta
Department of Physics, University of Rajasthan, Jaipur-302 004, India.

The problem of heat transport through semi-crystalline polymers has not been well understood. In absence of a suitable theoretical frame-work, various two phase models are used to interpret the observed thermal conductivity λ . These models consider semi-crystalline materials as a composite of anisotropic crystallites dispersed in isotropic amorphous medium. Authors suggest that two phase approach is not justified for polymers as the same polymeric chain runs through several ordered and disordered regions which makes motion of the structural units in these regions highly correlated. Recently, authors have developed a formalism $1/2$ for the heat transport through linear polymers considering phonons as the chief heat carriers. Predominant phonon-scattering processes have been identified for the temperature regions below and above T_g on the basis of the structural features; such as extent and strength of intermediate -range- order IRO, type and density of structural defects, effect of temperature on movements of structural units etc. Relations deduced for the dependence of conductivity on temperature predicts the thermal conductivity of linear amorphous polymers extremely well. In the present work it is shown that this approach is applicable to semicrystalline polymers also. It provides not only the correct values of λ over a wide range of temperature, but also explains the observed anisotropy in λ on extrusion in much more consistent manner than any other existing theory, IRO parameter correlates well with the draw ratio. Calculated values of λ for five semicrystalline polymers: for isotropic λ_{iso} , along the draw direction $\lambda_{||}$ and perpendicular to the draw direction λ_{\perp} are shown in figure 1, Δ are exptl. values $3/$ and full line is theoretical curve, max. dev. is 5%.

- /1/ Dashora P. Physica Scripta 45,399(1992) ibid 49, 611, (1994)
- /2/ Dashora P. and G. Gupta Polymer 37, 231 (1996).
- /3/ C.L. Choy, et.al, J. Appl. Polym. Sci. 26, 2325 (1981)

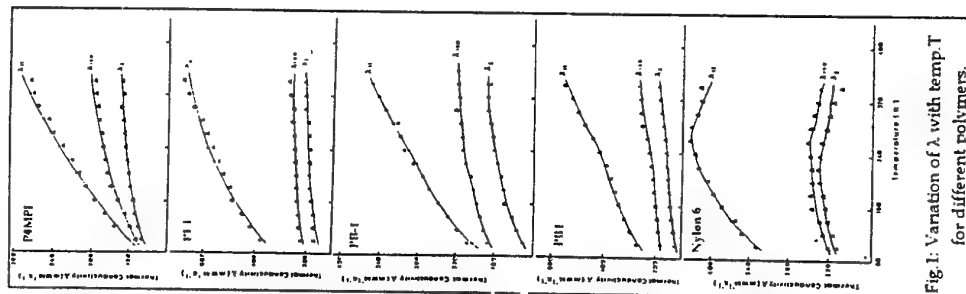
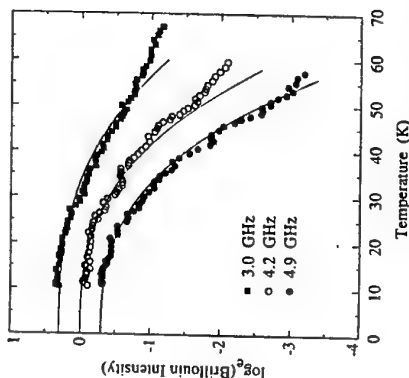


Fig.1: Variation of λ with temp. T for different polymers.

ANHARMONIC PHONON DECAY IN TeO₂: CONFIRMATION OF HERRING'S THEORY

E. P. N. Damen, A. F. M. Arts, and H. W. de Wijn
Faculty of Physics and Astronomy, and Debye Research Institute,
Utrecht University, P.O. Box 80000, 3508 TA Utrecht, The Netherlands

The decay of L phonons propagating along the [001] axis in TeO₂ has been measured by the use of a recently developed technique for the generation of monochromatic Fresnel-diffracted phonon beams in the gigahertz range [1]. The method relies on cw laser-induced thermomodulation of a metallic transducer evaporated onto the crystal, and permits measurement as a function of the temperature T at a set of angular frequencies ω . In addition to monochromaticity and tunability, the technique features substantial narrowness ($\sim 40 \mu\text{m}$) of the phonon beam with minimum divergence ($\sim 3^\circ$). Wave-vector selective detection via Brillouin scattering largely eliminates interference by secondary scattering. A few typical results at a depth of 2.0 mm below the transducer are displayed in the figure.



As was pointed out by Herring [2], in elastically anisotropic media L phonons are predominantly scattered by three-phonon processes $L + ST \rightarrow FT$. Using group-theoretical considerations, Herring established that the decay rate of L phonons is $\tau^{-1} = A\omega^2 T^6$, with $a + b = 5$, on the proviso that ω is in the acoustic range and that T is well below the Debye temperature. In the present case of L phonons propagating along [001] in TeO₂, which belongs to crystal class D_{4h}, the locus of ST wavevectors satisfying wavevector and energy conservation is a line in wavevector space, at least in the center of the Brillouin zone. This implies that $a = 2$ and $b = 3$. A circumstance further favoring $a = 2$ is that TeO₂ is very close to the rutile structure, which has the more symmetric crystal class D_{4h}, and whose slowness surfaces comply with $a = 2$ throughout the entire zone.

In the analysis of the data, a and b are extracted by assuming that the signal intensity depends on τ^{-1} according to $I = I_0 \exp(-z/v\tau)$, where z is the distance covered by the phonons, v is the sound velocity, and the prefactors I_0 pertain to a particular temperature scan. The output values are $a = 1.8 \pm 0.2$, $b = 2.8 \pm 0.2$, and $a + b = 4.6 \pm 0.3$. Indeed, a , b , and $a + b$ are in conformity with Herring's predictions.

- [1] E. P. N. Damen, A. F. M. Arts, and H. W. de Wijn, Phys. Rev. Lett. 74, 4249 (1995).
- [2] C. Herring, Phys. Rev. 95, 954 (1954).

NEUTRON SCATTERING STUDY AND LATTICE DYNAMICAL SIMULATION OF H₂O+He CLATHRATE

S.L.Dong, A.I.Kolesnikov and J.C.Li

Department of Physics, UMIST, PO Box 88, Manchester, M60 1QD, UK

Clathrate Hydrates (also called gas hydrates) are multi-component crystalline compounds with structures consisting of a net of H₂O (host) molecules hydrogen-bonded together like ice and enclosing molecules of small-diameter gases (guest). Its properties are of fundamental interest to condensed matter physics and chemistry as well as planetary astronomy.^{1,2,3} Common natural gas hydrates usually have two types of crystal structures (type I and type II Clathrate Hydrates). However, when guest gas molecule (atom) is small the host lattice can keep its ice structure.^{4,5} Neutron powder diffraction experiments showed that a gas hydrate lattice of H₂O+He (at pressures between 0.28 to 0.5 GPa) was almost the same as for ice II.⁵ Its dynamical characteristics could be different from ice II due to the interactions between host and guest molecules.

The vibrational dynamics of clathrate hydrates H₂O+He was studied *in situ* under pressure of He gas of 0.36 GPa using Inelastic Neutron Scattering (INS). The comparison of the obtained INS spectra with that for ice II measured previously at the same pressure showed that the high-energy peaks in both translation and libration regions slightly shifted towards to higher energies. This means that the resultant forces acting on water molecules were increased due to absorption of He atoms.

Lattice Dynamical simulation is a good method in analysing the INS spectra.^{6,7} A Force Constant Lattice Dynamical (FCLD) simulations was successfully used to describe the INS spectra of ice Ih under the assumption that there are two kinds of hydrogen bond strengths in ice Ih.⁷ Recently the calculated vibrational spectra for high pressure phase ice II were well fitted to measured INS data by introducing rather weak hydrogen bonds in ice II between water molecules with distorted local hydrogen-oxygen configurations.⁸

This report presents also the FCLD calculations for clathrate hydrates H₂O+He. The calculations were based on force field model for ice II and additionally Van der Waals interaction between water molecules and helium atoms were introduced. Indeed, from the comparison of FCLD calculations for both ice II and the clathrate hydrate it was demonstrated that the hydrogen bond strengths were slightly increased due to helium additions.

1. G.A. Jeffrey, *Inclusion Compounds*, (ed. J.L. Atwood, J.E.D. Davies and D.D. MacNicol, Academic Press, 1984) Vol. 1, Chapter 5 and Vol. 3, Chapter 3.
2. H. Tanaka and K. Kiyohara, *J. Chem. Phys.*, **98** (1993) 8110.
3. D. Blake, L. Allamandola, S. Sandford, D. Hudgins and F. Freund, *Science*, **254** (1991) 548.
4. W.L. Vos, L.W. Finger, R.J. Hemley and H. Mao, *Phys. Rev. Lett.*, **71** (1993) 3150.
5. D. Londono, J.L. Finney and W.F. Kuhs, *J. Chem. Phys.*, **97** (1992) 547.
6. B. Renker, *Physics and Chemistry of Ice* (eds. E. Whalley, S.J. Hones and L.W. Gold) 82-89 (University of Toronto Press, 1973).
7. J.C. Li and D.K. Ross, *Nature*, **365** (1993) 327.
8. S.L. Dong, Y. Wang, A.I. Kolesnikov and J.C. Li, *J. Chem. Phys.*, in press.

PHONON SCATTERING IN DIAMOND FILMS

V.B.Efimov, L.P.Mezhov-Deglin, M.K.Makova

Institute of Solid State Physics RAS, Chernogolovka, Moscow distr., 142432, Russia

We have studied thermal conductivity κ of free standing diamond films with different quality and sizes of the crystallites in bulk. The measurements were performed in the temperature range 10-350 K by steady-state heat flux technique. We have estimated value and temperature dependence of the phonon mean free path λ using the simple gas kinetic equation for thermal conductivity: $\kappa \approx 1/3 \lambda C_{ph}^* v$. The values of heat capacity C_{ph} and mean sound velocity v are known from literature for massive crystals

At high (room) temperatures the mean free path of phonons is limited by the phonon-phonon Umklapp interaction and phonon scattering on point defect in bulk. Both these processes lead to increasing of $\lambda(T)$ with cooling the sample but they have the different temperature dependencies. So from $\lambda(T)$ dependence one can judge on the quality (purity) of the sample.

At low temperatures the phonon-boundary scattering dominates and λ is limited by crystallite sizes. The mean free path of phonons in best of the samples has reached the value λ of a few microns at temperatures 20-70 K, that has agree with the middle sizes of crystalline estimated from X-ray measurements and from microphotos.

At lower temperatures the value of λ is increasing. It can be explained by the phonon penetration through the boundaries between crystallites. The temperature dependence of λ is closed to $\lambda(T) \sim T^{-(1/2)}$.

COMBINED INFRARED AND RAMAN STUDY OF THE OPTICAL PHONONS OF DEFECT-CHALCOPYRITE SINGLE CRYSTALS

A. Eifler, J.-D. Hecht, G. Lippold, V. Riede, W. Grill, G. Krauß * and V. Krämer*

Institut für Experimentelle Physik II, Universität Leipzig,
Linnéstraße 5, D-04103 Leipzig, Germany

Phone: +49-341-9732682, Fax: +49-341-9732699, e-mail: eifler@physik.uni-leipzig.de

* Freiburger Materialforschungszentrum, Albert-Ludwigs-Universität,
Stefan-Meier-Straße 21, D-79104 Freiburg, Germany

The defect-chalcopryrite ordered vacancy compounds show a wide range of interesting physical properties. In addition to the properties of applicational interest such as wide-gap, birefringence and strong photoconductivity they show various degrees of cation and vacancy ordering which is of more fundamental interest. The different crystallographic structures due to this ordering can be distinguished by observation of the infrared and Raman activities of the optical phonon modes.

In optically anisotropic media oblique phonon modes exist corresponding to extraordinary waves, which exhibit directional dispersion. For this reason in general oriented crystals are needed to determine the frequency as well as the symmetry classes of the optical phonons along principal directions. In this work we demonstrate that the combination of both infrared and Raman spectroscopy can lead to a reliable assignment of the optical phonon modes of the materials under investigation.

Whereas the lattice vibrational properties of $A^{III}B^{VI}_2C^{VI}_4$ defect-chalcopryrites with $B^{III} = Ga$ or In are well known, due to complications with respect to crystal growth and sample preparation much less is known about the phonon modes in the corresponding $A^{II}Al_2C^{VI}_4$ compounds. In the present work we report for the first time the combined infrared and Raman study of $HgAl_2Se_4$, $CdAl_2Se_4$ and $ZnAl_2Se_4$ single crystals grown by chemical vapour transport (CVT). For an oriented $CdAl_2Se_4$ single crystal the frequency dependence of the oblique phonon modes was observed by varying the angle between the main axis of the crystal and the optical beam in the backscattering Raman measurements.

The data obtained for the $A^{II}Al_2Se_4$ compounds are compared with the results for $A^{III}B^{VI}_2C^{VI}_4$ defect-chalcopryrites. The dependence of the properties of the lattice vibrations with respect to the variation of the elements is discussed. The infrared and Raman activities of the optical phonons of $ZnAl_2Se_4$ exhibiting a statistical distribution of a part of the aluminium atoms and all vacancies at sites of symmetry $4d$ (space group $I\bar{4}2m$) are compared with those of $ZnIn_2Se_4$, where the cations and vacancies are statistically distributed at all cationic sites.

THERMAL CONDUCTIVITY OF LaB_6 - THE ROLE OF PHONONS

K. Flachbart¹, M. Reiffers¹, Š. Molokáč¹, A. Belling², J. Bischof², E. Kononova³ and Y. Paderno³

¹Institute of Experimental Physics, Watsonova 47, SK-04353 Košice,

²Research Institute of Electrical Engineering, Prague, Czech Republic,

³Institute for Problems of Materials Science, Kiev, Ukraine

The thermal conductivity of a high conductivity metallic LaB_6 single crystal was measured in the temperature range between 0.7 K and 30 K. The striking point of the observed temperature dependence is the non-linear behaviour of the thermal conductivity at lowest temperatures, where a linear dependence is expected. Further measurements of electrical conductivity and in magnetic field suggest that the non-linearly originates from a scattering mechanism which leads to the decrease of the electronic component of thermal conductivity. Scattering processes of conduction electrons by phonons and magnetic impurities are discussed.

SOUND VELOCITY ANOMALY RELATED TO THE CHARGE ORDERING

IN $\text{La}_{1-x}\text{Sr}_x\text{MnO}_3$ AND $\text{La}_{1-x}\text{Ca}_x\text{MnO}_3$ H. Fujishiro¹, M. Ikebe¹, T. Kikuchi¹ and T. Fukase²¹ Faculty of Engineering, Iwate University, 4-3-5 Ueda, Morioka 020-8551, Japan² Institute for Materials Research, Tohoku University, 2-1-1 Katahira, Sendai 980-8577, Japan

Recently, interest of researchers in the fields of both elementary and applied physics has revived for perovskite based manganites $\text{R}_{1-x}\text{A}_x\text{MnO}_3$ ($\text{R}=\text{La}$ and trivalent rare-earth ions, $\text{A}=\text{Sr}$, Ba , Ca), because this system exhibits a variety of dramatic phenomena. Typical of such phenomena is the colossal magnetoresistance, which is a kind of metal-insulator transition induced by applied magnetic fields. The ferromagnetic metallic state (FMM) which is stabilized by the double exchange mechanism often becomes unstable against the formation of the charge ordering (CO) which is usually accompanied with the antiferromagnetic (AFM) order. In this system the occurrence of the CO transition can be conveniently monitored by observing anomalies in the sound velocity $v_s(T)$.^{1,3)} We have measured the sound velocity $v_s(T)$ of $\text{La}_{1-x}\text{Sr}_x\text{MnO}_3$ and $\text{La}_{1-x}\text{Ca}_x\text{MnO}_3$ polycrystals by the use of the pulse-superposition method between 4.2K (or 90K) and 290K. For $\text{La}_{1-x}\text{Sr}_x\text{MnO}_3$, we observed $v_s(T)$ anomalies associated with the CO transitions for the Sr concentration $0.48 \leq x \leq 0.75$ besides the polaron ordering transition centered at $x=1/8$.²⁾ Based on the observed anomalies we have made up a phase diagram of the charge ordering transition of $\text{La}_{1-x}\text{Sr}_x\text{MnO}_3$ as a function of T and X. For also $\text{La}_{1-x}\text{Ca}_x\text{MnO}_3$, we confirmed the $v_s(T)$ anomalies due to the polaron ordering transition centered at $x=1/8$. The overall features of the phase diagrams of $\text{La}_{1-x}\text{Sr}_x\text{MnO}_3$ and $\text{La}_{1-x}\text{Ca}_x\text{MnO}_3$ are very similar in spite of the difference in the e_g -electron bandwidth. The dilatation dL/L also showed clear anomalies at the same temperatures as the $v_s(T)$ anomalies. These experimental observations indicate extraordinarily large electron-lattice and/or spin-lattice couplings in these compounds.

¹⁾ A.P. Ramirez *et al.*: Phys. Rev. Lett. 76 (1996) 3188.²⁾ H. Fujishiro, M. Ikebe, K. Konno and T. Fukase: J. Phys. Soc. Jpn. 66 (1997) 3703.³⁾ H. Fujishiro, M. Ikebe and K. Konno: to be published in J. Phys. Soc. Jpn. 67 (1998).⁴⁾ P. Schiffer, A.P. Ramirez *et al.*: Phys. Rev. Lett. 75 (1995) 3336.RAMAN SCATTERING STUDY OF PbZrO_3 UNDER HIGH PRESSURE

H. Furuta, S. Endo

Research Center for Materials Science at Extreme Conditions, Osaka University, Toyonaka, Osaka 560-8531, Japan

L. C. Ming

Hawaii Institute of Geophysics and Planetology, University of Hawaii at Manoa, Honolulu 96822, HI, USA

M. Kobayashi

Graduate School at Engineering Science, Osaka University, Toyonaka, Osaka 560-8531, Japan

Raman scattering experiments have been carried out on antiferroelectric perovskite PbZrO_3 at room temperature under high pressure using a diamond anvil cell. The polycrystalline PbZrO_3 has pressurized up to 30 GPa. A new mode appears at 430 cm^{-1} and the mode at 210 cm^{-1} disappears into the background at 2.5 GPa. With further increasing pressure up to about 17.5 GPa, the Raman spectral features do not change, so much. At about 17.5 GPa two modes appear at 120 cm^{-1} and 260 cm^{-1} , respectively. On contrary, the mode at 180 cm^{-1} disappears at near 19 GPa. In spectra observed above 25 GPa, the background scattering dominates and only a few strong Raman modes are seen above the background level. These anomalous behaviors in the Raman spectra are consistent with the previous dielectric constant measurements and microscopic observation¹, indicating that two phase transitions occur at about 2.5 GPa and 17.5 GPa.

[1] Y. Kobayashi *et al.*: submitted to J. Phys. Chem. Solids.

NONEQUILIBRIUM ACOUSTIC PHONONS IN DIAMOND: GENERATION, SCATTERING, REFLECTION

T.I.Galkina, A.I.Sharkov, A.Yu.Klovov, R.A.Khmel'nitskii, V.A.Dravin, A.A.Gippius
P.N.Lebedev Physical Institute RAS, Leningrad pr. #53, Moscow, 117924 Russia

Nonequilibrium phonon propagation in diamond has been studied using "heat pulse technique", when phonons are generated near the surface of a sample either by heating (by electrical current or light) of a deposited metal film or by direct excitation of the sample by strongly absorbed light. In the case of diamond, the latter requires a powerful UV (≤ 200 nm) light sources which presents some difficulties.

Possibility of employment of heated thin (~ 100 nm) gold film as a generator of nonequilibrium phonons in diamond was studied both theoretically and experimentally. Within the framework of this problem: first, calculations of a mean temperature of a gold film deposited on diamond surface under pulsed heating were carried out as a result of numerical solution of a system of heat conduction equations taking account of temperature depending parameters (heat capacity, thermal conductivity coefficients of the film and substrate, as well as boundary resistance); second, the experimental measurements of photoresponse of bolometric structure diamond/gold film to a pulsed laser excitation were performed. The cooling times τ_c of Au film (about $100 \div 150$ ns) experimentally and calculated theoretically are in close agreement. It means that such a generator should not be used in heat pulse experiments with diamond samples of about 1 mm thick, since τ_c is much longer than duration of laser pulse (~ 10 ns) and the time of ballistic phonon propagation ($40 \div 60$ ns).

A novel method of phonons generation is proposed — photoexcitation of buried implanted layer. This layer turns out to be built in the host matrix of the sample, and therefore, one can assume its perfect acoustic match with the host matrix. The times of phonon generation by laser pulse are comparable with the laser pulse duration. Using this phonon generator, we were able to resolve the arrival of phonons of longitudinal and transverse polarization. Comparison of heat pulses observed in a «transition» geometry with those calculated by Monte Carlo method yields the constant of elastic phonon scattering. The experimentally found value ($A_{\text{exp}} = 2 \cdot 10^{-44} \text{ s}^{-3}$) coincides with that calculated taking account of phonon scattering by ^{13}C isotopes. Experiments and calculations performed for the «reflection» geometry with those calculated, results in conclusion that the interface diamond-liquid helium is, in fact, completely transparent for acoustic phonons.

SURFACE PHONONS ON Si(001)/As(2x1)

H. M. Tütüncü^{1,2}, S.C.A.Gay¹ and G. P. Srivastava¹

¹ Department of Physics, University of Exeter, Stocker Road, Exeter EX4 4QL, UK

² Sakarya Üniversitesi, Fen-Edebiyat Fakültesi, Fizik Bölümü, Adapazarı, Turkey.

(March 10, 1998)

Abstract

We present surface phonon calculations for the Si(001)/As(2x1) surface using the adiabatic bond-charge model within a repeated slab scheme. The structural and electronic information necessary for these calculations is obtained using the *ab initio* pseudopotential method [1]. We provide a detailed analysis of polarization characteristics of important surface phonon modes. The phonon spectrum of this surface is compared in detail with that of the Si(001)(2x1) surface presented in a recent bond-charge model study [2]. We find that the surface acoustic phonon modes are mainly localized on the As atoms due to the mass difference between As and Si atoms.

[1] S. C. A. Gay, S. J. Jenkins and G. P. Srivastava (submitted for publication)

[2] H. M. Tütüncü, S. J. Jenkins and G. P. Srivastava, Phys. Rev. B **56**, 4656 (1997).

PosA15

PHONON SCATTERING IN CRYSTALS WITH STRONGLY CORRELATED BISTABLE SUBLATTICE AND HYSTERETIC BEHAVIOUR OF THERMAL CONDUCTIVITY IN HTSC COMPOUNDS

A. P. Saiko, V. E. Gusakov, A. Jezowski*

Institute of Solid State and Semiconductor Physics, National Academy of Sciences, P. Brovki, 17, Minsk 220072, Belarus. gusakov@iftp.bas-net.by

*Institute for Low Temp. & Structure Research, Polish Academy of Sciences, 2 Okolna St., 50-422 Wrocław, Poland

The precise measurements reveal that there is a hysteresis in thermal conductivity $K(T)$ over a broad temperature range 70-230 K in high temperature superconducting $Yb_2Cu_3O_x$ (123) and $Rb_2Cu_3O_x$ (124; R= Dy, Gd, Eu) compounds. The measurements were performed on ceramic, polycrystal as well as single crystal specimens. It is particularly remarkable that for 123 compounds the hysteresis depends on the oxygen nonstoichiometry index: with $x=7$ the hysteresis curve has a one-loop and for oxygen deficient $x=6$ nonconducting compounds acquires two-loops with a certain path-tracing on cooling and heating of the sample.

We propose a theoretical description of this phenomenon with the generalized model of anharmonically unstable strongly correlated sublattice modulating acoustic phonon spectrum of the matrix lattice.

PosA16

AB INITIO PHONON SPECTRA FROM A SUPERCELL APPROACH

R. Heid, Max-Planck-Institut für Physik komplexer Systeme, Nöthnitzer Straße 38, 01187 Dresden, Germany

K.-P. Bohnen, Forschungszentrum Karlsruhe, Institut für Nukleare Festkörperphysik, P.O. Box 3640, 76021 Karlsruhe, Germany

We present a numerically efficient direct space approach to the calculation of complete phonon spectra of crystals from first principles, which represents a generalisation of the standard supercell technique. It only requires atomic force calculations and permits to deduce ab initio force constants even for systems with longer-range lattice interaction without involving large supercells [1]. We discuss first applications of this method to a variety of elemental metals (Ir, Rh, Ba, ...) with different lattice structures and interaction ranges. Calculations are performed employing a mixed-basis pseudopotential method in the local-density approximation to density-functional theory. We present results for phonon dispersions, density of states and interatomic force constants, and discuss the procedure to find optimal superlattice geometries. In the case of iridium, we predict pronounced dispersion anomalies along the [110] direction.

[1] R. Heid, K.-P. Bohnen, and K. M. Ho, Phys. Rev. B **57**, 7407 (1998)

OXYGEN CONCENTRATION DEPENDENCE OF RAMAN ACTIVE PHONONS WITH VARIABLE GRÜNEISEN PARAMETER IN $\text{YBa}_2\text{Cu}_3\text{O}_x$

T. Hirata

National Research Institute for Metals, 1-2-1, Sengen, Tsukuba, Ibaraki 305, Japan

Beginning with the mode Grüneisen parameter $\gamma_i = -(d\ln\omega_i/d\ln V)$, where V is the unit-cell volume and ω_i is the frequency of the i -th vibrational mode, the concentration dependence of phonon frequency is derived as $\ln(\omega_i/\omega_0) = (V_0\epsilon/\theta - \gamma_0)\ln(1 + \theta x/V_0) - \epsilon x$ under the condition that γ_i varies with x as $\gamma_i = \gamma_0 + \epsilon x$ (ϵ : constant), where ω_0 and V_0 are the corresponding values at $x=0$ and θ is the x derivative of V ($V = V_0 + \theta x$). It is highlighted that the derived equation is applied to the Raman-active modes in superconducting $\text{YBa}_2\text{Cu}_3\text{O}_x$ or $\text{YBa}_2\text{Cu}_{3-x}\text{Co}_x\text{O}_{7-\delta}$, which change in frequency with oxygen stoichiometry or Co concentration. The significance of variable Grüneisen parameter is stressed to reproduce the experimental data, focussing on the mode dependent Grüneisen parameter with reference to its size and sign.

86

PHONON SCATTERING ANOMALY IN THE DOPED MANGANESE OXIDE, $\text{La}_{1-x}\text{Sr}_x\text{MnO}_3$

H. Fujishiro and M. Ikebe

Faculty of Engineering, Iwate University, 4-3-5 Ueda, Morioka 020-8551, Japan.

Carrier-doped lanthanum manganites with perovskite-based structure have recently attracted renewed interest of researchers because this system exhibits a variety of dramatic phenomena such as the colossal magnetoresistance, field induced structural transition, charge ordering transition etc. The competition and interplay between various equally important mechanisms i.e., the double exchange, antiferromagnetic superexchange, Jahn-Teller effect, structural instability due to ion-radius mismatching, charge ordering and orbital ordering are considered to stage the dramas in the $\text{R}_{1-x}\text{A}_x\text{MnO}_3$ system ($\text{R} = \text{La}$ and rare-earth ions, $\text{A} = \text{Sr}$, Ba , Ca). We have measured the phonon thermal conductivity (κ_{ph}) of $\text{La}_{1-x}\text{Sr}_x\text{MnO}_3$ ($X \leq 0.5$) polycrystals in the temperature range from 10K to 300K. For typical samples the thermal diffusivity α_{ph} has been also measured under an identical experimental setup as the κ_{ph} measurement.¹⁾ For the Sr concentration $X \leq 0.17$ where the structural transition between rhombohedral to orthorhombic phase and the charge ordering transition centered at $X = 1/8$ ²⁾ take place, the phonon thermal conductivity κ_{ph} is markedly reduced especially in a low temperature region ($T < 80\text{K}$). With increasing X above $X = 0.18$, κ_{ph} is enhanced up to $X = 0.3$ but again is reduced as X approaches to 0.5 where the charge order transition centered at $X = 0.5$ occurs.³⁾ The experimental data of κ_{ph} are analyzed assuming additive scattering rate and the Debye phonon spectrum. The analyses indicate that the phonon scattering is anomalously enhanced especially in a low temperature region ($T \leq 50\text{K}$). We explain the observed reduction in κ_{ph} as being due to a kind of the two-level phonon scattering caused by unstable oxygen lattice sites in the vicinity of the lattice transformations. We have observed this kind of anomalous scattering in several oxide compounds such as $\text{La}_{2-x}\text{Sr}_x\text{CuO}_4$.

¹⁾ M. Ikebe, H. Fujishiro, T. Naito and K. Noto: J. Phys. Soc. Jpn. **63** (1994) 3107.

²⁾ H. Fujishiro, M. Ikebe, K. Konno and T. Fukase: J. Phys. Soc. Jpn. **66** (1997) 3703.

³⁾ H. Fujishiro, M. Ikebe and K. Konno: to be published in J. Phys. Soc. Jpn. **67** (1998).

⁴⁾ M. Ikebe and H. Fujishiro: submitted to this conference.

Local-mode thermodynamics of filled skutterudite antimonides

V. Keppens¹, D. Mandrus¹, B. C. Sales¹, B. C. Chakoumakos¹, P. Dai¹, R. Coldea¹,
M. B. Maple², D. A. Gajewski³, E. J. Freeman², and S. Bennington¹

¹ Oak Ridge National Laboratory, Solid State Division, P.O. Box 2008, Oak Ridge TN
37831

² Department of Physics and Institute for Pure and Applied Physical sciences,
University of California San Diego, La Jolla California 92093, USA

³ ISIS facility, Rutherford Appleton Laboratory, Chilton Didcot, Oxon, UK

Recently, it has been reported that filled skutterudite antimonides such as $\text{LaFe}_3\text{CoSb}_{12}$ show a drastic decrease in the thermal conductivity (κ) compared to their unfilled analogues. This reduction is primarily due to the presence of the rare-earth atom that fills the voids in the skutterudite structure and vibrates locally in an oversized atomic "cage". These local modes strongly scatter phonons and, therefore, are expected to have a marked effect on the lattice dynamics of these materials. We present Resonant Ultrasound Spectroscopy (RUS) and specific heat data for both filled ($\text{LaFe}_3\text{CoSb}_{12}$) and unfilled (CoSb_3) skutterudites, as well as neutron scattering measurements on $\text{LaFe}_3\text{Sb}_{12}$ and $\text{CeFe}_3\text{Sb}_{12}$. These data reveal that the La-filled skutterudite exhibits an unusual thermodynamic behavior, characterized by the presence of 2 low-energy localized modes. These low-energy vibrational modes, which are not present in the unfilled counterpart CoSb_3 , give the first unambiguous evidence for the "rattling" behavior of the rare earth in the structure.

ULTRASONIC ATTENUATION IN YTTRIA-STABILIZED ZIRCONIA

Kenta Kirimoto, Kohji Nobugai[†], Tatsuro Miyasato

Department of Computer Science and Electronics, Kyushu Institute of Technology, Iizuka, Fukuoka 820-8502, Japan
[†]The Institute of Scientific and Industrial Research, Osaka University, 8-1 Mihogaoka, Ibaraki, Osaka 567-0047, Japan

The ultrasonic attenuation in $\text{ZrO}_2(\text{Y})$ single crystal was measured by means of a pulse-echo method at temperatures from 300K to 430K. And the power dependence of the ultrasonic attenuation was measured at room temperature.

Single crystals $\text{ZrO}_2(\text{Y})$ containing 9.6 mol% and 10 mol% Y_2O_3 were prepared as samples for the present experiment. The dimension of the sample was $7 \times 7 \times 20 \text{ mm}^3$. Both end faces of the samples were polished optically flat. A ZnO thin film transducer was deposited by the rf-magnetron-sputtering onto the end face of the samples. The attenuation coefficients were obtained from the decay of the echo pattern.

The attenuation of 80MHz longitudinal acoustic waves propagating along $\langle 100 \rangle$, $\langle 110 \rangle$ and $\langle 111 \rangle$ directions was measured, and it was made clear that the attenuation increased with increasing temperature at temperatures from 300K to 430K. This attenuation curve is assumed to be the lower temperature side of the relaxation attenuation peak, because in other experiments we observed a relaxation peak for 10MHz longitudinal waves at temperatures from 500K to 540K. On the other hand, the power dependence of ultrasonic attenuation showed that the attenuation decreased with increasing acoustic intensity. This power dependence, in other words, the saturation of ultrasonic attenuation also depended on the yttrium-ion concentration, and high yttrium-ion concentration reduced the saturation. The saturation mechanism may be related to the two level systems composed of two equivalent oxygen sites, but the details are not known at this moment.

NEUTRON SPECTROSCOPY OF HIGH-DENSITY AMORPHOUS ICE

A.I. Kolesnikov¹, J.C. Li¹, N.C. Ahmad², C.-K. Loong³, J. Nipko³, D. Yocum³
and S.F. Parker⁴

¹Department of Physics, UMIST, PO Box 88, Manchester, M60 1QD, UK

²The University of Surrey, Guildford, Surrey GU2 5XH, UK

³Argonne National Laboratory, Argonne, IL 60439-4814, USA

⁴ISIS Facility, Rutherford Appleton Laboratory, Chilton, Didcot, Oxon, OX11 0QX, UK

One of the interesting results from the investigation of the structure and dynamics of ice was the observation of the phase transition from hexagonal ice-Ih to high-density amorphous (hda) ice by applying pressure ~10 kbar at low temperatures (T<130 K) [1]. The density of hda-ice (~1.31 g/cm³ at 10 kbar) is about 40% higher than that of ice-Ih (0.94 g/cm³ at ambient pressure). The inelastic neutron scattering (INS) spectrum of hda-ice H₂O in the range of translational and librational intermolecular vibrations (2 to 200 meV) was studied recently in Ref. 2 and 3. Nevertheless, the behaviour of this amorphous state does not seem to be completely understood, and the proposed models of the amorphization process [4,5] are ambiguous. In the present report, we present the INS spectra measured for a recovered hda-ice in the range of intramolecular vibrations up to 500 meV. The comparison of the present spectra with those measured early for other ice phases indicates that hda-ice is a disordered form of high-density ice-VI, which brings new light to the origin of the transition ice-Ih → hda-ice.

References:

1. O. Mishima, L.D. Calvert and E. Whalley, *Nature* **310** (1984) 393; and **314** (1985) 76.
2. A.I. Kolesnikov et al., *J. Phys.: Condens. Matter* **6** (1994) 375.
3. J.C. Li, *J. Chem. Phys.* **105** (1996) 6733.
4. E. Whalley et al., *J. Phys.* **48** (1987) C1-429.
5. J. S. Tse et al., *J. Chem. Phys.* **92** (1990) 3992.

NEUTRON SPECTROSCOPY OF FULLERITE HYDROGENATED UNDER HIGH PRESSURES

A.I. Kolesnikov^{1,2}, V.E. Antonov¹, I.O. Bashkin¹, J.C. Li², A.P. Moravsky³,
E.G. Ponyatovsky¹ and J. Tomkinson⁴

¹Institute of Solid State Physics RAS, 142432 Chernogolovka, Moscow District, Russia

²Department of Physics, UMIST, PO Box 88, Manchester, M60 1QD, UK

³Institute of Chemical Physics RAS, 142432 Chernogolovka, Moscow District, Russia

⁴ISIS Facility, Rutherford Appleton Laboratory, Chilton, Didcot, Oxon, OX11 0QX, UK

A recent inelastic neutron scattering (INS) study of the C₆₀ hydrofullerite synthesized at 620 K under a hydrogen pressure of 6 kbar then quenched to liquid nitrogen (spectrometer KDSOG-M at IBR-2, Dubna, Russia) [1] has shown that the quenched sample consisted of the C₆₀H_x molecules, x ≈ 24, packed as the bcc lattice and also interstitial hydrogen molecules, in amount of 1.4-H₂ molecules per C₆₀H_x molecule. The C₆₀H_x molecules were stable under normal conditions whereas interstitial hydrogen left the sample upon annealing at 300 K.

This report presents the INS data from hydrofullerite prepared and quenched under a higher hydrogen pressure of 30 kbar. The spectra were measured at 24 K in the range of the energy transfer from 2 to 500 meV using the high-resolution time-of-flight spectrometer TFXA (ISIS, RAL, UK). Both the as-prepared (quenched) state and the final state (after annealing for 3 hours at room temperature) were studied. The main features in the INS spectra and their behaviour upon annealing showed that the present as-prepared hydrofullerite also consisted of C₆₀H_x molecules with molecular hydrogen dissolved onto interstitial sites. However, the spectral features due to interstitial molecular hydrogen in the new hydrofullerite differed markedly from those of hydrofullerite after the 6 kbar synthesis. Two peaks observed at about 15.5 and 31 meV are close to energies of the first transitions between the rotational states of the free hydrogen molecule, E_{0,1} = 14.7 and E_{1,2} = 29.4 meV. The peak at 9.0 meV is close to the first roton peak of the two-dimensional molecular hydrogen, E₀₋₁ = 7.35 meV. There is another remarkable feature in the INS spectra of hydrofullerite, a peak at ~13 meV. This feature is very close to the vibrational modes characteristic of polymeric C₆₀. The report presents a detailed analysis of the experimental spectra.

1. A.I. Kolesnikov, V.E. Antonov, I.O. Bashkin, G. Grosse, A.P. Moravsky, A.Yu. Muzychka, E.G. Ponyatovsky and F.E. Wagner, *J. Phys.: Condens. Matter*, **9** (1997) 2831.

RAMAN SCATTERING IN Mg-DOPED CuGeO_3

H. Kuroe, H. Soto, T. Sekine, R. Masuda*, I. Tsukada*, and K. Uchinokura*

Department of Physics, Sophia University, 7-1 Kioi-cho, Chiyoda-ku, Tokyo 102-8854, Japan

*Department of Applied Physics, The University of Tokyo, 7-3-1 Hongo, Bunkyo-ku, Tokyo 113-8656, Japan

We have studied the Raman scattering in $\text{Cu}_{1-x}\text{Mg}_x\text{GeO}_3$ ($x = 0, 0.016, 0.06, \text{ and } 0.08$). The Raman spectra observed in the Mg-doped samples are compared with those in Zn- and Si-doped samples. In the sample of $x = 0$ and 0.016 , in which the spin-Peierls (SP) transition occurs, a folded phonon mode at 368 cm^{-1} which is induced by the formation of the lattice dimerization in the SP phase is observed. It weakens and broadens in the sample of $x = 0.016$, indicating that the SP transition is suppressed by the Mg-doping. In the sample of $x = 0.08$, we have observed a broad band of which width and intensity strongly depend on the wavelength of the incident light. It has not been observed in pure CuGeO_3 , Zn-doped samples and Si-doped ones. It is probably assigned to photoluminescence. In the polarized spectra of the broad band, we observe periodic structures, which probably originates from the cascade process of a phonon emission.

PHONONS IN THE NON-CONVERTED STATE OF DyCu_2 S. Kramp^{1,2}, N.M. Pyka¹, M. Loewenhaupt² and M. Braden³¹Institut-Langevin, B.P. 156, F-38042 Grenoble Cedex 9²Institut für Angewandte Physik, TU-Dresden, D-01062 Dresden³Laboratoire Léon Brillouin, C.E. Saclay, F-91191 Gif-sur-Yvette Cedex

Intermetallic compounds of type RCu_2 show a variety of interesting magnetic phenomena due to magnetic anisotropy. The a-axis magnetic moments of DyCu_2 are ordered antiferromagnetically below T_N . Applying a strong magnetic field along the c-direction results in an Ising axis conversion, i.e. the former c-axis behaves then like the a-axis. This conversion is accompanied by a jump in the magnetostriction of $\delta l/l = 4\%$. The conversion process is expected to be phonon assisted. In order to provide a basis for experiments in the converted state, we present first phonon measurements in the non-converted state of DyCu_2 along $[100]$ and $[001]$ together with a lattice dynamical model. The LA-phonons along the a-axis exhibit an anomalous temperature behavior already in this non-converted state.

POLARON RENORMALIZATION AND LIFE-TIME BROADENING EFFECTS ON RAMAN SCATTERING UNDER MAGNETIC FIELD.

V. López-Richard[†], G. E. Marques,
Departamento de Física, Universidade Federal de São Carlos,
13565-905, São Carlos, SP, Brazil
and

C. Trallero-Giner,
Departamento de Física Teórica, Universidad de La Habana
10400 C. Habana, Cuba.

The one phonon Raman scattering efficiency for III-V and II-VI zincblende-type semiconductors in high magnetic fields including the valence band admixture has been obtained. We have developed a microscopic theory for the magneto-Raman scattering in the framework of the Luttinger-Kohn Hamiltonian.

The Raman profiles are calculated as a function of magnetic field B_0 and laser frequency ω_L within the deformation potential and Fröhlich type of electron-phonon interaction.

The valence-band mixing has strong influences on the Raman profile and on the shape of resonant peaks. The calculated Raman intensity, according to the Luttinger-Kohn Hamiltonian, shows a number of new resonances related to the van Hove-like type of singularities in the density of the intermediate electron-hole states that could not be obtained with a simple parabolic model for the electronic structure. A relevant effect of the band mixing can be explained in the case of Raman scattering assisted by Fröhlich interaction when evident differences are obtained between the two scattering configurations with parallel Faraday geometries $\vec{z}(\sigma^+, \sigma^+)z$ and $\vec{z}(\sigma^-, \sigma^-)z$.

For a realistic picture of the resonances, an exact calculation of the life-time broadening of the intermediate electronic states assisted by LO-phonon has been carried out including the dependence on the laser incident energy, magnetic field and Landau quantum number. Based on these grounds, the essential features of recent magneto-Raman experiments in bulk GaAs can be explained, which confirms the strong effects of the electron-phonon interaction on the enhancement of the energy broadening of the Landau state.

The sharp resonances obtained by magneto-Raman scattering allow also the identification of polaron effects on the electronic band structure as was confirmed by introducing the magneto-polaron self energy in the renormalization of the electron Landau levels. It reproduces the splitting of the correspondent resonant peak obtained experimentally. It has been proved in recent works that precise measurements of the slopes of renormalized interband transition fan lines should allow one to determine not only the reduced effective mass but also the electron and hole masses separately.

Acknowledgments: V. López acknowledges FAPESP for financial support of this work. G.E. Marques acknowledges CNPq for partial financial support. Also, the authors are indebted to T. Ruf who provided the experimental data used in this work.

[†]Departamento de Física Teórica, Universidad de La Habana, 10400 C. Habana, Cuba.

DYNAMICS OF THE CUBIC LATTICES WITH LONG - RANGE INTERACTION

E.V. Manzhelii, E.S. Sytkin

B. Verkin Institute for Low Temperature Physics & Engineering,
National Academy of Sciences of Ukraine,
47 Lenin Ave., Kharkov, 310164, Ukraine.

The influence of long - range interaction on phonon dispersion characteristics of simple cubic lattice (SC), body - centred cubic lattice (BCC) and face - centred cubic lattice (FCC) was studied. It is known, that long-range interaction, even the next - nearest neighbour (NNN) interaction, significantly affects the dynamical properties of above - mentioned systems. Note, that if only the nearest neighbours (NN) interaction is considered, vector models of SC and BCC lattices are unstable, while the account of far - off neighbours (NNN in particular) stabilises them. Dispersion characteristics were calculated in scalar and vector models with the NNN interaction taken into account. It was found that in scalar model of FCC lattice if only the NN interaction is taken into account, the dispersion law along the entire line $K_x + K_y = \pi/a$, does not depend on K_z (here K_x, K_y, K_z are the components of the wave vector, a is the lattice constant). This causes the singularity in the density of states at the top boundary of the phonon spectrum. If NNN interaction is accounted, the singularity vanishes. The role of noncentral interaction was analysed. It appeared, that in specific cases even in cubic lattices there is a considerable difference between transverse velocities of the sound, which corresponds to strong elastic anisotropy. In such highly anisotropic systems the role of noncentral interaction is known to be quite considerable. The influence of NNN interaction on fundamental properties of purely shear surface waves with horizontal polarisation (SH - waves) was analysed. It was shown that in SC lattices one - component surface waves only exist if NNN interaction is accounted. For FCC and BCC lattices the consideration of NNN interaction turns one - partial surface waves into two - partial.

Ab-initio lattice dynamics studies of the vibrational spectra of ice

L.Morrison and S.Jenkins
 Department of Physics
 University of Salford
 Salford, UK
 M5 4WT

We present studies of the vibrational properties of a number of ice structures as evaluated by ab-initio lattice dynamics. Calculations are performed within the generalized gradient approximation to density functional theory using the ab-initio pseudopotential method. Dynamical properties are determined by finite difference evaluation of the dynamical matrix using atomic forces. The resulting normal modes are analysed in detail by projection onto pure intra and inter molecular modes of the water molecules. The importance of configurational disorder is assessed by comparison of results from numerous different proton arrangements in similar supercells. Both low pressure, tetrahedrally coordinated, and high pressure phases are studied.

Calculated vibrational density of states are compared with results from quasi elastic neutron scattering experiments and the microscopic origin for various features in the spectra explained. In particular, the role of coupling between the dynamics of the various types of bond which characterise the structures (covalent bonds, hydrogen bonds and inter sub-lattice bonds) is discussed.

EVIDENCE OF STRONG ELECTRON- PHONON COUPLING
IN DOUBLE LAYERD CUPRATE SUPERCONDUCTORS

K. Moltida and K. Suzuki

Department of Physics, Hokkaido University, Sapporo 060-0810, Japan.

In a previous paper, we proposed an explanation for the anomalies observed in the c-axis infrared optical conductivity of the underdoped crystals such as $\text{YBa}_2\text{Cu}_3\text{O}_x$ ($x = 6.5 \sim 6.8$) at low temperatures: a sudden decrease in oscillator strength of $\approx 320 \text{ cm}^{-1}$ phonon mode and an appearance of a broad band at $\approx 400 \sim 450 \text{ cm}^{-1}$ [K. Moltida, Physica C 282-287 (1997) 1063]. That is, the anomalies result from renormalization due to superconductivity of the B_{1u} O(2), O(3) in-phase phonon mode. For the phonon mode we previously predicted that it can strongly couple with the holes in the CuO_2 plane [K. Moltida, Physica B 219&220 (96) 210].

In order to discuss the relation between the broad band and superconductivity in detail, we analyzed the optical conductivity data of a natural underdoped cuprate $\text{YBa}_2\text{Cu}_3\text{O}_x$ [D.N. Basov et al. Phys. Rev. B 50 (1994) 3511]. This crystal is appropriate for avoiding the complexities that might be induced by inhomogeneity in atomic arrangement present in the $\text{YBa}_2\text{Cu}_3\text{O}_x$ system. As a result, this broad band can be described as a phonon using a Lorentzian curve with a large line width ($\approx 170 \text{ cm}^{-1}$). Further this spectrum disappears above a temperature ($82 \sim 90$) slightly upper than T_c (80K) but clearly below the spin gap starting temperature ($\approx 160\text{K}$). This indicates that the appearance of the broad band is connected with the superconductivity, considering that the local superconducting correlations develop below the temperature slightly upper than T_c .

On the other hand, we estimated the strength (square of the effective plasma frequency) of the phonon into which the B_{1u} O(2), O(3) in-phase phonon mode at lower temperatures i.e. the broad band changes at higher temperatures, by assuming that the B_{1u} O(2), O(3) out-of-phase phonon mode does not change its strength as temperature increases. The strength estimated is only 17 % at 82K of that of the dome-like spectrum at 10K, gradually decreases as temperature increases and becomes 6 % at 300K. This characteristic of the temperature dependence of the strength is almost same also in the $\text{YBa}_2\text{Cu}_3\text{O}_x$ system. Its origin is not clear at the moment.

Since the derived changes in the B_{1u} O(2), O(3) in-phase phonon mode due to superconductivity is so considerable, this shows that coupling between this phonon mode and the holes is strong. Therefore we should investigate the mechanism that induces the high-temperature superconductivity in not only underdoped cuprate superconductors but also optimally doped by taking into account of this coupling since the mechanism is considered common for the both cuprate superconductors.

ELASTIC ANOMALIES WITH THE TWO SPIN-STATE TRANSITIONS IN LaCoO_3 S. Murata, S. Isida, M. Suzuki, Y. Kobayashi, K. Asai, and K. Kohn¹

University of Electro-Communications, Chofu, Tokyo 182-8585, Japan

¹ Waseda University, Okubo-3, Tokyo 169-8555, Japan

LaCoO_3 exhibits two broad magnetic-electric transitions, one near 100 K and a second near 500 K. These two transitions have been interpreted as due to successive spin-state transitions of Co^{3+} ($3d^4$) ions; dominantly from LS (low spin; $S=0$) to IS (intermediate spin; $S=1$) at the first and from IS to HS (high spin; $S=2$) at the second transition.¹⁾ The energies of these spin-states are considered to depend on the lattice deformation as being manifested in anomalous lattice expansions accompanied by the spin-state transitions.

We examined the spin-state transitions of LaCoO_3 by the ultrasonic experiment, which is very powerful to investigate phenomena coupled with the lattice deformation. Figure 1 shows the temperature dependence of the elastic modulus along [111]. There are anomalous lattice softening in two temperature regions; a rather sharp one starts around 30 K and a broad one starts around 300 K. The modulus was reproduced reasonably well (solid line) by a model calculation assuming the three spin states coupled with the lattice deformation. This fact confirmed that the anomalous softening arises from the spin-state transitions. We also observed an increase of the absorption (inset) around 100 K suggesting the increase of the fluctuation of the spin states. The present study demonstrates a substantial coupling between the lattice deformation and the spin states, and supports the three-spin-states model.

1) K. Asai *et al.*,

J. Phys. Soc. Jpn. 67 290 (1998).

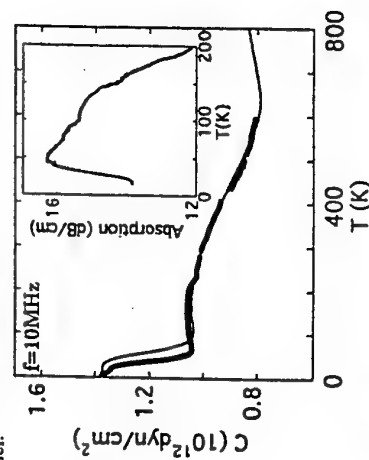


Fig1. Temperature dependences of the elastic modulus and the absorption of LaCoO_3 .

PSEUDOLATTICE VIBRATIONS IN SMECTIC LIQUID CRYSTALS

Hideyuki Nakayama, Yukiko Minagawa, Sachiko Yajima, and Kikujiro Ishii

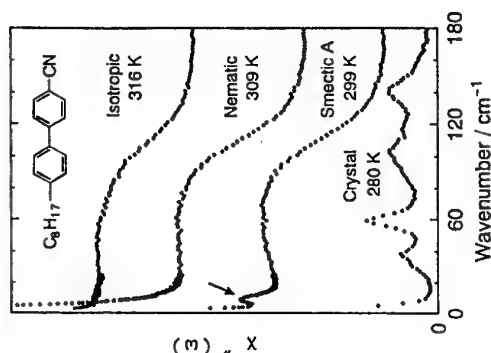
Department of Chemistry, Gakushuin University,

Mejiro 1-5-1, Toshimaku, Tokyo, 171-8588 Japan

Recently, low-frequency Raman spectra have been studied well to see the molecular motion in molecular liquids. However, very few similar spectra have been reported for liquid crystals. One of the causes of this is the elastic scattering of the laser light due to the polydomain structure of liquid crystals. We tried to prepare liquid-crystal samples with a small number of domain boundaries by applying the Bridgman method for the crystal growth. We obtained spectra clear enough for the analysis of the low-frequency region, in which lattice-vibration bands of molecular crystals are usually observed.

The figure below shows Raman spectra of 4-octyl-4'-cyanobiphenyl (8CB) in various phases. These spectra are corrected for the thermal excitation. It is seen that, for the smectic and nematic phases, a broad band peaked at about 70 cm^{-1} is observed. This band is similar to that observed for the isotropic liquid, and seems to reflect the low-frequency molecular motion in the nonperiodic structure of liquid crystals. In addition to this, it is worth noting that a small and sharp band, which is not observed in the nematic and isotropic phases, was observed around 10 cm^{-1} for the smectic phase.

A similar low-frequency additional band was also observed in the smectic phase of other cyanobiphenyls. These bands can be fitted by the damped-oscillator function, but not by the relaxational function. Taking account of these facts and of the layer structure of the smectic phase, these bands are considered to be the pseudolattice vibration propagating along the direction perpendicular to the layers. Thus it is very interesting that fairly long-range coherent vibrations exist in liquid crystals.



NONLINEAR QUANTUM DYNAMICS OF LOCAL MODES: PERFECT AND DISORDERED ALKALI HALIDE CRYSTALS

Dmitri Nevedrov and Vladimir Hizhnyakov

Institute of Theoretical Physics

University of Tartu

Tähe 4, EE2400 Tartu, Estonia

We study the time evolution of strongly excited local vibrations anharmonically interacting with phonons in three-dimensional cubic lattice. Recently developed nonperturbative theory [1] of stepwise quantum decay of strongly excited local mode associated either with an impurity center or strong vibrations of host atoms in perfect lattice (s.c. self-localized mode) [2] is applied to perfect and disordered alkali halides: $KCl:Na$, $KCl:F$, KI , NaI . The lattice dynamics calculations are based on a shell model Green's functions. The step-wise two-phonon relaxation, phenomena of emission of phonon bursts, quasimonochromatic spectrum of emitted phonons, dependence of the local mode frequency on its amplitude are confirmed by numerical calculations.

It was found that sharp explosions like emissions of phonons take place at the amplitude of the mode of about 0.3 Å or larger. We predict that the lifetime of self-localized modes is finite, there is no stage in the decay process which shows an exponential behaviour. The effect can highlight new ways in generation of ultrashort phonon pulses. Finally, we give several experimental facts which support our theory and suggest other possible ways of experimental realization,

1. V Hizhnyakov, Phys. Rev. B **53**, 13981 (1996); V. Hizhnyakov, D. Nevedrov, Z. Phys. Chem **201**, 301 (1997).
2. V Hizhnyakov, D. Nevedrov, Phys. Rev. B **56**, R2809 (1997).

PHASE TRANSITION AND EXCESS SPECIFIC HEAT IN RS-ARS MIXED CRYSTALS

N. Noda, K. Shimizu, R. Nozaki and Y. Shiozaki

Division of Physics, Hokkaido University

N10W8, Sapporo, 060-0810, Japan

Rochelle salt (RS) is a characteristic ferroelectric, which undergoes two successive phase transitions turning from the paraelectric phase to the ferroelectric one and again to the paraelectric one with decreasing temperature. Ammonium Rochelle salt (ARS) is isomorphous to RS in the paraelectric phase, but it is not ferroelectric. Although ARS is polar in the lower temperature phase, the polarization cannot be reversed by an electric field. The polar axis of ARS is parallel to the b -axis in contrast with the a -axis in RS. RS_{1-x}ARS_x mixed crystal system is divided into four regions according to the dielectric properties⁰: $0 \leq x \leq 0.025$ (region I), $0.025 \leq x \leq 0.18$ (region II), $0.18 \leq x \leq 0.9$ (region III), $0.9 \leq x \leq 1.0$ (region IV). The mixed crystals in the region I show similar properties to RS. In the region II, no phase transition occurs. The mixed crystals in the region III undergo a ferroelectric phase transition and the polar axis is parallel to the a -axis. The character of the mixed crystals in the region IV is similar to that of ARS.

The specific heat of RS shows very small anomalies around the two transition points.^{1,2} The anomalous behaviour of the specific heat in ARS is quite different from that in RS and exhibits a very large sharp peak at the transition point.³

On the other hand, in the region III, the specific heat anomaly is small. However, the jump at the transition point increases with x .^{3,5} Their behaviour is explained very well by the Landau type free energy. In general, in the uniaxial ferroelectrics, the thermodynamic quantities can be well described by the classical Landau theory up to the extreme vicinity of the transition point, since the fluctuation effect is suppressed by the long-range dipole-dipole interaction.⁶ Therefore, the divergence of the specific heat is weakened. In addition, in this case, the fluctuation have the anisotropy: The transverse fluctuation for the polar axis gives a large contribution. In the region III, it can be considered that the fluctuation effect, which is not so strong, increases with x and this is reflected to the increase of the specific heat jump. Moreover the fluctuation increasing is thought to be large for the direction along the b -axis. It can be related to the change of the polar axis from a -axis in the region III to b -axis in the region IV, and also related to the decrease of the peak value of the static dielectric constant along the a -axis as x increases in the region III.⁷

We will give an explanation about the dielectric and the thermal behaviour around the transition point in RS-ARS with taking account of the fluctuation effect. In this consideration, the results of the structural study will be also included.

References:

- 1) Y. Makita and Y. Takagi, *J. Phys. Soc. Jpn.* **13** (1958) 367.
- 2) A. J. C. Wilson, *Phys. Rev.* **54** (1938) 1103, J. Helwig, *Ferroelectrics* **7** (1974) 225, M. Tatsumi, T. Matsuo, H. Suga and S. Seki, *J. Phys. Chem. Solids* **39** (1978) 427.
- 3) N. Noda, H. Nakano, H. Haga, R. Nozaki and Y. Shiozaki, *J. Kor. Phys. Soc.* **29** (1996) S513.
- 4) N. Noda, H. Haga, T. Kikuta, R. Nozaki and Y. Shiozaki, *Ferroelectrics* **168** (1995) 169.
- 5) N. Noda, H. Haga, H. Nakano, R. Nozaki and Y. Shiozaki, *Ferroelectrics* **184** (1996) 293.
- 6) A. I. Larkin and D. E. Khmel'nitskii, *Sov. Phys. JETP* **29** (1969) 1123.

RAMAN SCATTERING STUDY OF $\text{Cu}(\text{Ge}_{1-x}\text{Si}_x)\text{O}_3$

Norio Ogita^A, Yasuhiro Tsunazumi^A, Osamu Fujita^B
 Jun Akimitsu^B and Masayuki Udagawa^A

^AFaculty of Integrated Arts and Sciences, Hiroshima University,
 Kagamiyama 1-7-1, Higashi-Hiroshima 739-8521, Japan

^BDepartment of Physics, Aoyama Gakuin University,
 Tokyo 157, Japan

CuGeO_3 shows Spin-Peierls (SP) transition at 14K. Substituting Si to Ge site, the SP transition temperature (T_p) decreases with increasing Si concentration. In order to clarify the lattice dynamics and magnetic excitations in $\text{Cu}(\text{Ge}_{1-x}\text{Si}_x)\text{O}_3$, temperature-, magnetic field- and polarization-dependence of Raman scattering spectra of $\text{Cu}(\text{Ge}_{1-x}\text{Si}_x)\text{O}_3$ have been measured for $x=0, 0.005, 0.01, 0.015$ and 0.02 . From the normal mode analysis, the lattice is mainly stabilized by the Ge-O bond. The Si substitution increases the Ge-O interaction, because the energy of the Ge-O vibration in uniform phase increases. The zone-folded phonons due to cell doubling appear in the higher temperature region than T_p . This means that the lattice instability occurs in the higher temperature and T_p should increase if the lattice instability is primary for SP transition. However, the actual T_{SP} decreases with the increase of x . This discrepancy between the lattice dynamical result and the actual T_p is understood by the decrease of the one dimensional spin correlation length. Therefore, the decrease of the magnetic correlation length by the Si-doping is important for the SP transition in $\text{Cu}(\text{Ge}_{1-x}\text{Si}_x)\text{O}_3$.

From the magnetic field dependence, the following new result is obtained. The peak at about 30cm^{-1} has been observed even in the magnetic phase, where the spin gap due to SP transition vanishes. This peak was assigned as the magnetic excitation related to the spin gap. However, the present observation concludes that this peak is not the magnetic excitation, since the phonons due to the cell doubling have been observed simultaneously. Thus, this peak at 30cm^{-1} is assigned as the soft phonon mode for the lattice distortion already pointed out in our previous paper and also the lattice distortion exists even in the magnetic phase.

Dynamical Properties of One-Dimensional Lennard-Jones Lattice

Tsuneysu Okabe and Hiroaki Yamada
 Graduate School of Science and Technology,
 Niigata University, Niigata 950-2081, JAPAN

Dynamical properties of one-dimensional system with large number of degrees of freedom, such as FPU model and ϕ^4 model, have been extensively investigated since original studies in early times [1, 2]. However one-dimensional Lennard-Jones (LJ) chain has not been studied except for some early works in 1970's [3, 4], although it keeps basic interest in the nonlinear dynamics.

We carried out computer simulation by symplectic integrator with adequate numerical accuracy [5, 6]. In a transition region between quasiperiodic (solid-like) and strongly chaotic (gas-like) motion the characteristics of the LJ lattice system with nearest-neighbor interaction appear. The energy dependence of maximum Lyapunov exponents (MLE), which is an indicator for stochasticity, shows a plateau region (P-region) between the weakly chaotic and strongly chaotic region. In the P-region the MLE is insensitive to change of energy, different from the FPU and soft-core potential.

The difference of energy dependence of the MLE between LJ and soft-core is due to the convexity of the potential form. The absence of convexity is a remarkable feature of the LJ potential, which does not exist in other potential. It is shown that the above P-region is well correspond to an energy region which the local instability of the LJ potential surface becomes dominant.

Moreover the characteristics of phase space structure which create the characteristic dynamics are also revealed by Poincare plots [6]. Especially, in a low density region it is shown that a (clustered state like) cooperative particle motion can be well observed [7].

1. For example, M. Pettini and M. Landolfi, *Phys. Rev. A* **41**, 768 (1990) and references therein; K. Fukamachi, *Europhys. Lett.* **26**, 449 (1994), *Physica. B* **219**, 411 (1996).
2. L. Casetti, R. Livi and M. Pettini, *Phys. Rev. Lett.* **74**, 375 (1995).
3. P. Bocchieri, A. Scotti, B. Bearzi and A. Loinger, *Phys. Rev. A* **2**, 2013 (1970); G. Contopoulos, L. Galgani and A. Giorgilli, *Phys. Rev. A* **18**, 1183 (1978).
4. K. Yoshimura, *Physica D* **104**, 148 (1997).
5. T. Okabe, H. Yamada and M. Goda, *Int. J. Mod. Phys. C* **7**, 613 (1996).
6. T. Okabe and H. Yamada, *Int. J. Mod. Phys. B* (1998), to be published.
7. T. Okabe and H. Yamada, *Mod. Phys. Lett. B*, submitted.

PHONON STUDY OF TEMPERATURE EVOLUTION OF STRAIN IN GaAs/Si(001) AND GaAs/Si(111) HETEROSTRUCTURES.

L. G. Quagliano, D. Orani and A. Ricci
I.M.A.I.-C.N.R., P.O. Box 10, via Salaria km 29.300
00016 Monterotondo Scalo, Roma, Italy
Z. Sobiesierski

Department of Physics and Astronomy, University of Wales
College of Cardiff, P.O. Box 913, Cardiff CF1 3TH, Wales, U.K

Heteroepitaxy of GaAs films on Si substrates is a promising technique for combining the advantages of GaAs-based photonic devices with those of the highly developed Si technology. However, a lattice mismatch of about 4.1% between GaAs and Si and a large difference between thermal expansion coefficients between the two materials contribute to strains and dislocations and prevent the growth of high-quality GaAs epilayer.

Raman spectroscopy has been used to characterize the strain and its temperature dependence in 4.1 μm GaAs layers grown on Si (001) and Si (111) substrates, grown by M.B.E., in the temperature range 100-500 K. The amount of strain in GaAs films has been estimated from the frequency shift of the optical phonon modes respect to the values of bulk samples measured under the same experimental conditions. For GaAs/Si(111) heterostructure polarization selection rules have been used to separate the various components of the optical phonon modes.

For temperatures lower than 400 K shift towards lower frequencies with respect to the bulk frequencies of the observed phonon modes has been observed. We attribute this behavior to the presence of a tensile strain in the GaAs layers, greater in the (111) growth direction than in the (001) one. This strain is the "thermal" strain arising from the difference in thermal expansion coefficients between GaAs and Si. Whereas, for temperatures greater than 400 K shift of the phonon modes to higher frequencies has been observed. This compressive strain is due to the larger lattice constant of GaAs compared to that of the substrate. Therefore, the observed temperature dependence of phonon peak positions indicates the temperature evolution of strain for GaAs/Si heterostructures. These results confirm the accuracy of Raman spectroscopy for studying quantitatively the strain present in heteroepitaxial layers.

SOFT PHONON AND BISMUTH CONTENT IN FERROELECTRIC $\text{SrBi}_2\text{Ta}_2\text{O}_9$

Seiji Kojima and Itaru Saitoh
Institute of Applied Physics, University of Tsukuba, Tsukuba, Ibaraki
305-8573, Japan.

Currently among bismuth layer-structured ferroelectrics $\text{Bi}_2\text{A}_{m-1}\text{B}_m\text{O}_{3m+3}$, the compounds of $m=2$ become to be the most important materials in the field of ferroelectric memory. These materials undergo ferroelectric phase transitions from tetragonal to orthorhombic system above the room temperature. However, their fundamental properties of ferroelectric phase transitions have been not yet well studied. The lattice instability related to a ferroelectric phase transition of $\text{SrBi}_2\text{Ta}_2\text{O}_9$ was studied by Raman scattering in the temperature range between 80 K and 958 K. The lowest optical mode of $\text{SrBi}_2\text{Ta}_2\text{O}_9$, at 28 cm^{-1} , shows remarkable softening towards $T_c = 608\text{ K}$. The influence of bismuth content to the soft optic mode was also studied. It is found that the damping factor of the soft mode decreases markedly when the bismuth content increases. The microscopic origin of marked change of damping was discussed in relation to the defects at Sr and Bi sites.

HIGH-PRESSURE BRILLOUIN STUDY ON HYDROGEN CHLORIDE UP TO 8 GPa

S. Sasaki, K. Kamabuchi, T. Kume, and H. Shimizu

Department of Electrical and Electronic Engineering, Gifu University,

1-1 Yanagido, Gifu 501-1193, Japan

CREST, Japan Science and Technology Corporation,

Kawaguchi, Saitama, 332-0012, Japan

Solid hydrogen chloride (HCl) is one of the simplest hydrogen-bonded crystals. With decreasing temperature, HCl undergoes the transitions to phase I (orientationally disordered cubic) at 158.9 K, to phase II (orientational disordered orthorhombic) at 120.0 K and to phase III (ordered orthorhombic) at 98.4 K. In phase I and II, HCl molecule rotates at each lattice point, connecting with other molecules by hydrogen-bonds. The purpose of this paper is to determine the elastic properties of HCl under pressure at 300 K by Brillouin spectroscopy, and is to investigate the anomalous elastic property in orientationally disordered phase.

For the loading of HCl in a diamond anvil high-pressure cell (DAC), gaseous HCl was sublimated by spraying its vapor into a small cylindrical gasket hole (diameter 0.2 mm, depth 0.2 mm) of the DAC cooled in a liquid nitrogen bath. After adequate pressure was applied, the DAC was warmed to room temperature. In order to determine the elastic properties, a single crystal was always grown in the DAC at freezing pressure of 0.7 GPa and at 300 K. Brillouin spectra were measured in the 60° or 90° scattering geometry using a tandem Fabry-Perot interferometer (JRS). In this geometry, the wave vectors of observed phonons lie in the plane parallel to the culet of diamond anvils. Therefore, the dependence of velocities on angle ϕ in above plane can be measured by rotating the DAC about the axis perpendicular to the culet of diamond anvils. Three ratios of elastic constants to density (C_{ij}/ρ) of solid HCl are determined by applying the least-squares fitting method between the theoretical function in cubic system and angle ϕ dependence of experimental velocities.^[1]

Figure 1 shows the pressure dependence of three ratios of C_{ij}/ρ . Each C_{ij}/ρ increases against pressure. The least-square errors assuming the cubic system slightly increase at 4.5 GPa, which means that the solid-solid phase transition occurs. However, this increase is not so large that it seems to be nearly cubic system. The low-pressure phase between 0.7 and 4.5 GPa exactly corresponds to phase I, but high-pressure phase above 4.5 GPa is possibly different from the phase II in which lattice constants considerably deviate from the cubic one. Consequently, we propose that the solid phase above 4.5 GPa is distinguished from the phase II in low-temperature and is named as phase I'. The elastic anisotropy reflecting the property of molecular rotations shows almost constant ($A = 3.0$) at each pressure, which is considered to be a consequence of the competition between the molecular rotation-translation coupling [2] and the hindrance to molecular rotation by hydrogen-bonds between the molecules.

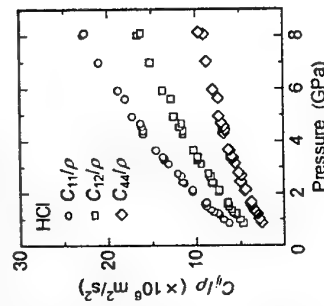
[1] H. Shimizu and S. Sasaki, *Science*, **257**, 514 (1992).[2] S. Wonneberger and A. Hüller, *Z. Phys. B-Condensed Matter* **66**, 191 (1987).

Fig. 1. Pressure dependence of three ratios of elastic constants to density for solid HCl at 300 K.

RAMAN STUDY OF HIGHLY PROTONATED LiNbO_3 THIN FILM WAVEGUIDESI. Savatinova,¹ E. Liarokapis² and I. Savova¹¹Institute of Solid State Physics, Bulgarian Academy of Sciences, Tsarigradsko Chaussee 72, 1784 Sofia, isavatin@phys.acad.bg.²Department of Physics, National Technical University, Athens 157 80, Greece, eliaro@central.ntua.gr.

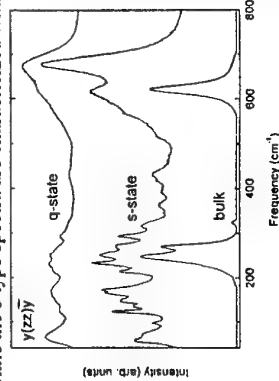
Proton-Lithium exchanged (PE) lithium niobate ($\text{Li}_x\text{H}_{1-x}\text{NbO}_3$) waveguides have attracted much attention because of the possibility to fabricate effective electrooptic and acoustooptic devices. A problem which should be solved before the practical applications of these devices are the various phase modifications which are formed at different temperatures and proton concentrations. During the last years it became clear that several rhombohedral β_i phases exist in addition to the ferroelectric phase of the pure LiNbO_3 crystal, some of which are metastable at room temperature.

Multimode PE waveguides have been produced in congruent z-cut LiNbO_3 substrates. The H-concentration was changed by annealing applying two different rates of cooling: quick (q) and slow (s). The value of the extraordinary refractive index change $\Delta n_e(q)$ in the q-process is higher than the s-value $\Delta n_e(s)$ with about $5 \cdot 10^{-3}$ at $\lambda = 633$ nm. With time $\Delta n_e(q)$ decreases to the equilibrium value $\Delta n_e(s)$. The changes in the refractive index from q- to s-cooling are reversible implying that a phase transition from metastable state to equilibrium takes place. The results from of the optical measurements are confirmed from Raman spectra.

At high proton concentration ($x_H > 0.56$) where the existence of β_i phases is supposed, the q- and s-type samples show very different Raman scattering, being also different from the scattering of the pure substrate (see figure). The q-type spectra consist of rather wide bands, while the s-type spectra are characterized with some additional narrow bands (at $< 300 \text{ cm}^{-1}$).

The diffused character of the Raman spectra in the q-type process can be explained with the presence of one or more disordered high-temperature β phases which have been frozen at room temperature by the quick cooling. The q-state disorder is probably originated from internal strains or randomly distributed H and/or Li ions.

In result, some changes in the spontaneous polarization and other parameters of the crystal lattice could take place becoming the structural mechanism of the phase transitions in the $\text{LiNbO}_3/\text{HfNbO}_3$ system.



Acknowledgments

Work supported by the Bulgarian Foundation of Science (Contract F-419), the Commission of the European Communities (Contract COP959) and the NATO grant HTECH.LG 961117.

OPTICAL PHONON ATTENUATION IN D-WAVE SUPERCONDUCTORS

A. Sergeev^{1,2}, Ch. Preis¹, and J. Keller¹¹ Dep. of Physics, University of Regensburg, D-93040 Regensburg, Germany
² Moscow Pedagogical University, Moscow 119482, Russia

Attenuation of longitudinal and transverse optical phonons in *d*-wave superconductors due to the electron-phonon interaction is calculated by employing the Kubo method. The electron-phonon interaction is considered in the frame of reference moving together with the lattice [1] that allows us to exclude from consideration the inelastic electron-impurity scattering. The screening of the longitudinal and transverse electromagnetic fields is taken into account for various values of the electron momentum relaxation time τ , the phonon frequency ω_q , and wave vector q . Analytical expression for the attenuation coefficient in the superconducting state α_s are derived in few limiting cases.

The most interesting results are obtained for $\omega_q \tau > 1$ and $q < \omega_q/v_F$ (v_F is the Fermi velocity). Here the attenuation coefficient may be presented as

$$\frac{\alpha_s}{\alpha_n} = \frac{\tau_n}{\omega} \int \left(\tanh \left(\frac{\epsilon}{2T} \right) - \tanh \left(\frac{\epsilon + \omega_q}{2T} \right) \right) \left(\rho(\epsilon) \gamma(\epsilon + \omega_q) + \rho(\epsilon + \omega_q) \gamma(\epsilon) \right),$$

where α_n is the phonon attenuation in the normal state [2], $\rho(\epsilon)$ is the quasiparticle density of state, and γ is the imaginary part of the electron self-energy in the superconducting state. The phonon attenuation is calculated numerically in the unitary limit and in the Born approximation for the electron-impurity scattering. It is found, that the value and temperature dependence of the attenuation coefficient are strongly dependent on the value of the electron-impurity potential that can explain the observed sensitivity of experimental data on the sample quality.

In the limit of $\omega_q \tau < 1$, $qv_F \tau < 1$, it is convenient to use the effective electron-phonon vertices, derived in Ref. 3. In this region of parameters peculiarities of the longitudinal dielectric function in the superconducting state practically do not manifest themselves in the attenuation coefficient.

The research of A.S. is supported by the Alexander von Humboldt Stiftung.

- [1] T. Tsuneto, Phys. Rev. B **121**, 402 (1961).
- [2] M. Yu. Reizer, Phys. Rev. B **38**, 10398 (1988).
- [3] M. Yu. Reizer and A.V. Sergeev, JETP **63**, 616 (1987).

PHONON SCATTERING IN ORIENTATIONALLY DISORDERED PHASE OF SOLID METHANE

S.A. Smirnov, V.A. Konstantinov, V.G. Manzheli, V.P. Revyakina

B. Verkin Institute for Low Temperature Physics and Engineering, National Academy of Sciences, 47 Lenin avenue, Kharkov, 310064, Ukraine,
e-mail: sasmirnov@ilt.kharkov.ua

Isochoric thermal conductivity (λ) of solid methane samples with molar volumes 30.5 and 31.1 cm³/mole has been studied in its orientationally disordered (OD) phase within the temperature range 35 - 140 K.

Above the temperature of transition of methane into the OD phase its isochoric thermal conductivity increases in the beginning with increasing temperature, passes through gentle sloping maximum, and decreases further up to the melting temperature. Thermal conductivity maximum shifts to the side of higher temperatures with increasing density of the samples. The observed unusual temperature dependence of CH₄ isochoric thermal conductivity is assigned to the effect of interaction of phonons with correlated molecular rotations.

The total thermal resistance $W = 1/\lambda$ is the sum of phonon - phonon $W_{pp} = 1/\lambda_{pp}$ and phonon - rotational $W_r = 1/\lambda_r$ thermal resistances: $W = W_{pp} + W_r$. In principle, both the components can be calculated on the basis of the crystal field potential by using the Debye temperature and effective quadrupolar charge as fitting parameters. However, even when calculating a phonon - phonon component of thermal conductivity there are certain difficulties in determining its absolute values. It is known that the results of the calculation of lattice thermal conductivity by the methods of Clemens, Callaway, Debye, and Leibfried - Schlemmer diverge by an order of magnitude even when one and the same crystalline potential is taken. This is connected with different methods of taking into account the laws of conservation of energy and quasi - momentum.

To determinate phonon-phonon component of thermal resistance of solid methane we used modified method of reduced coordinates. The advantage of this method lies in its simplicity and independence from model taken. It is well known that by a number of properties, in particular, by structure and parameters of pair potential of central intermolecular interaction, the OD phase of solid CH₄ is close to solidified inert gases, especially to krypton. Comparing thermal resistances of methane and krypton in coordinates reduced to molar parameters (W/W_{mol} , T/T_{mol}) for the same reduced molar volumes V/V_{mol} we can extract phonon-rotational component of thermal resistance.

We took as reduction parameters $T_{mol} = \epsilon \sqrt{k}$, $\lambda = k/r^2 \sqrt{\epsilon/m}$, and $V_{mol} = N \sigma^3$, where r - is the nearest-neighbor distance, and ϵ and σ - are parameters of Lennard - Jones potential. Since there is a considerable divergence in the values of pair potential ϵ and σ obtained from different sources, we used instead ϵ and σ temperatures and molar volumes of methane and krypton in critical points as reduced parameters T_{mol} and V_{mol} .

It was found that isochoric thermal conductivity of solid methane correlates well with a view of free rotation of molecules at the crystal lattice sites at premelting temperatures. At about 90 K and higher thermal resistance of methane is caused by phonon - phonon scattering merely. With decrease in temperature phonon-phonon scattering goes down, simultaneously phonon-rotation one increases monotonically and dominates near 20K. Volume dependence of total thermal conductivity is specified by phonon-phonon part predominantly.

ROLE OF THE Nb IMPURITIES ON THE THERMAL CONDUCTIVITY (Ta_{1-x}Nb_xSe₂)₁ ALLOYS IN THE VICINITY OF THE PEIERLS TRANSITION

A. Smolnata,¹ A. Bilušić,¹ E. Tutiš,¹ H. Berger² and F. Lévy²

¹Institute of Physics, Bijenička 46, POB 304, HR-10 001 Zagreb, Croatia

²Institut de Physique Appliquée, E. P. F. L., CH-1015 Lausanne, Switzerland

We report the investigation of the thermal conductivity of a series of pure and niobium-doped quasi one-dimensional alloys (Ta_{1-x}Nb_xSe₂)₁ with $x=0,0.01,0.1$ (nominal concentration) in the chain direction, in the temperature range 100K-340K. This study is the continuation of the previous one, related to the comparison of the thermal conductivity of different quasi one-dimensional compounds: (NbSe₂)₁, (NbSe₂)₃ and K_{0.3}MoO₃. In that study we have pointed out a very specific feature of the thermal conduction in charge-density-wave solids in the vicinity of the Peierls transition. Our results show that the Peierls transition in the pure (TaSe₂)₁ specimens is smeared and suppressed in the alloys (Ta_{1-x}Nb_xSe₂)₁. The temperature of the Peierls transition T_P and the low temperature energy gap E_g decreases linearly by increasing the impurity concentration. The results of detailed analysis of the thermal conductivity provide evidence for the collective mode aspects of the heat conduction in this system. There exist significant additional contributions to the thermal conductivity originating from the thermally assisted phason motion and charge-density-wave fluctuations. By increasing the concentration of the niobium impurities the charge-density-waves are less developed, and the additional contributions to the thermal conductivity are significantly reduced.

MINIMUM THERMAL CONDUCTIVITY OF THE Nb₁Te₂14

A. Smolnata,¹ A. Bilušić,¹ H. Berger²

¹Institute of Physics, Bijenička 46, POB 304, HR-10 001 Zagreb, Croatia

²Institut de Physique Appliquée, E. P. F. L., CH-1015 Lausanne, Switzerland

We have studied the thermal conductivity of the newly synthesized quasi-one-dimensional polytelluride Nb₁Te₂14 in the temperature range 4K-340K. Electrical conductivity in the chain direction at room temperature is $\sigma_{\text{cr}} \approx 0.2 \Omega^{-1} \text{m}^{-1}$. By lowering temperature electrical conductivity shows a semiconducting behavior with slow temperature dependent activation energy. Thermal conductivity at low temperatures shows a behavior like in dielectric crystals. The estimated Debye temperature from low temperature thermal conductivity $\theta_D \approx 105 \text{ K}$ indicates that acoustic phonons carry most of the heat current in these semiconducting materials. The phonon mean free path is of the order of the lattice parameter, and the temperature dependence of the thermal conductivity is expected to deviate from the $1/T$ law, to saturate or even to have a slight increase at the temperatures above Debye temperature. Indeed, at the temperatures above θ_D , thermal conductivity of Nb₁Te₂14 slowly increases showing the minimum value around 200K, with a low room temperature value of $\kappa \approx 3 \text{ Wm}^{-1}\text{K}^{-1}$ as in disordered materials. Therefore this semiconductor crystals would be interesting in designing thermoelectric refrigerators and generators.

INFLUENCE OF Zn SUBSTITUTION ON THE THERMAL CONDUCTIVITY OF Pr_2CuO_4

A.V.Sologubenko^{1,2}, D.F.Brewer¹, G.E.Eksoipididis¹, A.L.Thomson¹

¹ School of Chemistry, Physics and Environmental Sciences, University of Sussex, Falmer, BN1 9QJ Brighton, UK

² Low Temperature Laboratory, Kharkov State University, 310077 Kharkov, Ukraine

Existing experimental data for the compounds Pr_2CuO_4 and Nd_2CuO_4 show that the thermal conductivity reaches high values (the highest in the copper oxide family) with a peak in the temperature range 20-30 K. This thermal conductivity has been regarded as having a phononic origin and the high values have been attributed to a high quality of single crystal lattice and a weak phonon-defect scattering. We present the measurements on the thermal conductivity of polycrystalline $\text{Pr}_2\text{Cu}_{1-x}\text{Zn}_x\text{O}_4$ compound ($x=0, 0.003, 0.02$) in the temperature range 15 - 300 K. Our measurements for Pr_2CuO_4 exhibit the peak near 30 K with maximum value which is only by a factor of less than two lower than those of the single crystal measurements indicating that the excitations causing the thermal conductivity are not affected significantly by the grain boundaries in our samples. Our experiments show that comparatively small amount of Zn (0.3% and 2%) being substituted for the Cu substantially damp the thermal conductivity peak and shift it to higher temperatures. This effect is difficult to explain by the phonon-defect scattering because the masses and ionic radii of Cu and Zn differ small. On the other hand, because the substitution of Cu to Zn breaks the magnetic ordering of Cu spins, our results are a strong evidence of the prevalence of magnetic excitations in the heat transport in Pr_2CuO_4 . We come to a conclusion that phonon thermal conductivity of $(\text{Pr,Nd})_2\text{CuO}_4$ is much smaller than it was expected before.

LOWER LIMIT OF PHONON MEAN FREE PATH IN THE DEBYE MODEL OF THERMAL CONDUCTIVITY

A.V.Sologubenko

School of Chemistry, Physics and Environmental Sciences, University of Sussex, Falmer, BN1 9QJ Brighton, UK;

Low Temperature Laboratory, Kharkov State University, 310077 Kharkov, Ukraine

Methods of accounting for the minimum mean free path of phonons used to calculate the lattice thermal conductivity are analyzed in terms of the Debye model. The concept of a lower limit of the thermal conductivity has been shown^{1,2} to be valid for both amorphous materials at temperatures higher than the thermal conductivity plateau and disordered crystals as a high-temperature limit. In this paper we analyze the lattice thermal conductivity of a number of crystalline materials revealing a weaker than $1/T$ temperature dependence for the thermal conductivity at high temperatures. It is shown that correct consideration of the minimum mean free path in connection with specific mechanisms of phonon scattering allows one to calculate not only the high-temperature limit of the thermal conductivity but also the temperature dependence at lower temperatures. It is noted that consideration of the minimum mean free path of phonons is essential in analyzing the temperature dependence of the thermal conductivity for crystals in which phonons are scattered strongly, in particular high- T_c copper oxide cuprates.

¹ D.G.Cahill, S.K.Watson, and R.O.Pohl, *Phys.Rev. B* **46**, 6131 (1992)

² G.A.Slack, *Solid State Phys.* **34**, 1 (1979).

ANISOTROPY OF THERMAL RELAXATIONAL MODE IN KHCO_3 STUDIED BY IMPULSIVE STIMULATED THERMAL SCATTERING

Shigehiro Takasaka, Yuhji Tsujimi and Toshirou Yagi

Research Institute for Electronic Science, Hokkaido University, Sapporo 060-0812, JAPAN

The antiferrodistortive KHCO_3 undergoes a structural phase transition of an order-disorder type at $T_N = 318$ K. The molecular unit of the order-disorder mechanism is a $(\text{HCO}_3)_2$ plane dimer. It has been found that the dimer-dimer interaction plays the important role for the phase transition.[1] All dimers are on the cleavage plane of (4 0 -1).

The dimer-dimer interaction has been investigated from the viewpoint of the transport dynamics of the thermal phonons. For this investigation, the thermal relaxational mode of KHCO_3 has been observed by impulsive stimulated thermal scattering (ISTS), which is a time-resolved spectroscopy possible to measure the relaxational mode with relaxational time longer than 1 nsec. The coherent thermal relaxational modes with wave vectors $q \parallel [0 1 0]$ and $q \parallel [4 0 -1]$ (perpendicular to $[0 1 0]$) are successfully excited by the use of Nd:YLF pulse laser (Quatronix 4217). The wavelength and the pulse width of the laser output are 1064 nm and 60 psec, respectively.

Figure 1 shows the typical time dependence of the intensity of the excited mode at room temperature. From semi-logarithmic plot in an inset of the figure, it is clear that the observed thermal relaxational mode has a single relaxation time. We find a quite large anisotropy in τ : $\tau = 1.84$ μsec along $q \parallel [0 1 0]$ and $\tau = 4.72$ μsec along $q \parallel [4 0 -1]$. This result clearly indicates that there exists a very large anisotropy in the dimer-dimer interaction. The temperature dependence and the anisotropy of the relaxation time τ near T_N are now going to be investigated.

[1] S. Takasaka, Y. Tsujimi and T. Yagi: Phys. Rev. B 56 10715 (1997).

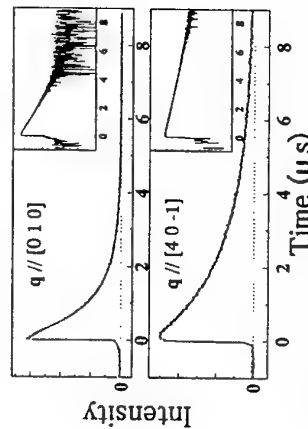


Figure 1: Time dependence of the intensity of the excited thermal relaxational mode at room temperature.

SAW ATTENUATION IN C_{60} THIN FILMS AT LOW TEMPERATURES

Tsuyoshi Takase, Young Sun and Tatsuro Miyasato

Department of Computer Science and Electronics,
Kyushu Institute of Technology, Iizuka, Fukuoka 820-8502, Japan

Since the peculiar features of C_{60} and fullerene family have been reported, they have been investigated by means of Raman scattering, NMR and X-ray diffraction, etc. Especially, C_{60} which has the highest molecular symmetry in the fullerenes, has some interesting properties. The most attractive behavior is the phase transition in solid C_{60} . X-ray diffraction measurements showed that solid C_{60} has fcc structure above 260K and sc structure below 260K, and some reports have been given about this transition. The calorimetry measurements showed that phase transition at 260K is λ -type transition. It was expected that the ultrasonic method was available to investigate dynamics of transition, and the ultrasonic attenuation measurements in C_{60} thin films were carried out by using the SAW devices.

The sample was deposited by vacuum evaporation method directly onto the surface of a SAW device. In the present experiment, a quartz substrate was used as a SAW device. The two types of SAW devices were used, namely one had a 40MHz fundamental-frequency and the another had a 80MHz fundamental-frequency. The SAW attenuation were measured at temperatures between 150K and 300K, and the ultrasonic frequencies were 120MHz, 160MHz, 240MHz and 280MHz in the present measurement.

Though the SAW attenuation gradually decreased with decreasing temperatures less than 300K, the attenuation drastically increased at 260K and showed peak at around 240K. The SAW attenuation gradually decreased with decreasing temperatures less than 240K till 150K. The transition temperature was almost independent for each attenuation curve, namely transition temperature was independent on frequency. The peak temperature which was about 240K, slightly shifted to lower temperatures with increasing in frequencies. The magnitude of attenuation below 240K were proportional to the square of the acoustic frequencies, ω^2 . The attenuation curves obtained by decreasing temperatures were compared with that by increasing temperatures, but the hysteresis of the attenuation curves was not observed.

It is expected the following description. There is a relaxation mechanism in sc structure below 260K, and this relaxation system is destroyed by the λ -type phase transition from sc to fcc structure at 260K. There may be a different type of mechanism in fcc structure above 260K.

TRANSPORT OF NON-EQUILIBRIUM PHONONS IN HIGH DISORDERED FERROELECTRICS CERAMICS.

S.N. Ivanov*, E.P. Smirnova**, A.V. Turanov*, E.N. Khazanov*

* Institute of Radioengineering and Electronics Russian Academy of Sciences, 103907, Mohovaja st. 11, Moscow, Russia.
 ** A.F. Joffe Institute, Russian Academy of Sciences, 194021, St. Petersburg, Russia.

The propagation processes of weakly nonequilibrium phonons in a number of ferroelectric ceramics were studied experimentally by heat pulse method. It was measured the signal maximum arrival time t_M and its dependence on temperature T and length of the sample L . For all samples we have the diffusive regime of phonons transport $t_M \sim L^2$ and values of $D_{eff} L^2 / t_M$ were close to recovered from thermal properties. But the dependences of t_M on temperature allow to divide investigated ferroelectric ceramics into groups. In the group I we have ceramics with diffusive phase transition due to ionic disordering: $PbMg_{1/2}Nb_{2/2}O_3$, $PbSc_{1/2}Nb_{1/2}O_3$, solid solution on their bases and $Pb_{1-x}Zr_xTi_{0.33}Ln_x$ ($x=0,06-0,1$). For that ceramics $t_M \sim T^{-1}$. There are no differences $t_M=f(T)$ characteristics for monocystal and ceramic's samples and effect grain boundaries on t_M is absent. Such results are predicted in [1] and explained by glass-like behavior of thermal properties of ceramic's materials. In the group II we have ceramics with sharp phase transition: $BaTiO_3$. In this classic ferroelectric $\partial t_M / \partial T < 0$, so t_M has the other slope and depends on scattering on the grain boundaries. This result is explained within the scope of theoretic model [2].

[1] V.T. Kozub, A.M. Rudin, H.R. Schober. Phys Rev B. 1994-1, 50, N°9, p. 6032-6046.

[2] A.G. Kozorezov, J.K. Wigmore, C.Erd, A. Peacock, A.Poelaert. Phys.Rev. B. 1997-to be published.

SPIN-PHONON INTERACTION IN THIN MAGNETIC FILMS

E.V. Tartakovskaya, B.A. Ivanov
 Institute for Magnetism NASU, Kiev, Ukraine.

We investigated spin-phonon interaction in two different physical models. The first one describes truly two-dimensional easy-plane antiferromagnets such as Langmuir-Blodgett films. It is obvious that in such a case elastic interaction between films and corresponding substrates is negligible and we can regard the film as elastic plane. It is shown here that the interaction of the magnetic subsystem with the lattice phonons stabilizes the long-range magnetic order at low temperatures. The mechanism establishing long-range order is not related with the square-root modification of the dispersion relation for spin waves. We estimate the corresponding transition temperature and compare it with experimental data [1]. The magnetoelastic gap is ordinarily much smaller than the exchange integral and for this reason the transition temperature is much smaller than exchange energy. Below this temperature long-ranged magnetic order exists. It is obvious that as the temperature increases, long-ranged magnetic order is destroyed via a phase transition and the thermodynamic characteristics have a singularity at the point of this transition in contrast to the Berezinskii-Kosterlitz-Thouless transition, where a macroscopic order parameter does not arise.

The second model of interest describes ultrathin films $Fe/Cu(Ag,Au)$, e.i., ferromagnetic film on nonmagnetic substrate. In such a case the film is strongly bounded with substrate. The system can be represented as elastic media occupying a half-space (substrate) with three-dimensional lattice phonons interacting with surface magnons. The particular difference between that system and the model of literally two-dimensional magnet considering above becomes apparent from investigation of the ground state. In truly two-dimensional system we must take into account the spontaneous deformations. As in three-dimensional crystals, it leads to the well-known consequences, namely, the magnetoelastic gap appears in the energy of quasi-particles [2]. On the contrary, in the case when the film and substrate have the similar elastic properties, the dimensionality of magnetic and elastic subsystems are different. As following, spontaneous deformations and magnetoelastic gap are equal to zero. Peculiarities of spin-phonon interaction in that nontrivial situation are discussed here and dependence of phonon-magnon branches energy from the angle between two-dimensional wave vector and magnetization is analysed. It is shown particularly that due to the phonon-magnon interaction the surface Rayleigh waves spreading in some special directions begin penetrate deep into substrate without damping.

1. B.A.Ivanov and E.V.Tartakovskaya, JETP Lett., 63, No.10, p.835 (1996).

2. E.A.Turov and V.G.Shavrov, Sov.Phys.Usp. 26, 593 (1983).

PHONON RAMAN STUDY IN $\text{La}_{1.476}\text{Nd}_{0.4}\text{Sr}_{0.125}\text{CuO}_4$

S. Nimori^A, H. Hata^B, N. Ogita^B, F. Nakamura^C, S. Sakita^C,
N. Kikugawa^C, T. Fujita^C, and M. Udagawa^B

^AVenture Business Laboratory, Hiroshima University
Kagamiyama 1-4-1, Higashi-Hiroshima 739-8527, Japan

^BFaculty of Integrated Arts and Sciences, Hiroshima University

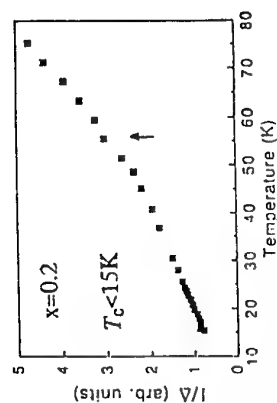
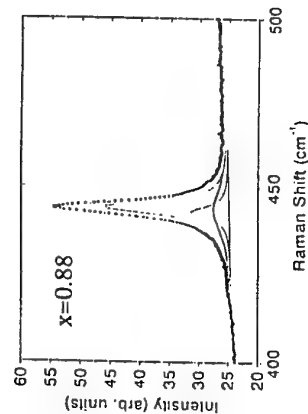
Kagamiyama 1-7-1, Higashi-Hiroshima 739-8521, Japan

^CDepartment of Physics, Hiroshima University

Kagamiyama 1-3-1, Higashi-Hiroshima 739-8526, Japan

At the carrier concentration of $x=1/8$, the suppression of superconductivity and the appearance of the low-temperature tetragonal structure have been known for $\text{La}_{2-x}\text{Ba}_x\text{CuO}_4$ and Nd-doped $\text{La}_{2-x}\text{Sr}_x\text{CuO}_4$ (1/8 problem). To clarify the lattice dynamical properties of this problem, the totally-symmetric phonons of $\text{La}_{1.476}\text{Nd}_{0.4}\text{Sr}_{0.125}\text{CuO}_4$ have been investigated by Raman scattering. $\text{La}_{1.476}\text{Nd}_{0.4}\text{Sr}_{0.125}\text{CuO}_4$ undergoes the following successive structural phase transitions; High temperature tetragonal (THT) for $T > \sim 470\text{K}$, Mid-temperature orthorhombic (OMT) for $\sim 470\text{K} > T > 77\text{K}$, Low temperature orthorhombic (OLT) for $77\text{K} > T > 66\text{K}$, and Low temperature tetragonal (TLT) for $66\text{K} > T$, respectively.

Among five phonon modes observed at room temperature, the energies of three modes at 231, 276, and 428cm^{-1} increase by 2cm^{-1} in the OLT and TLT phases. However, two modes at 120 and 155cm^{-1} show the remarkable change in TLT. The energy of the former, which is known as soft mode for OMT, decreases by 10cm^{-1} , and the latter, which is La/Nd vibration along the c-axis, splits into two peaks. From the normal mode calculation, the energy decrease of the soft mode and the lower energy peak at 155cm^{-1} is well explained by the decrease of the inter-atomic interaction of La-Cu by about 20%. However, for the higher energy peak at 155cm^{-1} , other additional interaction should be taken into account. According to neutron scattering, magnetic correlation develops in TLT. Then, the atomic interaction of Nd-Cu increases by the additional magnetic interaction between Nd and Cu ions. Therefore, it can be concluded that the magnetic interaction between Nd and Cu is enhanced in the TLT phase for $\text{La}_{1.476}\text{Nd}_{0.4}\text{Sr}_{0.125}\text{CuO}_4$.



PHASE TRANSITION OF ZERO-DIMENSIONAL HYDROGEN-BONDED CRYSTALS STUDIED BY RAMAN SCATTERING

J. Watanabe, M. Kasahara and T. Yagi

Research Institute for Electronic Science, Hokkaido University, Sapporo 060-0012, Japan

From our studies on the dynamics of zero-dimensional hydrogen-bonded systems such as $\text{K}_3\text{D}_x\text{H}_{1-x}(\text{SO}_4)_2$, $\text{K}_3\text{D}_x\text{H}_{1-x}(\text{SeO}_4)_2$ or $\text{Rb}_3\text{D}_x\text{H}_{1-x}(\text{SeO}_4)_2$, we have found several interesting results by Raman scattering as follows; in the H-D mixed crystals, (1) the length of the deuterium-related hydrogen-bond (D-hydrogen bond) is independent of the D-concentration x , while that of the proton-related hydrogen bond (H-hydrogen bond) lengthens with increasing x , (2) below 60K, some quantum mechanism like zero-point vibration seems to influence the motion of protons or deuterons in addition to the thermal excitation. It is possible to observe the proton-related Raman line and the deuterium-related one separately in the ordered phase of the sulfate salts, though in case of the selenite salts, it is not.

The characteristic time of the motion of the proton or deuterium τ_c is obtained from the temperature-dependence of the linewidth of the ν_2 internal mode. Figure 1 shows a three-line fit for the ν_2 mode Raman spectrum just below $T_c=91.9\text{K}$ for the crystal of $x=0.88$. Figure 2 shows the temperature-dependence of the inverse of the anomalous part of the Raman-linewidth which is proportional to τ_c^{-1} . A slight anomaly is found around 55K. This inflection suggests the existence of some quantum mechanical process like zero-point vibration or tunneling for the hydrogen (deuterium) motion.

THE PHONON DISPERSION OF WURTZITE CdSe

F. Widulle, A. Göbel, T. Ruf, A. Debernardi, R. Lauck, and M. Cardona
Max-Planck-Institut für Festkörperforschung, D-70569 Stuttgart, Germany

S. Kramp and N. M. Pyka

Institut Laue-Langevin, B.P. 156, F-38042 Grenoble Cedex 9, France

Wide-gap II-VI semiconductors, like CdS, CdSe or ZnSe, are presently of great interest for a variety of optic and optoelectronic applications, such as filter glasses made from nanoparticles or green-blue quantum-well lasers. The properties of such low-dimensional systems depend to a considerable degree on their lattice-dynamics and the electron-phonon interaction, which, unfortunately, are not well known in many cases, even for bulk crystals. This lack of knowledge has two main reasons: (i) Many of these compounds contain cadmium, a very strong neutron absorber due to the presence of 12.2% ^{113}Cd in the natural element. This makes dispersion measurements by inelastic neutron scattering impossible. (ii) Many systems have wurtzite structure and/or contain semicore d electrons. The theoretical modelling of their phonon dispersion is therefore very difficult. We have recently circumvented these obstacles and measured the phonon dispersion of wurtzite CdS made from weakly absorbing ^{114}Cd by inelastic neutron scattering while also performing *ab-initio* calculations of the lattice dynamics [1].

Here we present data of the phonon dispersion in wurtzite CdSe obtained from inelastic neutron scattering measurements ($T = 300\text{ K}$). For this purpose we have grown a crystal from highly enriched and very weakly absorbing ^{116}Cd and natural Se (diameter: 10 mm, length: 12 mm). Modes from various dispersion branches were measured along the $\Gamma - A_1$, $\Gamma - M$, and $\Gamma - K - M$ directions. The peaks observed are compared with *ab-initio* and shell model calculations. Note that neither experimental dispersion data nor theoretical predictions for wurtzite CdSe have been available up to now.

Due to the more similar masses of the cations and anions in CdSe as compared to CdS, the upper six optical branches lie very close together, and the eigenvectors show a stronger mixing of cadmium and selenium displacements. The frequencies of the two silent B_1 modes in the zone centre are 14.5 meV and 23.0 meV. These Raman and infrared inactive modes can only be determined by inelastic neutron scattering. They are crucial input parameters for fits of lattice-dynamical models to the measured phonon dispersion.

[1] A. Debernardi *et al.*, Solid State Commun. **103**, 297 (1997).

ANHARMONICITY OF $\text{Fe}_{72}\text{Pt}_{28}$ MEASURED WITH ELASTIC AND INELASTIC NUCLEAR SCATTERING OF SYNCHROTRON RADIATION

^{1,2} N. Wiele, ² H. Franz, ³ O. Leupold, ² W. Petry

¹ ESRF, B.P. 220, 38043 Grenoble CEDEX, France; ² TU-München, Physik Department E13, James-Frank-Str. 85748 Garching, Germany, ³ Universität Hamburg II-Institut für Experimentalphysik, Luruper Chaussee 149, D-22761 Hamburg

The phonon density of states (DOS) is usually determined from incoherent neutron measurements or calculated by fitting a model to phonon dispersion relations measured by coherent neutron scattering.

The DOS can be measured directly by using inelastic nuclear absorption of synchrotron radiation without any fitting.

We examined the system $\text{Fe}_{72}\text{Pt}_{28}$ to find out the influence of the atomic potential's anharmonicity on the invar effect. Neutron measurements showed a softening of the T_{110} -branch in ordered $\text{Fe}_{72}\text{Pt}_{28}$. In the DOS obtained by nuclear resonant absorption the softening appears as a temperature dependent peak.

The anharmonic effect could also be demonstrated by changes of the Lamb-Mössbauer-factor by means of nuclear forward scattering. For a harmonic lattice the Lamb-Mössbauer-factor decreases exponentially with temperature. In the case of ordered $\text{Fe}_{72}\text{Pt}_{28}$ the dependence is even stronger

EFFECT OF NONPARABOLICITY ON FREE-CARRIER ABSORPTION IN n-TYPE InSb FILMS FOR POLAR OPTICAL PHONON SCATTERING

Chhi-Chong Wu¹ and Chau-Iy Lin²

¹ Institute of Electronics, National Chiao Tung University, Hsinchu, Taiwan

² Department of Applied Mathematics, National Chiao Tung University, Hsinchu, Taiwan

The free-carrier absorption in n-type InSb films has been studied for quantum well structures fabricated from III-V semiconducting materials where the polar optical phonon scattering is predominant. We consider here two special cases: the electromagnetic radiation is polarized parallel to the layer plane and perpendicular to the layer plane separately. The energy band of electrons in semiconductors is assumed to be nonparabolic. Results show that when the electromagnetic radiation is polarized parallel to the layer plane, the free-carrier absorption coefficient is independent of temperature in a small quantum region such as $d < 30 \text{ \AA}$, but the absorption coefficient oscillates with the quantum well and depends upon the temperature in the region of larger film thickness. It is also shown that the free-carrier absorption coefficient decreases monotonically with increasing the photon frequency. However, if the film thickness decreases, the temperature dependence of the absorption coefficient disappears at low temperatures. When the electromagnetic radiation is polarized perpendicular to the layer plane, the dependence of the free-carrier absorption coefficient on the quantum well, the photon frequency, and temperature becomes quite complicated and does not show in a regular way.

HIGH-FREQUENCY DIELECTRIC CONSTANT OF KDP OBTAINED BY POLARITON DISPERSION

Shinya Yoshioka, Yuhji Tsujimi and Toshiro Yagi

Research Institute for Electronic Science, Hokkaido University, Sapporo 060-0812, JAPAN

Impulsive stimulated Raman scattering (ISRS) experiments have been performed in the polariton regime to determine the polariton dispersion relation of KDP. Polaritons are successfully excited and observed in the time domain at several scattering angles θ which gives the magnitude of the wavevector of the excited mode. Figure 1 shows some examples of the observed ISRS signals at $\theta = 0.57$ degree. ISRS signal is proportional to the squared real time response function of the excited mode. By the numerical analysis using a damped harmonic oscillator as the response function, frequency and damping of the mode are obtained. Figure 2 shows the dispersion relation of the polariton mode at several temperatures. From the slope of the dispersion relation shown in Fig. 2, dielectric constant is calculated. Its temperature dependence obeys Curie-Weiss law with the Curie constant in good agreement with the previous result of the dielectric measurement in several ten MHz region. This agreement indicates the observed oscillation definitely comes from the ferroelectric mode. No additional dispersion is concluded between several ten MHz and the polariton frequency region considered here (several hundred GHz).

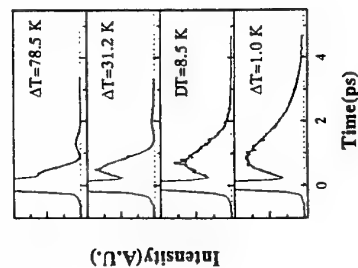


Figure 1 Temperature dependence of the observed ISRS signal with the scattering angle 0.57 degree.

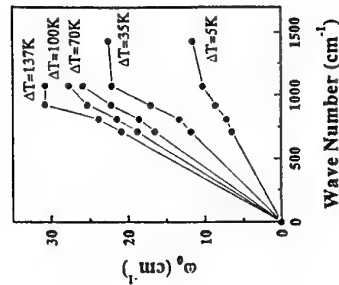


Figure 2 The dispersion relation of the polariton at several temperatures. $\Delta T = T - T_c$, here T_c is the phase transition point.

PHONON DISPERSION EFFECTS ON THE MOTION OF SMALL POLARONS IN MOLECULAR SOLIDS

Marco Zoli

Dipartimento di Matematica e Fisica

Sezione INFN, Università di Camerino

62032 Camerino, Italy

zoli@camserv.unicam.it

ABSTRACT

I study the motion of polarons as a function of temperature in the context of a molecular crystal model in which the discreteness of the lattice is accounted for. The model is based on a non linear Schrödinger equation which can be solved perturbatively if the conditions for the existence of small polarons are assumed. The polaron bandwidth and the site jump hopping probability have been calculated versus temperature and dimensionality. It is found that the crossover temperature T_g^* between band-like and hopping motion is reduced in low dimensional systems due to the enhanced importance of the off-diagonal scattering processes. By increasing the polaron binding energy the bandwidth narrows and the hopping probability quickly drops hence, T_g^* is shifted upwards. The dispersion in the phonon spectrum is a vital ingredient for the validity of the model. The first and second neighbors intermolecular force constants which parametrize the pair interactions strongly affect the values of the ground state polaron bandwidth and of the hopping probability. We discuss the relevance of the model to high T_c superconductors in which polaronic features in the transport properties have been pointed out.

PosB1

OBSERVATION OF ENERGY LOSS BY A HOT TWO-DIMENSIONAL ELECTRON GAS INTO COUPLED PLASMON-OPTIC PHONON MODES

H. Al Jawhary, A. G. Kozorezov, and J. K. Wignmore
Physics Department, Lancaster University, Lancaster. LA1 4YB UK.

We have obtained direct evidence from nanosecond phonon pulse experiments that the dominant mechanism for energy loss by a hot two dimensional electron gas (2DEG) in the temperature range approximately 20 - 55 K is via excitation of coupled plasmon-optic phonon modes. The phonon pulses emitted by the excited 2DEG in a gated GaAs/AlGaAs heterojunction were detected directly by superconducting bolometers as a function of power loss per electron, P/e , which determined the temperature of the hot 2DEG, and also, for the first time, of 2D carrier density, which could be varied through the field effect of gate bias. As in earlier work [1,2] at fixed carrier density it was found that a well-defined change in the slope of the phonon flux versus power loss occurred at $\sim 10^{-12}$ W/e. This feature was originally interpreted as the change from acoustic to optic phonon emission as the dominant energy loss mechanism, but the above figure is inconsistent with the accepted value of the deformation potential coefficient.

Our recent experiments on gated heterostructures show that the value of P/e at which the change of slope occurs is a strong function of 2D carrier density. Taking data from several samples, including some published by other workers, we find that an increase of carrier density from 2 to $11 \times 10^{15} \text{ m}^{-2}$ corresponds to a decrease in P/e from 8 to 2×10^{-12} W/e. This result provides clear evidence that the excitation of plasmon-optic phonon coupled modes is important in the energy loss process, and we believe that observed feature corresponds to the crossover from dominant energy loss by the lower (plasmon-like) coupled mode to that by the upper (phonon-like). A detailed comparison has been made with the calculations of Kawamura et al [3]. Several other problematic features of the phonon data are also explained by this model, notably the unexpectedly low intensity of the longitudinal phonon flux, and the power dependence of the transverse phonon flux below the crossover.

- [1] Hawker P, Kent A J, Hughes O H, and Challis L J, *Semicond. Sci. Technol.* **7** 829 (1992)
- [2] Wignmore J K, Erol M, Sahraoui-Tahar M, Ari M, Wilkinson C D W, Davies J H, Holland M, and Stanley C, *Semicond. Sci. Technol.* **8** 322 (1993)
- [3] Kawamura T, Das Sarma S, Jalabert R, and Jain J K, *Phys. Rev.* **B42** 5407 (1990)

PosB2

ELECTRON-PHONON RELAXATION IN QUANTUM WIRES IN A QUANTIZING MAGNETIC FIELD

Samvel M. Badalyan and Mher Aghasyan
Department of Radiophysics, Yerevan State University, 1 A. Manoogian St., 375049 Yerevan, Armenia
Garnett W. Bryant
National Institute of Standards and Technology, Gaithersburg, MD 20899 USA

We have calculated electron energy and momentum relaxation due to acoustic and optical phonons in quantum wires subjected to a quantizing magnetic field.

Currently semiconductor nanostructures with one-dimensional electron systems attract considerable interest both for unraveling novel fundamental phenomena and for possible device applications, such as quantum wire lasers. Rapid carrier relaxation is crucial for many of technological applications of nanosystems. Therefore, understanding and characterizing carrier relaxation in quantum wires are important for controlling carrier dynamics in thermalization, optical, and transport processes as well as for identifying lateral confinement effects in quantum wires.

We develop a theory for calculations of the energy and momentum relaxation rates of a test electron as well as for the relaxation rate of electron temperature for whole electron gas exposed to the quantizing magnetic field. We consider electron-phonon interaction due to deformation and piezoelectric acoustic phonons as well as due to polar optical phonons. We derive analytical expressions for the intra- and inter-subband relaxation rates which are represented as an average of some kernel over electron wave functions in directions of the electron confinement. Using these expressions and numerical forms of the appropriate electron wave functions, one can easily evaluate the relaxation rates in quantum wires with different shapes of the cross section (for instance, in T- or V-shaped quantum wires). We discuss analytically the relaxation rates in quantum wires with a rectangular and parabolic confining potential as a function of the initial electron energy (or electron temperature) for different values of the magnetic field. By considering limiting cases of the ratio of the cyclotron frequency to the strength of the lateral confinement, we obtain results for electron relaxation in one- and two-dimensional electron systems, as well as for the magnetic field free cases.

AB INITIO LATTICE DYNAMICS, GROUP VELOCITIES AND ELECTRON-PHONON COUPLING IN METALS

R. Bauer, A. Schmid, P. Pavone, and D. Strauch

*Institut für Theoretische Physik,
Universität Regensburg, D-93040 Regensburg*

We employed a linear-response approach based on density-functional theory in the plane-wave pseudopotential representation to calculate lattice dynamical properties of metals. We show the accuracy of this approach by evaluating group velocities in Al and Mg, which reveal Kohn anomalies in the phonon dispersion curves. We compare the group velocities to the experiment and find very good agreement.

We then studied the nonadiabatic behavior of some simple metals by determining the imaginary part of the phonon selfenergy due to electron-phonon coupling at the adiabatic phonon frequencies. The selfenergy yields a finite lifetime of the phonon states and determines various measurable effects of the electron-phonon coupling, like the Eliashberg function of superconductivity and transport properties in the normal state. We present calculated phonon linewidths and find good agreement with experimental data in the case of Nb. Furthermore, we show theoretical Eliashberg functions, and again we find reasonable agreement with tunneling data in most cases. The role of the phonons involved in the electron-phonon coupling turned out to be very sensitive to the details of the electronic structure, which therefore has to be determined very accurately.

Finally, we used the calculated coupling functions to determine the temperature dependence of the electrical resistivity in Na and Nb by evaluating reciprocal relaxation times.

CONFINED OPTICAL PHONON EFFECTS ON THE BAND GAP RENORMALISATION IN QUANTUM WIRE STRUCTURES

C. R. Bennett¹, K. Güven² and B. Tanatar²

¹Department of Physics, University of Essex, Colchester, CO4 3SQ, England
²Bilkent University, Department of Physics, 06533 Ankara, Turkey

The band gap renormalisation (BGR) due to the electron-hole gas is very important in semiconductor laser devices. With the prospect of a quantum wire laser, where the electrons and holes are quasi-one dimensional, it has now become vital to investigate the theoretical aspects of the BGR in these systems.

Experiments on these systems to measure the BGR involve the optical creation of an equal number of electrons and holes. Recent experimental results for higher dimensions have been compared with the quasi-static approximation of the BGR within the random phase approximation (RPA) without including optical phonons and, although the results seem to agree in some cases, it is not apparent when this approximation is valid. Also the plasmon-pole approximation for the polarisation (with many different definitions), where the oscillator strength is assumed to be at a single pole, is often employed due to its simple form. The effect of the optical phonons, which are always present but may couple to the particle excitations for certain densities, is often ignored as is the issue of the confinement of these optical modes.

We compare the fully dynamical calculation of the BGR for a quantum wire of circular cross-section within the RPA for the appropriate electron/hole density range with the results from the various plasmon-pole approximations and the quasi-static approximation with and without the bulk optical phonons included. It is shown that the quasi-static case is only valid for large densities. We include the confinement of the phonons through the use of the dielectric continuum (DC) model and show that the expected sum rule, which states that the result containing confined phonons be between the results containing either of the two bulk phonons, is still satisfied. We also investigate the multisubband case where the phonon coupling should become more important.

PHONOCONDUCTANCE OF QUANTUM WIRES

M. P. Blencowe¹ and A. Y. Shik^{2,3}¹ *The Blackett Laboratory, Imperial College, London SW7 2BZ, UK.*² *A. F. Ioffe Physical-Technical Institute, 194021 St. Petersburg, Russia.*³ *Present address: Energenius Centre for Advanced Nanotechnology, University of Toronto, Toronto M5S 3E4, Canada.*

Most theoretical investigations of the electron-phonon interaction in quantum wires have employed a simplified model in which the wire is infinitely long and of uniform width. In this case, only phonons with sufficient longitudinal momentum component to backscatter the electrons through $2k_F$ affect the wire conductivity, causing a reduction in the latter. However, real quantum wires are of finite length and nonuniform width joining large reservoirs. It has become clear that these features must be accounted for in the model in order to provide an explanation of the experimentally observed phonon conductivity properties. We present the results of our investigation using a more realistic quantum wire model. There are two basic contributions to the wire phononconductance. Phonon scattering in the reservoirs causes electron heating which produces a change in the wire conductance. This conductance-change is due to the strong energy dependence of the electron transmission probability through the wire, which in turn is due to the nonuniform electrostatic potential profile of the wire. The other contribution comes from phonon scattering in the wire region itself. For a nonequilibrium phonon distribution and transmission probability which is energy dependent, it is found that phonons which forward scatter the electrons can also affect the conductance. Adding the two basic contributions, the resulting net conductance change can be of either sign depending on the various electron and phonon distribution parameters.

In our investigations, we use the Landauer formula for the wire conductance since it is the best available approach for analytical and numerical study of the phononconductance. However, being a single electron description, Fermi-Dirac statistics are not properly taken into account and hence there is the fundamental issue of the validity of the Landauer approach. In particular, for elastic scattering the Landauer formula gives the correct description for the conductance, whereas for inelastic incoherent scattering, which includes phonon scattering, the Landauer formula is only approximate. We determine the conditions under which the Landauer formula provides a good approximation to the phononconductance.

ACOUSTIC SPECTROSCOPY OF DEEP CENTRES IN GaAs/AlGaAs
HETEROSTRUCTURES

P. Bury, I. Jamnický and V.W. Rampton*

Department of Physics, Zilina University, Veľký diel, 010 26 Zilina, Slovak Republic

*Department of Physics, University of Nottingham, University Park, Nottingham NG7 2RD, Great Britain

Two versions of the acoustic deep-level transient spectroscopy (A-DLTS) technique based on the acoustoelectric effect resulting from the interaction between an acoustic wave and heterostructure interfaces have been used to study deep centres in GaAs/AlGaAs heterostructures. The former uses an acoustoelectric response signal (ARS) produced by the heterostructure interface when a longitudinal acoustic wave propagates through the heterostructure. The latter uses the high frequency transverse acoustoelectric signal (TAS) arising from the interaction of a surface acoustic wave electric field and free carriers at the heterostructure interfaces.

The both ARS and TAS are extremely sensitive to any changes in the space charge distribution in the interface region so that their time development, after an injection bias voltage pulse has been applied, representing acoustoelectric transients reflects relaxation processes associated with the thermal recombination of excited carriers moving towards their equilibrium state. Since the amplitudes of these acoustoelectric signals are proportional to carrier density at the heterostructure interface, the decay time constant associated with the acoustoelectric signal amplitude is a direct measure of the time constant associated with the release of the carriers from deep levels after the excitation pulse. By investigating the temperature dependence of acoustoelectric transients characterizing the return to thermodynamic equilibrium, the activation energies and corresponding cross-sections can be determined.

Planar GaAs/AlGaAs heterostructure capacitors with electrodes in a field effect transistor configuration were investigated by both versions of the A-DLTS technique. We used a method of computer evaluation of isothermal acoustoelectric transients by applying a data compression algorithm and also including, in some cases, a method of digital filtering by convolution to calculate the deep centre's parameters. Several deep centres were found and their activation energies and corresponding cross-sections determined. The influence of gate voltage on the observed A-DLTS spectra were investigated by applying a bias voltage of -3, -5, and -7V. The measurement of the ARS as a function of gate voltage should correspond to the measurement at depletion conditions and shows considerable dependence of A-DLTS spectra on the applied gate voltage. The observed shift of practically all peaks of the A-DLTS spectrum with increasing bias voltage to lower or higher temperatures depending on the type of centre can be considered as the characteristic feature of interface states.

PHONON WAVE AND PARTICLE HEAT CONDUCTION IN SUPERLATTICES

Gang Chen

Mechanical and Aerospace Engineering Department
University of California, Los Angeles, CA 90095-1597

ABSTRACT

Significant reductions in both the in-plane and the cross-plane thermal conductivities of superlattices, in comparison to the values calculated from the Fourier heat conduction theory using bulk material properties, have been observed experimentally in recent years. Understanding the mechanisms controlling the thermal conductivities of superlattice structures is of considerable current interests for microelectronic and thermoelectric applications. In this work, phonon heat conduction in superlattices is studied based on three approaches: (1) the acoustic wave propagation, (2) ray tracing, and (3) the Boltzmann transport equation (BTE). The first two approaches are based on neglecting the internal scattering in superlattices. Based on a comparison of the results obtained from the first two approaches, it is concluded that phonon interference and tunneling in superlattices do not have significant influences on their overall thermal conductivities when the layers become thicker than 10 angstroms at room temperature. Heat conduction in most superlattices thus can be modeled based on the particle picture and solving the BTE. Phonon confinement and total internal reflection, however, can cause orders of magnitude reduction on the thermal conductivity of superlattices. In the BTE approach, both internal and interface scattering of phonons are considered. Different phonon interface scattering mechanisms are investigated, including elastic vs. inelastic, and diffuse vs. specular of phonons. Numerical solution of the BTE yields the effective temperature distribution, thermal conductivity, and thermal boundary resistance (TBR) of the superlattices. The modeling results show that the effective thermal conductivity of superlattices in the perpendicular direction is generally controlled by phonon transport within each layer and the TBR between different layers. The TBR is no longer an intrinsic property of the interface but depends on the layer thickness as well as the phonon mean free path. In the thin layer limit, phonon transport within each layer is ballistic and the TBR dominates the effective thermal conductivity of superlattices. Approximate analytical solutions of the BTE are obtained for this thin film limit. The modeling results based on partially specular and partially diffuse interface scattering processes are in reasonable agreement with recent experimental data on GaAs/AlAs and Si/Ge superlattices. Results of this work suggest that it is possible to make superlattice structures with thermal conductivity totally different from those of their constituting materials.

TRANSIENT GRATING DETECTION OF PICOSECOND ACOUSTIC PULSES

T. F. Crimmins, A. A. Maznev, K. A. Nelson

Abstract :

Picosecond acoustic pulses have traditionally been detected by measuring the change in reflectivity¹ or deflection² of a variably delayed probe pulse. In this work, we study picosecond acoustic responses in thin metal films detected by measuring diffraction efficiency from a transient, laser-induced diffraction grating, a technique in which the acoustic waves are excited by two crossed, ultrashort pump pulses and detected via the monitoring of the diffraction of a delayed probe pulse. In this technique, components normal to the film plane and propagation components in the film plane are generated and detected. This provides additional information, compared with the measurement of just one propagation component, on the material properties involved; as an example the determination of both the in-plane and through-plane sound velocities and corresponding elastic constants in a thin metal film is demonstrated. Additionally, this technique permits background-free detection of the acoustic phonons. Different contributions to the diffraction signal are considered, and it is concluded that strain-induced surface displacement is the primary diffraction mechanism. Measurements were performed on TiN, Ni, AlTiW, and TiN/Ti/AlTiN films.

[1] H. T. Grahn, H. J. Maris, and J. Tauc, "Picosecond Ultrasonics," *IEEE J. Quantum Electron.*, vol. QE-25, pp. 2562-2568, 1989.

[2] O. B. Wright, V. E. Gusev, "Ultrafast Generation of Acoustic Waves in Copper," *IEEE Trans. Ultrason. Ferroelec. Frequency Control*, vol. 42, pp. 331-338, 1995.

PHONON EMISSION BY WARM ELECTRONS IN GaAs QUANTUM WELLS: THE EFFECT OF WELL WIDTH ON THE ACOUSTIC-OPTIC CROSSOVER

A.J. Cross, A.J. Kent, P. Hawker, D. Lehmann¹, Cz. Jasiukiewicz² and M. Henini

¹Department of Physics, University of Nottingham, Nottingham NG7 2RD UK.

²Institute für Theoretische Physik, TU Dresden, D-01062 Dresden, Germany.

³Institute of Theoretical Physics, University of Wrocław, 50-204 Wrocław, Poland.

In this paper we describe heat pulse measurements of the phonons emitted by warm two-dimensional (2D) electrons in GaAs quantum well samples of various well widths ranging from 3 to 15 nm. The electrons were heated by applying short (≈ 10 ns) current pulses to the devices and the emitted phonons detected using superconducting aluminium bolometers. At low excitation power, sharp ballistic pulses of acoustic phonons were observed. At higher powers, the transverse mode pulse broadened and it developed a slowly decaying tail. Following from earlier work on GaAs heterojunctions [1, 2], we attribute the changes in the transverse pulse to the onset of optic phonon emission at an electron temperature of around 50 K. The optic modes rapidly undergo a series of decays ending in large-wavevector transverse modes which propagate diffusively and dispersively to reach the bolometer.

The power dissipation (per electron) at which the onset of optic phonon emission took place, P_{opt} , was seen to increase with decreasing well width, w (see figure). We attribute this to the increase of phase space for acoustic phonon emission as the well is narrowed: the maximum allowed perpendicular (to the 2D sheet) momentum component of the emitted phonon is given by $p_{\perp}(\max) \sim \hbar/w$, which means that more power can be dissipated by acoustic phonon emission at electron temperatures below 50 K. It was also observed that, as the well width was reduced, there was an increase in the ratio of the longitudinal acoustic (LA) to transverse acoustic (TA) emitted modes.

We have also carried out detailed theoretical calculations of the phonon emission based on a full model which includes the effects of acoustic anisotropy [3], screening and the finite "thickness" of the 2D gas. Comparing the results of the calculations with experiment, we find the same dependence on well width of the onset of optic phonon emission and the ratio LA/TA.

[1] P. Hawker et al. *Semicond. Sci. Technol.*, **7**, B29 (1992)

[2] J. K. Wignmore et al. *Semicond. Sci. Technol.*, **8**, 322 (1993)

[3] In this case acoustic anisotropy is included in the calculation of the electron-phonon matrix elements as well as in the propagation of emitted phonons to the detector. In earlier theories only the latter was considered.

CONFINED PHONONS AND PHONON-MODE PROPERTIES OF III-V NITRIDES WITH WURTZITE CRYSTAL STRUCTURE

D. Alexson (a), Leah Bergman (a), Mitra Dutta (b), K. W. Kim (c), S. Komirenko (c), Robert J. Nemanich (a), B. C. Lee (d), Michael A. Stroscio (b), SeGi Yu (c)

(b) U.S. Army Research Office, PO Box 12211, RTP, NC 27709 USA

(a) Physics Department, North Carolina State U., Raleigh, NC 27695 USA

(c) ECE Department, North Carolina State U., Raleigh, NC 27695 USA

(d) Physics Department, Inha University, Incheon, Korea

This paper discusses recent applications of the Loudon model [1] to derive the Frohlich interaction Hamiltonian as well as the electron-optical-phonon scattering in wurtzite crystals [2]. These results demonstrate that the optical-phonon branches support mixed longitudinal and transverse modes due to the anisotropy of the wurtzites. Moreover, it is found that the scattering rates due to longitudinal-like modes are similar to those obtained with the cubic Frohlich Hamiltonian; however, the scattering rates due to the transverse-like modes can be strongly enhanced relative to the cubic case over a range of angles with respect to the c-axis. These results for the bulk case have recently been extended to the case of dimensionally-confined wurtzite systems and it is found that there is a complex spectrum of confined phonon modes for the III-V nitrides of wurtzite crystal structure [3]; confined modes are found to be more complicated than the corresponding modes in crystals of cubic symmetry. Furthermore, this paper presents theoretical [4] and experimental [5] analyses of the mode behavior of phonons in wurtzite crystals. The theoretical treatment of the mode behavior is based on the modified random element isodisplacement (MREI) model which correctly explains the one-mode behavior of selected ternary III-V nitrides with wurtzite crystal symmetry. These results provide a partial foundational basis for the many recent works in electronics and optoelectronics based on wurtzite structures.

1. R. Loudon, *Adv. Phys.*, **13**, 423 (1964); W. Hayes and R. Loudon, *Scattering of Light by Crystals*, (Wiley, New York, 1978).

2. B. C. Lee, K. W. Kim, M. Dutta, and M. A. Stroscio, "Electron-Optical-Phonon Scattering in Wurtzite Crystals," *Phys. Rev. B*, **56**, 997-1000 (1997).

3. B. C. Lee, S. Komirenko, K. W. Kim, Michael A. Stroscio, and M. Dutta, "Optical Phonon Confinement and Scattering in Wurtzite Heterostructures," to be published (1998).

4. SeGi Yu, K. W. Kim, Leah Bergman, Mitra Dutta, and Michael A. Stroscio, "Long Wavelength Optical Phonons in Ternary Nitride-based Crystals," to be published (1998).

5. Leah Bergman, Mitra Dutta, Dimitri Alexson, and Robert J. Nemanich, "Raman Studies of Mode Behavior in III-V Nitrides with Wurtzite Crystal Structure," to be published (1998).

ACCOUNT FOR THE OPTICAL PHONON DISPERSION IN EXCITON ATTENUATION

N.I. Grigorchuk

Institute for Physics of Semiconductors Ukrainian Acad. of Sci., 45 Nauka Ave., 252022 Kyiv-22, Ukraine.

For the models of crystals with both large and small exciton radii the theoretical studies of the effect of LO-phonon dispersion on frequency and temperature dependence of the exciton attenuation is carried out. This study showed that increase of dispersion of the LO-phonons in the crystals with large exciton radius results in the shift of the low frequency edge of the phonon emission range which usually remains the same for all temperatures, when the dispersion is not accounted for. Emission extends to the long wave side of the spectrum and, in principle, can reach the exciton band bottom for the maximal dispersion. For the frequencies above the exciton band bottom this results in the non-zero attenuation even for zero temperature. For the crystals with small exciton radii the mentioned features are less pronounced since for them difference of the dynamics of the exciton and the hole is more essential as the phonon wave length is always greater than the exciton radius. The frequency shift of the attenuation trough with the simultaneous decrease of its absolute value result in the characteristic rise of the attenuation in the region above the exciton band bottom. The frequency dependence of the attenuation in a wide interval of exciton radii from 10 till 200 Å is illustrated. The temperature dependence of the attenuation in this frequency region ($E_0 \leq \hbar\omega \leq E_0 + \Omega_0$) attains finite values even at $T \rightarrow 0$ due to the possible contribution of the phonon emission processes. As the rule the dispersion increases attenuation but for the low temperature and high dispersion value there exists the temperature region for which the decrease of attenuation is possible. Choice of the formula for exciton radii calculation is important for the crystals for which the value of β does not exceed $1/4$. The GaAs and LiF crystals were chosen as the models for illustrations.

Phonons in self-consistent metallic SLAB.

T. Gwizdalla

Dept. of Solid State Physics, University of Łódź
Pomorska 149/153, 90-236 Łódź

There are many methods of attempting the problem of lattice dynamics of limited samples, such as surfaces or thin films. In our calculations we use the SLAB method, which is based on replacing of the continuous distribution of the wave vector component, which is perpendicular to the surface, with the discrete one.

The crucial point of as well many Molecular Dynamics, as all SLAB type calculations is to determine the correct shape of potential curve. As the potential we use the function obtained by thermal renormalization of the initial function chosen for 0 K. This renormalization is made due to self-consistent Siklos Green's functions method and tested by comparing the thermal vibrations obtained using calculated parameters with those well known from experiments. It may be noticed the similarity between potential functions for various metals having the same crystallographic structure.

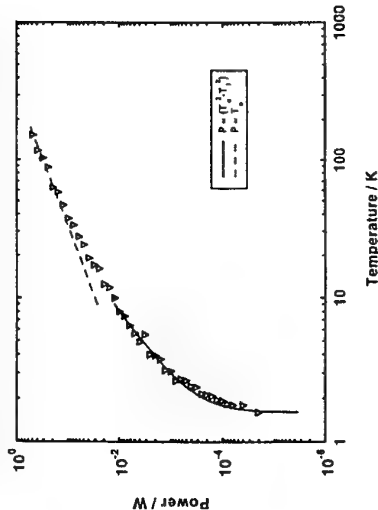
This method allows us then to calculate density functions, dispersion curves and layer dependence of various dynamical characteristics for unreconstructed metallic crystals with relaxed distances between surface layers.

HEAT PULSE STUDIES OF THE ENERGY RELAXATION RATE OF HOT ELECTRONS IN N-TYPE GaN EPILAYERS

P Hawker, A J Kent, T S Cheng and C T Foxon
Department of Physics, University of Nottingham, Nottingham NG7 2RD, UK.

GaN is likely to prove of considerable importance in the future development of microwave power devices and blue light emitters. Theoretical predictions suggest at least an order of magnitude greater power output should be possible in comparison with an equivalent GaAs device. It is envisaged that such devices could run at extremely elevated temperatures possibly even orange heat. In this regime hot carrier energy relaxation processes will have a profound effect on device performance. We present measurements of the electron energy relaxation rate between 1 and 130K made by a non-equilibrium phonon pulse technique.

The device was based on a 0.5µm thick $n^+(2 \times 10^{18} \text{ cm}^{-3})$ GaN epilayer grown on a c-axis sapphire substrate. An active area ($2 \times 10^{-7} \text{ m}^2$) was defined by diffused aluminium contacts. The carriers are briefly heated by an electrical pulse and subsequently relax by phonon emission. By comparing the device resistance during the excitation pulse we have deduced the energy relaxation rate of the hot electrons. The figure shows a linear dependence on temperature above about 10K as expected, since $q_{ph} \sim 2k_f$, where q_{ph} is the dominant thermal phonon wavevector, at this temperature. Below 10K, a quadratic dependence is observed consistent with piezoelectric coupling in the dirty limit ($q_{ph} l_{elastic} < 1$, where $l_{elastic}$ is the electron elastic mean free path). In contrast to GaAs, acoustic phonon coupling appears to be the dominant energy relaxation mechanism at least up to 130K. This observation is consistent with the unusually high values of piezoelectric coupling constant and longitudinal optical phonon energy in GaN. By depositing a



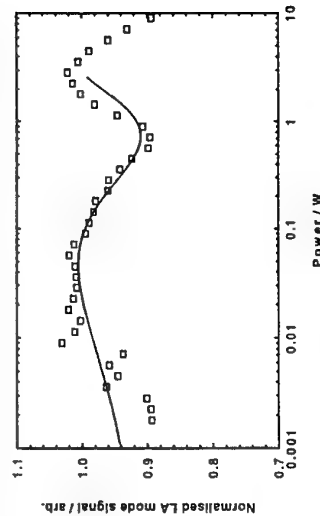
superconducting bolometer on the opposite crystal surface we were able to observe directly the emitted phonons. Sharp longitudinal and transverse mode signals typical of coupling to acoustic modes were observed with an intensity that scaled linearly with power throughout the temperature range.

MEASURING THE SIZE OF BURIED QUANTUM DOTS USING PHONONS

P Hawker, A J Kent and M Henini
Department of Physics, University of Nottingham, Nottingham NG7 2RD, UK.

An area of continued controversy in the growth of self-aligned quantum dots (QD) is their size and shape. Surface dots can be relatively easily imaged using a number of techniques (e.g. STM and AFM) but this is not possible for buried dots which may be more useful in the commercial device context. We present measurements of the size of buried self-aligned InAs QDs in GaAs made by studying the reflection of pulses of non-equilibrium phonons from the dot layers. The technique is non-destructive in contrast to TEM where the sample must be cleaved and thinned.

We have investigated a range of samples with various numbers of dot layers and interlayer spacings, each grown by depositing 1.8ML of InAs on (100) GaAs. Using a thin film resistive heater, short (~20ns) pulses of non-equilibrium phonons were directed at the dot layers and the reflected component was detected using a superconducting aluminium bolometer. The resulting time-of-flight traces allowed the individual acoustic modes (longitudinal, LA and transverse, TA) to be identified and their intensities were measured as a function of heater input power. The figure shows the LA mode intensity normalised to the heater power as a function of heater power for a fifteen dot layer sample. A horizontal line at $y=1$ would correspond to signal directly proportional to power. Instead, we observe a decrease at the lowest powers and a pronounced dip around 1W. We suggest both features can be explained in terms of interference of acoustic waves reflected from the upper and lower surfaces of individual dots. Taking into account the π phase change that occurs at the InAs→GaAs interface, destructive interference occurs for $\lambda_d \rightarrow \infty$ (low power limit) and $\lambda_d/2 = h$, where h and λ_d are the dot height and dominant thermal phonon wavelength respectively. We have modeled the interference process by approximating the heater spectrum to a



single peak at wavelength λ_d , and the result is shown as a solid line in the figure. We obtain $h \approx 3.3\text{nm}$. The only other adjustable parameter is the fraction of surface covered by dots. From the depth of the dip at 1W (~10%), and assuming that the buried dot layers have the same areal number density as observed in surface dot samples grown under the same conditions, we deduce a dot diameter of 230nm.

By analysing the relative sizes of the TA and mode converted (LA→TA, TA→LA) phonon signals it should be possible to obtain more information concerning the geometrical shape of the dots and work towards this end is in progress.

Interface and confined phonons in stepped quantum wells.

P. Kinsler*, R. W. Kelsall, P. Harrison.
*Institute of Microwaves and Photonics, School of Electronic and Electrical Engineering,
 University of Leeds, Leeds LS2 9JT, United Kingdom.*

Layered GaAs/(Ga_{1-x}Al_x)₂As heterostructures confine not only the quantum states of the electrons, but also those of the phonons. Here we consider details of the phonon modes in stepped (asymmetric) quantum wells[1], in contrast to many existing calculations which assume bulk-like phonon modes. Scattering processes control the utility of a given emitter design. Electron-electron scattering cannot be ignored in these devices, but electron-phonon scattering still has a crucial role[2].

The DCM: This is a continuum theory based on electromagnetic boundary conditions[3]. Using the dielectric continuum model (DCM), the dominant phonon modes are confined LO phonons; and interface polaritons (IP), which are often just called interface phonons. The total scattering rates obtained using the DCM are known to be reasonably accurate in the types of structures we consider. The confined LO phonons have sinusoidal interaction potentials that are completely confined to each layer. In contrast, the IP potentials vary exponentially, and tend to be localised at the interfaces – however the details of the structure affect this localisation greatly. Each IP has its own dispersion curve, and for the structures considered here there are six branches.

The IP dispersions: The electrostatic potentials and the electric displacement field perpendicular to each interface must be continuous for an IP mode. These potentials were solved analytically to obtain a dispersion relation, then used to determine the amplitudes in each layer of each mode. We find 6 modes, which at $k = 0$ correspond to either the TO or LO phonon energies in the barrier, step, or well. These dispersion relations were unlike those in a symmetrical system, in that at large k the branches do not pair off.

The IP potentials: In simple square quantum well structures, there are simple symmetric and antisymmetric interface phonon modes. However, in our asymmetric quantum wells the presence of asymmetry and extra interfaces affects the interaction potentials of the interface polaritons, as well as the electronic wavefunctions. In particular, we now have an IP mode localised at the step edge in the middle of the well. As the scattering rates depend on the overlap of these, it is clear that some of the IP modes will interact more strongly with particular electronic states than others, because of both the different energies and localisations of the branches. What this means in practice is that although for the square well case the results of the bulk-phonon approach are adequate, we cannot rely on this to be true in general.

[*] email P.Kinsler@elec-eng.leeds.ac.uk

[1] P. Harrison, R.W. Kelsall, J. Appl. Phys. **81**, 7135 (1997).

[2] P. Kinsler, P. Harrison, R.W. Kelsall, submitted to Phys. Rev. B.

[3] B.K. Ridley, *Electrons and phonons in semiconductor multilayers*, (Cambridge University Press, 1997).

OBSERVATION OF THERMALLY ACTIVATED
QUASIPARTICLE INTERACTION

BY BALLISTIC ELECTRON TRANSPORT AND ELECTRON FOCUSING

S. Knauth, A. Boehm*, and W. Grill
 Institut für Experimentelle Physik II der Universität Leipzig,
 Linnéstr. 5, D-04103 Leipzig, Germany

* MPI für Festkörperforschung - Grenoble High Magnetic Field Laboratory
 25, avenue des Martyrs, F-38042 Grenoble Cedex 9, France

Electron focusing patterns originating from ballistic electron transport in single crystalline materials are observed in transmission. Spatially resolved excitation by scanning electron microscopy and detection by a point contact is employed for imaging.

The electron-phonon respectively the electron-electron interaction has been studied by observation of the thermal dependence of the focusing patterns in the temperature range of 5 to 20 K. Results are presented for bismuth and tungsten. Effects concerning the simultaneous emission of thermally excited phonons by the electron beam are discussed.

CONFOCAL SCANNING ACOUSTIC MICROSCOPY IN AIR AT NORMAL CONDITIONS AT MHZ-FREQUENCIES CLOSE TO THE PHONON-CUTOFF-REGIME

W. Grill*, T. J. Kim*, Z. Kojro*, M. Schmachtl*, and M. Schubert*,

* Technical University of Wrocław, Institute of Telecommunication and Acoustics,

Wybrzeże Wyspiańskiego 27, PL-50-370 Wrocław, Poland

* Institut für Experimentalphysik II der Universität Leipzig,

Linnéstr. 5, D-04103 Leipzig, Germany

A scanning acoustic microscope with phase and amplitude contrast (vector contrast) operating in air at normal conditions has been developed. Focusing transducers with and without impedance matching layers were manufactured and employed for the generation of focused ultrasonic waves and the spatially resolved detection of reflected or transmitted waves.

Frequencies up to 11 MHz have been employed. At 1.27 MHz a lateral resolution of about 220 μm is achieved. The distance resolution reaches 10 nm for 1 s total signal acquisition time. It is in the vicinity of the average distance of 3 nm between the molecules in air at normal conditions. Images in amplitude and phase contrast and 3-dimensional representations of the surface topography of various objects have been obtained in reflection.

Technical details of the instrument including the focusing air transducers and the signal and data processing are explained. Applications are demonstrated.

RENORMALIZATION OF ACOUSTIC PHONON SPECTRA AND RUDIMENTS OF PEIERLS TRANSITION IN FREE-STANDING QUANTUM WIRES

S. M. Komirenko (a), K. W. Kim (a), V. A. Kochelap (b), Mitra Dutta (c), Michael A. Stroscio (c)

(a) ECE Dept., North Carolina State U., Raleigh, NC 27709 USA

(b) Dept. of Theoretical Physics, Institute of Semiconductor Physics, Ukrainian Academy of Sciences, Kiev, 252650, Ukraine

(c) U.S. Army Research Office, PO Box 12211, RTP, NC 27709 USA

ABSTRACT

In this paper presents an analysis of the Peierls transition [1] for a system of one-dimensional electrons and acoustic phonons confined in a free-standing quantum wire. In this analysis, electrons and phonons are coupled via the deformation potential interaction and electron-electron interactions are treated in the mean field approximation. [2-4] Moreover, potential energy contributions due to acoustic-phonon-induced variations in the electron density are taken into account in modelling the coupled one-dimensional electron-phonon system. This formalism facilitates the investigation of the renormalized acoustic phonon spectrum as well as the role of screening effects. Based on this formalism, cusp-like features are found in the dispersion relation for a free-standing quantum wire at the wavevectors where the Peierls transition is predicted to occur. Furthermore, this formalism predicts the possibility of the Peierls transition in free-standing quantum wires fabricated from semiconductor materials with large dielectric permittivity.

REFERENCES

1. R. E. Peierls, *More Surprises in Theoretical Physics* (Princeton University Press, Princeton, 1991); *Quantum Theory of Solids* (Clarendon, Oxford, 1955).
2. SeGi Yu, K. W. Kim, M. A. Stroscio, G. J. Iafrate, A. Ballato, *Phys. Rev. B* **50**, 1733 (1994).
3. N. Nishiguchi, *Phys. Rev. B* **50**, 10970 (1994).
4. V. A. Kochelap, V. N. Sokolov, *Sov. Phys. JETP, Letters*, **25**, 18 (1978); V. A. Kochelap and V. N. Sokolov, *Phys. Status Solidi, b*, **120**, 565 (1983).

GENERALIZED INTERFACE ACOUSTIC WAVES PIEZOELECTRICALLY COUPLED TO EMBEDDED TWO-DIMENSIONAL ELECTRON SYSTEM

Yuriy A. Kosevich

Max-Planck-Institut für Physik komplexer Systeme, D-01187 Dresden, Germany

Experiments on the propagation of surface acoustic waves (SAW) across the surface of a heterostructure containing two-dimensional electron system (2DES) showed that SAW technique can be used as a powerful probe of the (diagonal) conductivity σ_{xx} of the 2DES (see, e.g., [1-3]). In most cases, 2DES is placed at a $GaAs/AlGaAs$ heterojunction on a finite distance d from free surface of the structure, and the wave number k in most recent experiments can be so large that the product kd is more than unity [4,5]. In this case the 2DES can be considered as embedded in bulk of $GaAs$ crystal. In the present work we consider the propagation of interface acoustic waves (IAW), caused by and localized at a conducting 2DES embedded in bulk of cubic piezoelectric crystal (of the $GaAs/AlGaAs$ type). It is shown that the IAW with a sagittal polarization can propagate along the [110] direction in the (001) plane of the 2DES due to the internal (local) screening of the electrostatic potential by the 2DES with $2\pi\sigma_{xx} > \epsilon v_s$, where v_s is the acoustic wave velocity, ϵ is the dielectric constant of the crystal (see also [6,7]). The IAW, contrary to the SAW in the structure [5], cannot be consistently described by the perturbation of the nonpiezoelectric wave since localized IAW do not exist in the absence of piezoelectric coupling. The important conclusion is that generalized IAW can propagate in the $GaAs$ crystal, when the IAW displacement amplitude decays from the 2DES into the bulk and towards the free surface nonmonotonously, with spatial oscillations. The period of spatial oscillations as well as the possibility of propagation of generalized IAW are determined by the acoustic anisotropy of the crystal, as in the case of generalized SAW in cubic crystals [8]. The existence of generalized IAW with amplitude, nonmonotonously decaying towards the free surface, can substantially effect the coupling of short-wavelength SAW to the 2DES embedded in bulk of $GaAs$ crystal.

1. A. Wixforth, J.P. Kotthaus, and G. Weimann, Phys. Rev. Lett. **56**, 2104 (1986).
2. V.M. Rampton *et al.*, Semicond. Sci. Technol. **7**, 641 (1992).
3. R.L. Willet, Advances in Physics **46**, 447 (1997).
4. R.L. Willet, K.W. West, and L.N. Pfeiffer, Phys. Rev. Lett. **75**, 2988 (1995).
5. S.H. Simon, Phys. Rev. B **54**, 13 878 (1996).
6. Yu.A. Kosevich, Progr. Surf. Sci. **55**, 1 (1997).
7. Yu.A. Kosevich, C. Eckl, and A.P. Mayer, *unpublished*.
8. Yu.A. Kosevich, E.S. Sytkin and A.M. Kosevich, Progr. Surf. Sci. **55**, 59 (1997).

ENERGY LOSS OF HOT ELECTRONS IN DOUBLE BARRIER RESONANT TUNNELLING STRUCTURES

A.V. Kulikowski, M. Giltrow, A.G. Kozorezov, M. Sahraoui-Tahar and J.K. Wignmore,
School of Physics and Chemistry, Lancaster University, Lancaster. LA1 4YB UK

and

J.H. Davies, C.R. Stanley, B. Vogel and C.D.W. Wilkinson,
Dept. of Electronic and Electrical Eng., Glasgow University, Glasgow. G12 8QQ UK

We have used phonons as a direct probe of the energy loss processes of hot electrons in $GaAs/AlGaAs$ double barrier resonant tunnelling diodes (DBRTD). The use of nanosecond pulses and lithographically defined superconducting aluminium bolometers resulted in high resolution in both time and space. We have been able to identify various regimes of energy loss with respect to the bias voltage and therefore electron energy. The particular processes were distinguishable due to the differing spatial and spectral distributions of the emitted phonons.

The energy of the tunnelling electrons was tuneable via the device bias voltage, with a bandwidth of a few meV. At low bias voltages (<400 meV), the dominant energy loss mechanism was the excitation of coupled plasmon-optic phonon modes in the heavily-doped collector of a device. The transverse (TA) phonons observed resulted mainly from the decay and down-conversion of cascades of these coupled modes, whilst the lower frequency longitudinal (LA) phonons arose from heating of the Fermi gas in the collector.

At higher biases, although still below the resonant tunnelling peak, a distinct transition in the TA voltage dependence could be seen, which was identified as the onset of Γ -L and L-L intervalley transfer. These processes generated intervalley optic phonons, which decayed through anharmonic down-conversion via a different route to that of the coupled modes. This was also clearly observed in the detected LA phonon flux as a different spectral distribution above the threshold energy. The value of the intervalley deformation potential coupling constant, D_{TL} , could be determined from the results.

At bias voltages beyond the resonant tunnelling peak, we have found evidence for phonon emission through inelastic tunnelling via the excitation of interface phonons.

PosB21

THEORY OF THE ELECTRON PHONON INTERACTIONS IN THE InSb MOSFET

Saadi Lamari
Institut de physique
Université Ferhat Abbas
Sétif 19000 Algeria

Abstract

The 2D electron gas in a InSb Mosfet presents a very rich system where numerous processes can take place. Reliable calculations on this system are however complicated by the intricate band structure of this material which besides being a narrow gap semiconductor is also polar.

In the present work I present the results of my investigations on the electron phonon interactions in the system.

I use a multiband (6 X6) Kane Hamiltonian for the band structure from which I deduce the subband structure self-consistently within the effective mass approximation and self-consistent LDA. Use is made of the Fröhlich hamiltonian for optical phonons and deformation potentials for the acoustic phonons in the e-phonon part of the Hamiltonian. I use both slab and interface phonons to calculate the relaxation time τ .

I also investigate the cases where the bulk optical phonon energy $\hbar\omega_{LO}$ is resonant with either the intersubband spacing or the Landau spacing of the levels.

The different processes involved are clarified and discussed and our results are compared to existing experiments with which they show satisfactory agreement.

The use of our theory for other systems (e.g. quantum wells, superlattices...) is also pointed out.

PosB22

Confinement of optical phonon modes in thin $(GaAs)_n(AlAs)_n$ Superlattices

K. Lambert and G.P. Srivastava

Department of Physics, University of Exeter, Stocker Road, Exeter, EX4 4QL, United Kingdom

Abstract

We present theoretical investigations of atomic vibrations in thin $(GaAs)_n(AlAs)_n$ superlattices grown along the symmetry directions [001], [110] and [111] using the *adiabatic bond charge model*. We find that optical phonon modes get confined for all layer thicknesses, including the monolayer case. In particular we show that the energy gap between the primary and secondary confined longitudinally optic modes is dependent upon the direction of growth in addition to the period of thickness of the superlattice. We show that the direction dependence is due to the polarity of the system. We also calculate the unfolding behaviour of the confined superlattice frequencies and provide a comparison with experimental Raman peaks.

THERMAL CONDUCTIVITY OF SHORT PERIOD $(\text{GaAs})_n/(\text{AlAs})_n$ SUPERLATTICES

W. S. Capinski and H. J. Maris

Department of Physics, Brown University, Providence, RI 02912, USA

T. Ruf, M. Cardona, and K. Ploog

Max-Planck-Institut für Festkörperforschung, Heisenbergstr. 1, D-70569 Stuttgart, Germany

D. Scott Katzer

Naval Research Laboratory, Washington, D.C. 20375

We present measurements of the thermal conductivity κ_L in the direction normal to the interfaces of a family of periodic $(\text{GaAs})_n/(\text{AlAs})_n$ superlattices. The thickness of the GaAs and AlAs layers ranged from $n = 1$ to 40 monolayers. The measurements were obtained by an optical pump-and-probe technique and made over the temperature range of 100 to 375 K. We find a general decrease in κ_L with a decrease of the superlattice period. For the samples with $n \leq 10$ the conductivity at 300 K was lower than the conductivity of the $\text{Al}_{0.5}\text{Ga}_{0.5}\text{As}$ alloy. We will discuss the decrease in κ_L compared to the bulk constituents in terms of extrinsic and intrinsic scattering mechanisms.

VIBRATIONAL PROPERTIES OF SPONTANEOUSLY ORDERED GaInP_2

A. Mascarenhas, H.M. Cheong, F. Alsina, and J. M. Olson

National Renewable Energy Laboratory, 1617 Cole Boulevard, Golden, CO 80401

GaInP_2 alloys grown by MOCVD on (001) GaAs substrates exhibit a spontaneous CuPt-type ordering along the $[\bar{1}11]$ or $[1\bar{1}\bar{1}]$ directions, depending on the growth conditions and the substrate misorientation. These structures resemble monolayer superlattices of $\text{Ga}_{0.5-\eta}\text{In}_{0.5+\eta}\text{P}/\text{Ga}_{0.5-\eta}\text{In}_{0.5+\eta}\text{P}$ along the ordering direction in where the value of the order parameter η ($0 \leq \eta \leq 1$) depends on growth conditions. Due to this ordering, the symmetry of the crystal changes from the T_d symmetry of zinc-blende to trigonal C_{3v} symmetry. The electronic, optical, and lattice-dynamical properties of the ordered alloy reflect this change in symmetry. So far, several symmetry-induced phenomena, including valence-band splitting, birefringence, pyroelectricity, and superlattice phonon modes, have been observed and found to be consistent with the C_{3v} symmetry of the ordered crystal.

In Raman scattering measurements taken from the (001) growth surface, three extra phonon peaks at 60, 205, and 354 cm^{-1} have been observed for ordered GaInP_2 samples. The two lower-frequency modes at 60 and 205 cm^{-1} are identified as due to the 'zone-folded' transverse and longitudinal acoustic phonon branches, respectively, and the extra mode at 354 cm^{-1} as due to a longitudinal mode. The nature of these extra peaks was investigated using far-infrared reflection and transmission measurements and micro-Raman scattering measurements in the $(\bar{1}10)$ and $(\bar{1}\bar{1}1)$ backscattering geometries, and in the right-angle scattering geometry between the (001) and $(\bar{1}\bar{1}0)$ surfaces. In addition, resonance Raman scattering measurements on the (001) growth surface show a pronounced resonance near the fundamental band gap of the ordered material. These results are interpreted in terms of the electronic structure and the lattice dynamic properties of the ordered alloys.

HETERODYNE TRANSIENT GRATING DETECTION OF ACOUSTIC AND OPTIC PHONONS

A. A. Maznev, T. F. Crimmins, K. A. Nelson

Abstract:

A novel optical arrangement for the heterodyne detection of laser-induced transient gratings, based upon the use of an optical phase mask instead of a beam splitter for probe and reference beam separation, provides phase stability and control without the need for active stabilization. This dispersion-free optical arrangement can also be used to separate and recombine the two pump pulses used in transient grating experiments, resulting in complete spatial overlap between the two pulses with markedly improved k vector accuracy. In this work, measurements of acoustic and optic phonons using this technique are made and shown to have superior signal to noise ratios and phase sensitivity. Additionally, the technique is applied to accurately determine low-frequency phonon-polariton dispersion curves as well as acoustic phonon responses in bulk and thin film materials.

SURFACE VIBRATIONAL MODES AND REFLECTION TIMES OF PHONONS IN A FINITE-SIZE SUPERLATTICE

Seiji Mizuno and Shin-ichiro Tamura

Dep. of Appl. Phys., Hokkaido University, Sapporo 060-8628, Japan

We study theoretically the interaction of bulk phonons with surface vibrational modes in a finite size superlattice with a free surface. A phonon incident normally on the superlattice from a substrate is perfectly reflected, i.e., the reflection rate is unity irrespective of frequency (Fig.1). However, it comes back to the substrate with a large time delay when the frequency coincides with an eigenfrequency of the surface mode.

This temporal delay is explained in terms of "phase time" defined by the frequency derivative of the scattering phase shift. We derived an analytical expression of the phase time. Figure 2 shows the phase time calculated for an AlAs/GaAs superlattice. We see sharp peaks within the lowest and third frequency gaps (at about 0.3 THz and 0.9 THz). We also derived approximate but explicit formulas for these peaks, and show that these are due to the resonant interaction of an incident phonon with a vibrational mode localized near the surface. To see this resonant behavior more explicitly, we calculated numerically the time evolution of the phonon wave packet (Fig.3). Figure 3 shows that the large amplitude stays near surface for a long time and is gradually emitted toward the substrate. The sharp peaks in Fig.2 correspond to the temporal delay demonstrated in Fig.3. Our results suggest the observability of the surface vibrational modes by a time-resolved phonon reflection experiment.

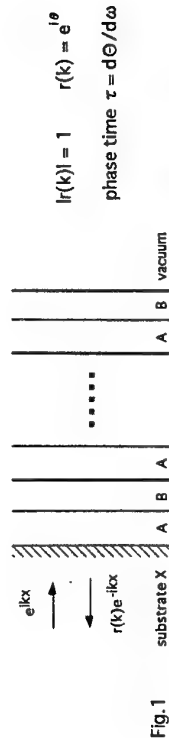


Fig.1

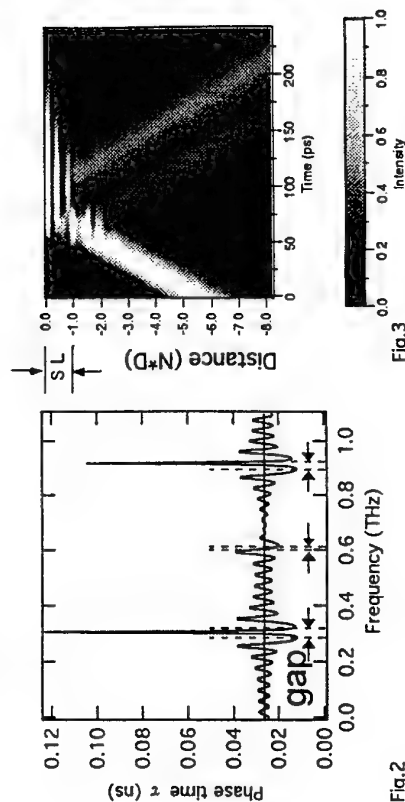


Fig.2

Fig.3

COHERENT PHONONS IN MIXED SEMIMETALS AND SEMIMETAL SUPERLATTICES

S. Nakashima^a, M. Hase^a, K. Mizoguchi^a, H. Harima^a, K. Sakai^b,
S. Cho^c, A. DiVenere^c and J. B. Ketterson^c

^aDepartment of Applied Physics, Osaka University,
Suita, Osaka 565-0871, Japan

^bKansai Advanced Research Center, Communication Research
Laboratory, Kobe, Hyogo 651-24, Japan

^cDepartment of Physics and Astronomy, Northwestern
University, Evanston, Illinois 60208, USA

Pump-probe technique using fs laser pulses has enabled us to generate and detect the coherent phonons in solids. Time resolved reflectivity signals for semimetals such as Bi and Sb have showed strong oscillations due to optic phonon generations.

In this work we have measured coherent phonons in a Bi_{1-x}Sb_x mixed crystal system and Bi-Sb superlattices using a reflection type pump-probe technique and compared with results of Raman measurements.

Bi-Sb mixed crystals are of three-mode type, and A_{1c} type Raman bands corresponding to the stretching vibrations of Bi-Bi, Bi-Sb and Sb-Sb bonds are observed at around 100, 130 and 150 cm⁻¹, respectively. Three coherent phonons with the A_{1c} species are also observed in this mixed crystal system. The frequencies of the coherent phonons coincide with those of the Raman bands, while the relative amplitude of the coherent phonons differs from Raman intensity profile of the A_{1c} modes, presumably because the resonant effect may contribute to the Raman intensity.

Using multiple pulse trains we were able to selectively excite either of the three components in Bi-Sb mixed crystals.

For Bi-Sb superlattices we have observed coherent oscillations of the A_{1c} optic phonons confined in each constituent layer and folded acoustic (FA) phonons which are extended over a whole region. We have also found a phonon mode localized at the interface of Bi and Sb layers, which corresponds to the Bi-Sb mode in the mixed crystals. The frequency of the coherent FA phonons increases as the superlattice period is reduced. It is to be noted that the decay time of the coherent FA mode with frequencies of 0.1-4 THz is very short (~10 ps) compared with that of the GaAs-AlAs superlattices. The short time decay might be due to strong attenuation of high frequency acoustic phonons due to the scattering of free carriers and escape of the coherent phonons from local area probed by the probe pulses.

Coherent phonon spectroscopy is a powerful tool to measure phonons with wide range of frequencies simultaneously.

Anomalous Velocity Change of Surface Wave near the Gelation Point

Hirofumi Okabe, Keiichi Kuboyama,¹ Kazuhiro Hara and Shoichi Kai

Department of Applied Science, Faculty of Engineering, Kyushu University,
Hakozaki, Higashi-ku, Fukuoka 812-8581, Japan

¹Venture Business Laboratory, Kyoto University,
Yoshida Honmachi, Sakyo-ku, Kyoto 606-8317, Japan

We studied the properties of surface waves during the gelation process of tungstic acid gel by time resolved surface wave measurements.¹⁾ The experimental results agreed qualitatively with the known theoretical results²⁾ of the viscoelastic model in an equilibrium system except near the gelation point. Near the sol-gel transition point of tungstic acid, we found interesting features in the time variation of the velocities. Namely, the velocities of the surface waves had a maximum near the gelation point, decreased once rapidly, and again increased gradually as the gelation proceeded. The anomaly is clearly shown in the time dependence of the wave number exponent x ($\omega \sim k^x$), too. The x of tungstic acid was about 1.4 (the values 1.5 and 1.0 indicate surface tension and elastic wave, respectively) in the sol state and rapidly decreased to 1.0 at the gelation time. Nakanishi et al³⁾ had tried to explain this anomalous velocity changes by the viscoelastic model. However, further investigation is necessary to clarify the mechanism of this particular property. So, we have measured that of the gelatin and silica gel, and the viscoelasticity of all samples.

In the sol state, all samples showed the same frequency dispersion as that of water. After the sol-gel transition time, the velocities of all samples increased considerably. In particular, the increase of velocity in tungstic acid was larger than that in gelatin and silica gel, and this property may be due to the difference of elasticity. This result reflects the fact that as gelation proceeded, the network structure spread and elasticity emerged. While, the frequency dispersion of tungstic acid in the gel state disappeared, that of gelatin and silica gel remained after the gelation point. The x of gelatin was about 1.4 (same as tungstic acid) in the sol state and decreased gradually after the gelation point. As the gelation progressed, it approached a value of about 1.2. On the other side, the x of silica gel remained near 1.5 after the gelation point. However, the absolute values of complex viscosity of all samples haven't shown anomalous changes near the gelation point. There may be another essential difference in addition to the fact that the gelation process of tungstic acid proceeds much faster than that of gelatin and silica gel.

References

- 1) K. Motonaga, H. Okabe, K. Hara, K. Matsushige: Jpn. J. Appl. Phys., **33** (1994) 2905.
- 2) J. L. Harden, H. Pleiner, P. A. Pincus: J. Chem. Phys., **94** (1991) 5208.
- 3) S. Kubota and H. Nakanishi: Prog. Theor. Phys. Suppl., **126** (1997) 359.

ACOUSTODYNAMIC METHODS OF INVESTIGATIONS OF SEMICONDUCTORS DEFECTS

Ya.M.Olikh, V.F.Machulin, R.K.Savkina

(Inst. of Semiconductor Physics of NASU, pr.Nauki,45,Kyjiv,Ukraine,252028)

A novel alternative low-temperature method of the structural perfection controlling of the semiconductor crystals is the ultrasound (US) treatment in the frequency range (0.1-100) MHz. These possibilities are based on the phenomenon of intensive (beyond threshold) ultrasound interaction with nonequilibrium defects in semiconductors [1]. In many further works qualitative conclusions were made as to the possibility of using such an "active sound" for modification of the samples parameters [2].

We are looking for enlarging essentially of the possibilities of traditional physical investigation techniques by using of the US loading of samples during the measurement process. Under the US loading of a semiconductor sample a special state of the crystal defect structure comes into being while certain defects appear to be acoustosensitive. Their acoustostimulated transition into metastable states is accompanied by changes in electrical, optical, photoelectrical, etc. parameters of the sample. Complex all-round investigations of these changes over a wide range of temperatures at varying US characteristics (amplitude, polarization and frequency) performed on the model prototype semiconductors samples will result in comprehensive understanding of the physics of US interaction with nonequilibrium defects and in stating up the scope of the method as well as optimal US treatment conditions.

The physical processes in crystals with dislocational mechanism of US interaction (A_2B_3 -compound and their solid solutions) are understandable [1,2]. However the situation remain open to question for the nonpiezoelectrical crystals without dislocations (Si, Ge, A_3B_5 -compound).

In this work we have presented the results of intensive ultrasonic waves using for acceleration of the radiation-induced defects (RD) annealing process on one hand and for investigations of RD in Ge crystals by acoustodynamic Hall method on the other hand. Ultrasound accelerates on the efficacy of RD disintegration and electrical activation of the transmutation doped impurities. On certain stages of annealing in Ge crystals the defect structure with high sensitivity to US is realized. Reversible changes of the electrophysical parameters have taking place during US loading. Investigations of the amplitude, frequency and kinetic of transition processes allow to obtain information about defects and their structure.

In paper the possibilities of acoustodynamic Hall method are discussed.

I.V.Ostrovskij, JETP Lett., 1981,v.34, p.467, (in Russian).

2.Ya.M.Olikh, Ju.Shavlyuk. Fiz.Tverd.Tela, 1996,v.38,p.3365,(in Russian).

ACOUSTIC PHONON SCATTERING IN TWO DIMENSIONAL CARRIERS IN GAAS

F.F.Ouali, H.R.Francis, H.C.Rhodes.

Department of Physics, University of Nottingham, NG7 2RD, UK.

Abstract

The phonon scattering contribution to the mobility (μ_{ph}) of a two dimensional carrier gas cannot be readily separated from the impurity scattering (μ_{ex}) since the latter may depend on temperature because of the temperature dependence of screening.

In the present work, we present a new experimental technique which separates the two components at low temperatures and allows each to be obtained as a function of temperature. In this, we do not make any assumptions about the temperature dependence of extrinsic scattering but use the fact that the energy loss rate of hot carriers due to acoustic phonons, $P \propto T_e^2 - T_l^2$, (T_e and T_l are the carrier and lattice temperature respectively) where n lies between one and seven(five) for screened deformation(piezoelectric) scattering. In our temperature range $n=2-3$. To estimate the phonon contribution to the mobility at a temperature T_l , we measure the mobility of the device μ for the same input power P at two temperatures: (a) T_l and (b) $T_0 \ll T_l$ (T_0 is such that phonon scattering is negligible).

If the corresponding carrier temperatures are such $(T_e)_H \gg T_l$ and $(T_e)_L \gg T_0$, the carriers have the same temperature T_c in both conditions and the difference $\mu_H - \mu_L$ is then used to estimate phonon scattering at T_l .

The technique is applied to GaAs in the temperature range 4.2-20K. Four heterojunctions 2DEGs with electron densities in the range $(1-3) \times 10^{11} \text{ cm}^{-2}$ and mobilities in the range (0.2-1) $\times 10^6 \text{ cm}^2$ were used. The results show that μ_{ex} is only weakly temperature dependent. The measured μ_{ph} and its temperature dependence are discussed and compared with theoretical calculations [1] and other experimental measurements where impurity scattering was assumed to be temperature independent [2,3]. We also present measurements on high mobility holes grown on (311A) substrate.

[1] Karpus (1990), *Semicond. Sci. Technol.* 5, 691.

[2] Stromer et al (1990), *Phys. Rev B* 41, 1287.

[3] Harris et al (1990), *Surf. Sci.* 229, 113.

STIMULATED PHONON EMISSION IN SUPERLATTICES

S A Cavill, A V Akimov*, F F Ouali, L J Challis, A J Kent and M Henini

Dept. of Physics, Nottingham University, University Park, NG7 2RD

* Permanent address: Ioffe Physical-Technical Institute, 26 Polytechnicheskaya str, 194021 St. Petersburg, Russia

Abstract

In earlier studies, we have made measurements of the transient effects on the tunnel current in double barrier tunnelling structures produced by a pulse of non-equilibrium phonons. The signals were attributed to phonon assisted tunnelling from the emitter to the donor state [1] and to the intrinsic ground state of the quantum well [2].

In the present work, we have extended our studies to superlattices. We have made the first experimental observations of phonon assisted tunnelling in a superlattice. The sample used is a weakly coupled, lightly doped AlAs/GaAs superlattice tunnelling device. Non-equilibrium phonons are generated by applying ~100 ns long electrical pulses to a constantan heater evaporated opposite the sample. The resulting transient change in the tunnel current, ΔI , is measured as a function of time, applied bias and heater temperature T_h .

As the bias voltage increases, and hence the energy separation of the levels in neighbouring wells, ΔI rises to a peak and then falls, approximately tracing out the Planckian spectrum of phonons in the heat pulse. The voltage at the peak increases approximately linearly with temperature. Time-of-flight measurements indicate that ΔI is caused predominantly by transverse (TA) ballistic phonons. We attribute the response ΔI to assisted tunnelling between two neighbouring quantum wells as a result of stimulated phonon emission. Measurements in the Wannier-Stark regime and in magnetic fields are in progress.

[1] F F Ouali *et al* (1995), *Phys. Rev. Lett.* **75**, 308 and E S Moskalenko *et al.* (1997), *High Magnetic Fields in the Physics of Semiconductors*, Eds G Landwehr and W Ossau, World Scientific, p 453.

[2] D N Hill *et al* (1997) *Phys. Stat. Sol. (b)* **204**, 431.

COMPUTER EXPERIMENT ON SURFACE WAVES IN NON-LINEAR CRYSTALS

S. Ozawa^a, R. Komuro^a, Y. Hiki^b^a Applied Physics Group, Faculty of Engineering, Ibaraki University, Nakanarusawa, Hitachi 316-0033, Japan^b Faculty of Science, Tokyo Institute of Technology, Emeritus, 39-3-303 Motoyoyagi, Shibuya-ku, Tokyo 151-0062, Japan

Molecular dynamics computer simulation is carrying on for studying lattice excitations in model crystals. The study started from the case of one-dimensional crystal [1] was extended recently to the case of two-dimensional square crystal [2]. In the present work, three-dimensional case is further intended to be investigated. For the present, the simulation is aimed to observe surface excitations in thin crystals. In our simulations, mass-spring model crystals are used; central forces are considered between nearest neighbor atoms; a lattice anharmonic potential up to the fourth order is taken into account; and magnitudes of the anharmonicity comparable with those observed in crystals of real materials are adopted. An input pulse displacement is given to specific atoms in the crystal and the displacements of all atoms are computed. It was found that, when the applied input pulse was small, medium, and large, then phonons, a single soliton, and multiple solitons were respectively produced as excitations in the crystal. Mutual collisions of phonons and solitons in one-dimensional crystals, and collisions of phonons and solitons with different kinds of lattice defects in one-dimensional and two-dimensional crystals were investigated with success. In the present case of three-dimensional crystal, surface atoms of a thin crystal are displaced and displacements of all atoms are computed. Produced excitations are considered to be sharply localized to the surface, and surface solitons are expected to be produced rather easily since the lattice anharmonicity is large at the surface of the crystal. Study of the surface (mechanical) solitons is physically interesting, and also seems to be important for possible practical applications.

[1] S. Ozawa and Y. Hiki: *Physica B Condensed Matter* **219 & 220** (1996) 473.

[2] H. Tanaka, S. Ozawa and Y. Hiki: *Jpn. J. Appl. Phys.* **37** (1998), in press.

SECOND AND THIRD-ORDER ELASTIC CONSTANTS FOR EFFECTIVE ISOTROPIC MEDIA FOR ALL LAUE GROUPS

A. Duda and T. Paszkiewicz
Institute of Theoretical Physics, Wrocław University,
PL-50-204 Wrocław, pl. Maxa Borna 9

Properties of long wavelength acoustic phonons are defined by the set of independent components of the tensor of second order elastic constants $C_{\mu\nu}$ ($\mu, \nu = 1, \dots, 6$). Their number varies from 21 for the lowest triclinic to 2 for most symmetric isotropic media. The wider set of elastic constants for a less symmetric structure is reduced to the set corresponding to a more symmetric structure by imposing some conditions on elastic constants.

Even the simplest kinds of phonon-phonon processes, that is, three phonon anharmonic spontaneous decay processes, are characterised by the whole set of independent third-order elastic constants $C_{\mu\nu\lambda}$. Their number varies from 54 to 3. Together with elastic scattering processes the mutual phonon interactions determine the evolution of the spectral composition of nonequilibrium phonon systems. Therefore, such evolution is studied analytically as well as in computer simulations (cf. [2]).

Due to their complexity, even spontaneous decay processes usually are studied in equivalent effective isotropic media [2]. For such studies it is indispensable to know the elastic constants of the second and third order for effective isotropic media represented respectively as $C_{\mu\nu}^{(eff)}$ and $C_{\mu\nu\lambda}^{(eff)}$. For the cubic elastic media $C_{\mu\nu}^{(eff)}$ and $C_{\mu\nu\lambda}^{(eff)}$ were calculated by Tamura [2], who used the method applied by Fedorov for the second order elastic constants. Using the method of averaging of components of elastic constants tensors over all orientations of axes of the laboratory frame we derived expressions for both kinds of effective elastic constants for all eleven Laue symmetry groups and checked the consistency of obtained results using the mentioned conditions. For cubic media our results agree with [2]. We checked that these effective isotropic *linear* elastic media are stable.

Additionally for cubic and transversely isotropic media we proved that our method of obtaining effective nonlinear elastic media reduces the complicated spectra of relaxation rates related to elastic scattering in anisotropic media to the simple, purely discrete spectrum which is characteristic for all isotropic media [3].

References

- [1] M. T. Labrot, A. P. Mayer, R. K. Wehner, P. E. Obermayer, J. Phys. C **1** (1989) 8809.
- [2] S. Tamura, Phys. Rev. B **31** (1985) 2574.
- [3] T. Paszkiewicz, M. Wilczyński, in: Dynamical Properties of Solids v. 7, Phonon Physics The Cutting Edge, ed. G. K. Horton and A. A. Maradudin (North Holland, Amsterdam, 1995), p. 257.

CONFINED ACOUSTIC PHONONS AND ELECTRON TRANSPORT IN QUANTUM WIRES: A NUMERICAL ANALYSIS OF THE CHARACTERISTIC PARAMETERS

N. Perrin
Laboratoire de Physique de la Matière Condensée de l'Ecole Normale Supérieure
24, rue Lhomond
75231 Paris Cedex 05, FRANCE

The acoustic phonons quantization in metallic nanostructures is expected to lead to peculiar features in the electron transport properties. When experimentally observed these features are rather small as in the case of the dynamical resistance of thin wires. A numerical analysis of the electron transport through the different parameters involved in the problem is presented here: an attempt is done to determine the best conditions for the electron transport to exhibit these features.

Destruction of weak localization by phonon flux in δ -doped GaAs

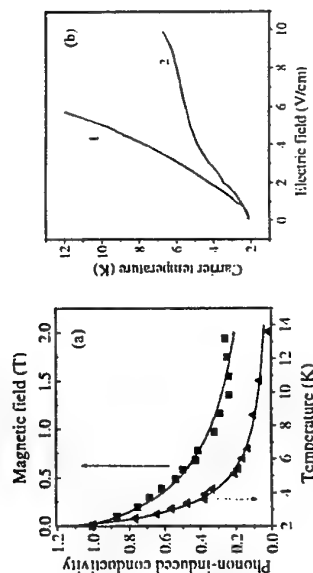
D. Poplavsky†, B. Danilchenko†, and H. Kostial§

† Institute of Physics of NASU, Prosp. Nauki 46, 252650 Kiev, Ukraine
§ Paul-Drude-Institut für Festkörperforschung, Hausvogteiplatz 5-7, 10117 Berlin, Germany

The effects of quantum interference of carriers are observed in low-dimensional systems with strong elastic scattering of carriers and caused by constructive interference of counterpropagating electron waves [1]. This leads to negative correction to conductivity. It is known that processes of nonelastic scattering as well as external magnetic field change the phases of wave functions thus leading to the destruction of weak localization and increasing the conductivity. The most widely used experimental method of weak localization study is magnetotransport measurements at different temperatures.

We present another approach for the study of weak localization - phonon-induced conductivity (PIC) measurements using time-of-flight phonon spectroscopy. Low mobility 2DEG formed in δ -Si doped GaAs with carrier concentration $5 \cdot 10^{11} \text{ cm}^{-2}$ was studied. Phonon flux that was incident on 2DEG increased its conductivity. Responses from both LA and TA phonon modes were observed. Also magnetoresistivity measurements at different temperatures were carried out and showed the presence of weak localization in the system under investigation. The temperature dependence of phase-breaking time τ_0 was extracted indicating the Nyquist mechanism of phase relaxation. PIC measurements were performed at different carrier temperatures and values of magnetic field perpendicular to δ -layers (see Fig. a). The suppression of PIC normalized to phonon flux was observed at $\approx 15 \text{ K}$ that corresponds to the temperature of suppression of weak localization observed in magnetoresistivity measurements. It is supposed that observed PIC signals correspond to the destruction of weakly localized states by phonon flux. Increase of the temperature or external magnetic field reduces the number of weakly localized carriers thus decreasing the value of PIC.

PIC caused by the destruction of weak localization reflects only the properties of 2DEG. Thus temperature and electric field behavior of PIC enables to deduce the dependence of 2DEG temperature on heating electric field (Fig. b-2). It does not coincide with the dependence extracted from conductivity data that corresponds to the mixture of 2D and 3D electron subsystems (Fig. b-1). The obtained dependencies are in qualitative agreement with calculations [2].



[1] G. Bergmann, Phys. Rep. 107, 1 (1984).

[2] H. Kostial et al, Phys. Rev. B 47, 4485 (1993).

PANDA: A NOVEL TRIPLE-AXIS SPECTROMETER UNDER CONSTRUCTION AT THE HIGH FLUX REACTOR FRM-II OF MUNICH

N.M. Pyka¹, M. Loewenhaupt² and S. Kramp^{1,2}¹Institut-Laue-Langevin, B.P. 156, F-38042 Grenoble Cedex 9²Institut für Angewandte Physik, TU-Dresden, D-01062 Dresden

At present the high flux research reactor FRM-II is under construction at Munich, Germany. Two triple axis spectrometers (TAS), one operated with thermal and one with cold neutrons, will be installed within the scope of the primary instrumentation. We shall present the cold spectrometer PANDA which will be optionally operated with polarised neutrons and which will have a spin-echo equipment. This instrument largely profits from its vicinity to the reactor and uses all possibilities of state-of-the-art neutron optics. PANDA will be a unique TAS with respect to neutron flux, energy resolution and energy- and Q-range.

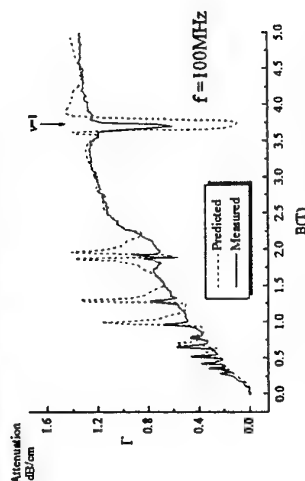
SAW ATTENUATION BY THE LOCALISED STATES OF A 2D CARRIER SYSTEM IN A MAGNETIC FIELD.

V.W Rampton, I Kennedy, C J Mellor, B Bracher*, M Henini, Z R Wasilewski† and P T Coleridge†.

Department of Physics, University of Nottingham, University Park, Nottingham NG7 2RD UK
 *CMF, Rutherford Appleton Laboratory, Chilton Didcot, OX11 0QX, UK
 †Microelectronics Division, NRC, Ottawa, Canada.

The attenuation and dispersion of a surface acoustic wave (SAW) propagating on a surface under which a 2 dimensional electron system (2DES) or a 2 dimensional hole system (2DHS) has been established, depends on the conductivity, σ_{xx} , of the 2DES or 2DHS. [Wixforth et al. 1989]. In the quantum Hall effect regime, σ_{xx} varies with filling factor and can tend to zero at integral filling factor. However, we find that the attenuation of high frequency SAW does not return to zero at these values of magnetic field. We interpret this as due to localised electron or hole states which do not contribute to the conductivity but can interact with the SAW. A theoretical account of the interaction was given by Rampton et al. [1992].

We have made experiments using GaAs/AlGaAs heterojunctions with both a 2DES and with a 2DHS. SAW at frequencies up to 2GHz, magnetic fields up to 16T and at temperatures down to 300mK were used. The samples were in the form of a Hall bar so the longitudinal and transverse resistivities could be measured and the conductivity of the 2D layer was found. This enabled us to predict the SAW attenuation and dispersion due to the extended electron states. An extra attenuation was found at integral filling factors and is attributed to the localised states. The figure below shows a typical result for a 2DES.



The ratio of attenuation to dispersion by the localised states is given by the product of the frequency and wavevector of the SAW and the relaxation time of the localised electron states. We have found that relaxation times are of the order of 10^{-11} s. The dependence on sample and on whether the carriers are electrons or holes will be discussed.

References

- Wixforth A, Schriha J, Wasserman M, Kothaus J P, Weimann G and Schlapp W *Phys.Rev.* 40 7874-87 (1989)
- Rampton V W, McEnaney K, Kozorezov A G, Carter P J A, Wilkinson C D W, Henini M and Hughes O H *Semicond. Sci. Technol.* 7 641-47 (1992)

POINT-CONTACT SPECTROSCOPY OF THE ELECTRON-PHONON INTERACTION IN RENi, (RE - RARE EARTHS)

M. Reiffers¹, E. Kačmarčíková² and T. Saloňová²

¹Institute of Experimental Physics, Watsonova 47, SK-04353 Košice,

²Faculty of Sciences, Safarik University, park Angelinum, SK-041 54 Košice, Slovakia

The comparison of the characteristic point-contact spectra of heterocontacts between $RENi_2$ ($RE = La, Ce, Pr, Nd, Sm, Dy, Y$) and Cu is presented. It is shown that the contribution of electron-phonon interaction to the electron-quasiparticle interaction function is qualitatively similar. This contribution have characteristic small maximum at ≈ 8 meV and a broad maximum at ≈ 18 meV which are connected with phonons of $RENi_2$. Last maximum and small maximum at 30 meV are connected with phonons of Cu. This observation is in an agreement with very similar lattice constants for all $RENi_2$, and it supports the manner of subtracting the phonon part of electrical resistivity of bulk samples. The main differences among characteristic properties of $RENi_2$ compounds originate from low energy part of the electron-quasiparticle interaction function.

Vibrational Density of States of Thin Films Measured by Inelastic Scattering of Synchrotron Radiation

R. Röhlberger¹, A. Bernhard¹, E. E. Alp², E. Burkel¹, A. I. Chumakov³, J. Metge³, R. Rüffer³, W. Sturhahn², and T. S. Toellner²

¹ *Universität Rostock, Fachbereich Physik, August-Bebel-Str. 55, 18055 Rostock, Germany*

² *Advanced Photon Source, Argonne National Laboratory, Argonne, Illinois 60439, USA*

³ *European Synchrotron Radiation Facility, BP 220, 38043 Grenoble Cedex, France*

Low dimensional structures like thin films very often exhibit properties that differ considerably from those of corresponding bulk materials. Special deposition techniques allow preparation of disordered and amorphous materials far away from thermal equilibrium that exhibit unique electronic, magnetic and vibrational properties. The latter are often influenced by the structure of the layer system, especially in the case of propagating excitations like phonons.

Due to its outstanding brilliance and large wave vector, synchrotron x-rays offer a unique possibility for inelastic spectroscopy on thin films. In the experiments discussed here, we employ the recently developed technique of inelastic nuclear resonant scattering [1-3] to the measurement of the vibrational density of states (VDOS) of thin films. In this method, Mössbauer isotopes like ⁵⁷Fe serve as energetic analyzers in the samples. The yield of nuclear decay products, e.g. fluorescence photons, as a function of energy gives a direct measure of the VDOS of the ⁵⁷Fe in the sample. In case of thin films, the signal can be significantly enhanced by making use of interference effects in grazing incidence geometry. The generation of standing waves in the film under study leads to a yield enhancement of 4 - 100, depending on the absorption in the film.

As a first application of this new method, we have studied phonon damping in thin films of ⁵⁷Fe in the thickness range of 10 - 30 nm. The damping is attributed to lifetime broadening of phonons in the confined geometry and could be phenomenologically described with the model of a damped harmonic oscillator.

In another experiment the VDOS of a 13 nm thick layer of sputtered FeBO₃ was determined, where the fraction of ⁵⁷Fe in Fe was only 2 % (natural abundance). The measurement was possible due to a 10-fold enhancement of the x-ray intensity in a Pd/FeBO₃/Pd waveguide structure. The amount of ⁵⁷Fe in that sample was equivalent to one monolayer. Thus, the high sensitivity of the method together with the inherent isotope specificity allows to investigate local vibrational properties of low dimensional systems, perhaps down to the atomic level. The experiments clearly demonstrate a great potential for inelastic spectroscopy of thin films at 3rd generation synchrotron radiation sources.

[1] M. Seto, Y. Yoda, S. Kikuta, X. W. Zhang, M. Ando, Phys. Rev. Lett. 74, 3828 (1995)

[2] W. Sturhahn, T.S. Toellner, E.E. Alp, X. Zhang, M. Ando, Y. Yoda, S. Kikuta, M. Seto, C. W. Kimball, and B. Dabrowski, Phys. Rev. Lett. 74, 3832 (1995)

[3] A. I. Chumakov, R. Rüffer, H. Grünsteudel, H. F. Grünsteudel, G. Grübel, J. Metge, O. Leupold, and H. A. Goodwin, Europhys. Lett. 30, 427 (1995)

[4] R. Röhlberger, W. Sturhahn, T. S. Toellner, P. Hession, K. W. Quast, M. Hu, J. Sutter, and E. E. Alp (to be published)

Phonon Measurement on Graphite and Hexagonal Boron Nitride Films on Ni(755)

E. Rokuta, A. Itoh, T. Tanaka, K. Yamashita, S. Otani^{*} and C. Oshima

Department of Applied Physics, Waseda University, 2-8-26 Nishiwaseda, Shinjuku, Tokyo

169-0051, Japan

^{*}National Institute for Research in Inorganic Material, 1-1 Namiki, Tukuba 305-0044,

Ibaraki, Japan

Recently, fundamental explorations in material science have been intrigued by new types of compounds including π electrons such as fullerenes, nanotubes, one sheet of graphite and hexagonal boron nitride (*h*-BN), and BNC compounds.

In a previous work [1], we have grown epitaxial monolayer films of *h*-BN on Ni, Pd and Pt(111), and have measured the phonon dispersion of the films by means of high resolution electron energy loss spectroscopy (HREELS); the experimental dispersion curves indicate the peculiar features of the vibrational frequencies of the *h*-BN films on Ni(111).

In this work, we have tried to grow monolayer nano-ribbons of graphite and *h*-BN. The substrate used in this experiment is a clean Ni(755) surface, which consists of narrow terraces lengthening to the <110> direction: the width of the (111) terrace is about 1.3 nm. Hence, we tried to form the nano-ribbons of graphite and *h*-BN and to detect the edge phonons, of which vibrational amplitudes are localized at the nano-ribbon edge.

The experiment concerning *h*-BN films on the vicinal surface is in progress. After a 100 L exposure in borazine gas, almost stoichiometric boron and nitrogen were adsorbed on the surface at about 450 °C, which were clarified by HREELS and Auger electron spectroscopy (AES). The measured HREEL spectrum is quite different from ones measured on the (111) surfaces. Several large loss peaks located at 90-100 meV, which are assigned to be the optical phonons with the displacements perpendicular to basal planes. In 170-190 meV, the broad peak consisting of plural peaks was detected. Although this peculiar spectrum does not evidently exhibit the formation of the nano-ribbons at present, the phonon dispersion measurement will clarify the structure and properties of this new thin films. Combining LEED observation and AES measurement with HREELS data, we discuss the growth process of the nano-ribbon, the atomic structure and the phonon dispersion.

[1] E. Rokuta, Y. Hasegawa, K. Suzuki, C. Oshima and A. Nagashima, PRL 79 (1997) 4609.

Phonons in Hexagonal Boron Nitride Films on Transition Metal Surfaces and
Analysis of Dispersion Curves based on Lattice Dynamics

E. Rokuta and C. Oshima

Department of Applied Physics, Waseda University, 2-8-26 Nishiwaseda, Shinjuku, Tokyo
169-0051, Japan

In recent years, much attention has been devoted to hexagonal boron nitride (*h*-BN). *h*-BN is a typical layered material with strong anisotropic bonds likewise graphite. We have formed epitaxial monolayer *h*-BN films on Ni, Pd and Pt (111), and measured phonon dispersion of the monolayer films by means of high resolution electron energy loss spectroscopy (HREELS) [1]. The data measured on the three surfaces clarified some qualitative information concerning the properties and structures of the films, which are summarized as follows. (1) While the energy of the transverse optical phonon with out-of-basal-plane polarization is lower on Ni(111) than the energy of the bulk counterpart, those on both Pd and Pt (111) are agreement with the bulk one. (2) The energies of the transverse optical phonon with in-plane polarization are almost same or slightly higher, compared to the corresponding bulk ones. On the contrary, all the observed longitudinal optical (LO) phonons have the lower energies than the bulk LO phonon due to weaker macroscopic electric fields produced by the polarization of the constituent ions in the films. (3) The measured dispersion curves of *h*-BN/Ni(111) suggest that the *h*-BN films form a rumpled structure.

In order to obtain some quantitative information, we have tried to reproduce the measured curves by calculations based on lattice dynamics. Although sophisticated models like a shell model were generally required to reproduce the phonon dispersion in ionic *h*-BN, force constant model was applied in the first step, because no information of parameters were available. For the sake of the simple structure of a *h*-BN film, the eigen problems that offer the phonon dispersion are solved analytically at high symmetry point of Γ and K in 2 dimensional Brillouin zone. Hence, the force constants should have been determined almost uniquely by solving a linear set of equations constructed with the measured energies. Nevertheless, there were discrepancies between the calculated dispersion and the measured one, which suggested there were some limits to the applied force constant model which successfully had reproduced phonon dispersion in graphite films [2]. In our talk, we will show the improved curve fitting based on the shell model, and will discuss about the results.

[1] E. Rokuta, Y. Hasegawa, K. Suzuki, C. Oshima and A. Nagashima, PRL 79 (1997) 4609.

[2] for example, T. Aizawa, R. Souda, Y. Ishizawa, H. Hirano, T. Yamada, K. Tanaka and C. Oshima, Surf. Sci. 237 (1990) 194.

EXCITON-PHOON SCATTERING EFFECTS
ON THE COHERENT CONTROL OF
EXCITON DECAY

S.M. Sadeghi and J. Meyer

The University of British Columbia,
Department of Physics and Astronomy, 6224 Agricultural
Road,

Vancouver, B.C., Canada V6T 1Z1

We theoretically study the role of exciton-phonon scattering in the coherent control of near band-gap exciton (E1-HH1) emission spectra in quantum wells. The coherent control is caused by tuning two intense infrared fields to become near resonant with various transitions between three sets of exciton states (E1-HH1, E2-HH1, and E3-HH1) associated with electrons in three conduction subbands (E1, E2, and E3) and holes in the valence band (HH1), forming an atomic-like Ξ , V, or Λ system. We characterize these systems in terms of the scattering processes between the coupled excitons and phonons and show how they determine the coupling mechanisms. It is shown that this provides control over the decay of E1-HH1 excitons via adjustment of one- or two-photon coupling of the coupled excitons, giving rise to drastically different near-band-gap emission spectra. These results are then discussed in terms of the exciton-phonon scattering rate effects on the type of the quantum interferences involved in these spectra.

HIGH-RESOLUTION BRILLOUIN SCATTERING OBSERVATION OF FERROELASTIC SOFT PHONON, USING SPHERICAL FABRY-PÉROT INTERFEROMETER AND COMPUTER CONTROLLED SPECTRA ACCUMULATION

Mizuho Sanada* and Toshirou Yagi**

*Department of Electrical Engineering, Kyushu Kyoritsu University,
Kitakyushu 807-8585, Japan

**Research Institute for Electronic Science, Hokkaido University,
Sapporo 060-0812, Japan

A high-resolution Brillouin scattering system has been developed for the purpose of observing and analysing spectral shape of low frequency (~100MHz) phonon. A spherical Fabry-Pérot interferometer which has a sufficient resolution of about 10^3 is utilized. However, with such a high-resolution spectrometer, even the frequency of light from a longitudinal single mode laser is not stable enough during a long period of time required for obtaining spectrum. In order to avoid the influence of this instability in light source, we developed a computer controlled procedure of estimating the amount of frequency deviation during each sweep of spectrometer, rejecting spectra assessed not reliable, aligning spectra with positions of Rayleigh lines, then accumulating.

The soft acoustic mode of ferroelastic crystal $KD_3(SeO_3)_2$ has been observed by applying the present system. The Brillouin spectra are well explained in terms of damped harmonic-oscillator. The temperature dependence of the damping constant shows no anomalies in contrast with that of the frequency.

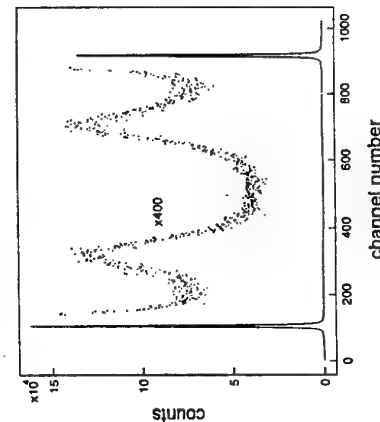


Figure 1 An example of spectrum observed with the present high-resolution Brillouin scattering system using a spherical Fabry-Pérot interferometer which has a free spectral range of 2.0GHz. The full width at half maximum of obtained Rayleigh line is no more than 16MHz. The result of numerical analysis of this spectrum shows the Brillouin shift of 560MHz and the damping constant of 270MHz, which corresponds to the width of Brillouin line.

DETECTION OF NONEQUILIBRIUM PHONONS BY THE EXCITON LUMINESCENCE IN CdTe/CdMnTe QUANTUM WELLS

A.V.Scherbakov, A.V.Akimov, and V.P.Kochereshko

A.F.Ioffe Physical-Technical Institute, Russian Academy of Sciences, 194021 St.Petersburg, Russia
D.R.Yakovlev, W.Ossau and G.Landwehr

Physikalisches Institut der Universität Würzburg, 97074 Würzburg, Germany

T.Wojtowicz, G.Karczewski and J.Kossut

Polish Academy of Sciences, Institute of Physics, 02-668 Warszawa, Poland

We present results of the first experiments on the detection of subterahertz acoustic phonons by means of luminescence from CdTe quantum well (QW) surrounded by semimagnetic (Cd,Mn)Te barriers. The idea of the experiments is to elevate the temperature of the Mn-ion system by nonequilibrium phonons and thus to decrease the giant Zeeman splitting of the exciton states.

The studied structure is grown by molecular beam epitaxy on semi-insulating 0.38 mm thick GaAs substrate and contains four CdTe QWs of widths 9.0 nm, 4.0 nm, 1.8 nm and 1.2 nm. The QWs are separated by 50 nm $Cd_{0.6}Mn_{0.4}Te$ barriers. A 10-nm constant film evaporated on the side of the GaAs substrate was heated by current pulses to act as a phonon generator. Nonequilibrium phonons were injected into the GaAs substrate which played a role of a filter for high-energy (> 1 meV) phonons. The phonons that do propagate in the GaAs reach the CdTe/(Cd,Mn)Te QW structure located in an external magnetic field and excited by cw 50 mW Ar-laser with a diameter of the focused spot on the sample 0.3 mm. As a result nonequilibrium phonons induce changes in the exciton luminescence.

The dynamic shift $\delta E_B(t)$ of the exciton line induced by nonequilibrium phonons was measured at two points having different distances, r , from the phonon generator. The leading edges of the phonon-induced luminescence signals showed a delay with increasing r in good agreement with the ballistic time of flight for LA and TA phonons in GaAs. Thus we conclude that our phonon detector is sensitive to low-energy (<1 meV) phonons that are known to be ballistic in GaAs. For some values of r , magnetic field, B , and phonon generator power, P , we also detect a diffusive microsecond trailing edge which reflects the arrival of high energy (>>1 meV) phonons. A surprising result is obtained for the trailing edges of the measured signals for low magnetic field, $B=2$ T, and high $P=160$ W/mm². The measured signal decays faster the further the detector is located from the phonon generator. This behavior is very unusual in experiments involving nonequilibrium phonons and is contrary to the results of earlier and numerous studies of phonon propagation. The explanation of such unusual behavior can be found in the analysis of the spin-phonon interaction in the semimagnetic material.

Our results lead to the conclusion that apparently both direct and indirect processes of phonon interaction with Mn ions govern the phonon-induced signal $\delta E_B(t)$. Direct processes are induced by the resonant phonons with $\hbar\omega = g_{mn} \mu_B B$ and for $B=3$ T $\hbar\omega=0.3$ meV, which corresponds to the phonons with ballistic phonon propagation in GaAs. Indirect processes are supposed to be associated with Orbach processes and are mediated by the spin clusters which interact with high-energy phonons. The proposed phonon detection technique has a potential for application as a subterahertz phonon spectrometer with a high resolution (<0.1 meV).

PROPOSED MODEL OF MIXED ELECTRON (HOLE)-PHONON SCATTERING IN THE INTERMEDIATE CONCENTRATION REGION, P.C. SHARMA, Department of Physics, Tuskegee University Tuskegee, AL 36088, USA

At the intermediate doping concentration, the electronic states are analyzed using inhomogeneity model, according to which the impurity states exist both in nonmetallic and metallic regions. By calculating the nonmetallic and metallic impurity concentrations in each doped sample, it is found that all the impurities are nonmetallic at low concentrations and all are metallic at high concentrations while at intermediate concentrations both nonmetallic and metallic impurity states coexist. Hence the new electron-phonon scattering model in the intermediate concentration has been proposed, for the first time, which is known as 'mixed electron-phonon scattering.

MEASURING SYSTEM FOR THE DETERMINATION OF NONLINEAR ELASTIC AND ELECTROMECHANICAL PROPERTIES IN SOLIDS

U. STRAUBE, H. BEIGE

Fachbereich Physik, Martin-Luther-Universität Halle-Wittenberg, Friedemann-Bach-Pl. 6, D-06108 Halle/Saale, Germany

ABSTRACT

The measurement equipment for the determination of nonlinear elastic and electromechanical coefficients [1] was improved. We apply time variable uniaxial stresses or electric fields to solid samples that are examined with pulsed ultrasound. A new broadband sampling oscilloscope (HP54750A) allows a higher accuracy and resolution of time measurements in the picosecond range. An arbitrary waveform generator produces the pulse bursts. This improves the jitter behaviour and the spectral purity of the signal produced by the transmitter stage. We have designed and built a new pulse amplifier based on a ceramic power triode circuit to drive the transducer. Automatic high accuracy measurements of velocity and attenuation are now possible from room temperature down to the temperature of liquid nitrogen. All relevant instruments of the temperature regulation and the ultrasound measurement block are connected via IEEE-buses. The computers for the temperature control, for the ultrasound measurement and for the final data processing are connected in a local network. Results found near ferroic phase transitions are presented.

[1] U. Straube, P. Grau, S. Fadeew, H. Beige, *acta physica slovaca*, 46, (1996), 727.

LOCALIZED EXCITATIONS IN DILUTED MAGNETIC $\text{Cd}_{1-x}\text{Mn}_x\text{Te/Cd}_{1-y}\text{Mn}_y\text{Te}$, $\text{ZnSe/Zn}_{1-y}\text{Mn}_y\text{Se}$ SEMICONDUCTOR SUPERLATTICES

Devki N. Talwar

Department of Physics, Indiana University of Pennsylvania
Indiana, PA 15705-1087, USA

Raman scattering and far-infrared spectroscopy are considered to be the well known primary tools for the investigation of vibrational properties of solids. In recent years, the ability of far-infrared reflectivity (FIR) [1] and Raman scattering [2] to probe confined phonons in diluted magnetic semiconductor (DMS) alloys and superlattices (SLs) have been documented. In the optical-phonon region, the Raman spectra of the $\text{Cd}_{1-x}\text{Mn}_x\text{Te/Cd}_{1-y}\text{Mn}_y\text{Te}$ SLs with superlattice axis along [001] show optical phonons 'confined' to the well or the barrier layer when the corresponding dispersion curves do not overlap, whereas 'propagating' optical phonons are observed when they do. In $\text{ZnSe/Zn}_{1-y}\text{Mn}_y\text{Se}$ SLs, the strain arising from lattice mismatch gives rise to shifts in the optical-phonon frequencies. The purpose of the present work is to investigate (i) the reflectivity spectra of CdTe/CdMnTe thick multiple heterostructures in the FIR range up to 250 cm^{-1} and (ii) to study the folded acoustic and optical phonons in [001] $\text{Cd}_{1-x}\text{Mn}_x\text{Te/Cd}_{1-y}\text{Mn}_y\text{Te}$ and [001] $\text{ZnSe/Zn}_{1-y}\text{Mn}_y\text{Se}$ SLs within a second-neighbor eleven parameter rigid-ion-model (RIM11). For CdTe , MnTe , ZnSe , and MnSe materials, the short-range forces in the RIM11 are optimized by using the neutron scattering and transformed Raman data of phonons and the elastic constant values. The long-range Coulombic forces are evaluated exactly by using an Ewald summation method. The influence of composition and disorder in ternary compounds $\text{Cd}_{1-y}\text{Mn}_y\text{Te}$ and $\text{Zn}_{1-y}\text{Mn}_y\text{Se}$ is described within a modified random-element iso-displacement model generalized to layered structures with arbitrary wavevectors and composition profiles. Theoretical results are compared and discussed with the existing FIR and Raman data. Due to the significant difference in the masses of Cd and Mn, the ternary $\text{Cd}_{1-x}\text{Mn}_x\text{Te}$ alloy exhibits a 'two-mode' behavior having two pairs of lines characteristic of zone center 'CdTe-like' and 'MnTe-like' LO-TO phonons. In contrast, the behavior of optical phonons in $\text{Zn}_{1-y}\text{Mn}_y\text{Se}$ exhibits a mixed-mode behavior intermediate between 'two-mode' and 'one-mode' - the LO phonons of ZnSe continuously evolves into that of MnSe (LO₁) while the TO phonon (TO₁) and one of the component of the Mn²⁺ impurity mode in ZnSe (LO₂) merge into the gap mode of Zn in the hypothetical zinc-blende 'MnSe'. The other Mn²⁺ impurity mode (TO₁) transforms into the TO phonon of 'MnSe'. In the $\text{CdTe/Cd}_{1-x}\text{Mn}_x\text{Te}$ and $\text{ZnSe/Zn}_{1-y}\text{Mn}_y\text{Se}$ SLs, we compare and discuss our results for the calculated interface modes, acoustical and optical folded phonons with the existing Raman data.

[1] S. Perkowitz *et al.* Physical Review B38, 5565 (1988).

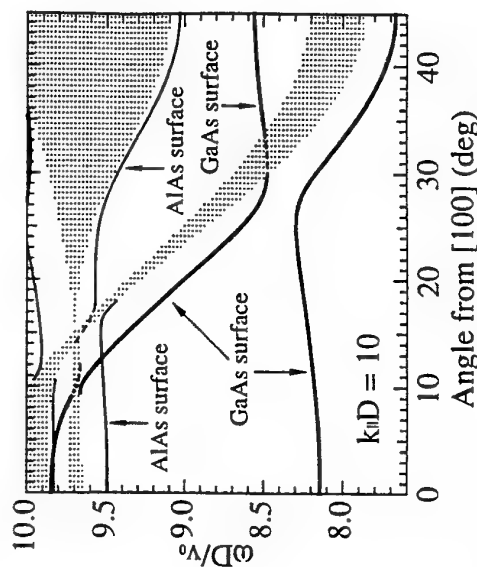
[2] R. W. G. Syme, D. J. Lockwood, M. M. Dion and J. J. Dubowski, Solid State Commun. 103, 239 (1997); E. K. Suh *et al.* Physical Review B36, 4316 (1987).

Surface phonons in one-dimensional periodic superlattices

Takashi Aono, Yukihiko Tanaka, and Shin-ichiro Tamura

Department of Applied Physics, Hokkaido University, Sapporo 060, Japan

We study theoretically the surface acoustic phonons propagating on semi-infinite, periodic superlattices consisting of anisotropic, elastic layers of cubic symmetry. We consider the cases where the surface is parallel (case A) and perpendicular (case B) to the layer interfaces. Case A: Conventional transfer-matrix method is employed to derive the dispersion relations of surface modes. We find the existence of surface localized modes inside the frequency gap of bulk phonon as well as below bulk band. Pseudosurface branches are also found inside the bulk frequency band. A remarkable feature is the existence of a pseudosurface branch which links a surface phonon branch below the bulk band to a branch inside the frequency gap (see the figure shown below). Case B: The plane-wave expansion method is employed to derive the dispersion relations. The surface phonon branches exist only below the bulk band. The frequency gap and the folding effect of surface phonons are found at the boundary of the mini-Brillouin zone. Pseudosurface branches are also found inside the bulk frequency band. Numerical examples are given for AlAs/GaAs superlattices with AlAs surface or GaAs surface, and the anisotropy of the dispersion relations is investigated. Focusing characteristics of ballistically propagating surface and pseudosurface phonons are also studied.



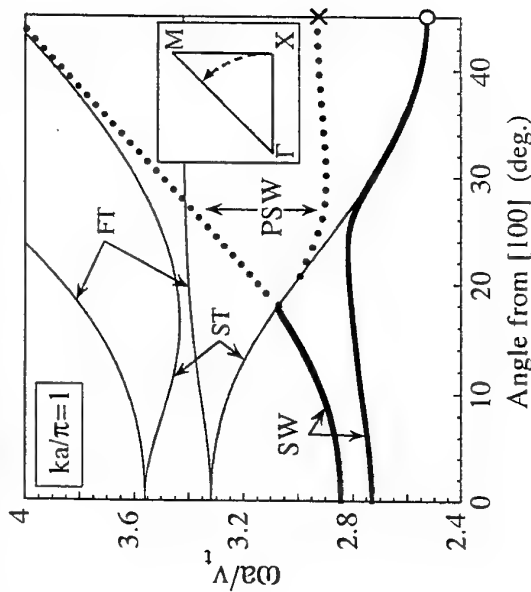
Angular dependences of the surface and pseudosurface phonon frequencies in the periodic superlattice consisting of AlAs and GaAs with the same layer thicknesses. Solid (dashed) lines are the surface (pseudo-surface) mode branches. Dotted regions are the bulk bands. $k_{||}D=10$ (D : periodicity) and $v_s=3.33 \times 10^5$ cm/s.

Two-dimensional phononic crystals: surface acoustic waves

Yukihiro Tanaka and Shin-ichiro Tamura

Department of Applied Physics, Hokkaido University, Sapporo 060, Japan

Surface localized modes of acoustic waves in two-dimensional periodic elastic structures, or two-dimensional phononic crystals, are studied theoretically by taking account of the elastic anisotropy of constituent materials. The surface assumed is perpendicular to the axis of the periodic arrays of cylinders embedded in a background material. The dispersion relations of surface mode are calculated for circular cylinders of AIA's which form a square lattice in a GaAs matrix. The folding and anisotropy of surface mode branches as well as the existence of several pseudosurface wave (PSW) branches are found. The figure shown below exhibits the angular dependence of the dispersion curves for $ka/\pi=1$ (k : wave number, a : lattice constant), i.e., along the dashed line in the inset. The lower bold line is the generalized Rayleigh wave similar to the one in the bulk solid and the upper bold line is the folded surface wave branch which continues into the bulk band as PSW's plotted by dashed lines. We also present the stop band distributions of both the surface and bulk modes, which would be relevant to compare the ultrasound imaging experiment.



Angular dependences of the surface wave (SW) and pseudosurface wave (PSW) frequencies. At 45° true surface wave appears in the PSW branch as indicated by cross. Thin solid lines are bulk slow-transverse (ST) and fast-transverse (FT) waves travelling parallel to the surface.

MAGNETOACOUSTIC DETERMINATION OF DEFORMATION POTENTIAL

A. V. Tkach

Institute for Metal Physics, Ural Department of the Russian Academy of Sciences,
18, Kovalevskaya st., Ekaterinburg 620219, Russia

Up to now, geometric characteristics of the Fermi Surfaces (FS) have been investigated quite well for a number of metals. There is plenty of data also on the electron velocities over the FSs. As to another local property of a state -- the deformation potential (DP), it describes variations of the electron energy due to a lattice deformation -- it remains insufficiently studied.

A possible approach to this problem consists in using a relationship between the averaged DP and the area change of effective orbit under a deformation in a quantizing magnetic field. Unfortunately, these later data are available with a restricted accuracy of 10–15% and few effective orbits have been investigated only. The reason is that a combination of complicated quantum oscillation techniques (for example, oscillatory magnetostriction and torque) has to be used in the measurements. This report demonstrates some opportunities of a more simple non-oscillatory method. The level of ultrasonic attenuation α in a classically high longitudinal magnetic field $H||q$ (q is the ultrasound wave vector) can be shown to give the same information on the deformation potential, averaged over an effective orbit. For the case of shear deformation of Mo and W, a comparison is made of the DP-values over the ρ -orbits, evaluated : a) on the basis of quantum oscillation data [1,2] in conjunction with formula of Ref.[3] (which is expected to be approximately correct in this case), and b) from the α measurements with shear waves propagating along $q||H||[001]$. Full consistency of results is revealed, but the ultrasonic data have an essential advantage of a better accuracy. Moreover, in the case of longitudinal ultrasound propagation, this method gives us an opportunity to evaluate, for the first time, corresponding DP-value over the τ -orbit on the FS of W.

This work was supported in part by the Russian Foundation for Basic Research.

REFERENCES

1. M.J.G. Lee, J.M. Perz, D.J. Stanley *Phys.Rev.Lett.* **37**, (1976), 537.
2. J.M. Perz, K.P. Des Rues, M.J.G. Lee, D.K. Mak, *Phys.Rev. B* **19**, (1979), 4901.
3. N.G. Bebenin, N.S. Yartseva, *Sol.St.Comm.* **73**, (1990), 579.

Phonon Hole Burning at Low Temperature
 Fujio TSURUOKA
 Department of Physics, Kurume University
 Asahimachi 67, Kurume
 Fukuoka 830-0011, JAPAN

We have observed phonon hole burning phenomena, in which piezoelectric powder resonantly absorb oscillating electric field. Its fundamental idea originates from the hole burning phenomenon which is related with absorption of oscillating electromagnetic field or light.

Piezoelectric particle are known to oscillate resonantly and their resonant frequencies are determined by the particles dimension, the crystallographic angle and the oscillation mode. Experimental specimen are prepared by sieving mechanically crushed particles. Large number of particles with different figure and size, as a whole, have widely and moderately spread resonance frequency spectrum. In this spectrum, holes are written by applying large amplitude pulsed rf electric field. We call these results as phonon hole burning.

The mechanism of hole formation has been studied. So far, our experimental results show that the holes are composed of modification in the oscillation characteristics of particles whose resonant frequencies correspond to the hole in the spectrum. The depth of holes is described with the absolute amplitude of applied pulses.

At this time, the mechanism of hole formation is studied by observation of holes at liquid nitrogen temperature and by comparison of the results with those obtained at room temperature. The amplitude of particle oscillation introduced is concerned with damping constant of oscillation, which depends upon the temperature. And plastic deformation of particle, which we propose as the hole formation mechanism, may be influenced by the temperature.

Non-linear excitations in one-dimensional electron-phonon systems

Loredana Valente
 Dipartimento di Scienze Fisiche, Università di Napoli
 Mostra D'Oltremare Pad.19, 80125 Napoli, Italia
 e-mail: valente@na.infn.it

Electrons and phonons interacting on a lattice can be described by the Su-Schrieffer-Heeger model $H = -\sum_{n,\sigma} t_{n+1,n} (c_{n+1,\sigma}^\dagger c_{n,\sigma} + h.c.) + \sum_n \frac{1}{2} \frac{p_n^2}{M} + \frac{K}{2} (u_{n+1} - u_n)^2$, with $t_{n+1,n} = t_0 - \alpha(u_{n+1} - u_n)$. It exhibits the *Peter's instability*: a lattice distortion of wave vector $2k_F$ opens up a gap in the electronic spectrum at the Fermi surface. The fundamental issue is the persistence (or not) of the broken symmetry depending on e-ph coupling strength, phonon frequency and commensurability. The continuum theory provides an effective description of the long-distance behaviour of the model, assuming that the fields are slowly varying on the scale of the lattice spacing. There are two different cases: *incommensurate* and *commensurate*, depending on the number of electrons and sites. Some insight can be gained in limiting cases. In the antiadiabatic limit, the effective Lagrangian is given by the Gross-Neveu model, $L = \sum_{s=1}^N \bar{\psi}^s(x) (\gamma_\mu \frac{\partial}{\partial x_\mu}) \psi^s(x) + \frac{1}{2} g_{GN}^2 (\sum_{s=1}^N \bar{\psi}^s(x) \psi^s(x))^2$, having a $SU(N)$ and a chiral symmetry. The dimerized phase is the one with $\langle \bar{\psi}^s \psi^s \rangle \neq 0$.

Role of defects in inducing phase transitions. If the creation energy of defects is less than zero, the broken symmetry can be restored: an example is provided by the ϕ^4 theory.

Commensurability effects. The higher order commensurate case can be studied by using a coherent state approach. Quantum fluctuations are described through the phase $\alpha_p = \frac{2\pi p}{N}$, defining the location of the center of the defect, and the corresponding state $|p\rangle = S(p)|0\rangle$, with $|0\rangle$ the vacuum state for both phonons and electrons, $S(p)$ quantum operator creating an adiabatic configuration with phase α_p . Nucleation of pairs of defects occurs when the creation energy of the defect is less than zero. The nature of the new *undistorted* phase arising from effects of quantum fluctuations can be inferred from Lang-Firsov like methods. Anyway, the continuum approximation can be useful but there are some discrepancies with the discrete system, due to different excitations in the systems. Undoubtedly the incommensurate case presents a higher sensitivity to quantum fluctuations.

QUANTUM DECAY OF SELF-LOCALIZED MODES IN ANHARMONIC SYSTEMS

M. Wagner and A. Sauerzapf

Institut für Theoretische Physik, Universität Stuttgart,
Pfaffenwaldring 57, 70550 Stuttgart, Germany

Phone: 0049/711/685 5204 (M. Wagner)

0049/711/685 5211 (A. Sauerzapf)

Fax: 0049/711/685 5098

E-Mail: wagner@theo3.physik.uni-stuttgart.de

achim@theo3.physik.uni-stuttgart.de

Abstract

In a previous paper [1] it has been shown that self-localized (solitary) modes (SLS) in anharmonic systems may be described by means of a unitary transformation such that the solitary mode is incorporated in the dynamics of a single anharmonic oscillator (SAO), which is classically decoupled from the other degrees of freedom. In a quantum description the SLS is to be viewed as a kind of a "coherent state", which however is subject to quantum decay. This decay process within the dynamics of the SAO is well-described by another unitary transformation and will be discussed in our presentation. Specifically, we will exemplify our procedure by applying it to the Fermi-Pasta-Ulam chain. We finally will contrast the features of the quantum decay with that due to residual decay channels of classical nature.

[1] M. Wagner, A. Sauerzapf, *Physica D* (1998), in print

ELASTIC PROPERTIES OF TiN/Zn SUPERLATTICES: A BRILLOUIN SCATTERING STUDY

A. Yoshihara

Faculty of Science and Engineering, Ishinomaki-Senshu University,
Ishinomaki, Miyagi, Japan

We-Hyo Soe and R. Yamamoto

Institute of Industrial Science, University of Tokyo,
Roppongi, Minato-ku, Tokyo, Japan

We have investigated the Rayleigh surface wave (RSW) velocities of TiN/Zn superlattices deposited on MgO substrates for several superlattice periods ranging from 30 nm to 0.6 nm using Brillouin scattering at room temperature. Brillouin spectra were excited by the *p*-polarized 532 nm line from a solid state laser with an output power of 150 mW in a single cavity mode, and backscattered light was analyzed using a (3+3)-pass tandem Fabry-Perot interferometer. Since we found that the superlattices give extremely weak RSW scattering intensities, we deposited Al layer of about 20 nm in thickness on the top surface of each superlattices to enhance the RSW scattering.

Figure 1 shows an example of RSW spectrum, and Fig. 2 gives the RSW velocity as a function of the superlattice period. The Al layers introduced two effects on the RSW spectra: the RSW velocity slightly increases (about 3 % in our superlattices) due to the stiffening effect, and a broad quasi-elastic peak appears as rather higher background in Fig. 1. The RSW velocity is almost independent of the superlattice period (-4.4 ± 0.1 km/s) within the experimental accuracy. The present results are very similar to the ones already reported on the Al-coated NbN/AlN (R. Bhadra *et al.* : Appl. Phys. Lett. 54 (1989) 1409) and TiN/(V_xNb_{1-x})N (P. B. Mirkarimi *et al.* : J. Appl. Phys. 71 (1992) 4955) superlattices using Brillouin scattering.

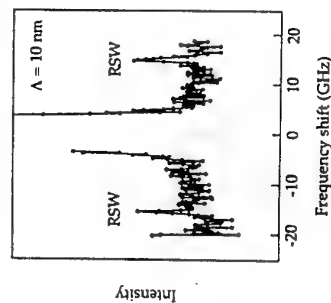


Fig. 1 An example of RSW spectrum.

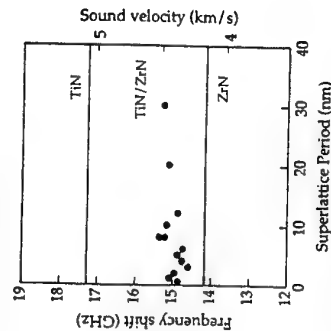


Fig. 2 The sound velocity as a function of the superlattice period.

INTERACTION OF NON-EQUILIBRIUM ELECTRONS WITH PHONONS IN BULK GaN AND GaN/AlGaN QUANTUM WELLS

N.A.Zakhleniuk, C.R.Bennett, B.K.Ridley, and M.Babiker

Department of Physics, University of Essex, Colchester CO4 3SQ, UK

Wide-gap semiconductors such as GaN have become increasingly important because of their potential for use in optoelectronic devices operating in the blue to ultraviolet wavelength range, as well as in electronic devices operating at high temperatures and extremely large electric fields. Several GaN-based heterostructures have been grown recently and, with improving techniques, good quality GaN/GaN quantum wells will, no doubt, be produced in which the scattering of the electrons by the lattice vibrations is the dominant mechanism. This prospect makes the study of electron-phonon interactions in bulk GaN and GaN-based quantum wells of considerable importance.

Previous investigations of electron-phonon phenomena in GaN were performed mostly for the equilibrium state of the electron system. There are also some purely numerical studies employing Monte Carlo techniques to model the non-equilibrium processes in the electron-phonon system of GaN. Such studies by their nature, do not provide insight into the underlying basic physics.

In this report we present the first theoretical analytical study of transport phenomena in bulk GaN as well as in GaN-based quantum wells under non-equilibrium conditions. Our recent investigation of the electric field dependence of carrier mobility in low-dimensional structures has shown a non-monotonous behaviour and the dependence is characterised by a change in gradient when the scattering by the deformation acoustic phonons is more important than that by the piezoelectric phonons. An important feature of the III-nitride materials is their very large optical phonon energy which is about 90 meV in GaN. This is the main reason behind the fact that the interaction of electrons with deformation and piezoelectric phonons controls transport phenomena within wide ranges of electric fields and lattice temperatures. We have shown that at relatively small electric fields the electron mobility is controlled by the piezoelectric phonons, while for higher electric fields the mobility is controlled by the deformation acoustic phonons. A more dramatic change in the electric field dependence of the mobility takes place at very high electric fields when the optical phonons dominate.

In our analysis the electron gas is assumed to be non-degenerate, but this condition is not consistent with the electron temperature approximation. On going beyond the electron temperature approximation, we have obtained a set of new distribution functions for non-equilibrium electrons in GaN-based quantum wells with many electron subbands included. Our theory predicts novel non-linear regimes of transport phenomena in quantum wells due to electron-phonon interaction which will be presented and discussed.

PosC1

THE INFLUENCE OF HYDROGEN CHARGING ON THE GLASSY LOW TEMPERATURE PROPERTIES OF A POLYCRYSTALLINE NBTI-ALLOY

S. ABENS¹, A. GLADUN, M. JÄCKEL, D. LIPP and S. SAHLING
Institut für Tieftemperaturphysik, Technische Universität Dresden, D-01062 Dresden, Germany

We measured the thermal conductivity, specific heat and heat release of polycrystalline $Nb_{0.7}Ti_{0.3}$ at low temperatures. Further we charged our samples with hydrogen and investigated the influence of the H-charging on these thermal properties for different charging concentrations.

In pure NbTi, below one Kelvin, all of these thermal properties show amorphous low temperature behaviour, predicted by the standard tunneling model [1,2]. The thermal conductivity follows the T^2 -dependence, the specific heat is proportional to the temperature T and the heat release increases with $T_1^2 - T_0^2$ (T_0 : final temperature after cooling down from the initial equilibrium temperature T_1) and varies proportional to the inverse of time (t^{-1}) (e.g. [3]). From the measured heat release and thermal conductivity we obtained the typical parameters of the standard tunneling model: the distribution parameter $\bar{P} = 5 \cdot 10^{44} J^{-1}m^{-3}$ and the coupling constant $\gamma_0 = 1.2 eV$. These values are in good agreement with measurements of the internal friction and speed of sound in a NbTi-alloy with similar composition, made by Van Cleve et al. [4].

By charging our samples with hydrogen, the heat release increases nearly proportional with the hydrogen concentration. The distribution parameter obtained from heat release measurements reaches, for example for $NbTi_{10\%}$ a value of $5 \cdot 10^{45} J^{-1}m^{-3}$, ten times larger as in pure NbTi. Similar behaviour is also visible in the measured specific heat, but in comparison to the heat release the specific heat is enhanced only by a factor of two between pure NbTi and $NbTi_{10\%}$.

Considering this increase of the distribution parameter \bar{P} and the prediction of the tunneling model for the thermal conductivity ($\lambda \propto (\bar{P}\gamma_0^2)^{-1/2} T^2$), we would expect a remarkable decrease of the thermal conductivity of NbTi_{10%} below one Kelvin. But this behaviour did not occur in our measurements. Moreover it increases by a factor of four.

A possible explanation for these features can be found in the assumption of two different types of tunneling system. In pure NbTi the tunneling system can be described by diffusionless phase transition ($\omega - \beta$ -transition) as discussed in [4]. By charging with hydrogen these tunneling systems are suppressed and a new kind of tunneling system is built by the hydrogen, characterized in particular by another value of the coupling constant. Taking the measurement of the heat release and the thermal conductivity of NbTi_{10%} into account, we obtained for the coupling constant $\gamma_1 = 0.2 eV$.

[1] P.W. Anderson, B. Halperin and S. Varma, Philos. Mag. 50, 1 (1972).

[2] W.A. Phillips, J. Low Temp. Phys. 7, 351 (1972).

[3] O.A. Parshin, S. Sahling, Phys. Rev. B 47, 5677 (1993).

[4] J.E. Van Cleve, A.K. Raychaudhuri, R.O. Pohl, Z. Phys. B 93, 479 (1994).

¹supported by Deutsche Forschungsgemeinschaft, Sa 549 / 1-3

PosC2

BACK TUNNELING AND PHONON EXCHANGE EFFECTS IN SUPERCONDUCTING TUNNEL JUNCTION X-RAY DETECTORS

V.A. Andrianov, P.N. Dmitriev*, V.P. Koshelets*, M.G. Kozin, I.L. Romashkina, S.A. Sergeev, V.S. Shpinel
 Institute of Nuclear Physics, Lomonosov Moscow State Univ., 119899 Moscow, Russia
 *Institute of Radio Engineering and Electronics RAS, 103907 Moscow, Russia

Superconducting tunnel junctions (STJs) are promising devices for X-ray and lower-energy photon detection with high energy resolution and low energy threshold. One of the features of high quality STJs is the possibility for nonequilibrium quasiparticle to tunnel from one electrode to another one many times (back or multiple tunneling). It leads to amplification of the output signal (Gray effect) but at the same time worsens the energy resolution [1].

In the present work effects of back tunneling were studied for STJs of a simple structure Nb/Al/AlOx/Nb (240/8/2/120 nm) with the areas of the tunnel barrier 400, 1800 and 6400 μm^2 . The normal state resistance of the barrier was $2 \cdot 10^{-5} \Omega cm^2$.

Pulse height spectra from STJs irradiated by ⁵⁵Mn X-rays were measured at $T=1.4 K$ depending on the bias voltage and applied magnetic field. The signals from the counter electrode were approximately 5 times more weak than signals from the base one due to more short lifetime of quasiparticles.

Effects of back tunneling were observed in the temporal shape of the pulses. Output signals from the charge sensitive preamplifier were fitted by the expression

$$Q(t) = \frac{Q}{1+p} \left[(1 - \exp(-\gamma_1 t)) + p(1 - \exp(-\gamma_2 t)) \right] \quad (1)$$

where γ_1^{-1} and γ_2^{-1} are effective lifetimes of quasiparticles in electrodes 1 and 2 respectively, Q is the collected charge. Effect of back tunneling is described by the second term in (1). Expression (1) is an approximate solution of linear differential equations of Rothwarf and Taylor under conditions γ_1, γ_2 and $|\gamma_1 - \gamma_2| \gg \gamma_1, \gamma_2$, with γ_1 and γ_2 being effective tunneling times. The contribution of back tunneling is estimated as $p \approx \gamma_2 / \gamma_1$.

The results of fitting were parameters γ_1, γ_2 and p for the counter electrode, pulses from which were the most sensitive to back tunneling. Values of p proved to be several times higher than the above estimation. The discrepancy increases with increasing size of the junction. This means that the excitation resulting from X-ray absorption in one electrode is redistributed between both electrodes. The most probable candidate for this process is the exchange of 2 Δ -phonons. Usually it is accepted that due to the small recombination rate of quasiparticles the number of 2 Δ -phonons is small and their exchange between the electrodes has no noticeable effect on the STJ-performance. However simple estimations show that the density of the excess quasiparticles is considerably higher than the density of thermal excitations. Therefore the recombination rate is increased. Correspondingly the number of 2 Δ -phonons and their exchange between the STJ electrodes is increased also.

The role of 2 Δ -phonon exchange in STJ-performance depends upon the conditions of the heat exchange between STJ and the substrate and on the STJ design. It seems that the dependence of the effective lifetime on the junction size may be attributed to this effect. It is also possible that the pulses of anomalous polarity were not observed in a number of works due to exchange of the 2 Δ -phonons.

[1], N.E. Booth and D.J. Goldie, Supercond. Sci. Technol. 9 (1996) 493.

AN AD HOC DYNAMICAL MODEL STUDY OF LATTICE DYNAMICS OF METALLIC GLASS $\text{Mg}_{70}\text{Zn}_{30}$

J. R. Campanha

Departamento de Física, UNESP, Rio Claro, C.P. 178

CEP 13500-230 Rio Claro, SP, Brasil

M. M. Shukla

Departamento de Física, UNESP, Bauru, C.P. 473

CEP 1700-360, Bauru, SP, Brasil

About a decade back Bhatia and Singh [1] had developed an ad hoc dynamical model of metallic glass by considering interionic interactions effective between nearest neighbours. We [2] have very recently modified this model by including the interionic interactions out to second neighbours also rectifying a mistake in the electron-ion dynamical matrix and applied successfully to the study of lattice dynamics of metallic glass $\text{Ca}_{70}\text{Mg}_{30}$. In the present work we have applied our scheme to metallic glass $\text{Mg}_{70}\text{Zn}_{30}$ and have obtained good agreement between the theoretical and the experimental phonon dispersion relations for the longitudinal branch.

[1] A. B. Bhatia and N. Singh, Phys. Rev. B **31**, 4751 (1985)

[2] M. M. Shukla and J. R. Campanha, 9th International Conference on Rapidly Quenched and Metastable Materials. August 25-30, 1996. Bratislava, Slovakia. J. Materials Science and Engineering A. Supplement **111** (1997)

LOW FREQUENCY ACOUSTIC PROPERTIES OF NEUTRON-IRRADIATED QUARTZ

J. Classen,¹ I. Rohr,¹ C. Enss,¹ S. Hunklinger,¹ and C. Laermans²

¹ Institut für Angewandte Physik, Universität Heidelberg
Albert Ueberle-Str. 3-5, 69120 Heidelberg, Germany

² Department of Physics, Katholieke Universiteit Leuven
Celestijnenlaan 200D, B-3001 Leuven, Belgium

Neutron-irradiated quartz is an interesting model system to investigate the density, the dynamics, and perhaps the nature of tunneling defects in tetrahedrally coordinated solids like vitreous silica. By variation of the irradiation dose it is possible to study the transition from an almost perfectly crystalline to an entirely amorphous state. Over the past years the elastic properties of neutron-irradiated quartz has been investigated in detail above 0.3 K by means of ultrasonic experiments. We have carried out low frequency acoustic (vibrating reed) measurements on samples with six different neutron doses up to $2 \times 10^{20} \text{ n/cm}^2$ in the wide temperature range from 7 mK to 300 K. In all samples a temperature dependence of the sound velocity and of the internal friction indicative of the presence of tunneling states with a broad distribution of energies and relaxation times is found. From both measured quantities the "macroscopic coupling constant" $C = \bar{P}\gamma^2/\rho v^2$ could be derived where \bar{P} is the density of states of tunneling systems (assumed to be constant), γ the coupling constant between phonons and tunneling systems ("deformation potential"), ρ the mass density, and v the sound velocity. The parameter C increases approximately linearly with increasing irradiation dose for small doses and saturates for high doses. However, even for the highest irradiation dose, where the sample is completely amorphous, C remains smaller than in vitreous silica by almost a factor of two. The monotonic dose dependence of C observed in our experiments is particularly interesting in comparison with recent ultrasonic measurements where for a certain crystal orientation a non-monotonic dependence of C on the neutron dose has been observed [V. Keppens and C. Laermans, Nucl. Instr. and Meth. in Phys. Res. B **91**, 346 (1994)]. Possible implications of these results on the microscopic nature of the tunneling states in SiO_2 are discussed.

ELASTIC PROPERTIES OF NEON AND ARGON FILMS

J. Classen, M. Heitz, J. Meier, and S. Hunklinger

Institut für Angewandte Physik, Universität Heidelberg
Albert Ueberle-Str. 3-5, 69120 Heidelberg, Germany

When noble gases are quench-condensed onto a cold substrate they form solid films with a high degree of disorder. Due to the simple interatomic interaction they are a promising model system to learn more about tunneling defects which are known to occur both in polycrystalline monatomic films and in amorphous mixtures of two noble gases. We have used surface acoustic waves at frequencies 100 - 1000 MHz to investigate the elastic properties of neon and argon films of thickness ~ 100 nm at temperatures from the Millikelvin range up to the sublimation threshold. First results on the number and the dynamics of tunneling states at different annealing stages of the films are reported.

ULTRASONIC VELOCITY CHANGES IN BULK NEUTRON-DISORDERED SILICON

M. Coeck^{1,2}, C. Laermans¹ and E. Peeters^{1,*}¹ : Katholieke Universiteit Leuven, Dept. of Physics, Celestijnenlaan 200 D, B-3001 Heverlee, Belgium² : SCK•CEN, Dept. BR2, Boeretang 200, B-2400 Mol, Belgium

During the past few decades several experiments have shown that glasses exhibit universal properties which differ from those in crystals. Below a few Kelvin this anomalous behavior can be very well described by the tunneling model [1], postulating the presence of low-energy excitations called tunneling states (TS). These are atoms or groups of atoms which can have two equilibrium positions and can therefore quantummechanically tunnel in a double asymmetric potential well. They have a wide distribution of energies and relaxation times and appear with an almost constant density of states. It was first believed that these TS could only occur in typical glass-forming amorphous solids having a low average coordination of the individual atoms. Also in partly disordered low-coordinated solids such as neutron-irradiated quartz, TS have been observed.

In order to explore the possibility of the presence of these states in topologically higher constrained disordered solids and to study their properties, we have performed measurements of the ultrasonic (MHz range) velocity changes $\Delta v/v$ in bulk neutron-irradiated silicon single crystals. The irradiation with fast ($E > 0.1$ MeV) neutrons up to doses of 1.7 and 3.2×10^{21} n/cm² is seen to induce amorphous regions into the silicon, leading to an amorphous volume fraction of 3.7 and 4.1 % respectively [2]. Using bulk single-crystalline silicon as a starting material excludes the influence of large voids and low density regions inherent to amorphous silicon films made by sputtering which were previously used for this kind of research [3].

Here we present the results obtained from measurements of $\Delta v/v$ as a function of temperature (0.3 - 30 K). Our measurements show a pronounced difference between the behavior of the irradiated and the unirradiated material. Furthermore, the irradiated material shows a remarkable similarity with the predictions of the tunneling model, putting in evidence the possibility of the introduction of TS in high coordinated materials. Measurements of $\Delta v/v$ performed for two different irradiation doses also show that the logarithmic increase observed at low temperatures becomes steeper for higher irradiation doses, indicating a higher density of states of TS for higher irradiation doses and thus for higher amorphous volume fractions. We also performed numerical fits on these data. The results will be discussed in the framework of the tunneling model and the soft potential model.

* : Now at SRON, P.O. Box 800, NL-9700 AV Groningen, The Netherlands

[1] P. W. Anderson, B. I. Halperin and C. M. Varma, *Phil. Mag.* 25 (1972) 1; W. A. Phillips, *J. Low Temp. Physics* 7 (1972) 351.[2] M. Coeck, C. Laermans, R. Provoost and R. E. Silverans, *Mat. Sc. Forum.* 258-263 (1997) 623-628.[3] J. E. Graebner et al., *Phys. Rev. B* 29 (1984) 3744 and *Phys. Rev. B* 29 (1984) 5626; von Haumer et al., *Phys. Rev. Lett.* 44 (1980) 84.

FREQUENCY DEPENDENT DIELECTRIC INVESTIGATIONS OF POLYCARBONATE FROM 100 mK TO 300 K AT HYDROSTATIC PRESSURES

Th. Eggert*, G. Köbernik, M. Jäkel and A. Gladun

Institut für Tieftemperaturphysik, Technische Universität Dresden, D-01062 Dresden,
Germany

We measured the dielectric response of polycarbonate (PC) at frequencies between 1 and 200 kHz. In the accessible temperature range (100 mK - 300 K) we were able to examine thermally activated processes as well as tunneling systems. For the application of hydrostatic pressures (up to 0.4 GPa) a self clamping oil pressure cell was used.

Since the measurements were carried out at various frequencies, the barrier height V and the attempt frequency ν_0 of the thermally activated process could be determined using the Arrhenius law. We found that up to 0.3 GPa V remains unchanged with increasing pressure while ν_0 is enhanced several decades. This behaviour is not surprising because the binding forces of the polymer molecule are not affected by the pressure, but due to the higher density (with increasing pressure) [1] the thermally moving molecule units are hindered in motion.

In the tunneling regime ($T < 1$ K) the relative permittivity exhibits a minimum, arising from resonant and relaxational interaction of the electric ac field with the two level systems (TLS) [2]. Application of pressure increases slightly the slope of the relaxational branch and shifts the minimum to lower temperatures. The first effect is explained with the standard tunneling model (STM) [3] by an increase of Pp^2 . Here P is the number of TLS per unit volume per unit energy, and p the average dipole momentum. The minimum temperature T_{min} is proportional to $\sqrt[3]{\nu^2/\gamma^2}$, with ν as the velocity of sound and γ as the deformation potential. Since ν increases under pressure [4] γ has to increase much stronger to explain the shift of T_{min} .

[1] M. Jäkel, F. Weise, J. Opitz, R. Geilenkeuser, *Cryogenics* **38** (1998) in the press

[2] S. Hunklinger, M. v. Schickfus, *Amorphous Solids*, Ed.: W.A. Phillips, Springer Verlag, Berlin, Heidelberg, New York (1981) p. 81

[3] W.A. Phillips: *J. Low Temp. Phys.* **7** (1972) p. 351

P.W. Anderson, B.I. Halperin, C.M. Varma, *Philos. Mag.* **25** (1972) p. 1

[4] R. Geilenkeuser, F. Weise, M. Jäkel: *Czech. J. Phys.* **46** (1996) p. 2251

* supported by the Deutsche Forschungsgesellschaft through Ja 677/3-2

LATTICE DYNAMICAL CALCULATION OF PHONON SCATTERING AT A DISORDERED INTERFACE

G. Fagas, A.G. Kozorezov, C.J. Lambert, J.K. Wignmore

School of Physics and Chemistry, Lancaster University LA1 4YB, Lancaster UK

Using the exact dynamical matrix for a fcc cubic crystal with central nearest neighbor interactions, we solve numerically the phonon transmission(reflection) problem through a disordered planar interface between two identical semi - infinite leads. The disorder is introduced as a random variation of masses or spring constants with or without correlation along the plane of the interface. The overall transmission is controlled by phonon scattering, exhibiting strong frequency dependence with increasing incident phonon frequency. We also calculate the full scattering matrix and obtain complete scattering angle dependencies. The angular distribution of the scattered phonons is shown to exhibit a frequency dependence which arises from the correlation induced finite width of the disordered spectral distribution.

HIERARCHICAL STRUCTURE OF THE POTENTIAL LANDSCAPE IN GLASS

Y. Ben-Ezra and V. Fleurov

Beverly and Raymond Sackler School of Physics and Astronomy

Tel Aviv University

Tel Aviv 69978, Israel

Hypothesis of two-level systems in glasses was introduced as a phenomenological explanation of linear temperature dependence of the specific heat of amorphous solids (dielectric, spin and metallic glasses) at low temperatures and various other anomalies. In spite of the fact that a large number of papers has been published devoted to theoretical consideration of the model only few of these address the problem of a microscopical explanation of how these double-well potentials (DWP) appear.

Using the Monte Carlo simulation we show that there are DWPs in $Al_{90}La_{10}$ metallic glass appearing as sort of elementary parts of more complicated landscape.

Glassy systems clearly break ergodicity. A physical system often displays different kinds of thermal equilibria when observed on different time scales. The model of hierarchically constrained dynamics for glassy relaxation was checked for $Al_{90}La_{10}$ metallic glass. For system containing 500 atoms several levels of hierarchy are observed. Types of atomic motion for different hierarchy levels are determined.

We conclude that our simulation demonstrate clearly that the energy landscape even of this rather small glassy system is arranged hierarchically. The transitions between the wells of the landscape correspond to local rearrangements of atomic structure which can involve one or more atoms depending on the level of the hierarchy.

MICROREFRIGERATION AND THE PHONON DEFICIT EFFECT

Armen M. Gulian

(USRA/US Naval Research Laboratory, Washington, DC 20375, USA)

A long while ago the benefit of using non-symmetric superconducting tunnel structures was argued for electron cooling. In SIS/TS structure the extraction of electron excitations from smaller gap thin-film superconductor S' via tunneling into the larger gap "banks" S was predicted by Parmenter to reduce the effective temperature in S' . His work actually pioneered the theory of order-parameter enhancement in conditions of nonequilibrium superconductivity. Subsequent studies considered the possibility of tunnel junction refrigeration. Experimental and theoretical studies were performed related to this mechanism (of microrefrigeration) in superconducting tunnel structures, which resulted into practical realization of the effect. The initial studies were focused on the effective electronic temperature of the smaller gap superconductor (in the ultimate case of the smallest gap $S' \rightarrow N$ one deals with the most effective SINIS structure). This intrinsic electron cooling is promising for "on-chip" applications.

A wider application range is possible when cooling also involves the crystalline lattice. In this case it is possible to refrigerate externally attached objects, such as a membrane. We paid attention to the Joule heating which exists because of finite resistance of tunnel structures and treated the refrigeration using the concept of the "phonon deficit" effect. This effect arises when superconductors are driven towards nonequilibrium and deals with the negative phonon fluxes in some spectral range of the phonons, related to the gap energy. The involvement of the crystalline lattice results in counter play of the phonon deficit effect with the Joule heating. For SIS junctions both mechanisms are proportional to V^2 , where V is the voltage across the junction and the heating is typically stronger than the cooling power of the phonon deficit mechanism. For asymmetric junctions SIS' the cooling power becomes linear in V , so that for sufficiently small voltages the net difference may result in a cooling.

In this report we are discussing: a) the relevance of the phonon deficit effect to the microrefrigeration problem; b) some theoretical possibilities to raise the overall effectiveness of refrigeration; c) some ways to reach this goal in practice.

EVOLUTIONS OF LOW-FREQUENCY RAMAN SCATTERING SPECTRUM, THERMAL AND ELASTIC PROPERTIES OF

DEHYDRATED POLYACRYLAMIDE GEL WITH INCREASING TEMPERATURE

Kazuhiro HARA, Atsushi NAKAMURA¹, Nobuyasu HIRAMATSU¹ and Akihiro MATSUMOTO²

Department of Applied Science, Faculty of Engineering, Kyushu University,

Hakozaki, Higashi-ku, Fukuoka 812-8581, Japan

¹*Department of Applied Physics, Faculty of Science, Fukuoka University,*

Nanakuma, Jonzan-ku, Fukuoka 814-0180, Japan

²*Osaka Municipal Technical Research Institute,*

Morinomiya, Joto-ku, Osaka 536-8553, Japan

In the present study, comparative investigations of evolutions of the low-frequency Raman scattering spectrum, thermal property and complex elastic stiffness of dehydrated polyacrylamide (PAAm) gel were carried out with increasing temperature from room temperature.

In the measurement of the thermal property by a differential scanning calorimeter (DSC), a thermal anomaly was observed around 60°C (at a temperature increasing rate of 10°C/min). In the measurement of temperature dependence of the complex elastic stiffness (at a rate temperature increasing of 8°C/min), the real part of the complex elastic stiffness (storage modulus) decreased remarkably around the temperature where the thermal anomaly has been observed (T_g). Besides, the imaginary part (loss modulus) showed a peak around T_g . Because these features resembled those commonly observed around the glass transition temperature in the non-crystalline polymers, the occurrence of the glass transition was confirmed in the dehydrated PAAm gel around T_g .

In the observation of the Raman scattering spectrum with increasing temperature, remarkable decrease in the scattering intensity of a peak in the low frequency region (which looked like the boson peak usually observed in the amorphous materials). However, the low-lying peak could be still distinguished even far above the glass transition temperature which was confirmed by the thermal and elastic measurements. This feature can come from the complex structure of the dehydrated PAAm gel compared with the usual glass.

ON THE WAVEVECTOR DEPENDENCE OF THE BOSON PEAK IN SILICATE GLASSES AND CRYSTALS

M. J. Harris, ISIS Facility, Rutherford Appleton Laboratory, Chilton, Didcot, Oxon, OX11 0QX, United Kingdom

M. T. Dove, Department of Earth Sciences, University of Cambridge, Downing Street, Cambridge, CB2 3EQ, UK

J. M. Parker, Department of Engineering Materials, Sheffield University, Mappin Street, Sheffield, S1 3JD, UK

So many amorphous materials display low temperature anomalies in their specific heats that they are generally regarded as being universal properties of the glassy state. These anomalies are usually of two kinds. The first concerns the observation that, while many crystals obey the Debye law $C \propto T^3$ for temperatures less than say, 1 K, glasses with the same chemistry frequently display the law $C \propto T$ at correspondingly low temperatures. In addition, glasses such as silica, SiO_2 , contain an excess specific heat over crystalline phases in a higher temperature regime, where $T \sim 10$ K. This second observation is tied in with the appearance of the ubiquitous Boson peak in inelastic neutron and Raman spectra. A satisfactory microscopic description of both anomalies has so far proved elusive, and over the last year, controversy has developed over the Boson peak in particular.

Our previous work [1] demonstrated that a plausible explanation for the Boson peak is that it arises simply from the dispersion characteristics of transverse acoustic modes in both crystals and glasses. We develop this argument further and put it on a much firmer footing, by investigating the *wavevector dependence* of the Boson peak in inelastic neutron data. We make use of new results from an inelastic neutron scattering study of several crystalline polymorphs of SiO_2 (cristobalite and quartz), and a number of silicate glasses (pure silica, SiO_2 , and three glasses in the alkali silicate series $(\text{K,Li})_2\text{Si}_2\text{O}_5$). In addition to the Boson peak, we also investigate the role of the lower-energy floppy modes in the inelastic spectra, and show that they are controlled by chemical effects. We find that in all cases, the inelastic features in the glasses may be explained simply by these arguments, developed from phonon dispersion models of the crystals.

[1] M. T. Dove, M. J. Harris, A. C. Hannon, J. M. Parker, I. P. Swinson and M. Gambhir, *Phys. Rev. Lett.* **78**, 1070 (1997).

IMAGING PHONONS IN SUPERCONDUCTORS*

M.R. Hauser^a, R. Gaitskell^b, J. Short and J.P. WolfePhysics Department and Materials Research Laboratory
University of Illinois at Urbana-Champaign, Urbana, IL 61801

Abstract

Phonon imaging has provided detailed information about the ballistic propagation and scattering of phonons in semiconductors and insulators at low temperatures. Until now, the technique has not been applied to metallic crystals because high frequency phonons scatter strongly from free electrons. However, the phonon scattering can be greatly reduced in a superconducting metal for phonons with energy less than twice the superconducting gap, as shown by heat-pulse experiments in Pb by Narayanamurti, et al., in Sn by Pannetier et al., and in Nb by Gaitskell et al. We report here the first phonon-imaging experiments in superconductors: single crystals of Nb and Pb. Phonon-focusing caustics are observed in both materials, and these structures are used to study the spatial migration of nonequilibrium phonons and quasiparticles. In this talk, we concentrate on Nb, for which we have conducted computer simulations to model the propagation of interacting quasiparticles and phonons. The experimental data show strong dependences on the excitation intensity and are only partly explained by the simulations. We expect that the imaging of ballistic phonons in superconductors will prove useful for probing temporal and spatial development of nonequilibrium excitations.

*Research supported by Department of Energy grant DOE 45439.

^aPresent Address: Shell E & P Technology Co., Houston, TX 77025^bPresent address: Center for Particle Astrophysics, University of California at Berkeley, Berkeley, CA 94720RELAXATION OF THERMAL PROPERTIES
OBSERVED IN GLASSESY. Hiki^a, H. Takahashi^b, Y. Kogure^c^aFaculty of Science, Tokyo Institute of Technology, Emeritus,
39-3-303 Motoyogoi, Shibuya-ku, Tokyo 151-0062, Japan^bApplied Physics Group, Faculty of Engineering, Ibaraki University,
Nakanarusawa, Hitachi 316-0033, Japan^cTeikyo University of Science & Technology,
Uenohara, Yamanashi 409-0193, Japan

Using the improved hot-wire method, simultaneous measurement of the thermal conductivity κ and the thermal diffusivity D of solids can conveniently be carried out [1]. The experimental method is as follows. In a small fused-quartz cylindrical specimen cell, a thin heating wire with two attached potential leads is stretched along its axis. Melted specimen is poured into the cell. The thin wire enclosed in the specimen acts as a heating element and a thermometer. By observing the change with time of the wire temperature after a constant electric current is applied, the values of κ and D of the specimen can be determined. The heat capacity per unit volume $C = \kappa/D$ is also obtained. The method was used to study the stabilization in phosphate glasses below the glass transition. After annealing at room temperature, the temperature of the specimen was rapidly increased to an annealing temperature T and was kept constant. Then the hot-wire measurement was quickly made for determining the values of κ , D and C . The measurement was repeated with adequate intervals of the annealing time t . The time dependence was found to be $\kappa \propto \exp[(-t/\tau(\kappa))]$ etc. with respective relaxation times $\tau(\kappa)$ etc. By performing the experiments at various temperatures T , the τ vs T relation was determined [2]. The observed relaxations are considered to be due to a stabilization process caused from the unstable-metastable transition. Discussion will be focused to interpret the fact found in the experiment, $\tau(\kappa) \sim \tau(C)$.

[1] H. Takahashi, Y. Hiki and Y. Kogure, Rev. Sci. Instrum. 65 (1994) 2901.

[2] Y. Hiki, H. Kobayashi, H. Takahashi and Y. Kogure, Prog. Theor. Phys. Suppl. 126 (1997) 245.

Nonequilibrium Phonon Propagation in Vitreous Silica

Hiroshi Ikari

Department of Physics, Faculty of Education, Shizuoka University,
Ohya 836 Shizuoka City, 422-8529 Japan

Time of flight measurements of vitreous silica at 2.08K have been performed in the low excitation energy where the excitation surface is isolated from the He bath. The anharmonic decay of high frequency phonons is estimated from quantitative comparisons between the experimental and theoretical decay rate for the quasidiffusive propagation regime. The observed decay rate is two orders of magnitude larger than that calculated in terms of the second and third order elastic constants at room temperature, which is in contrast to the successful predictions of the quasi-diffusive phonon propagation in Si crystal. This rapid decay reflects unusual anharmonicity of the lattice in silica glass. When liquid helium is in contact with the excitation surface, a dramatic reduction in the diffusive tail is observed. In order to evaluate the effect of phonon losses into the helium bath, a Monte Carlo calculation which simulates the experimental conditions has been performed. The vacuum case assumes 100% specular reflection from the surface, and the liquid helium case assumes a 3% loss rate into the helium with each incidence at the surface, which is ten times greater than the transmission coefficient predicted by the acoustic-mismatch theory.

PECULIAR SUPPRESSION OF THE SPECIFIC HEAT AND BOSON PEAK INTENSITY OF DENSIFIED SiO_2 GLASS

Y. Inamura¹, M. Arai¹, O. Yamamuro², T. Matsuo³, N. Kitamura³, T. Otomo¹ and
S.M. Bennington⁴

¹ High Energy Accelerator Research Organization, 1-1 Oho, Tsukuba 305, Japan
² Chemistry Department, Osaka University, 1-1 Machikaneyama, Toyonaka 560, Japan
³ Government Industrial Research Institute of Osaka, 1-8-31 Midorigaoka, Ikeda, Japan
⁴ Rutherford Appleton Laboratory, Chilton, Didcot, Oxon OX110QX, UK

Abstract

The low temperature thermal properties, i.e. specific heat (Cp), of densified vitreous silica are investigated as a function of the density from 2.2g/cc for normal density to 2.64g/cc for the highest density. It is believed that the low energy dynamics of intermediate range structure is responsible for the universal properties of non-crystalline system[1]. Hence, we have modified the intermediate range structure of vitreous silica artificially by densification in order to investigate the effects on the thermal properties from the modified structure. We reported the detailed results on the structural and dynamic evolution[2], which showed a large upward shift of the Boson Peak on densification by RAMAN scattering. Although observed specific heat (Figure 1) has peculiar features as well, those cannot be explained by the observed evolution of Boson Peak because the density dependence of that intensity was not clear. This time we observed the Boson Peak of both normal and densified SiO_2 glass in detail by neutron scattering (Figure2). This result indicates that the evolution by densification are not simple shift of the peak but the huge suppression of the intensity of a vibrational mode. This result can explain also the suppression of the additional specific heat at around 10K, which is thought to be attributed to the Boson peak. Hence, with the structural studies[2], we believe that the structure causing the suppressed mode is an important constituent for the intermediate range structure, which is attributed to the thermal properties of SiO_2 glass.

Reference [1] Pohl and Zeller, Phys. Rev. B5(1971)2029
[2] Y. Inamura et al. J. Non-Cryst. Solids to be published

Figure 1
Specific Heat for normal and densified
 SiO_2 glass

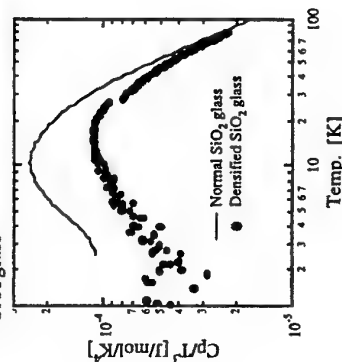
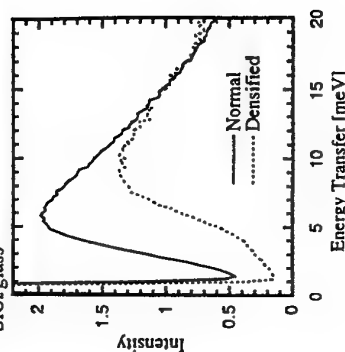


Figure 2
Boson Peak of normal and densified
 SiO_2 glass



FLUCTUATION PROPERTIES OF THIRD SOUND TRANSMISSION IN RANDOM MEDIA

Hironori Kawashima, Keiya Shirahama and Kimio Kono

Institute for Solid State Physics, Univ. of Tokyo,

Roppongi 7-22-1, Tokyo, Japan

Third sound is a surface wave on a superfluid helium film. It involves a longitudinal oscillation of superfluid component parallel to the substrate, with the normal component stationary.

We studied the localization properties of third sound in one-dimensional random lattices, the glass substrates on which aluminum strips were randomly distributed. Third sound pulses are propagated on both the patterned substrate and the blank substrate (with no strip) under the same conditions. The transmission spectrum is obtained by dividing the power spectrum of the wave form which was propagated on the patterned substrate by that on the blank substrate. The measurement was done at 0.7 K to reduce the attenuation effect.

In the random media the spectrum shows prominent suppression due to the weak localization effect. In addition to that a large fluctuation is observed in the suppressed region. The properties of this fluctuation is analysed in terms of the weak localization theory. The fluctuation of the transmissivity is expected to contain essential information of the randomness.

The measurement on two-dimensional random lattices is now in progress.

MICROMECHANISMS OF DISLOCATION-PHONON INTERACTION IN SOLIDS AT LOW AND HIGH TEMPERATURES

Valery P. Kisel

Institute of Solid State Physics, 142 432 Chernogolovka, Moscow
distr., RUSSIA; Fax: +7 (096) 576-41-11; E-Mail: kisel@issp.ac.ru

The main findings of this work are the demonstration of the key-role of dislocation mechanisms in thermal (TC) conductivity of insulators (solid helium, alkali halides, etc.), metals and semiconductors at low/high temperatures, and the scaling behaviour of the stresses for dislocation interaction with phonons (PS) and lattice physical imperfections (DS) at different length scales under heat or dislocation flow under different tests.

The matrix nano/microparticles of impurity phase (and dislocation loops around them) are the main obstacles for dislocation vibrations or motion due to the crucial role of dislocation double cross-slip mechanism [1], so the mobile dislocations are the key-obstacles for dispersion of phonons, and the temperature and impurity concentration influence on the TC and TEC (thermal expansion coefficient) can be well understood if the local temperature-dependent lattice mismatch stresses between matrix and nanoprecipitates will be taken into consideration [1-3].

This conclusion is confirmed by:

1. The same "size effect", the surface roughness effect, the sensitivity of TC, TEC and the parameters of plastic flow to temperature, predeformation and heat prehistory, morphology, composition and concentration of impurities, crystallographic symmetry [2], and work-hardening of solids at low/high temperatures.
2. The same dependences of orientation angle anisotropy for TC, TEC and plasticity in the n.c.p. crystals.
3. The spread of TC and deformation data points (curves) usually increases with temperature or thermal resistance decrease, and it disappears at high temperatures.
4. The non-monotonous temperature behaviour of TC, TEC is similar to the low-, moderate temperature and in the vicinity of the melting point yield stress anomalies in insulators, metal and disordered alloys, crystalline gases [1-3]. It can be easily estimated with high accuracy (the value of $T_{max,min}$ and the analytical forms for the

left/right wings of $k(T) = (T \text{ to } T)^{-1}$ and $k(T) = T^{-3}$ through the

temperature dependence of thermal expansion mismatch between precipitates and the matrix in solid helium [2], insulators, metals and semiconductors, etc.

5. Second-phase nano- or microprecipitates are always present in every so-called "solid solutions" or alloys with the tendency to the miscibility gap at any concentration or temperature. The local stresses around these particles play the crucial role in the effect of dislocation cross-slip and climb on the TC, TEC and yield-stress "anomalies" at low and ultra-low temperatures [1-3], and this is proved by the scaling of deformation stresses with the PS in the same materials.

1. Kisel, V. P. et al., Phil. Mag., 1993, v. 67A, No 2, p.343-360.
2. Kisel, V. P., II Int. Conf. on Cryocrystals and Quantum Crystals, Polanica-Zdroj, 7-12 Sept. 1997, Poland, Abstracts Pl-13, P2-24.
3. Kisel, V. P., Mater. Sci. Forum, 1993, v. 119-121, p. 227-232.

SPIN-LATTICE RELAXATION OF PARAMAGNETIC SPIN IN PHOSPHATE GLASS UNDER HIGH MAGNETIC FIELD

N. Kitamura, I. Matsubara, R. Funahashi, *H. Ohia, **H. Nojiri, **S. Mitsudo,

**T. Sakon and **M. Motokawa

Osaka National Research Institute, AIST, 1-8-31 Midorigaoka, Ikeda, Osaka 563-8577, Japan

**Faculty of Science, Kobe University, 1-1 Rokkodai, Nada, Kobe 657, Japan*

***Institute for Material Research, Tohoku University, 2-1-1 Katahira, Aoba, Sendai 980-77, Japan*

Magnetic relaxation phenomena of dilute spin system in amorphous solids are related to low energy lattice vibration in a random network, because a certain vibration state is excited selectively through an energy transfer from spin to phonon system by spin-lattice interaction. Thermal energy in the temperature region, where universality of thermal properties is observed in amorphous solids, corresponds to several Tesla of magnetic field. Thus the measurements of magnetization under a high magnetic field are important for understanding the low energy excitation. Time-domain magnetization and ac susceptibility measurements have been performed for binary calcium metaphosphate glass doped with Cu^{2+} ions under magnetic fields.

The magnetization under pulse magnetic field exhibits slow spin-lattice relaxation time of the order of 10^{-4} sec in the glass, while it is faster than 10^5 sec in the polycrystalline solid. The relaxation time has third power dependence on magnetic field, B , and is independent of the concentration of copper ion above 3 Tesla. Below 1 Tesla, it has B^3 dependence and increases with increasing copper concentration from the analysis of ac susceptibility. The B^3 dependence will be explained by a model assuming constant density of state against vibration energy. Almost constant behavior below 1 Tesla is still unclear. However, the observation of dependence of copper concentration on relaxation ratio suggests that the vibration state is strongly localized in small areas. Because the coupling between spin and vibration state should have a dependence of copper concentration when the scale of the localization is smaller than with average distance between copper ions.

BOSON PEAK IN ALKALI BORATE GLASS

Seiji KOJIMA and Masao KODAMA*,

Institute of Applied Physics, University of Tsukuba, Tsukuba, Ibaraki 305-8573, Japan

#Department of Industrial Chemistry, Kumamoto Institute of Technology, Ikeda, Kumamoto 860-0082, Japan

The detailed composition dependence of boson peak in alkali borate glass was measured using Raman scattering spectroscopy. In cesium borate glass, the peak frequency of boson peak is independent on the composition. With the increase of Cs composition an additional peak appears in the shoulder of the boson peak at above 100 cm^{-1} , and increases in intensity markedly above $x_m = 0.3$, where the sound velocity shows a maximum. While in lithium borate glass, the boson peak frequency changes markedly with the linear relation to sound velocity. The additional peak does not appear in this glasses. The correlation between the boson peak frequency and the sound velocity was discussed in these glasses. The detailed composition dependence of internal vibration bands was also studied. The correlation between the intensities of these bands and the sound velocities was also discussed.

INTERNAL FRICTION AND RELAXATION MECHANISMS OF F-DOPED SiO₂ GLASSES

Hiroshi KOBAYASHI[1], Toshio KOSUGI[2] and Yoshiaki KOGURE[3]

[1] National Research Laboratory of Metrology, Umezono, Tsukuba, Ibaraki 305, Japan

[2] Faculty of Science, Hiroshima University, Higashi-Hiroshima 739, Japan

[3] Teikyo University of Science and Technology, Kitatsuru-gun, Yamanashi 409-01, Japan

SiO₂ glass is one of the materials for studying complex systems in which many scientists recently have strong interest. We have been measuring both the low temperature dependence of the internal friction and the Young's modulus of Ge-doped, O-excessive and O-deficient SiO₂ glasses. The analysis using the thermal relaxation model with a double well potential has succeeded in providing an explanation of these phenomena. With this model, the internal friction is attributed to the lateral motion of the bridging oxygen atoms across the Si-O-Si bridge.

In the present paper, we report the measurements of the internal friction and the Young's modulus of F-doped SiO₂ glasses in the temperature range of 1.6 K to 250 K. First, SiO₂ soot rods were obtained from SiCl₄ by the VAD method, and then the rods were heat-treated at high temperature in an atmosphere of SF₆ and He gases. These rods were sintered at the temperature of 1500°C, and SiO₂-4mol%F and -8mol%F glasses were obtained. In this process, it is supposed that the O atoms are substituted by F atoms as Si-F. Pure SiO₂ glass which was obtained by the direct method was prepared and used as the standard of SiO₂ glasses.

The internal friction of pure SiO₂, SiO₂-4mol%F and -8mol%F glasses are not very different except for their peak values, which show a few % differences at 35 K. In contrast, the Young's modulus of SiO₂-4mol%F and -8mol%F glasses are 7.5% and 15% less than that of pure SiO₂ glass respectively. The theory of thermal relaxation shows internal friction $IF \propto n/E$, where n is particles (bridging oxygen atoms) moving in a double well potential and E is Young's modulus. With the increment of fluoride content, the values of n and E decrease in the same manner, which it is thought, cancels the change of IF .

It is concluded that this relaxation model can explain the mechanical dynamics of SiO₂ glasses very well.

ACOUSTIC WAVES LOCALIZED AT A PLANAR DEFECT IN CRYSTAL

A.M.Kosevich, E.S.Syrkin, and A.V.Tutov

Theoretical Division, Institute for Low Temperature Physics and Engineering
310164, 47 Lenin Avenue, Kharkov Ukraine

The planar defect effect on the phonon spectrum in fcc crystal is studied. Shear horizontal (SH) surface waves are investigated. The nearest and next-nearest neighbour interactions are calculated. Such an accounting leads to the appearance the ordinary as well as the generalized interface waves in the short wavelength region. The conditions of the transition are sufficient respectively to the change of the bulk vibrational iso-energy surface connectivity. The characteristics of the generalized interface waves (the additional spatial oscillation period for the wave amplitude, damping parameter) as well as the features on the density of the quasilocalized phonon states are described and they could be visible in the measurements of the non-elastic scattering of the low-energy particles by the interface. The cases of the free surface and the interface are considered. There are only low-energy states in the case of the free surface (lying under the edge of the continuous spectrum). There are both low- and high-energy states in the case of interface. The planar defect is described as the force change between two adjacent crystal layers. One can separate the eigen modes into two classes depending on their symmetry relatively the defect plane. So, there are symmetrical and antisymmetrical waves having the energy both below and under the edge of the bulk band. The transition from the ordinary (monotonic dumping) to the generalized (oscillation dumping) surface waves occurs in the short wavelength region, and this area can not be described in the framework of the elasticity theory.

INTERNAL FRICTION OF $\text{TiO}_2\text{-SiO}_2$ GLASST. Kosugi, H. Kobayashi¹, Y. Kogure²

Faculty of Science, Hiroshima University, Higashi-Hiroshima 739, Japan

¹National Research Laboratory of Metrology, Tsukuba 305, Japan²Teikyo University of Sci. & Tech., Uenohara, Yamanashi 409-01, Japan

Anharmonic state or relaxational motion of atoms in solids characterizes the glassy state. The concepts, for instance, such as double-well potential (DWP), tunneling two-level state (TLS), β relaxation due to a cage motion of atoms by thermal activation, α relaxation due to irreversible diffusion of atoms near the glass transition temperature, are often considered. However, in any real glasses, the microscopic structure of relaxational motions are not clear so far, although there have been successful studies based on the phenomenological approaches by using TLS model or the extended models such as the soft potential model (SPM).

We have measured internal friction of $\text{GeO}_2\text{-SiO}_2$ glasses to clarify the microscopic structure for the relaxational motion in SiO_2 glass at low temperatures, and explained the substitution effect of Ge atom to Si atom site not only qualitatively but also quantitatively among different Ge concentrations (0, 5, 10, 24, 100%) by the T model, where the O atom in Si-O-Si bridge moves to relax transversely to the bridge.

To understand how the distribution of DWP parameters such as the barrier height are determined, we recently measured the internal friction (50kHz) of 5.7 mol% $\text{TiO}_2\text{-SiO}_2$ glass between 1.6 and 300 K. As a result, we find the shift of the broad peak of internal friction to the lower temperature side, i.e., the peak temperature T_p shifts to 29 K from 33 K in pure SiO_2 . In the case of $\text{GeO}_2\text{-SiO}_2$ glasses, T_p shift to higher temperatures. If we pay attention to the bond angle of Si-O-R (R= Ti or Ge), the increase of the angle seems to correspond to the decrease of T_p or the barrier height of DWP.

TUNNELING — THERMAL ACTIVATION CROSSOVER IN NEUTRON IRRADIATED QUARTZ.

C. Laermans¹ and D.A. Parshin²¹Department of Physics, Katholieke Universiteit Leuven, Celestijnenlaan 200D, B-3001 Leuven, Belgium.²St. Petersburg State Technical University, 195251, Polytechnicheskaya 29, St. Petersburg, Russia.

The low-temperature internal friction data in neutron-irradiated and amorphous quartz are compared. The region of the tunneling plateau in irradiated quartz extends to much higher temperatures in comparison with amorphous SiO_2 . It is interpreted within the soft-potential model that two-level systems in irradiated quartz have higher crossover temperature, T_c , from tunneling to thermal activation than in the glassy state. The characteristic energies, W , of the particles in the double-well potentials are estimated. Their difference is ascribed to higher effective masses of the tunneling centers inside the amorphous network than in the distorted crystalline regions of irradiated quartz. The high value of T_c in neutron irradiated quartz explains also why the onset of the tunneling plateau can still be seen in the ultrasound data at high frequencies where one does not expect to see the tunneling states anymore.

UNEXPECTED BEHAVIOUR OF THE TUNNELING STATES-PHONON COUPLING IN NEUTRON-IRRADIATED QUARTZ AS A FUNCTION OF DOSE.

V. Keppens^{1,2} and C. Laermans¹

1. Katholieke Universiteit Leuven, Dept. of Physics, 3001 Leuven, Belgium.
2. Oak Ridge National Laboratory, Solid State Division, Oak Ridge, Tenn., USA.

Neutron irradiated crystalline quartz turned out to be very interesting for the study of the low temperature (LT) dynamic properties related to the anomalies in amorphous solids. It is very appropriate as a model for the glassy state because of the possibility of introducing increasing degrees of disorder by varying the neutron dose and monitoring the induced tunneling states (TS)(1)

An extensive ultrasonic study was carried out in our group for different neutron doses involving attenuation measurements and variation of the velocity determination for different doses and crystallographic directions. At relatively low volume fraction of the created amorphous regions the macroscopic coupling strength C of the TS increases monotonically with increasing neutron dose mainly due to the increasing density of states (DOS) and it was expected that this increase would be continued and saturate when the full network disorder is reached.

Previously an indication was found, for the decrease of C with increasing dose, after the initial increase in x-cut quartz crystals (2). In this work we report new low temperature ultrasound measurements for doses in the high dose region (0.3 K to 20 K; ~200 MHz). The data confirm the unexpected non-monotonic behaviour of C with dose, at least for the x-cut crystals. However, this behaviour is not found when the ultrasonic wave propagates in the z-direction: a systematic increase with neutron dose is observed up to the saturation value for the fully disordered crystal.

The results will be discussed in view of the microscopic model which was put forward for the TS in neutron irradiated quartz as rotations of coupled SiO_4 tetrahedra related to the microtwins in (at least part of) the sample (1). It is remarkable that the maximum of C (and of the DOS) occurs for a dose for which the amount of microtwins in the sample is expected to be saturated.

1. C. Laermans and V. Keppens, Phys. Rev. B **51**, 8158 (1995) and references therein.
2. V. Keppens and C. Laermans, Nucl. Instr. and Meth. in Phys. Res. B **91**, 346 (1994).

SAW DIAGNOSTICS OF GaAs SURFACE STRUCTURE.

T.A. Briantseva*, T.J. Bullough**, D.V. Ljoubchenko**

I.A. Markov*, E.M. Tolmachev*,

*Institute of Radioengineering and Electronics, Russian Academy of Sciences
11 Mokhovaya Str., 103907, Moscow, Russia.

**The University of Liverpool, Materials Science and Engineering,
Department of Engineering, Liverpool, L69 3BX, UK.

Sensitivity of surface acoustic waves (SAW) to the surface state of the crystals is well known [1,2]. In this work GaAs semi-insulating samples with SAW transducers disposed at (111) surface were under study. SAW transducers were preliminary formed as Al thin film interdigital structure that allowed to operate at the central frequency 65 MHz. The surface of the samples with transducers was cleaned only by organic solutions such as iso-propanol, dimethyl-formamide because the presence of Al stripes eliminated the treatment by chemical nonorganic etchants. Since GaAs surface was not preliminary treated in etchants with following annealing it was expected to be covered by thick oxide layer (Ga_2O_3 , $\text{Ga}_2(\text{OH})_4$). SAW parameters were measured by means of measuring stand which allowed to measure the amplitude and phase variations of the output signals ($A_m = A_{\text{out}} - A_{\text{in}}$, $\varphi_m = \varphi_{\text{out}} - \varphi_{\text{in}}$) after the preset time intervals and to indicate them by IBM PC. This stand gave sensitivity of measurements: the amplitude - 0.04 dB, the phase - 2° , the time - 10 ms; dynamic range of setup was 90 dB. The insertion losses were ~18dB in the whole scheme with the sample turned on. The maximum signal of frequency synthesizer was 0.7 V at zero induced attenuation, the input impedance of the whole scheme was 50 Ohm. Evaporation of Au and irradiation of the sample by light were performed through the mask between the transducers. The obtained results of this work combined with the results obtained by microscopy (optical and SEM) and electronography show that SAW is sensitive not only to the state of the natural oxide layers (composition, the shapes of blocks, etc.) but also to the state of GaAs subsurface layer. It turns out that free Ga and As atoms are able to migrate from GaAs surface into grain or block boundaries of oxide layers and fill them by the formed defective GaAs islands. These GaAs islands can absorb SAW energy at grain boundaries and be decomposed resulting in formation of more perfect oxide layer. The formation of dense oxide layer leads to the reorientation of GaAs surface and changes the direction of SAW maximum velocity $[2 \bar{1} \bar{1}] \rightarrow [00 \bar{1}]$ that is indicated by variations of phase velocity.

Thus, the investigation of SAW interactions with surface and subsurface layers of the crystals is very useful because SAW may be both the source of artificial mechanical stresses and their indicator.

References

1. Design of an Ultrahigh-Vacuum Compatible System for Studying the Influence of Acoustic-Waves on Surface Chemical Processes. Mitrelias T., Ostanin V.P., Gruyters M., King D.A. Applied Surface Science, 1996, Vol.101, pp.305-310.
2. Acoustic Wave Enhancement of the Catalytic Oxidation of Carbon Monoxide Over Pt. Kelling S., Mitrelias T., Matsumoto Y., Ostanin V.P., King D.A. Journal of Chemical Physics, 1997, Vol.107, No.14, pp.5609-5612.

HEAT PULSE BALLISTIC PHONONS INTERACTION WITH OPTICAL COHERENT EXCITED IMPURITY SYSTEM

V.N.Lisin, A.M.Shcheda, B.M.Khabibullin, V.A.Zuikov, V.V.Samartsev
Zavoisky Physical-Technical Institute of RAS,

Sibirsky trakt, 10/7, Kazan, 420029, Russia, Phone: (8432)763681,
fax: (8432)765075, e-mail: vlisin@diomis.kfti.kcn.ru

It is studied the effect of the ballistic phonons of heat pulses of the nanosecond duration on the inverted photon echoes in ruby with the concentration of Cr^{3+} ions of 0.2 wt.% and 0.03 wt.% and in $\text{LaF}_3:\text{Pr}^{3+}$ for 4777 Å ($^3\text{P}_0 - ^3\text{H}_4$) transition with the concentration of Pr^{3+} ions of 1 wt.% at temperature 2 K. The heat pulse ballistic phonons are generated by fast (~10 ns) electrical excitation of thin ($\sim 10^{-6}$ - 10^{-5} cm) Cu-film, by resistance 50Ω, deposited on to one polished face of a sample in parallel axes C_3 . The photon echo was used as the phonon detector. It was observed experimentally the full recovering of the echo intensity in the ruby and significant on the ions Pr^{3+} in LaF_3 if the each impurity ion was interacted with two alike phonon pulses after the recording and, accordingly, reading laser pulses. The basic property of the photon echo, which allows to use of one as a detector of processes without coherent losses, lies in an independence of the echo intensity from inhomogeneity width. This has allowed to conclude that the main effect of the ballistic phonon pulses consists in shifts of the energy levels, instead of in relaxation transitions. It is unexpected result, which do not be interpreted within the framework of usual representation about the mechanism of action heat phonons on impurity ions. To study the interaction mechanisms the some attention was given to measurements, conducted under different duration of the phonon pulses and different delay times between them, to investigation of additivity and commutativity of the phonon pulses action and to comparison of the theoretical and experimental results.

PHONON SCATTERING AND IR-SPECTRA OF OXYGEN-RELATED DEFECTS IN GALLIUM ARSENIDE - ASPECTS OF QUANTITATIVE PHONON SPECTROSCOPY

F.Maier, K.Laßmann Universität Stuttgart, I.Physikalisches Institut, Pfaffenwaldring
57, 70550 Stuttgart

Version: March 20, 1998 Key Words: GaAs:O, phonon spectroscopy, IR spectroscopy

Depending on growth conditions and thermal history a number of oxygen-related defects is known to occur in oxygen-doped gallium arsenide apparent as resonance lines in the IR transmission spectra. Of these, interstitial (Ga-O-As) and quasi-substitutional (Ga-O-Ga) oxygen have been identified by the stress dependence and the Ga and O isotope shifts. Here we report on the investigation of GaAs:O by phonon spectroscopy showing that in such samples there is a number of specific phonon scattering resonances in the energy range from about 0.5 meV to 4 meV.

By systematic variation of doping conditions and heat treatment we have tried to relate the varying intensities of the phonon resonances to changes in the IR spectra. For this to do a quantitative analysis of the phonon spectra was necessary. As regards the effect of multiple scattering on the line shape we performed numerical simulations as was done previously for the quantitative determination of interstitial oxygen in silicon [1]. Since the relevant phonon resonances are lower in energy in GaAs:O than in Si:O, some simplifications used in [1] are not valid here. Also, it turned out, that the influence of the junction/substrate interface on the (frequency dependent) transmission characteristic is different for gallium arsenide varying distinctly with the orientation. These differences have been included in an improved calculation of the emission spectrum to obtain emitter/detector transfer characteristic. As a result we obtain good correlation between four relatively sharp phonon resonances (1.70 meV, 1.85 meV, 1.98 meV and 3.76 meV) and the 845 cm^{-1} IR line associated with interstitial oxygen Ga-O-As. However, from the stress and temperature dependence no clear-cut model for the low-energy motion of interstitial oxygen in GaAs as yet was found when compared to the rotational motion in Ge and the 2D-oscillation in Si. Two further broad lines around 2.1 meV and 2.7 meV are possibly due to an oxygen-boron complex. A sometimes very deep resonance at 1.65 meV appearing after thermal treatment has no IR counterpart and is probably not related to oxygen.

[1] C. Wurster, E. Dittrich, W. Scheitler, K. Laßmann, W. Eisenmenger, and W. Zulehner, Proc. of PHONONS 95, Sapporo, 1995, Physica B 219&220, 763 (1996)

BRILLOUIN SCATTERING STUDY OF ACOUSTIC PHONONS IN
SUPERCOOLED LIQUID OF LOWER ALCOHOLS

Genzou MATSUI and Seiji KOJIMA

Institute of Applied Physics, University of Tsukuba,
Tsukuba, Ibaraki 305-8573, Japan.

Currently the glass transition has been studied extensively. The investigation of phonons in supercooled liquid is the one of the subjects of fundamental physics and is important for understanding the dynamical nature of the glass transition. On the other hand, the glass as disordered material has been investigated due to the interest in their many potential applications for optical devices. In this circumstance, Brillouin scattering technique of a very short acquisition time has been developed. We have constructed the experimental setup combined by multi-pass Fabry-Perot interferometer and highly sensitive CCD detector. This enables one to measure a Brillouin spectrum in a few seconds. Using this system, we have studied the temperature dependence of Brillouin shift and its width in a supercooled state of lower alcohols. This molecular liquid is known as the fragile liquid and behaves corporative relaxation in a supercooled state. It was found that a cusp like anomaly appeared in the width of Brillouin components near its maximum. Such a phenomenon has been explained as the resonance between a structural relaxation and phonon modes. However such anomaly has been poorly understood up to now. The analysis based on the Mori-Zwanzig formula is proposed to clarify the corporative phenomena on a mesoscopic scale.

ANISOTROPIC THERMAL TRANSPORT
OF 2D QUASICRYSTALS OF DECAAGONAL Al-Ni-Co SYSTEM

M.Matsukawa, M.Yoshizawa, K.Noto, Y.Yokoyama¹ and A. Inoue²

Faculty of Engineering, Iwate University, 4-3-5 Ueda, Morioka 020, Japan

¹ Faculty of Engineering, Himeji Institute of Technology, Himeji 671-22, Japan

² Institute for Materials Research, Tohoku University, Sendai 980, Japan

The anisotropic thermal conductivity of 2D quasicrystals of decagonal Al-Ni-Co system has been measured over the wide range of temperature. The thermal conductivity value along the periodic axis shows the nearly same behavior as dirty alloy systems. The quasiperiodic thermal conductivity exhibits a typical plateau dependence similar to that of disordered systems. The anisotropic behavior of the measured thermal conductivity has been discussed on the basis of phonon relaxation time approximation. It is found that the main contributions of phonon scattering processes in the periodic and quasiperiodic directions are phonon-electron interaction and point-defect scattering effect arising from Penrose tiling, respectively. A small increase above the plateau region in the quasiperiodic transport indicates hopping conduction of localized vibration modes assisted by phonons such as fracton excitations in disordered systems.

LOCALISED VIBRATIONS INDUCED BY 3d CHARGED IMPURITIES IN II-VI SEMICONDUCTORS - A NOVEL APPROACH

Mazurenko V.G., Sokolov V.I.* and Kislov A.N.

Ural State Technical University, Ekaterinburg, Russia
* Institute of Metal Physics of Ural Branch of RAS, Ekaterinburg, Russia

Transition metal impurities in II-VI semiconductors are isoelectronic ones and have neutral charge state with respect to the lattice. After photoionisation into allowed bands or capture of carriers into 3d - shell they become charged with respect to the lattice and induce very intensive localised vibrations. An extremely sensitive experimental technique used in our work for detection of localised vibrations and extended theoretical analysis of experimental data for ZnSe:Ni and ZnO:Ni may be considered as a new approach to an investigation of localised vibrations induced by 3d charged impurities.

We have been investigating donor and acceptor excitons of 3d impurities in II-VI compounds for which there is a change in the number of electron in 3d shell, -1 for the former and +1 for the latter, under photoexcitation. The excited carrier is confined in a hydrogenlike orbit by the coulomb field of the impurity since it is charged with respect to the lattice. For detection of donor or acceptor excitons of 3d impurities we have been using a sensitive modulation technique of electroabsorption, which is very good adapted for an observing hydrogenlike systems in semiconductors [1]. The experimental electroabsorption spectra of II-VI compounds doped with Ni contain zero phonon lines and their strong lattice repetitions. It was shown [1] that Ni impurity excitons interact with the lattice vibrations transforming as irreducible representations which are compatible with the symmetry of the d^7 configuration ground state for Ni donor exciton and the d^9 configuration ground state for Ni acceptor exciton. The most intensive vibrational replicas of Ni donor exciton zero phonon line appears to have a combination character $\omega_{01} + n \omega_l$, where ω_{01} is the frequency of the motion of mainly second sphere ions, and ω_l is the frequency of the motion mainly of first sphere ions.

The defect vibrations in ZnSe:Ni and ZnO:Ni crystals induced by Ni impurity ions having a charge state of -1 (d^7 configuration) or +1 (d^9 configuration) with respect to the lattice are described. The calculations have been carried out in the framework of a recursive scheme in a shell model with the account of coulomb interaction for a cluster containing about 1000 ions. This approach permits to account of charge state of impurities. Increasing of the cluster sizes does not bring about essential quantitative changes to results of calculations. The lattice relaxation near the charged Ni impurity under consideration was also taken into account. The localised vibrations frequencies for A_1 , E and T_2 symmetry modes have been obtained and projected to the nearest two co-ordination spheres of the Ni impurity. Model calculations have enabled an interpretation of the vibronic structure in the experimental electroabsorption spectra of Ni impurity excitons in ZnSe:Ni, ZnO:Ni crystals. It was shown that defining factors in arising the localised fluctuations are a deforming a lattice near defect and its charge condition.

1. Sokolov V.I., Semiconductors, 1994, 28, 329-342

LOW FREQUENCY RAMAN PEAK AND ELASTIC ANOMALY OF DEHYDRATED HEAT-TREATED EGG-WHITE GEL

Aisushi Nakamura, Kazuhiro Hara¹, Nobuyasu Hiramatsu and Akihiro Matsumoto²

¹Department of Applied Physics, Faculty of Science, Fukuoka University,
Nanakuma, Jonan-ku, Fukuoka 814-0180, Japan

²Department of Applied Science, Faculty of Engineering, Kyushu University,

Hakozaki, Higashi-ku, Fukuoka 812-8581, Japan,

³Osaka Municipal Technical Research Institute,

Morinomiya, Joto-ku, Osaka 536-8553, Japan

The opaque heat-treated egg white gel turns in to a transparent substance by dehydration, which looks like a glass. We performed the observation of Raman spectrum of the dehydrated heat-treated egg white gel (abbreviated as DHTEWG hereafter) and found that there existed a pair of peaks in the low frequency region, which was similar to the boson peak observed commonly in many glasses. Therefore, in order to examine the glass transition in DHTEWG, we also measured the viscoelastic stiffness of DHTEWG with increasing temperature. In the measurement, the storage modulus decreased remarkably and the loss modulus showed a broad peak around the temperature where a thermal anomaly had been observed. Because these features are usually observed in the noncrystalline polymers around the glass transition temperature, the occurrence of the glass transition was confirmed in DHTEWG around T_g , namely, which meant that DHTEWG could be regarded as a glass.

However, we also noticed that there was a quantitative difference in the low-lying mode frequency between DHTEWG and some monomer glasses. Therefore, in order to clarify one of the effects on the low frequency Raman spectrum, the heat treatment of egg white, we also observed the low frequency Raman spectra of dehydrated egg white (DEW) without the heat treatment and compared with those of DHTEWG. From this investigation, a notable difference has been revealed in the low-lying band frequency: in DEW, it was approximately the same as that of the boson peak reported on many amorphous materials or glasses, on the other hand, in DHTEWG, the frequency was 2~3 times as much as that value.

A STUDY OF NETWORK DIMENSIONALITY IN CHALCOGENIDE GLASS BY LOW FREQUENCY RAMAN SCATTERING

Department of Physics, Graduate School of Science c/o Murase lab.,
Osaka University 1-1 Machikaneyama, Toyonaka 560-0043, Japan

M.Nakamura, O.Matsuda, Y.Wang and K.Murase

Recently, low frequency Raman spectral results are reported for $\text{Ge}_x\text{Se}_{1-x}$ glasses, and discussed on the basis of fracton dynamics and rigidity percolation[1]. The Raman intensity reduced by Bose factor, $I(\omega)/[n(\omega)+1]$ which are proportional to the vibrational density of states show a power-law dependence of the frequency, $g(\omega)\propto\omega^{\theta-1}$, in a low frequency region. The \bar{d} called spectral dimensionality is non-integer value.

The quantitative estimation of structural dimensionality of the network glass has not been made as yet. However, it is definitely clear that the glass structures have a certain dimension, such as polymeric glass(1D-like) and vitreous silica (3D-like). The Ge-chalcogenide glasses whose dimensionalities can be controlled by composition ratio are suitable for investigating the network dimensionality of glass structures. For example, in $\text{Ge}_x\text{Se}_{1-x}$ glasses, Se-rich samples are 1D-like network mainly composed of Se-chain, and GeSe_2 has layered 2D-like network. It has been also reported that the GeSe_2 glass is 1D-network polymeric glasses.

In this study, we will propose the possibility of dimensionality analysis of the Ge-chalcogenide network glass by low frequency Raman scattering. The spectral dimensionality of stretching motion (\bar{d}_s) of $\text{Ge}_x\text{Se}_{1-x}$ glasses increases with Ge composition ratio[1] and that of $\text{Ge}(\text{S}_2\text{Se}_{1-x})_2$ decreases with S composition ratio as shown in Figure 1(a) and (b). We will discuss these experimental results in correspondence to the actual dimensionality of Ge-chalcogenide glasses. The spectral dimensionality \bar{d} is defined by $\bar{d} = 2D/(2 + \theta)$. Here, D is Hausdorff fractal dimensionality and θ the exponent giving the dependence of the diffusion constant on distance with $\theta > 0$. The slow diffusion is caused by the presence of "dead end" in the glass network. The experimental results on the behavior of \bar{d}_s are closely related to the diffusion exponent θ . It is expected that the lower dimensionality glass has more "dead end" resulting in the larger value of θ and the smaller value of \bar{d} . The value of \bar{d}_s can be regarded as an indicator of network dimensionality for network glass.

[1] M.Nakamura *et al.*, Phys.Rev.B (1998) (in press).

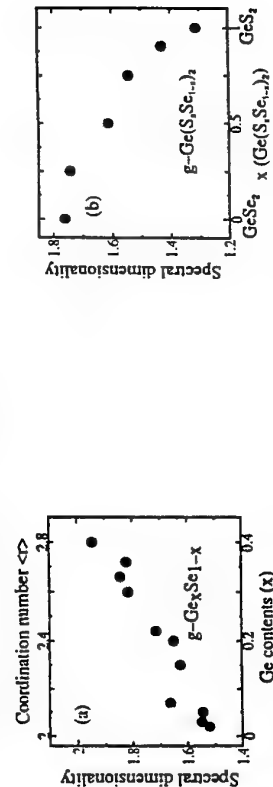


Figure 1: The behavior of \bar{d}_s for $\text{Ge}_x\text{Se}_{1-x}$ glasses(a) and $\text{Ge}(\text{S}_x\text{Se}_{1-x})_2$ glasses(b).

ANHARMONICITY OF VIBRATIONS AND QUASIELASTIC SCATTERING IN GLASSES

V.N. Novikov

Institute of Automation and Electrometry,
Russian Academy of Science, Novosibirsk, 630090, Russia

It is shown that the anharmonicity of vibrations leads to the quasielastic scattering in glasses and supercooled liquids. The vibrational self-energy term which arises due to anharmonic interaction provides the one-phonon quasielastic response. Estimations show that in the glass transition region the contribution of this mechanism to the quasielastic spectrum is dominant. The underlying fast relaxation process corresponds to the fluctuations of the vibration occupation numbers [1]. For the boson peak vibrations the respective relaxation time is of the order of a picosecond. The spectral shape of this fast relaxation is found. The amplitude of the quasielastic scattering intensity and its temperature dependence is estimated within the frames of the model and compared with experimental data on light scattering for various materials. The strength of the fast relaxation which is the integral ratio of the quasielastic to vibrational contribution was found to be proportional to the squared Grüneisen parameter.

It is shown that at high temperatures the quartic anharmonic term suppresses the contribution of the third order anharmonicity to the quasielastic scattering. As a result, a crossover temperature appears in the model; above this temperature the intensity of the fast relaxation does not increase anymore. This result is in a good agreement with the analysis of the Raman scattering data in B_2O_3 [2]. Within the frames of the model, the ratio of the crossover temperature to that of the glass transition is proportional to the inverse fourth - order anharmonic coefficient.

REFERENCES

1. V.N. Novikov, Phys. Rev. B 55, R14685 (1997).
2. A. Brodin, D. Engberg, L.M. Torell, L. Börjesson, A.P. Sokolov, Phys. Rev. B 53, 11511 (1996).

DIELECTRIC DISPERSION OF SiO_2 GLASS AT LOW TEMPERATURES

T. Ozaki, T. Ogasawara, T. Kosugi and T. Kamada

*Department of Physical Science, Faculty of Science, Hiroshima University,
Higashi-Hiroshima 739-8526, Japan*

It is interesting to know whether SiO_2 glass is a system of interacting relaxators which undergoes a structural phase transition in a low temperature region. We expect that a relaxation time τ of polarization shows an anomaly at a low temperature, if SiO_2 glass undergoes the phase transition. To examine this, we measured a low-frequency dielectric dispersion in a SiO_2 glass produced by using a soot method. Complex dielectric constants $\varepsilon^* = \varepsilon' - i\varepsilon''$ were obtained at frequencies of 10 Hz, 100 Hz, 1 kHz and 10 kHz in the temperature region from 3 K to 100 K. We analyzed ε^* , by using a least squares method, based on the following three assumptions. (1) τ obeys the Vogel-Fulcher law, $\tau = \tau_0 \exp[E(T - T_0)]$ and is distributed according to a normalized distribution function $f(E)$ of an energy parameter E . (2) ε^* is expressed as the superposition of the Debye formula with a weight of $f(E)$. (3) ε^* is independent of the frequency at 3 K. We found that $f(E)$ obtained at $T_0 = -1$ K and $\tau_0 = 1.2 \times 10^{-13}$ s best reproduced the measured ε^* . This shows that τ substantially obeys the Arrhenius equation, $\tau = \tau_0 \exp(E/T)$, and hence the cooperative interaction between relaxators is too weak to make SiO_2 glass undergo the structural phase transition even at low temperatures.

COMPARISON OF BALLISTIC PROPAGATION OF MOLECULAR AND PHONON BEAMS

T. Paszkiewicz and M. Pruchnik
Institute of Theoretical Physics, Wrocław University,
PL-50-204 Wrocław, pl. Maxa Borna 9, Poland

Narayanamurti and collaborators studied propagation of heat pulses in gaseous, liquid and solid helium [1, 2]. In particular they examined propagation of molecular pulses of ^3He and ^4He in helium vapour in both ballistic and hydrodynamic regime [1]. In their experiments linear dimensions of the heater and source as well as the distance between them were comparable. They concluded that heating of helium films produces Maxwellian pulses of the temperature T different than the ambient temperature T_0 . We present here kinetic description of ballistic molecular and phonon heat pulses in collisionless regime because the estimated (using experimental data of Narayanamurti et al [1]) mean free paths are approximately one order longer than the distance between source and detector.

Solving the collisionless Boltzmann equation containing a suitable source terms (cf. [3]) we study the explicit time and space dependence of these pulses for various types of sources and detectors — point and extended. For the source consisting of point-like source (or set of point sources) which radiates Maxwellian pulses of temperature T_1 and for both point and extended particle detectors, the agreement of our theoretical findings with experimental results of Narayanamurti et al [1, 2] for molecular pulses of ^3He and ^4He is quite satisfactory. The arrival times of pulses t_{arr} and the leading fronts of pulses agree quite well. In the agreement with the experimental findings the propagation velocity and the width of molecular pulses depend on T .

However, V. Narayanamurti drew our attention to the fact that the agreement is better for ^4He than for ^3He , which he attributed to the enormously large heat conductivity of superfluid ^4He films, which make them more homogeneously heated. Therefore, for weakly heated ^3He beams, we considered spatially inhomogeneous source consisting of a circle radiating Maxwellian pulses of temperature T_1 and a point source (a spot of "boiling" ^3He liquid) radiating Maxwellian pulses of the temperature T_2 ($T_2 > T_1$). For $T_2 \approx 2T_1$ (where $T_1 = 0.6$ K) we obtained a very good agreement with the experimental results of Narayanamurti et al [2]. For moderately heated ^3He films we considered more inhomogeneous film states with two point sources producing Maxwellian beams of different temperatures T_1, T_2 . Again, for $T_2 \approx 2T_1$ ($T_1 = 3.16$ K) the fit of our formula to the experimental findings is excellent.

We expect that our results shed some light on the problem of cooling crystalline specimens immersed in helium.

In comparison, we also considered pulses of phonons moving in an isotropic medium. We shown that phonon pulses (even Maxwellian ones) always have the form of narrow peaks moving with the group velocity.

References

- [1] K. Andres, R.C. Dynes, V. Narayanamurti, Phys. Rev. A **8**, 2501 (1973).
- [2] V. Narayanamurti, R.C. Dynes, K. Andres, Phys. Rev. B **11**, 2500 (1975).
- [3] Cz. Jasinkiewicz, T. Paszkiewicz, D. Lehmann, Z. Phys. B **96** 213 (1994).

COMPUTER EXPERIMENTS ON ANOMALOUS DIFFUSIVE PROPAGATION OF PHONON BEAMS IN CUBIC ELASTIC MEDIA CONTAINING POINT MASS DEFECTS

M. P. Blencowe[†], T. Paszkiewicz[‡] and M. Pruchnik[‡]

[†]The Blackett Laboratory, Imperial College, London SW7 2BZ UK,

[‡]Institute of Theoretical Physics, Wrocław University,

PL-50-204 Wrocław, pl. Maxa Borna 9

We considered mixed valence semiconductor alloys of cubic symmetry eg $\text{Sm}_x\text{La}_{1-x}\text{S}$, $\text{Sm}_x\text{Y}_{1-x}\text{S}$, $\text{Sm}_x\text{Tm}_{1-x}\text{S}$ and Tm_2Se . For some critical value of nonstoichiometry x the semiconductor-to-metal phase transition occurs [1]. This transition manifests in anomalies of elastic and transport properties. For example, for some critical value of x the sum of elastic constants ($C_{12} + C_{44}$) becomes very small and scattering processes of phonons by point mass defects accompanied by polarization conversion processes become very rare. Therefore, the standard derivation of the diffusion equation based on perturbation theory with respect to the small Knudsen number, which is valid when the effectiveness of processes which mix polarization and of processes chaoticising directions of phonon wave vectors are comparable [3], does not work and one has to modify it. The slowing down of elastic scattering processes with polarization conversion makes the corresponding diffusion coefficient D anomalously large. On the line $C_{12} = -C_{44}$ (aa -line), the conversion processes are forbidden and D exhibits a singularity [2].

To gain some understanding of the nature of this anomaly of the diffusion constant in the vicinity of aa -line we performed the set of computer experiments on the propagation of phonon beams scattered by point mass defects. At temperatures much lower than the Debye temperature and in the vicinity of aa -line only spontaneous phonon down conversion processes mix polarizations of phonons. Therefore, we included also phonon down conversion processes into our computer experiments and observed that they regularize the diffusion constant. We concluded that, differently than in the quasidiffusion regime, in the region of weak elastic scattering processes with conversion, the spontaneous down conversion processes reduce the diffusion coefficient.

References

- [1] H. Boppart, J. Magn.Magn. Mat. **47&48**, 436 (1985),
- [2] T. Paszkiewicz, M. Pruchnik, J. Low Temp. Phys., May, 1998,
- [3] T. Paszkiewicz, M. Wilczyński, in: Dynamical Properties of Solids, vol. 7, Phonon Physics, The Cutting Edge, ed. by G.K. Horton and A.A. Maradudin, North-Holland, Amsterdam, pp. 257-348 (1995).

Tunneling electric dipole defects in insulating glass: soft mode and spin-glass like transition

G. Busiello^a, R. Saburova^b

^aDipartimento di Scienze Fisiche "E.R. Caianiello", Università di Salerno
I-84081 Baronissi - Salerno, Italy,

^bIstituto Nazionale di Fisica della Materia, Sezione di Salerno, Salerno, Italy

^cPhysical - Technical Institute, Russian Academy of Science, Kazan, Russia

A theoretical study of the dynamics of the two-level systems (TLS) interacting both, with each other and with "lattice" vibrations in glass is presented. The spectrum and damping of the collective excitations is calculated. The frequency dependence and concentration of phonon lifetimes are analysed. It is shown that one of the collective modes becomes soft signaling about spin-glass-like phase transition in insulating glass. The theory of resonance phonon scattering by the two-level systems in the TLS with acoustic vibrations and strong interaction between TLS. The contribution of the collective excitations to the specific heat is determined.

HARMONIC VIBRATIONAL EXCITATIONS IN DISORDERED SOLIDS AND

THE "BOSON PEAK"

W. Schirmacher¹, G. Diezemann², and C. Ganter¹¹Phys. Dept. E13, Technische Universität München, D 85747 Garching, Germany²Institut für physikalische Chemie, Universität Mainz, Mainz, D 55099

Mainz, Germany

In order to obtain a model description of vibrational excitations in disordered solids (such as glasses or polycrystals) we consider a system of coupled classical scalar harmonic oscillators with nearest-neighbor interactions on a simple cubic lattice. The force constants are assumed to fluctuate from bond to bond according to a Gaussian distribution which is truncated at its lower end. The model is solved both by numerically diagonalizing the Hamiltonian and by applying the two-site coherent potential approximation (CPA). The results for the density of states (DOS) $g(\omega)$ are in excellent agreement with each other. If the system – due to the presence of negative force constants – is almost unstable the reduced DOS $g(\omega)/\omega^2$ exhibits a low-frequency peak ("boson peak"), which is a precursor phenomenon of the instability. We show that the occurrence of the boson peak is a generic phenomenon of a strongly disordered system of coupled harmonic oscillators.

In our model the phonon mean free path is very short in the frequency range of the boson peak but the states are not localized. This is shown by means of the level distance statistics.

We discuss the general trends of the boson peak phenomenon in disordered solids in terms of our model.

THERMAL CONDUCTIVITY OF $\text{Cu}_x\text{Sn}_{100-x}$ FILMS AT LOW TEMPERATURESR. Schmidt, Th. Franke, P. Häussler
TU Chemnitz, Institut für Physik, 09107 Chemnitz, Germany

$\text{Cu}_x\text{Sn}_{100-x}$ serves as a model substance to study amorphous systems. Among many other properties the resistivity, the thermopower and the Hall coefficient, as well as the low temperature specific heat and structural data are well known.

Here we report on the thermal conductivity of amorphous and polycrystalline samples prepared at $T = 5$ K on a microchip. The measurements were performed with an improved steady-state technique in the range from $1.2 \text{ K} < T < 360 \text{ K}$. We separate the electronic part from the total thermal conductivity with the Wiedemann-Franz law and discuss the main scattering processes contributing to the phonon-thermal conductivity. The amorphous samples show superconductivity below $T_c = 5.71 \text{ K}$ for $x = 20 \text{ at\% Cu}$ and below 1.2 K for 70 at\% Cu . After crystallization T_c becomes lower. In the amorphous state below T_c a T^2 -dependence due to disorder was observed. Above T_c phonon-electron scattering becomes important and λ^{Pa} follows T^n ($1 < n < 2$). The exponent n depends on structural disorder. At temperatures between $T = 3 \text{ K}$ and 30 K a plateau region due to low-energy excitations was found in the phonon part of the thermal conductivity. The plateau relates to structural anomalies at scattering vectors $k = 2k_F$ and shifts with increasing x to lower temperatures. For alloys with $x \geq 60 \text{ at\% Cu}$ it has also been observed after crystallization shifted to lower temperatures but vanishes after further annealing.

INELASTIC ELECTRON-BOUNDARY SCATTERING IN THIN FILMS

A. Sergeev

Dep. of Physics, University of Regensburg, D-93040 Regensburg, Germany
 Moscow Pedagogical University, Moscow 119482, Russia

Inelastic electron scattering at the interface between a conducting film and an insulating substrate provides a new channel for energy transfer from the film electrons to the substrate phonons. Its contribution to the Kapitza conductance is found to be $\hbar u \gamma / k_B \tau_{e-ph}$, where u is the sound velocity, γ is the Sommerfeld constant, and τ_{e-ph} is the electron-phonon energy relaxation time in the film. This mechanism is significant for conductors with strong electron-phonon coupling, or for an interface with a small value of the phonon transparency ($\alpha \leq 0.05$). Our results can explain the observed decrease of the Kapitza conductivity at the transition to the superconducting state [1], and an universal minimal value of the Kapitza conductance for pairs of materials with rather different acoustic impedances [1,2]. Due to the small value of the phonon transparency of the interface between YBaCuO film and any known substrate [3], the suggested mechanism probably gives a significant contribution to the conductance in this case.

In the wide temperature range the inelastic electron-boundary scattering in pure thin films determines the temperature-dependent part of the electrical conductivity (T^2 -term) and the electron dephasing rate. These effects are analogous to the effects of electron-impurity scattering in impure films [4].

Finally, this scattering mechanism results in a nonequilibrium component of the photoresponse with the picosecond decay time proportional to the film thickness that has been recently observed in YBaCuO ultrathin films [5].

The research is supported by the Alexander von Humboldt Stiftung.

- [1] E.T. Swartz and R.O. Pohl, *Rev. Mod. Phys.* **61**, 605, (1989).
- [2] R.J. Stoner and H.J. Maris, *Phys. Rev. B* **48**, 16373 (1993).
- [3] A.V. Sergeev, A.D. Semenov, P. Kouminov et. al, *Phys. Rev. B*, **49**, 9091 (1994)
- [4] N.G. Pitsina, G.M. Chulkova, K.S. Il'in, A.V. Sergeev, F.S. Pochinkov, E.M. Gershenzon and M.E. Gershenzon, *Phys. Rev. B* **56** 10089 (1997).
- [5] L. Shi, G.L. Huang, C. Lehan et. al, *Phys. Rev. B*, **48**, 6550 (1993).

LOW ENERGY VIBRATIONAL EXCITATIONS IN METALLIC GLASS ($\text{Mo}_{0.6}\text{Ru}_{0.4}\text{B}_{20}$) AND ITS ANOMALIES INDUCED BY SUPERCONDUCTIVITYK. Shibata¹⁾, Y. Yamazaki¹⁾, K. Matsuzaki²⁾, H. Takakura³⁾ and K. Suzuki¹⁾

¹⁾Institute for Materials Research, Tohoku University, SENDAI 980-8577, Japan

²⁾Mechanical Engineering Laboratory, Agency of Industrial Science and Technology, TSUKUBA 305-8564, Japan

³⁾National Research Institute for Metals, Sengen 1-2-1, TSUKUBA 305-85, Japan

We have investigated the low energy vibrational excitations; so called Boson peak in metallic glass ($\text{Mo}_{0.6}\text{Ru}_{0.4}\text{B}_{20}$) and its anomalies induced by superconductivity.

We prepared the superconducting metallic glass ($\text{Mo}_{0.6}\text{Ru}_{0.4}\text{B}_{20}$) ribbon sample by a single-roller melt-spinning technique.

It was showed that this sample had a sharp superconducting transition at $T_c = 6.0 \pm 0.1$ K and was a type II superconductor and the lower and upper critical field H_{c1} and H_{c2} were 23 Oe and 1.1 kOe respectively at 4.2 K. Its gap energy 2Δ was 1.8 meV.

We performed coherent inelastic neutron scattering measurements on LAM spectrometer in KEK, from room temperature to below T_c , with an energy resolution $\Delta E = 0.2$ meV at an elastic position.

At room Temperature, the spectrum; $G(Q, \omega) / \omega^2$ of the generalized vibrational density-of-states divided by ω^2 showed a broad peak of the low energy vibrational excitations with the peak energy $\hbar\omega_g = 3.3$ meV. The intensity of

low energy vibrational excitations around peak position showed a Q-dependence except Q^2 -dependence and had the first broad peak around $Q = 2.8 \text{ \AA}^{-1}$ where the structure factor $S(Q)$ had the first principal peak.

On the other hand, around T_c , the generalized vibrational density-of-states spectrum showed an anomalous enhancement in low energy range around a gap energy $2\Delta = 1.8$ meV. Its anomalous enhancement was starting below about 100K, and was increasing with decreasing temperature, and then had a broad maximum around T_c . Also this anomalous enhancement showed a Q-dependence and appeared around the first principal peak of $S(Q)$. It suggests that the low energy vibrational excitations; so called Boson peak in this metallic glass interacted strongly with the superconducting electrons.

LOCALIZED VIBRATIONAL STATES IN AMORPHOUS $Tb_{1-x}Fe_x$ FILMS AND PHONON-FRACTON CROSSOVER IN AMORPHOUS Fe_9Zr

W. Sturhahn, R. Röhlsberger¹, T.S. Toellner, and E.E. Alp
Argonne National Laboratory, Advanced Photon Source,
9700 South Cass Ave., Argonne, IL 60439, USA

T. Ruckert and W. Keune
Laboratorium für Angewandte Physik, Gerhard - Mercator - Universität Duisburg,
47048 Duisburg, Germany

We present measurements of the vibrational density of states of thin films (17.5 nm) of amorphous iron-terbium alloys and of amorphous Fe_9Zr (bulk). The novel PHOENIX (PHONon Excitation by Nuclear Inelastic absorption of X-rays) technique is used to selectively investigate vibrations at the iron positions. The vibrational properties of the amorphous material are distinctly different from those of the crystalline phases. In particular, the vibrational density of states of the thin films was measured with an energy resolution of 5.5 meV and we find a deviation from Debye-like scaling for low energies (5 meV - 15 meV). In case of the amorphous Fe_9Zr alloy, we achieved an energy resolution of 0.66 meV, which permits to observe the crossover from Debye-like to non Debye-like scaling. We explain this behavior with the fracton model and infer the existence of localized vibrational states. The presented data was obtained at sector 3-ID of the Advanced Photon Source.

This work is supported by US-DOE, BES Materials Science, under contract No: W-31-109-ENG-38.

¹present address: Universität Rostock, August - Bebel - Str. 55, 18051 Rostock, Germany.

MECHANICAL RESPONSES OF HELIUM FILM ADSORBED ON TWO-DIMENSIONAL MESOPOROUS HECTORITE

M. Hieda, M. Suzuki, H. Yano^a, N. Wada^a, and K. Torii^b

^aUniversity of Electro-Communications, Chofu, Tokyo 182, Japan

^bGovernment Industrial Research Institute of Tohoku, Miyagi-ku, Sendai 983, Japan

To investigate the mechanical responses of adsorbed 3He films to the vibration of substrates, we performed the ultrasonic measurements of two-dimensional mesoporous hectorite covered with thin 3He films (< 1.3 layers) in the temperature range 150 mK to 20 K.

Because of the very large surface area of hectorite (484 ± 3 m²/g), the change in elastic properties caused by the adsorbed 3He films was observed. Figure 1 shows the variation of the sound velocity and attenuation at 0.505 layer 3He film. The sound velocity increased drastically around 4K accompanied with the attenuation. It was found that the observed increase of the sound velocity is proportional to the film thickness, and that the temperature dependence of both the sound velocity and attenuation is well explained by the thermal activated relaxation process. This behavior suggests that the adsorbed 3He film is decoupled from the vibration of the substrate in the low temperature region.

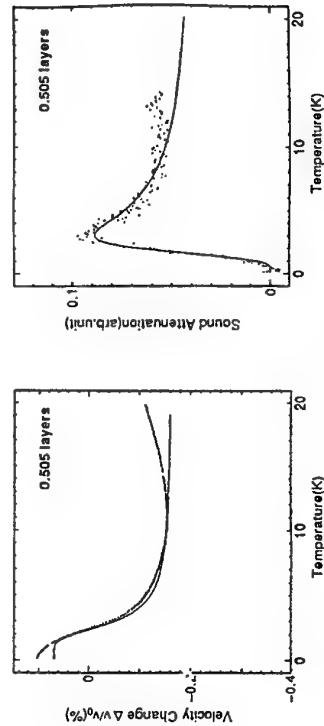


Fig. 1: Variation of the sound velocity and attenuation at 0.505 layer. Solid curves are calculated by assuming the thermal activated relaxation process.

Temperature Dependence of Depolarized Spectra in n-Propanol

Yasunari Takagi[†], Toru Yano[†] and M. Mikami [‡], Seiji Kojima[†][†]Department of Applied Physics and Chemistry,

The University of Electro-Communications, 1-5-1, Chofu, Tokyo 182, Japan

[‡] Institute of Applied Physics, University of Tsukuba, Tsukuba, Ibaragi 305, Japan

The liquid-glass transition in the n-propanol has been investigated from temperature dependence of the depolarized spectra. Temperature-dependence of spectra were measured with the backward scattering by using the Brillouin. The fitting analyses were performed using the spectral function of the Davidson-Cole. The relaxation time obtained was one order higher than one already reduced from the polarized spectra using the spectral function of the viscoelastic theory in single relaxation-time approximation. It was found that in the Brillouin scattering, the relaxation in the depolarized spectra differed from one coupled with the longitudinal acoustic phonon in the polarized spectra. Moreover, in comparison with the results of dielectric measurement, the relaxation in the depolarized spectra corresponds to the combined relaxation of II- and III-modes appeared in the high frequency side of I-mode, the intensity of which was the strongest in the dielectric measurement.

VIBRATIONAL CHARACTERISTICS OF CLUSTER-CLUSTER AGGREGATIONS

T. TERAQ and T. NAKAYAMA

Department of Applied Physics, Hokkaido University, Sapporo 060-8628, Japan

We investigate vibrational characteristics of cluster-cluster aggregations changing their formation conditions. At first, the aggregates are formed on a simple cubic lattice under different particle concentrations, and the density-density correlation functions have been calculated for these systems. A self-similar behavior has been realized on cluster-cluster aggregations at lower particle concentrations. We have calculated the frequency dependence of the density of states, showing a power-law behavior $\mathcal{D}(\omega) \propto \omega^{\bar{d}-1}$, where \bar{d} is a spectral dimension. The spectral dimensions \bar{d} for three-dimensional systems take a value $\bar{d} = 1.17 \pm 0.04$ for *diffusion-limited* cluster-cluster aggregation and $\bar{d} = 1.28 \pm 0.03$ for *reaction-limited* cluster-cluster aggregation, respectively. These results indicate that the density of states depends on a sticking probability of clusters when forming an aggregate. At higher particle concentrations, the crossover from extended phonons to strongly localized excitations is clearly observed.

We have also investigated the frequency dependence of the dynamical structure factor $S(q, \omega)$ and its scaling properties. A broad peak with a long tail extended to higher frequency is observed, which is in agreement with scattering experiments on silica aerogels. For lower particle concentrations, calculated results collapse onto a single universal curve, indicating that $S(q, \omega)$ satisfy the single-length-scaling postulate. On the contrary, $S(q, \omega)$ for the system with higher concentrations are not rescaled with a single characteristic length scale.

FREQUENCY AND TIME-RESOLVED SPECTROSCOPIC STUDY OF LIQUID-GLASS TRANSITION IN D-SORBITOL

Y. Tajima, M. Kobayashi and T. Yagi

Research Institute for Electronic Science, Hokkaido University, Sapporo 060-0812, Japan

D-sorbitol $[\text{HOCH}_2(\text{CHOH})_4\text{CH}_2\text{OH}]$ is a fragile glass-former with linear carbon-chains and hydrogen-bonded networks. The liquid-glass transition and melting points are $T_g = -7^\circ\text{C}$ and $T_m = 97^\circ\text{C}$, respectively.[1] The two step relaxation (α - and β -relaxations) in D-sorbitol is investigated in a wide frequency range of 7 decades from 1 MHz to 10 THz by three types of light scattering techniques; Raman scattering (0.6 ~ 10 THz), Brillouin scattering (1 GHz ~ 1 THz) and time-resolved spectroscopy (1 MHz ~ 1 GHz).[2]

Figure 1 shows the imaginary part of dielectric susceptibility $\chi''(\omega)$ evaluated from the scattered intensity obtained by depolarized Raman and Brillouin scatterings. The susceptibility $\chi''(\omega)$ shows minimum at a particular frequency ω_{min} , indicating β -relaxation of the mode coupling theory (MCT). The exponents a and b obtained from a fit to the equation $\chi''(\omega) = \chi''_{\text{min}} [b(\omega/\omega_{\text{min}})^a + a(\omega/\omega_{\text{min}})^b]/(a+b)$ are 0.9 ± 0.2 and 0.18 ± 0.04 , respectively. The exponent a can also be obtained from $\omega_{\text{min}} \propto (T - T_g)^{1/2a}$, and we have $a = 0.5 \pm 0.05$ and $T_g = 33 \pm 2^\circ\text{C}$. The values of a and b are clearly contradict with the condition of MCT giving relationship between them; $\Gamma(1-a)^2/\Gamma(1-2a) = \Gamma(1+b)^2/\Gamma(1+2b)$ where Γ represents a gamma function.

Frequency shift $\Delta\nu$ and width $\delta\nu$ of the Brillouin peaks of the longitudinal acoustic mode are plotted in Fig. 2 as a function of temperature. A peak of α -relaxation seems to exist near T_m as shown from the data of $\delta\nu$. To study α -relaxation sufficiently, the frequency range lower than 1 GHz (spectral resolution limit of Brillouin scattering) is now examined by the use of the time-resolved spectroscopy.

[1] C. A. Angell and D. L. Smith : J. Phys. Chem. **88** (1982) 3845.

[2] Y. Yang and K. A. Nelson : J. Chem. Phys. **103** (1995) 7722.

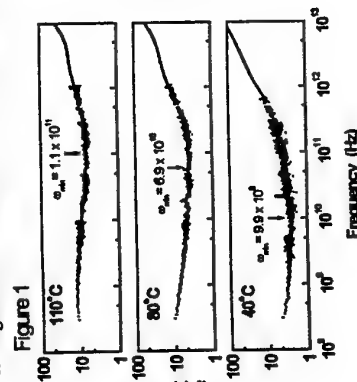


Figure 1

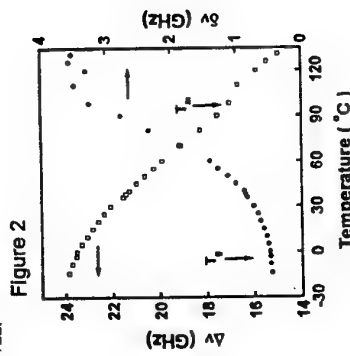


Figure 2

STUDIES OF ANISOTROPIC THERMOELECTRICITY IN LAYERED OXIDE MATERIALS AND TIME-RESOLVED PHONON KINETICS

Deborah Van Vechten (US Office of Naval Research, Arlington, VA 22217, USA), Kent S. Wood, Gilbert G. Fritz, James S. Horwitz, Rhonda M. Stroud, Ray C. Y. Auyeung, Jeungoo Kim, Syed B. Qadri (US Naval Research Laboratory, Washington, DC 20375, USA), Ashot L. Gyalamiryan, Vahan R. Nikogosyan (Physics Research Institute, Asharak, 378410, Armenia), Armen M. Gulian (USRA/US Naval Research Laboratory, Washington, DC 20375, USA)

One of the properties of the high temperature superconductors that has attracted considerable attention is the transient longitudinal voltage pulses that occur in the normal state following the absorption of light pulses in thin film samples. In this talk we will describe our experiments which unambiguously confirm that the observed effects arise from the thermoelectric response of these layered oxide materials to heat fluxes propagating vertically within the film, orthogonal to the voltage measurement axis. (Thermoelectric voltage and its inverse the Peltier effect are two phenomena which depend intimately on the coupling of electrons and phonons in a solid.)

Our measurements use sub-nanosecond trains of laser pulses in UV, visible (green) and IR wavelengths, directed onto patterned and unpatterned films, grown on a variety of substrates. Illumination is from either side of the film, and both spatially localized and homogeneous beams have been used. Good agreement of the measurable voltage characteristics with a macroscopic model based solely on the Seebeck tensor of the material is found.

We will also discuss the status of our efforts to use the temporal behavior of the experimental signal amplitude to derive a microscopic model of the electron and phonon kinetics within the film.

RIGIDITY PERCOLATION AND STRUCTURE OF Ge-Se SYSTEM

Y. Wang, M. Nakamura, O. Matsuda and K. Murase
Department of Physics, Graduate School of Science, Osaka University,
1-1 Machikaneyama, Toyonaka, Osaka 560-0043, Japan

Structural properties of $\text{Ge}_2\text{Se}_{1-x}$ ($0 \leq x \leq 0.33$) system are investigated by Raman scattering ($\geq 3 \text{ cm}^{-1}$) in a wide temperature range, 4-1200K. From changes of spectral shapes ($\geq 150 \text{ cm}^{-1}$) at various temperatures, information of the medium range structures and their changes during the glass-transition, crystallization and melting has been obtained.

Reducing the low frequency Raman intensity in the frequency range of 20-100 cm^{-1} by Bose factor, $n(\omega)+1$, the vibrational density of states suggests that glassy $\text{Ge}_2\text{Se}_{1-x}$ structure can be classed as a fractal structure. Stretching fractons appear in all the glasses, while bending fractons are observed only in the Se-rich samples. The threshold occurs at average coordination number, $\langle r \rangle$, of 2.4, which is the rigidity percolation old occurs at average coordination number, $\langle r \rangle$, of 2.4, which is the rigidity percolation threshold predicted by the Phillips-Thorpe constraint theory. In the higher frequency region, 150-350 cm^{-1} , temperature dependence of the Raman spectra shows that c- GeSe_2 like crystalline embryo increases with increasing temperatures above the glass-transition in the $\text{Ge}_2\text{Se}_{1-x}$ ($0.10 \leq x \leq 0.25$). In $\text{Ge}_2\text{Se}_{1-x}$ ($x=0.10, 0.15$), where no crystalline spectra are observed in our experimental period ~ 10 hours, the c- GeSe_2 like embryo appears and then resolves at melting point. At $x=0.18$, the crystallization of c- GeSe_2 easily occurs. The crystallization period abruptly changes at $x=0.18$ ($r=2.37$) which is related to the prediction basing on the constraint theory. The fragility of the glass-former is proposed, by Sokolov et al. recently, to be also described by the low frequency Raman spectrum which includes the boson peak and the quasielastic scattering. They described the fragility as I_{\min}/I_{\max} , where I_{\min} and I_{\max} are the Raman scattering intensities divided by the frequency, ω , and the Bose factor, $n(\omega)+1$, respectively, at the minimum close to the Rayleigh line, and at the maximum of the boson peak. In Ge-Se system, we find that the fragility increases with the decrease of the average coordination number.

THE PHONON ASSISTED SHIFT OF THE ENERGY LEVELS OF LOCALIZED ELECTRON STATES IN STATICALLY DISORDERED SOLIDS

I.A. Weinstein, A.F. Zatspin, Yu.V. Shchapova

Department of Physics and Technology, Ural State Technical University,
19 Mira Str., 620002 Ekaterinburg, Russia

The interaction between lattice vibrations and localized electron states in tails of the energy bands of non-crystalline solids has a great effect on their optical properties. As distinct from crystals, no unified opinion have been available so far with respect to the interpretation of the optical spectra taken at the fundamental absorption edge in disordered structures. The known semi-empirical approaches make use of model parameters, which, as a rule, are devoid of any physical content. Eventually, no information can be derived about the energy and the type of the interacting phonons in systems having a statically disordered atomic structure.

This study deals with the use of Fan's microscopic theory, as applied for description of the thermal shift of the optical absorption boundary taking glassy lead silicates as an example. The behavior of the fundamental absorption edge was examined experimentally and theoretically at various temperatures for different glass matrix compositions. The spectral and temperature dependences of the absorption coefficient determined for the region corresponding to optical transitions between localized states in band tails are described by Urbach's modified rule. The temperature shift to the long-wave region and the invariability of the slope of the spectral characteristic reflect the large role played by the static disorder in the formation of the absorption edge (the "frozen" phonon model), which is typical of many non-crystalline structures. However, the regularities in the observed shifts of the optical boundary suggest that the thermal movement of atoms (the dynamic phonon model) makes a considerable contribution to the processes of the thermally induced shift of the energy states in band tails of disordered systems.

The Fan-Radkowsky-Davydov formalism was used to estimate the effective energy of the phonons, which determine the temperature shift of the energy levels of the localized states of band tails. The experimental temperature dependences of the optical transitions are well described allowing for the effect that the lattice thermal expansion and the electron-phonon interactions have on the location of electron levels. The calculated phonon energies correlate with the results of the Raman spectroscopic examination of the said materials. They correspond to the frequency interval of long-wave acoustic vibrations induced by lead-oxygen bonds and different-valence lead ions distributed in the silicate matrix. The concentration dependences of the phonon frequencies and the optical gap exhibit peculiarities caused by the transformation of the type of the short-range structural order. The observed behavior of these energy characteristics agrees fairly well with measured parameters of the photo-induced and secondary electron emissions to whose mechanisms the participation of phonons is essential.

Thus, it was shown that the temperature effects taking place at the fundamental absorption edge in statically disordered systems can be correctly described if one allows for the contribution of the phonon subsystem. The approach discussed explains the temperature shift of the long-wave optical edge in glassy lead silicates by the interaction of the electron optical transitions between localized states with low-frequency deformation vibrations induced in the lead-oxygen sublattice.

THERMODYNAMICS OF IRREVERSIBLE HEAT GENERATION IN GLASSES AT LOW TEMPERATURES

Oliver B. Wright*

Department of Applied Physics, Faculty of Engineering,

Hokkaido University, Sapporo 060, Japan

*Also with PRESTO, Japan Science and Technology Corporation (JST), Kawaguchi 332,
Japan

Dissipation accompanying mechanical strain in glasses at low temperatures has been widely investigated by methods that rely on the response to a cyclic deformation. Typical examples are the measurement of internal friction in a vibrating reed experiment or with a torsional pendulum, or the measurement of ultrasonic attenuation. However, there have also been investigations based on the thermoelastic effect that can probe dissipation *within* a cycle of strain, rather than the response integrated over a single or several cycles as in the above examples.[1,2] In particular, experiments on silica, polymers and metallic glasses at low temperatures have shown that this instantaneous dissipation can be effectively accounted for by a model in which the occupation probabilities of the upper states of the two-level systems in glasses are treated as internal variables in the context of irreversible thermodynamics.[3,4] However, although the results of such calculations were given, the thermodynamical formalism has not been published. The purpose of this paper is to present these calculations and show how, through a proper consideration of the irreversible entropy production, the instantaneous temperature change under adiabatic conditions, or the instantaneous heat output under isothermal conditions, can be simply evaluated for a given applied strain variation.

A similar formalism can be used for variables other than stress or strain in glasses at low temperatures: for example, to predict the response to transient heating, as in experiments that measure the time-dependent specific heat of glasses, or to predict the heat generation on applying an electric field.

[1] O. B. Wright and W. A. Phillips, *J. Phys.*, Paris, **42**, C4, 1017 (1981); *Physica* **108B**, 859 (1981)

[2] H. Tietje, M. von Schickfus and E. Gmelin, *Z. Phys.* B **64**, 95 (1986)

[3] O. B. Wright, *Phil. Mag.* **B53**, 477 (1986)

[4] O. B. Wright and W. A. Phillips, *Phil. Mag.* **B50**, 63 (1984)

VORONOI ANALYSIS ON MICROSTRUCTURES OF LOCALIZED INSTANTANEOUS NORMAL MODES IN LIQUID Na

Wen-Jong Ma, Dept. of Physics, National Sun Yat-Sen University, Kaohsiung, Taiwan, R.O.C.

Ten-Ming Wu, Institute of Physics, National Chiao-Tung University, HsinChu, Taiwan, R.O.C.

Abstract

The instantaneous-normal-mode (INM) densities of states for liquid Na in realistic thermodynamic states have been calculated with molecular-dynamic simulation by Wu and Tsay¹. The regions for the high-frequency localized INMs of both the real-frequency and the imaginary-frequency lobes are determined through the size dependence of the INM participation ratio. It has been shown that each localized INM indeed has only one excitation center at the particle with the largest eigenvector projection component and the spatial size of the localization extends to its first nearest neighbor shell. In this paper, we perform a Voronoi analysis on the central particle of each localized INM, and then averaged with all localized INMs within a frequency bin. Through this study, we find that the microstructure around the center of a localized INM is strongly distorted, as compared with those of other particles in the liquid. The example microstructures of localized INMs with real and imaginary frequencies are also shown.

1. T. M. Wu and S. F. Tsay, *J. Chem. Phys.* **105**, 9281 (1996); *Prog. Theo. Phys. Suppl.* **126**, 343 (1997).

Dynamical Delocalization of One-Dimensional Disordered System with Lattice Vibration

Hiroaki Yamada

Faculty of Engineering, Niigata University, Niigata 950-21, JAPAN

The localization phenomena in one-dimensional disordered quantum systems (1-DDS) have been extensively studied since several decades ago. It is well known that almost all the eigenstates are localized under the presence of any disorder. The quantum diffusion of wave packet in the 1-DDS is in general suppressed within a finite length by the interference effect. On the other hand, stochastic perturbation will destroy the quantum coherence which is the origin of the Anderson localization, and the wave packet diffuses beyond the intrinsic localization length. Then the influence from the heat reservoir is modeled by stochastic forces applied to each of lattice sites.

A more interesting scenario of the electronic stochasticization is the possibility that the stochasticization is organized in the dynamically perturbed 1-DDS.

The dynamical perturbation is modeled by linear oscillator containing M independent (mutually incommensurate) frequency components [1]. The linear oscillator can be identified with a highly excited quantum harmonic oscillator [2]. For $M \geq 2$ a diffusive behavior emerges and the presence of finite localization length can no longer be detected numerically. The diffusive motion obeys a subdiffusion law characterized by the exponent α as $\xi(t)^2 \propto t^\alpha$, where $\xi(t)^2$ is the mean square displacement of wave packet at time t . With increase in M and/or the perturbation strength, the exponent α approaches rapidly to 1 which corresponds to the normal diffusion. Moreover, the space(x)-time(t) dependence of the distribution function $P(x, t)$ is reduced to a scaled form decided by α and an another exponent β such that $P(x, t) \sim \exp\{-const.(|x|/t^{\alpha/2})^\beta\}$, which contains the two extreme limits, i.e., the localization limit ($\alpha = 0, \beta = 1$) and the normal-diffusion limit ($\alpha = 1, \beta = 2$) in a unified manner. Some 1-DDSs driven by the oscillatory perturbation in different ways are examined and compared.

1. H. Yamada and K. S. Ikeda, in preparation.
2. H. Yamada and K. S. Ikeda, Phys. Lett. A222, 76(1996).

ANIHARMONIC EFFECTS OF PHONON SCATTERING FROM CRYSTAL SURFACES

P. Zieliński, *Institute of Nuclear Physics, ul. Radzikowskiego 152, 31-342 Kraków, Poland*
Z. Lodzińska, *Institute of Nuclear Physics, ul. Radzikowskiego 152, 31-342 Kraków, Poland*

It has been shown [1] that the amplitude of vibrations of the surface atoms can be significantly larger than the amplitude of atomic vibrations in the bulk of the crystal. This happens in particular whenever the vibrational frequency is close to the surface resonances or to edge singularities in LDOS. The harmonic approximation to the lattice dynamics of the crystal with surfaces then is insufficient even though it might correctly account for the phonon dynamics in the bulk.

Actuated by the above observation we have constructed a model in which the surface atoms of an otherwise harmonic crystal are additionally placed in an anharmonic local potential. Dispersionless substrates as well as substrates with strong spatial dispersion have been considered. Two kinds of theoretical treatment of such models have been applied. The first approach amounts to directly solving the equations of motion in analogy to the molecular dynamics (MD) method. The size of the model system then is always limited to a finite number of the unit cells. This limitation is avoided in the second approach in which the effective number of degrees of freedom is systematically reduced to those atoms which are explicitly subject to the anharmonic potential. The resulting equations of motion have been shown to take on the form of integro-differential equations of Volterra type. The influence of the eliminated harmonic degrees of freedom is reflected by the corresponding memory kernels. The explicit forms of such equations of motion will be presented for the most common one-dimensional substrates.

The response of the described systems to an oscillatory perturbation applied from outside as well as to the irradiation of the surface with phonons coming from the bulk have been studied. With increasing amplitude of the perturbation the surface atoms have been found to generate higher harmonics and/or subharmonics. At some ranges of the applied amplitudes and frequencies the motion of surface atoms becomes irregular and shows features of a chaotic intermittence.

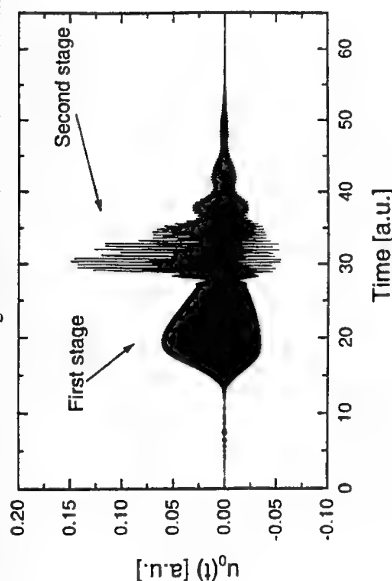


Fig. 1. Time-dependent displacement $u_s(t)$ of a surface atom as the response to a Gaussian wave-packet sent from the bulk. Visible are two stages of the reflection corresponding to a splitting of the wave packet due to spatial dispersion. Higher harmonics are present in the spectrum at the first stage, whereas the second stage shows a chaos-like irregularity.

[1] P. Zieliński, L. Dobrzyński and B. Djafari-Rouhani, Z. Phys. B 104, 299 (1997)

PHONON-ASSISTED DIFFUSION OF VACANCIES IN SOLID HELIUM

N.V. Zuev, V.V. Boiko, N.E. Dyumin, and V.N. Grigor'ev

B. Verkin Institute for Low Temperature Physics and Engineering, National
Academy of Sciences, 47 Lenin avenue, Kharkov, 310064, Ukraine.
e-mail: zuev@ilt.kharkov.ua

The method has been developed of direct measuring a self-diffusion coefficient in solid helium. The method consists of the measurement of shift velocity of porous membrane under action of a force, which is smaller than the fluidity threshold. The experiments have been carried out in hcp and bcc phases of ^4He at temperatures 1.3 - 1.8 K and molar volumes 20.3 - 21.0 cm^3/mole . The obtained data on self-diffusion coefficient have been analyzed together with the results of measuring the vacancy contribution in helium heat capacity and the compressibility. The temperature dependencies of the vacancy diffusion coefficient found can be described by exponential $D \sim \text{Dexp}(-W/T)$. The different mechanisms of vacancy motion have been considered: (i) classical thermoactive; (ii) the narrow band quasiparticles quantum (vacancion) diffusion; (iii) the quantum diffusion of the vacancion with wide band. The results obtained may be described self-consistently with the fit in the frames of the model of wide-band vacancion. The vacancion motion is determined by the one-phonon process (phonon-assisted diffusion). The value of wide band of vacancion is found from the comparison with the theoretical formulas available. The value of changes from 4K to 2K for ^4He and is 6.9K for bcc ^4He in temperature range studied. The obtained are larger values than temperature. In confirms the supposition that the vacancies represent wide-band quasiparticles in solid helium.

AUTHOR INDEX

Abe Y.	CP1.4	11	Bennington S.M.	GL1.5	16
Abens S.	PosC1	114	<u>Bennington S.M.</u>	LD2.1	8
Adams J.S.	PP3	39	Bennington S.M.	LD2.4	9
Aghasyan M.	PosB2	86	Bennington S.M.	PosA1	58
Ahmad N.C.	PosA21	68	Bennington S.M.	PosC16	121
Aichele N.	IS3	49	Berger H.	PosA41	78
Akimitsu J.	PosA33	74	Berger H.	PosA42	78
<u>Akimov A.V.</u>	EP2.1	30	Bergman L.	PosB10	90
Akimov A.V.	GL3.2	26	Bernhard A.	NT2.4	47
Akimov A.V.	NS2.1	6	Bernhard A.	PosB39	105
Akimov A.V.	PosB31	101	Bicout D.	EP3.2	54
Akimov A.V.	PosB44	107	Bilusic A.	PosA41	78
Akkermans E.	IQ4	51	Bilusic A.	PosA42	78
Al Jawhari H.	PosB1	86	Bischof J.	PosA10	62
Alexson D.	PosB10	90	Blencowe M.P.	NS1.1	2
Alp E.E.	NT2.3	47	Blencowe M.P.	PosB5	88
Alp E.E.	NT2.4	47	Blencowe M.P.	PosC37	132
Alp E.E.	PosC43	135	Bockowski M.	PosA4	59
Alp E.E.	PosB39	105	Boehm A.	PosB16	93
Alsina F.	PosB24	97	Bohnen K.-P.	PosA16	65
An C.P.	DS2	42	Bolko V.V.	PosC55	141
Andreev V.N.	CP2.5	36	Bonello B.	NT2.2	46
Andrianov V.A.	PosC2	114	Booth N.E.	PP5	40
Antonov V.E.	LD2.4	9	Böttger H.	DS3	43
Antonov V.E.	PosA22	68	Bracher B.	EP3.4	55
Aono T.	PosB48	109	Bracher B.	PosB37	104
Arai M.	GL1.5	16	Braden M.	LD2.3	9
Arai M.	PosA1	58	Braden M.	PosA24	69
Arai M.	PosC16	121	Bravin M.	PP5	40
Arts A.F.M.	CP1.1	10	Brennan C.J.	NT2.1	46
Arts A.F.M.	NT1.3	29	Bressoux R.	PI3.1	52
Arts A.F.M.	PI3.2	52	Brewer D.F.	PosA43	79
Arts A.F.M.	PosA6	60	Briantseva T.A.	PosC26	126
Arzel L.	PT4	13	Briggs G.A.D.	IQ1	50
Asai K.	PosA29	72	Bruckmayer M.	PP5	40
Auyeung R.C.Y.	PosC48	137	Bullough T.J.	PosC26	126
Babiker M.	NS1.4	3	Burkel E.	LD2.2	8
Babiker M.	PosB55	113	Burkel E.	NT2.4	47
Badalyan S.M.	PosB2	86	Burkel E.	PosB39	105
Bandler S.R.	PP3	39	Bury P.	PosB6	88
Bartels A.	CP2.1	34	Busiello G.	PosC38	132
Bashkin I.O.	PosA22	68	Bussmann-Holder A.	LD1.4	5
Bauer R.	PosB3	87	Bussmann-Holder A.	PosA2	58
Baumhoff S.	CP1.2	10	<u>Cabrera B.</u>	PP1	38
Beige J.	PosB46	108	Cain M.G.	PosA1	58
Belenky G.	NS1.2	2	Camacho J.	IS2	48
Belling A.	PosA10	62	Campanha J.R.	PosC3	115
Benedict K.A.	EP3.1	54	Cantarero A.	IS2	48
Ben-Ezra Y.	PosC9	118	Cantarero A.	PosA3	59
Bennett C.R.	NS1.4	3	Capinski W.S.	PosB23	97
Bennett C.R.	PosB4	87	<u>Cardona M.</u>	IS1	48
Bennett C.R.	PosB55	113	Cardona M.	IS2	48
Bennington S.M.	PosA19	67	Cardona M.	NS3.3	25

Cardona M.	PI1.3	33	Del Fatti N.	CP2.4	35
Cardona M.	PosA3	59	den Hartog R.	PP4	39
Cardona M.	PosA51	83	Dennis W.M.	NS2.2	6
Cardona M.	PosB23	97	Dennis W.M.	PI1.4	33
Cavill S.A.	PosB31	101	Devitt A.M.	EP3.1	54
Chakoumakos B.C.	PosA19	67	Dickmann S.	EP3.3	55
Challis L.J.	EP2.2	30	Dieleman D.J.	NT1.3	29
Challis L.J.	PosB31	101	Dietsche W.	EP2.2	30
Chen G.	PI3.4	53	Dietsche W.	IQ2	50
Chen G.	PosB7	89	Diezemann G.	PosC39	133
Cheng T.	EP3.1	54	Dijkhuis J.I.	GL3.2	26
Cheng T.S.	PosB13	92	Dijkhuis J.I.	NS2.1	6
Cheong H.M.	PosB24	97	DiVenere A.	PosB27	99
Cho S.	PosB27	99	Djotni K.	PP5	40
Chudnovsky F.A.	CP2.5	36	Dmitriev P.N.	PosC2	114
Chulkova G.M.	EP2.3	31	Dong S.L.	PosA7	61
Chumakov A.I.	NT2.4	47	Dorner B.	LD2.4	9
Chumakov A.I.	PosB39	105	Dove M.T.	PosC12	119
Classen J.	PosC4	115	Dravin V.A.	PosA13	64
Classen J.	PosC5	116	Duda A.	PosB33	102
Clegg P.	PP5	40	Duguet T.	EP3.2	54
Coeck M.	GL2.4	23	Dutta M.	NS1.2	2
Coeck M.	PosC6	116	Dutta M.	PosB10	90
Coldea R.	PosA19	67	Dutta M.	PosB18	94
Coleridge P.T.	EP3.4	55	Dyumin N.E.	PosC55	141
Coleridge P.T.	PosB37	104	Efimov V.B.	PI2.1	44
Courtens E.	GL1.4	15	Efimov V.B.	PI3.3	53
Courtens E.	PT4	13	Efimov V.B.	PosA8	61
Cowan M.L.	CP1.3	11	Eggert Th.	PosC7	117
Crimmins T.F.	NT2.1	46	Eifler A.	PosA9	62
Crimmins T.F.	PosB25	98	Eilenberger R.	DS1	42
Crimmins T.F.	PosB8	89	Eisenmenger W.	DE3	57
Cross A.J.	EP1.4	19	Eisenmenger W.	DS1	42
Cross A.J.	PosB9	90	Ekosipedidis G.E.	PosA43	79
Currat R.	PT3	13	Endo S.	PosA12	63
Dai P.	PosA19	67	Engel U.	LD1.1	4
Dalal N.	PosA2	58	Enss C.	DS2	42
Damen E.P.N.	PosA6	60	Enss C.	GL2.1	22
Damker T.	DS3	43	Enss C.	IS4	49
Danilchenko B.	DE4	57	Enss C.	PosC4	115
Danilchenko B.	PosA4	59	Enss C.	PP3	39
Danilchenko B.	PosB35	103	Esposito E.	PP5	40
Dashora J.	PosA5	60	Every A.G.	IQ1	50
Dashora P.	PosA5	60	Fagas G.	DS4	43
Davies J.H.	PosB20	95	Fagas G.	PosC8	117
de Vries M.A.	NT1.3	29	Falko V.I.	DS4	43
de Wijn H.	CP1.1	10	Fedotov V.K.	LD2.4	9
de Wijn H.W.	NT1.3	29	Feofilov S.P.	NS2.2	6
de Wijn H.W.	PI3.2	52	Feofilov S.P.	PI2.3	45
de Wijn H.W.	PosA6	60	Feoktsitov N.A.	NS2.1	6
Debernardi A.	PI1.3	33	Flachbart K.	PosA10	62
Debernardi A.	PosA51	83	Fleischmann A.	PP3	39
Dekorsy T.	CP2.1	34	Fleurov V.	PosC9	118

Flytzanis C.	CP2.4	35
Foret M.	GL1.4	15
Foxon C.T.	PosB13	92
Francis H.R.	PosB30	100
Franke Th.	PosC40	133
Franz H.	PosA52	83
Freeman E.J.	PosA19	67
Friedland K.	IQ2	50
Fritz G.G.	PosC48	137
Fujii Y.	IQ3	51
Fujishiro H.	PI2.2	44
Fujishiro H.	PosA11	63
Fujishiro H.	PosA18	66
Fujita O.	PosA33	74
Fujita T.	PosA49	82
Fukase T.	PosA11	63
Funahashi R.	PosC19	123
Furuta H.	PosA12	63
Gaitskell R.	PosC13	120
Gajewski D.A.	PosA19	67
Galkina T.I.	PosA13	64
Ganter C.	PosC39	133
García-Cristóbal A.	PosA3	59
Gay S.C.A.	PosA14	64
Geilenkeuser R.	GL2.3	23
Geller M.R.	PI1.4	33
Gerdau E.	NT2.4	47
Gershenson E.M.	EP2.3	31
Giehler M.	NS3.3	25
Giltrow M.	PosB20	95
Gippius A.A.	PosA13	64
Gladun A.	PosC1	114
Gladun A.	PosC7	117
Göbel A.	IS2	48
Göbel A.	PosA51	83
Gorfinkel V.B.	NS1.2	2
Gov N.	IQ4	51
Grigor'ev V.N.	PosC55	141
Grigorchuk N.I.	PosB11	91
<u>Grill W.</u>	NT1.1	28
Grill W.	NT1.2	28
Grill W.	PosA9	62
Grill W.	PosB16	93
Grill W.	PosB17	94
Grosse G.	LD2.4	9
Grzegory I.	PosA4	59
Gudra T.	PosB17	94
Gulian A.M.	PosC10	118
Gulian A.M.	PosC48	137
Gupta G.	PosA5	60
Gusakov V.E.	PosA15	65
Gusev V.E.	EP2.4	31
Güven K.	PosB4	87

Guzenko V.	PosA4	59
Gvasaliya S.N.	GL3.3	27
Gwizdalla T.	PosB12	91
Gyulamiryan A.L.	PosC48	137
Haddad G.I.	NS1.2	2
Halcoussis C.	LD2.2	8
Haller E.E.	IS3	49
Hannon A.C.	GL1.5	16
Hao H.-Y.	PI1.1	32
Hara K.	PosB28	99
Hara K.	PosC11	119
Hara K.	PosC32	129
Harima H.	CP2.3	35
Harima H.	PosB27	99
Harris M.	LD2.1	8
Harris M.J.	PosC12	119
<u>Harris M.J.</u>	PT1	12
Harrison P.	PosB15	93
Hase M.	CP2.2	34
Hase M.	CP2.3	35
Hase M.	PosB27	99
Hata H.	PosA49	82
Hauser M.R.	PosC13	120
Häussler P.	PosC40	133
Hawker P.	EP1.4	19
Hawker P.	PosB13	92
Hawker P.	PosB14	92
Hawker P.	PosB9	90
Hecht J.-D.	PosA9	62
Hehlen B.	GL1.4	15
Hehlen B.	PT4	13
Heid R.	PosA16	65
Heitz M.	PosC5	116
Henini M.	EP1.1	18
Henini M.	EP3.1	54
Henini M.	EP3.4	55
Henini M.	PosB14	92
Henini M.	PosB31	101
Henini M.	PosB37	104
Henini M.	PosB9	90
Hession P.	NT2.3	47
Hieda M.	PosC44	135
Hiki Y.	PosB32	101
Hiki Y.	PosC14	120
Hillmann K.	NT1.1	28
Hillmann K.	NT1.2	28
Hiramatsu N.	PosC11	119
Hiramatsu N.	PosC32	129
Hirata T.	PosA17	66
Hizhnyakov V.	PI1.2	32
Hizhnyakov V.	PosA31	73
Horstmann U.	GL3.4	27
Horwitz J.S.	PosC48	137

Houwman E.P.	PP5	40	Kennedy I.	PosB37	104
Hu M.	NT2.3	47	Kent A.J.	EP1.1	18
Hübner M.	IS4	49	Kent A.J.	EP1.4	19
Hunklinger S.	GL2.1	22	Kent A.J.	EP3.1	54
Hunklinger S.	PosC4	115	Kent A.J.	PosB13	92
Hunklinger S.	PosC5	116	Kent A.J.	PosB14	92
Hunklinger S.	PP3	39	Kent A.J.	PosB31	01
Iafrate G.J.	NS1.2	2	Kent A.J.	PosB9	90
Ikari H.	PosC15	121	Keppens V.	PosA19	67
Ikebe M.	PI2.2	44	Keppens V.	PosC25	126
Ikebe M.	PosA11	63	Ketterson J.B.	PosB27	99
Ikebe M.	PosA18	66	Khabibullin B.M.	PosC27	127
Il'in K.S.	EP2.3	31	Khazanov E.N.	PI2.4	45
Inaba Y.	PT4	13	Khazanov E.N.	PosA47	81
Inamura Y.	GL1.5	16	Khurunenko L.I.	IS3	49
Inamura Y.	PosC16	121	Khmelnitskii R.A.	PosA13	64
Inoue A.	PosC30	128	Kigugawa N.	PosA49	82
Inoue K.	PT4	13	Kikuchi T.	PosA11	63
Iobe A.	CP1.4	11	Kim J.	PosC48	137
Ishii K.	PosA30	72	Kim K.W.	NS1.2	2
Isida S.	PosA29	72	Kim K.W.	PosB10	90
Isobe M.	RS4	21	Kim K.W.	PosB18	94
Itoh A.	PosB40	105	Kim T.J.	NT1.1	28
Itoh K.M. I	S3	49	Kim T.J.	PosB17	94
Ivanov B.A.	PosA48	81	Kim Y.	PP3	39
Ivanov S.	PI2.4	45	Kink R.	PI1.2	32
Ivanov S.N.	PosA47	81	Kinsler P.	PosB15	93
Jäckel M.	GL2.3	23	Kirimoto K.	PosA20	67
Jäckel M.	PosC1	114	Kisel V.P.	PosC18	122
Jäckel M.	PosC7	117	Kisin M.	NS1.2	2
Jamnický I.	PosB6	88	Kislov A.N.	PosC31	129
Jasiukiewicz Cz.	EP1.4	19	Kisoda K.	CP2.3	35
Jasiukiewicz Cz.	PosB9	90	Kisoda K.	CP2.5	36
Jeannet J.-C.	NT2.2	46	Kitamura N.	GL1.5	16
Jenkins S.	PosA27	71	Kitamura N.	PosA1	58
Jezowski A.	PosA15	65	Kitamura N.	PosC16	121
Joffrin J.	CP1.2	10	Kitamura N.	PosC19	123
Kacmarčíková E.	PosB38	104	Klemens P.	DE1	56
Kai S.	PosB28	99	Klimashov A.	IQ2	50
Kamada T.	PosC35	131	Klokov A.Yu.	PosA13	64
Kambuchi K.	PosA37	76	Knauth S.	NT1.2	28
Kaplyanskii A.A.	NS2.1	6	Knauth S.	PosB16	93
Kaplyanskii A.A.	PI2.3	45	Kobayashi H.	PosC21	124
Karasik B.S.	EP2.3	31	Kobayashi H.	PosC23	125
Kasahara M.	PosA50	82	Kobayashi M.	PosC47	137
Kasahara M.	PT2	12	Kobayashi Y.	PosA29	72
Katagi J.	RS3	21	Köbernig G.	PosC7	117
Katayama-Yoshida H.	RS1	20	Kocevar P.	CP2.6	36
Katzer D.S.	PosB23	97	Kochelap V.A.	PosB18	94
Kawashima H.	PosC17	122	Kochereshko V.P.	PosB44	107
Keller J.	PosA39	77	Kodama M.	PosC20	123
Kelsall R.W.	PosB15	93	Koehl R.M.	NT2.1	46
Kennedy I.	EP3.4	55	Koenderink A.F.	NT1.3	29

Kogure Y.	NS2.4	7
Kogure Y.	PosC14	120
Kogure Y.	PosC21	124
Kogure Y.	PosC23	125
Köhler K.	CP2.1	34
Kohn K.	PosA29	72
Kojima S.	PosA36	75
Kojima S.	PosC20	123
Kojima S.	PosC29	128
Kojima S.	PosC45	136
Kojro Z.	PosB17	94
Kolesnikov A.	LD2.4	9
Kolesnikov A.I.	PosA21	68
Kolesnikov A.I.	PosA22	68
Kolesnikov A.I.	PosA7	61
Komirenko S.	PosB10	90
Komirenko S.M.	PosB18	94
Komuro R.	PosB32	101
Kono K.	PosC17	122
Konovalova E.	PosA10	62
Konstantinov V.A.	PosA40	77
Kosevich A.M.	DE2	56
Kosevich A.M.	PosC22	124
Kosevich Y.A.	PosB19	95
Koshelets V.P.	PosC2	114
Kostial H.	PosB35	103
Kosugi T.	PosC21	124
Kosugi T.	PosC23	125
Kosugi T.	PosC35	131
Kozin M.G.	PosC2	114
Kozorezov A.	PP4	39
Kozorezov A.G.	PosB1	86
Kozorezov A.G.	PosB20	95
Kozorezov A.G.	PosC8	117
Krämer V.	PosA9	62
Kramp S.	PosA24	69
Kramp S.	PosB36	103
Kraus H.	PP5	40
Krauß G.	PosA9	2
Kreft M.	DS2	42
Kuboyama K.	PosB28	99
Kuhl J.	CP2.6	36
Kühn R.	GL3.4	27
Kulikowski A.V.	PosB20	95
Kulinkin A.B.	PI2.3	45
Kume T.	PosA37	76
Kume T.	RS2	20
Kuroe H.	PosA23	69
Kuroe H.	RS4	21
Kurz H.	CP2.1	34
Laermans C.	GL2.4	23
Laermans C.	PosC24	125
Laermans C.	PosC25	126

Laermans C.	PosC4	115
Laermans C.	PosC6	116
Lamari S.	PosB21	96
Lambert C.J.	DS4	43
Lambert C.J.	PosC8	117
Lambert K.	PosB22	96
Lander G.H.	PT3	13
Lasjaunias J.-C.	PI3.1	52
Lassmann K.	DE3	57
Lassmann K.	DS1	42
Lassmann K.	IS3	49
Lassmann K.	PosC28	127
Lauck R.	PosA51	83
Lee B.C.	PosB10	90
Lehmann D.	EP1.4	19
Lehmann D.	PosB9	90
Lenkeit O.	NT1.1	28
Leupold O.	NT2.4	47
Leupold O.	PosA52	3
Levinson Y.	EP1.2	18
Lévy F.	PosA41	78
Lewis M.H.	PosA1	58
Li J.	LD1.3	5
Li J.	LD2.1	8
Li J.C.	LD2.4	9
Li J.C.	PosA21	68
Li J.C.	PosA22	68
Li J.C.	PosA7	61
Liarokapis E.	PosA38	76
Lin C.-J.	PosA53	84
Linsenmaier C.	IS3	49
Lioubtchenko D.V.	PosC26	126
Lipp D.	PosC1	114
Lippold G.	PosA9	62
Lisin V.N.	PosC27	127
Lodziana Z.	PosC54	140
Loewenhaupt M.	PosA24	69
Loewenhaupt M.	PosB36	103
Loong C.-K.	PosA21	68
López-Richard V.	PosA25	70
Ludwig S.	DS2	42
Luryi S.	NS1.2	2
Lushnikov S.G.	GL3.3	27
Luty F.	DS2	42
Ma W.-J.	PosC52	139
Machulin V.F.	PosB29	100
Maeda T.	NS2.3	7
Magyar P.	EP3.2	54
Maier F.	IS3	49
Maier F.	PosC28	127
Makova M.K.	PosA8	61
Maksimov J.	PI1.2	32
Mandrus D.	PosA19	67

Manzhelii E.V.	PosA26	70
Manzhelii V.G.	PosA40	77
Maple M.B.	PosA19	67
Maris H.J.	PI1.1	32
Maris H.J.	PosB23	97
Marmeggi J.C.	PT3	13
Marques G.E.	PosA25	70
Mascarenhas A.	PosB24	97
Masuda R.	PosA23	69
Matsubara I.	PosC19	123
Matsuda O.	PosC33	130
Matsuda O.	PosC49	138
Matsui G.	PosC29	128
Matsukawa M.	PosC30	128
Matsumoto A.	PosC11	119
Matsumoto A.	PosC32	129
Matsumoto K.	IQ3	51
Matsuo T.	PosC16	121
Matsuzaki K.	PosC42	134
Mayer A.P.	NS3.2	24
Maynard R.	PI3.1	52
Maznev A.A.	IQ1	50
Maznev A.A.	PosB25	98
Maznev A.A.	PosB8	89
Mazurenko V.G.	PosC31	129
McMorrow	D.F. PT1	12
Meier J.	PosC5	116
Meissner M.	GL2.2	22
Mellor C.J.	EP3.1	54
Mellor C.J.	EP3.4	55
Mellor C.J.	PosB37	104
Meltzer R.S.	NS2.2	6
Metge J.	PosB39	105
Meyer J.	PosB42	106
Mezhov-Deglin L.P.	PI2.1	44
Mezhov-Deglin L.P.	PI3.3	53
Mezhov-Deglin L.P.	PosA8	61
Michel K.-H.	PosA2	58
Mikami M.	PosC45	136
Minagawa Y.	PosA30	72
Misochko O.V.	CP2.5	36
Mitin V.V.	EP1.3	19
Mitsudo S.	PosC19	123
Miyasato T.	PosA20	67
Miyasato T.	PosA46	80
Mizoguchi K.	CP2.2	34
Mizoguchi K.	PosB27	99
Mizuno S.	PosB26	98
Molokác S.	PosA10	62
Moravsky A.P.	PosA22	68
Morrison I.	PosA27	71
Motida K.	PosA28	71
Motokawa M.	PosC19	123

Msall M.E.	IQ2	50
Murase K.	PosC33	130
Murase K.	PosC49	138
Murata S.	PosA29	72
Müssig H.	IS3	49
Nakamura A.	PosC11	119
Nakamura A.	PosC32	129
Nakamura F.	PosA49	82
Nakamura M.	PosC33	130
Nakamura M.	PosC49	138
Nakashima S.	CP2.2	34
Nakashima S.	CP2.3	35
Nakashima S.	CP2.5	36
Nakashima S.	PosB27	99
Nakayama H.	PosA30	72
Nakayama M.	CP2.2	34
Nakayama T.	GL1.1	14
Nakayama T.	GL1.2	14
Nakayama T.	GL1.3	15
Nakayama T.	PosC46	136
Naylor A.J.	EP1.1	18
Ndop J.	NT1.1	28
Nelson K.A.	NT2.1	46
Nelson K.A.	PosB25	98
Nelson K.A.	PosB8	89
Nevedrov D.	PosA31	73
Newanich R.J.	PosB10	90
Nikogosyan V.R.	PosC48	137
Nimori S.	PosA49	82
Nipko J.	PosA21	68
Nishiguchi N.	NS1.3	3
Nobugai K.	PosA20	67
Noda N.	PosA32	73
Nojiri H.	PosC19	123
Nori F.	PL2	1
Noto K.	PosC30	128
Novikov V.N.	PosC34	130
Nozaki R.	PosA32	73
Ogasawara T.	PosC35	131
Ogita N.	PosA33	74
Ogita N.	PosA49	82
Ohta H.	PosC19	123
Okabe H.	PosB28	99
Okabe T.	PosA34	74
Okuda Y.	IQ3	51
Olikh Y.M.	PosB29	100
Olson J.M.	PosB24	97
Orani D.	PosA35	75
Orbach R.L.	GL1.3	15
Oshima C.	PosB40	105
Oshima C.	PosB41	106
Otani S.	PosB40	105
Otomo T.	GL1.5	16

Otomo T.	PosC16	121
Ouali F.F.	PosB30	100
Ouali F.F.	PosB31	101
Ozaki T.	PosC35	131
Ozawa S.	PosB32	101
Paderno Y.	PosA10	62
Page J.H.	CP1.3	11
Pajot B.	IS3	49
Parker J.M.	PosC12	119
Parker S.F.	LD2.4	9
Parker S.F.	PosA21	68
Parshin D.A.	PosC24	125
Paskiewicz T.	PosA4	59
Paszkiewicz T.	PosB33	102
Paszkiewicz T.	PosC36	131
Paszkiewicz T.	PosC37	132
<u>Pavone P.</u>	LD1.1	4
Pavone P.	PosB3	87
<u>Peacock A.</u>	PP2	38
Peacock A.	PP4	39
Peeters E.	PosC6	116
Pentland I.A.	EP1.1	18
Perrin B.	NT2.2	46
Perrin N.	PosB34	102
Petry W.	PosA52	83
Pevtsov A.B.	NS2.1	6
Pipa V. I.	EP1.3	19
Pletl T.	LD1.1	4
Ploog K.	PosB23	97
Ploog K.H.	NS3.3	25
Poelaert A.	PP4	39
Ponyatovsky E.G.	PosA22	68
Poplavsky D.	DE4	57
Poplavsky D.	PosB35	103
Porschberg T.	GL2.3	23
Preis C.	PosA39	77
Prieur J.-Y.	CP1.2	10
Pruchnik M.	PosC36	131
Pruchnik M.	PosC37	132
Ptitsina N.G.	EP2.3	31
Pyka N.M.	PosA24	69
Pyka N.M.	PosB36	103
Qadri S.B.	PosC48	137
Quagliano L.G.	PosA35	75
Quast K.W.	NT2.4	47
Rampton V.W.	EP3.4	55
Rampton V.W.	PosB37	104
Rampton V.W.	PosB6	88
Reichardt W.	LD2.3	9
Reiffers M.	PosA10	62
Reiffers M.	PosB38	104
Revyakin V.P.	PosA40	77
Rhodes H.C.	PosB30	100

Ricci A.	PosA35	75
Ridley B.K.	NS1.4	3
Ridley B.K.	PosB55	13
Riede V.	PosA9	62
Riess J.	EP3.2	54
Röhlsberger R.	NT2.4	47
Röhlsberger R.	PosB39	105
Röhlsberger R.	PosC43	135
Rohr I.	PosC4	115
Rokni M.	EP1.2	18
Rokuta E.	PosB40	105
Rokuta E.	PosB41	106
Romashkina I.L.	PosC2	114
Roshko S.	DE4	57
Roshko S.	EP2.2	30
Roshko S.H.	EP3.1	54
Ross D.K.	LD2.1	8
Rossignol C.	NT2.2	46
<u>Roukes M.</u>	PL1	1
Ruf T.	IS2	48
Ruf T.	NS3.3	25
Ruf T.	PosA51	83
Ruf T.	PosB23	97
Rüffer R.	NT2.4	47
Rüffer R.	PosB39	105
Rump P.J.	PI3.2	52
Saburova R.	PosC38	132
Sadeghi S.M.	PosB42	106
Sahling S.	PosC1	114
Sahraoui-Tahar M.	PosB20	95
Saiko A.P.	PosA15	65
Saitoh I.	PosA36	75
Sakai K.	CP2.5	36
Sakai K.	PosB27	99
Sakita S.	PosA49	82
Sakon T.	PosC19	123
Sales B.C.	PosA19	67
Salmon G.L.	PP5	40
Salonová T.	PosB38	104
Samartsev V.V.	PosC27	127
Sanada M.	PosB43	107
Sasaki S.	PosA37	76
Sasaki S.	RS2	20
Sauerzapf A.	PosB53	112
Savatinova I.	PosA38	76
Savkina R.K.	PosB29	100
Savova I.	PosA38	76
Scherbakov A.V.	PosB44	107
Schirmacher W.	PosC39	133
Schmachtl M.	PosB17	94
Schmid A.	PosB3	87
Schmidt R.	PosC40	133
Schmitt M.	NS3.2	24

Schönefeld J.	PP3	39
Schönherr E.	IS2	48
Schriemer H.P.	CP1.3	11
Schubert M.	NT1.1	28
Schubert M.	PosB17	94
Schullatz M.	CP2.6	36
Seidel G.M.	PP3	39
Sekine T.	PosA23	69
Sekine T.	RS4	21
Selg M.	PI1.2	32
Sergeev A.	EP2.3	31
Sergeev A.	PosA39	77
Sergeev A.	PosC41	134
Sergeev S.A.	PosC2	114
Seto H.	PosA23	69
Seto H.	RS4	21
Seyfert C.	LD2.2	8
Sharkov A.I.	PosA13	64
Sharma P.C.	PosB45	108
Shchapova Yu.V.	PosC50	138
Shegeda A.M.	PosC27	127
Sheng P.	CP1.3	11
Shibata K.	PosC42	134
Shik A.Y.	PosB5	88
Shimizu H.	PosA37	76
Shimizu H.	RS2	20
Shimizu K.	PosA32	73
Shiozaki Y.	PosA32	73
Shirahama K.	PosC17	122
Shirai K.	RS1	20
Short J.	PosC13	120
Shpinel V.S.	PosC2 1	14
Shukla M.M.	PosC3	115
Silier I.	IS2	48
Simmons R.O.	LD2.2	8
Sinn H.	LD2.2	8
Siny I.G.	GL3.3	27
Smirnov S.A.	PosA40	77
Smirnova E.P.	PosA47	81
Smit G.D.J.	GL3.2	26
Smit G.D.J.	NS2.1	6
Smontara A.	PI3.1	52
Smontara A.	PosA41	78
Smontara A.	PosA42	78
Soifer Y.M.	PI2.4	45
Sokolov V.I.	PosC31	129
Sologubenko A.V.	PosA43	79
Sologubenko A.V.	PosA44	79
Srivastava G.	LD1.2	4
Srivastava G.P.	PosA14	64
Srivastava G.P.	PosB22	96
Stanley C.R.	PosB20	95
Straube U.	PosB46	108

Strauch D.	LD1.1	4
Strauch D.	NS3.2	24
Strauch D.	PosB3	87
Strehlow P.	GL2.1	22
Strehlow P.	GL2.2	22
Stroscio M.A.	NS1.2	2
Stroscio M.A.	PosB10	90
Stroscio M.A.	PosB18	94
Stroud R.H.	PosC48	137
Sturhahn W.	NT2.3	47
Sturhahn W.	NT2.4	47
Sturhahn W.	PosB39	105
Sturhahn W.	PosC43	135
Sun J.P.	NS1.2	2
Sun Y.	PosA46	80
Suski T.	PosA4	59
Suzuki K.	PosA28	71
Suzuki K.	PosC42	134
Suzuki M.	PosA29	72
Suzuki M.	PosC44	135
Syrkin E.S.	PosA26	70
Syrkin E.S.	PosC22	124
Tagantsev A.K.	PT4	13
Takagi Y.	PosC45	136
Takahashi H.	PosC14	120
Takahashi H.	RS3	21
Takakura H.	PosC42	134
Takasaka S.	PosA45	80
Takase T.	PosA46	80
Takesada M.	PT2	12
Talwar D.N.	NS3.4	25
Talwar D.N.	PosB47	109
<u>Tamura S.I.</u>	NS3.1	24
Tamura S.I.	PosB26	98
Tamura S.I.	PosB48	109
Tamura S.I.	PosB49	110
Tanaka T.	PosB40	105
Tanaka Y.	PosB48	109
Tanaka Y.	PosB49	110
Tanatar B.	PosB4	87
Tani M.	CP2.5	36
Taranov A.	PosA47	81
Taranov A.V.	PI2.4	45
Tartakovskaya E.V.	PosA48	81
Teng H.B.	NS1.2	2
Terao T.	PosC46	136
Thomson A.L.	PosA43	79
Tissue B.M.	NS2.2	6
Tkach A.V.	PosB50	110
Toellner T.S.	PosB39	105
Toellner T.S.	PosC43	135
Tollner T.S.	NT2.3	47
Tollner T.S.	NT2.4	47

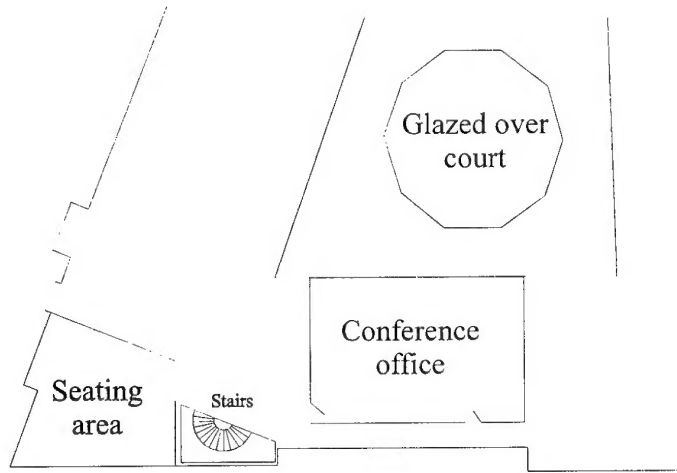
Tomkinson J.	PosA22	68
Torii K.	PosC44	135
Trallero-Giner C.	PosA3	59
Tsuji T.	RS2	20
Tsujimi Y.	PosA45	80
Tsujimi Y.	PosA54	84
Tsujimi Y.	PosC47	137
Tsukada I.	PosA23	69
Tsunezumi Y.	PosA33	74
Tsuruoka F.	PosB51	111
Tutis E.	PosA41	78
Tutov A.V.	DE2	56
Tutov A.V.	PosC22	124
Tütüncü H.M.	LD1.2	4
Tütüncü H.M.	PosA14	64
Tzortzakis S.	CP2.4	35
Uchinokura K.	PosA23	69
Udagawa M.	PosA33	74
Udagawa M.	PosA49	82
Ueda Y.	RS4	21
Vacher R.	GL1.4	15
Vagidov N.Z.	EP1.3	19
Valente L.	PosB52	111
Vallée F.	CP2.4	35
van der Voort M.	GL3.2	26
van der Voort M.	NS2.1	6
Van Vechten D.	PosC48	137
van Veghel M.G.A.	NT1.3	29
van Walree P.A.	CP1.1	10
Ventzek P.L.G.	EP2.4	31
Vines R.E.	NT1.4	29
Vogel B.	PosB20	95
Voltz S.	PI3.4	53
Wada N.	PosC44	135
Wagner F.E.	LD2.4	9
Wagner M.	PosB53	112
Wakamura K.	RS3	21
Wang Y.	PosC33	130
Wang Y.	PosC49	138
Wasilewski Z.R.	EP3.4	55
Wasilewski Z.R.	PosB37	104
Watanabe J.	PosA50	82
Weinstein I.A.	PosC50	138
Weiss G.	IS4	49
Weitz D.A.	CP1.3	11
Widulle F.	IS2	48
Widulle F.	PosA51	83
Wiele N.	PosA52	83
Wigmore J.K.	PosB1	86
Wigmore J.K.	PosB20	95
Wigmore J.K.	PosC8	117
Wigmore J.K.	PP4	39
Wilkinson C.D.W.	PosB20	95

Wolfe J.P.	NT1.4	29
Wolfe J.P.	PosC13	120
Wood K.S.	PosC48	137
Wright O.B.	EP2.4	31
Wright O.B.	PosC51	139
Wu C.-C.	PosA53	84
Wu T.-M.	PosC52	139
<u>Wurger A.</u>	GL3.1	26
Wybourne M.N.	NS1.3	3
Yagi T.	GL1.2	14
Yagi T.	PosA45	80
Yagi T.	PosA50	82
Yagi T.	PosA54	84
Yagi T.	PosB43	107
Yagi T.	PosC47	137
Yagi T.	PT2	12
Yajima S.	PosA30	72
Yamada H.	PosA34	74
Yamada H.	PosC53	140
Yamaguchi M.	GL1.2	14
Yamamuro O.	PosC16	121
Yamanaka A.	PT4	13
Yamashita K.	PosB40	105
Yamazaki S.	IQ3	51
Yamazaki Y.	PosC42	134
Yang H.	NS2.2	6
Yano H.	PosC44	135
Yano T.	PosC45	136
Yocum D.	PosA21	68
Yokoyama Y.	PosC30	128
Yoshida T.	IQ3	51
Yoshihara A.	PosB54	112
Yoshioka S.	PosA54	84
Yoshizawa M.	PosC30	128
Yu S.	NS1.2	2
Yu S.	PosB10	90
Zakharchenya R.I.	PI2.3	45
Zakhleniuk N.A.	NS1.4	3
Zakhleniuk N.A.	PosB55	113
Zaranek S.	NS3.4	25
Zatsepin A.F.	PosC50	38
Zeitler U.	EP3.1	54
Zeller F.	DE3	57
Zeller F.	IS3	49
Zhukova L.M.	PI2.4	45
Zielinski P.	PosC54	140
Zoli M.	PosA55	85
Zuev N.V.	PosC55	141
Zuikov V.A.	PosC27	127

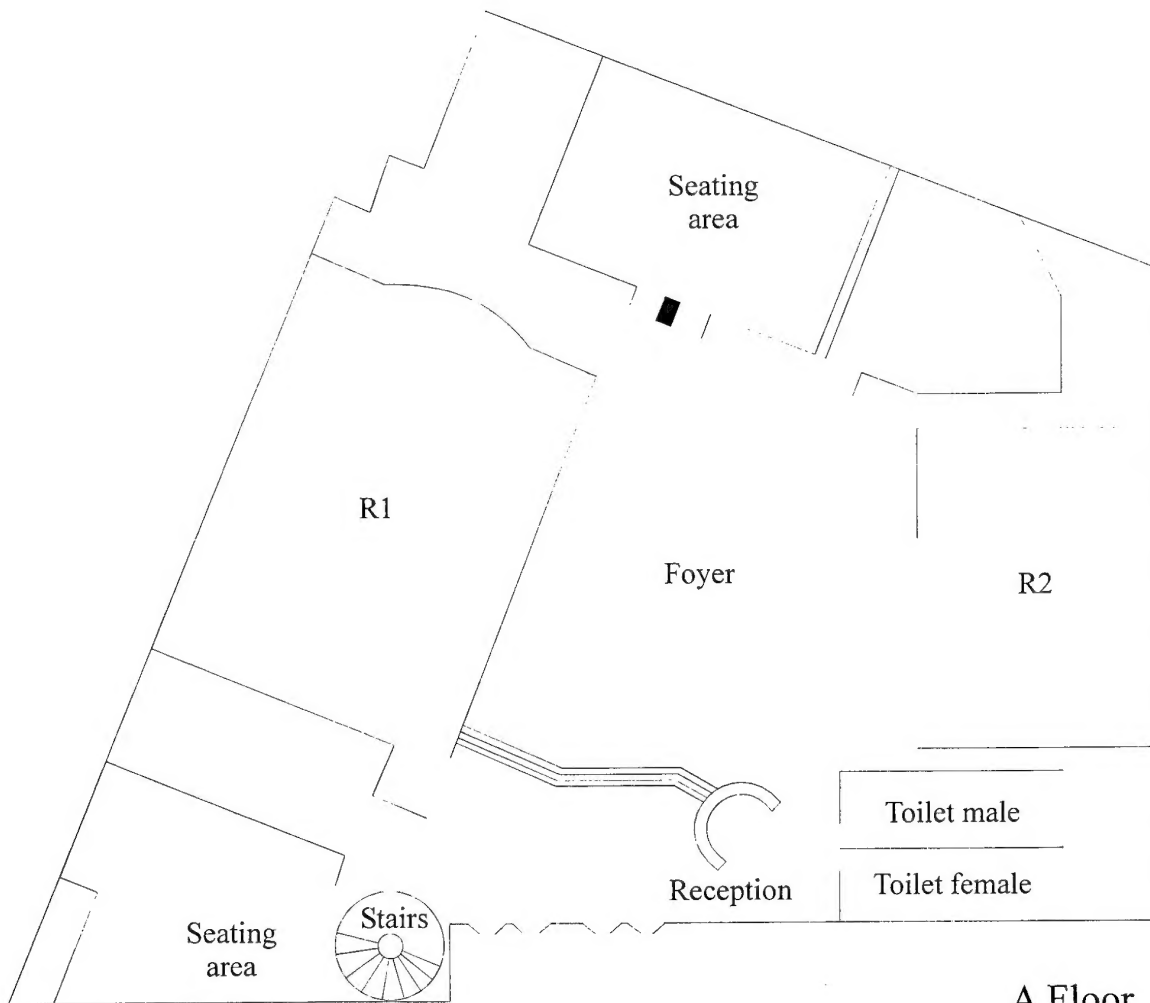
Bold = Corresponding author

Underlined = Invited speaker

George Fox Conference Centre



B Floor



A Floor

Monday 27 July		
09:00	Opening ceremony	
09:30	Plenary session	
10:50	<i>Refreshments</i>	
11:20	Nanostructures 1	Lattice dynamics 1
13:00	<i>Lunch</i>	
14:00	Nanostructures 2	Lattice dynamics 2
15:30	Poster session A (<i>Refreshments</i>)	
17:00	Coherent phonons 1	Phase transitions
19:00	<i>Dinner</i>	
20:30	<i>Conference reception</i>	

Tuesday 28 July		
09:00	Glasses 1	
10:50	<i>Refreshments</i>	
11:20	Electron-phonon interaction 1	Raman scattering
13:00	<i>Lunch</i>	
14:00	Glasses 2	Nanostructures 3
15:30	Poster session B (<i>Refreshments</i>)	
17:00	Nanostructures (discussion)	
19:00	<i>Dinner</i>	

Wednesday 29 July		
09:00	Glasses 3	New techniques 1
10:30	<i>Refreshments</i>	
10:50	Electron-phonon interaction 2	Phonon interactions 1
12:30	<i>Lunch</i>	
13:30	<i>Excursion departure</i>	
20:00	<i>Dinner</i>	

Thursday 30 July		
09:00	Coherent phonons 2	Particle detectors (highlight)
11:00	<i>Refreshments</i>	
11:30	Disordered systems	Phonon interactions 2
13:00	<i>Lunch</i>	
14:00	New techniques 2	Isotope effects (highlight)
15:30	Poster session C (<i>Refreshments</i>)	
17:00	Glasses and disordered systems (discussion)	
18:30	<i>Conference banquet departure</i>	
19:00	<i>Dinner</i>	

Friday 31 July		
09:00	Interfaces and quantum fluids	Phonon interactions 3
10:30	<i>Refreshments</i>	
10:50	Electron-phonon interactions 3	Defects
12:15	Closing ceremony	
13:00	Conference close	
13:30	<i>Lunch</i>	